MINISTRY OF EDUCATION AND SCIENCE OF UKRAINE
SUMY NATIONAL AGRARIAN UNIVERSITY

Qualifying scientific
on the rights of the manuscript

ZHIKE LIU

UDC 619:615.281.9

PHD THESIS

CONSTRUCTION OF MULTIPLEX PCR ASSAY BASED ON THE *CITE2* GENE TO IDENTITY SALMONELLA PULLORUM AND ITS EFFECTOR STEE IN PATHOGENICITY AND IMMUNITY

Field of knowledge: 21 - veterinary medicine
Specialty: 211 - veterinary medicine

Submitted for a scientific degree of Doctor of philosophy

The dissertation contains the results of own research. The use of ideas, results and texts of other authors have references to the relevant source Zhike Liu Zhike Liu.

Scientific supervisor (consultant): **Andrii Berezovskyi**,
Doctor of veterinary sciences, Professor

Sumy – 2023

ANNOTATION

Zhike Liu «Construction of multiplex PCR assay based on the *citE2* gene to identity *Salmonella* Pullorum and its effector SteE in pathogenicity and immunity» − Qualifying educational and scientific work on the rights of the manuscript. Dissertation for the degree of doctor of philosophy in the specialty 211 «Veterinary medicine» − Sumy National Agrarian University, Sumy, 2023.

The thesis is devoted to providing development and scientific justification of the prevention and accurate detection of *S*. Pullorum, and clarify the mechanism of persistent *S.* Pullorum infection in chickens. *S.* Pullorum is a host-specific pathogen, causes severe economic losses to the chicken farms, and also can induce an anti-inflammatory response in chickens. A rapid and accurate method can help us make corresponding prevention and control measures in clinical and food samples. Additionally, *S.* Pullorum effectors with anti-inflammatory function can be a unique drug candidate for targeting salmonellosis.

In order to confirm the pathogenic bacteria species and its drug susceptibility that causes severe diarrhea (pullorum disease) and systemic fatal diseases in chickens. The diseased chickens with suspected *S*. Pullorum from a large-scale chicken farms were subjected to bacterial culture identification and drug sensitivity test. *S.* Pullorum were the main pathogenic bacteria of the diseased chickens. Drug susceptibility test confirmed that the isolated *S.* Pullorum were resistant to amoxicillin, sulfamethazine, tetracycline and ciprofloxacin, but sensitive to ceftriaxone, ceftiofur and kanamycin.

The *citE2* gene and the interval sequence of SPS4_00301-SPS4_00311 gene existed in all *Salmonella* serovars, but the regions of difference in *citE2* was found only in *S*. Pullorum. The developed multiplex PCR system based on the two molecular markers can be as low as 6.25 pg/μL and 10^4 CFU/mL for genomic DNA and *S*. Pullorum cells, respectively. The developed multiplex PCR assay distinguished *S*. Pullorum from 33 different *Salmonella* serotypes and 13 non-

target species. The detection of egg samples artificially contaminated with *S.* Pullorum, *S.* Enteritidis and naturally contaminated 69 anal swab samples showed that results were consistent with the culture method.

In order to the analysis of the association of the type III secretion system encoded *steE* with *S.* Pullorum virulence, the *steE* deletion of *S.* Pullorum (Δ*steE*) strain was constructed using the λ-Red recombination system. We performed *in vitro* and *in vivo* analysis using HD-11 cells and chickens, infected with wild-type S. Pullorum (WT) or Δ*steE* strain, respectively. The results of virulence assay showed that the LD_{50} of Δ*steE* strain was 22.8 times higher than that of WT and Δ*steE* strains in chickens. The colonization experiment of bacteria showed that the overall change trend of the number of WT and Δ*steE* strains were similar in chicken livers, spleens, heart, bursas, and cecums, which increased first and then decreased. Compared to that in the WT strain, Δ*steE* strain reduced invasion and proliferation of bacteria in the infected HD-11 cells.

In addition, we analyzed the mRNA expression levels of effector genes and cytokines by qRT-PCR. SteE was associated with the regulation of various effector genes and inflammatory cytokines in HD-11 cells during *S.* Pullorum infection. Compared with those of the WT or Δ*steE*+*steE* strain-infected group, the mRNA transcript levels of *IL-12* and *IFN-γ* were significantly higher, whereas the *IL-10* mRNA expression was significant decreased in the Δ*steE* strain-infected liver and bursa, the *IL-4* mRNA expression displayed dramatically decreased transcriptional level in the Δ*steE* strain-spleen, cecum, and heart, and the *IL-10* mRNA expression was significantly lower in the Δ*steE* strain-infected spleen and cecum. The chickens infected with the Δ*steE* strain showed weak pathological lesions in the liver and spleen histopathological lesions compared to those in the WT strain.

To elucidate the mechanism via which *steE* regulators the Th1/Th2 cytokines expression in the case of *S.* Pullorum infection, we used *S.* Pullorum as a model pathogen to evaluate the role of *steE* in *Salmonella*-induced inflammation. We demonstrated that *steE* diminished the expression of Th1-related cytokines (*IFN-γ* and *IL-12*) and promoted the expression of Th2-related cytokines (*IL-4* and *IL-10*)

in HD-11 cells and chicken models of S. Pullorum infection. SOCS3 silencing suppressed the function of *steE* in HD-11 cells, led to the imbalance of Th1/Th2-related cytokines. *SteE* promoted SOCS3 expression by activating STAT3 in HD-11 cells. Moreover, *steE* inhibited NF-κB P65 expression and blocked its translocation to the nucleus by promoting SOCS3 expression.

In summary, the combined application of bacterial culture identification, drug sensitivity test analysis and the developed multiplex PCR system can accurately understand the distribution, drug resistance and detection of *S.* Pullorum, provide data support and a valuable tool for the purification of salmonellosis. In addition, s*teE* enhanced the persistent infection and virulence of *S.* Pullorum by regulating inflammation response in the case of *S.* Pullorum infection. Finally, our results also illustrated for the first time that *steE* regulated the expression of Th1/Th2 cytokines via modulation of the STAT3/SOCS3 and NF-κB axis that might be associated with the Th1/Th2 cells differentiation and could, therefore, be a novel therapeutic strategy against salmonellosis.

Based on the materials of the dissertation, methodological recommendations «**Construction of multiplex PCR assay based on the *citE2* gene to identity *Salmonella* Pullorum and its effector SteE in pathogenicity and immunity»** was developed and approved by the Academic Council of SNAU (Protocol № 5, dated 29.12.2022).

We recommend using the materials of the dissertation work when studying the courses "Veterinary microbiology", "Veterinary immunology" for masters of the Faculty of Veterinary Medicine of Sumy NAU.

And for the courses "Veterinary microbiology" and "Veterinary immunology" for masters of the Henan Institute of Science and Technology (HIST).

Keywords: *S.* Pullorum, host-specific pathogen, bacterial culture identification, drug susceptibility test, *citE2*, interval sequence, multiplex PCR, sensititivity and specificity, *steE*, HD-11 cells, chicken, virulence, colonization, inflammatory response, Th1/Th2 cytokines, STAT3/SOCS3, NF-κB P65.

АНОТАЦІЯ

*Zhike Liu. «*Конструкція мультиплексного ПЛР-тесту на основі гену CITE2 для ідентифікації *Salmonella pullorum* та її ефектора в патогенності та імунітеті». − Кваліфікаційна наукова праця на правах рукопису.

Дисертація на здобуття наукового ступеня доктора філософії за спеціальністю 211 «Ветеринарна медицина». − Сумський національний аграрний університет, м. Суми.

Дисертаційна робота присвячена розробці та науковому обґрунтуванню профілактики та точного виявлення *S. Pullorum*. У роботі був з'ясований механізм персистуючої інфекції *S. Pullorum* у курей. Виявилося, що *S. Pullorum* є специфічним патогеном, який спричиняє значні економічні втрати на фермах, а також може викликати запальну реакцію у курей. Тому швидкий і точний метод може допомогти розробити відповідні заходи профілактики та контролю в клінічних зразках і продукції птахівництва. Крім того, ефектори *S. Pullorum* з протизапальною функцією можуть бути унікальними для лікування сальмонельозу.

Були проведені дослідження для підтвердження виду патогенної бактерії та її чутливості до препаратів, яка викликає важку діарею (пуллорум) і системні смертельні захворювання у курей. Також була зроблена ідентифікація та тест на чутливість до препарату *S. Pullorum* у курей з великих пташиних ферм.

Відповідно тест на чутливість до лікарських засобів підтвердив, що виділені *S. Pullorum* були стійкими до амоксициліну, сульфаметазину, тетрацикліну та *іпрофлоксацину*, але чутливі до цефтріаксону, цефтіофуру та канаміцину.

Ген *citE2* та інтервальна послідовність гена SPS4_00301-SPS4_00311 існували у всіх сероварах *Salmonella*, але ділянки відмінності в *citE2* були виявлені лише у *S. Pullorum*. Така розроблена система мультиплексної ПЛР на основі двох молекулярних маркерів може досягати 6,25 pg/μL і 10^4 CFU/mL

для геномної ДНК та клітин *S.Pullorum*. А розроблений мультиплексний ПЛР аналіз дозволив виділити *S. Pullorum* у 33 різних серотипах *Salmonella* та 13 нецільових видів.

Дослідження проб з яєць, штучно контамінованих *S. Pullorum*, *S. Enteritidis* і природно забруднених 69 зразків анальних мазків, показали аналогічні результати.

Штам секреції III типу, кодованої *steE* вірулентної *S. Pullorum* та делецією *steE S.* Pullorum (Δ *steE*), був побудований за допомогою рекомбінаційної системи λ-Red 3. Також був проведений аналіз *in vitro* та *in vivo* з використанням клітин HD-11 і курей, інфікованих диким типом *S.Pullorum* (WT) та Δ *steE* . Таким чином, результати аналізу вірулентності показали, що LD_{50} був у 22,8 рази вищий у штаму ΔsteE, ніж штаму WT. Експеримент же з колонізації бактерій показав, що загальна тенденція зміни кількості штамів WT і Δ *steE* була аналогічною в курячій печінці, селезінці, серці, бурсі та сліпій кишці, які спочатку збільшувалися, а потім зменшувалися. Тому, порівняно з штамом WT, Δ *steE* штам зменшив інвазію та проліферацію бактерій в інфікованих клітинах HD-11.

Крім того, ми проаналізували рівні експресії мРНК ефекторних генів і цитокінів методом qRT-PCR, який SteE асоціювався з регуляцією різних ефекторних генів і запальних цитокінів у клітинах HD-11 при інфікуванні *S. Pullorum*. Порівняно з групою, яка була інфікована штамом WT або Δ *steE* + *steE*, рівні транскриптів мРНК *IL-12* та *IFN-γ* виявилися значно вищими, тоді як *IL-10* експресія мРНК була значно знижена в печінці та бурсі, що інфікована штамом Δ *steE*, Експресія мРНК *IL-4* показала різке зниження рівня транскрипції в штамі Δ*steE* у селезінці, сліпій кишці та серці, а експресія мРНК *IL-10* була значно нижчою в селезінці та сліпій кишці, що інфіковані штамом Δ *steE*. У курчат, заражених штамом Δ *steE* , виявилися незначні патологічні ураження в печінці та гістопатологічні ураження селезінки порівняно з аналогічними у WT.

Для того, щоб з’ясувати механізм, за допомогою якого регулятори *steE*

Th1/Th2 викликають експресію цитокінів при інфікуванні *S. Pullorum*, використовували *S. Pullorum* як модельний патоген для оцінки ролі *steE* у запаленні, який викликала *Salmonella*. Ми продемонстрували як *steE* зменшує експресію Th1-пов'язаних цитокінів (*IFN-γ* та *IL-12*) і сприяє експресії Th2-споріднених цитокінів (*IL-4* та *IL-10*) у клітинах HD-11 та куриних моделях інфекції *S. Pullorum*, а сайленсінг SOCS3 пригнічував функцію *steE* в клітинах HD-11, що призводило до дисбалансу Th1/Th2-пов'язаних цитокінів. Відповідно *SteE* сприяв експресії SOCS3 шляхом активації STAT3 у клітинах HD-11. Крім того, *steE* інгібував експресію NF-B P65 і блокував її транслокацію до ядра шляхом сприяння експресії SOCS3.

Таким чином, комбіноване застосування ідентифікації бактеріальної культури, аналіз тесту на чутливість до препарату та розробка мультиплексної системи ПЛР може точно визначити поширення, лікарську стійкість та виявлення S. *Pullorum*, забезпечити підтримку даних і цінний інструмент для знищення сальмонельозу. А також steE підсилює стійку інфекцію та вірулентність *S. Pullorum*, регулюючи реакцію запалення у випадку інфекції *S. Pullorum*.

Отже, наші результати вперше показали, що steE регулює експресію цитокінів Th1/Th2 за допомогою модуляції осі STAT3/SOCS3 і NF-κB, яка може бути пов'язана з диференціацією клітин Th1/Th2 і, відповідно, може бути розроблена нова терапевтична стратегія проти сальмонельозу.

За матеріалами дисертації розроблено та затверджено Вченою радою СНАУ методичні рекомендації «**Побудова мультиплексного ПЛР-тесту на основі гена *citE2* для ідентифікації *Salmonella* Pullorum та його ефектора SteE у патогенності та імунітеті» (протокол № 5 від 29.12.2022**), у яких було рекомендовано використовувати матеріали дисертаційної роботи під час вивчення курсів «Ветеринарна мікробіологія», «Ветеринарна імунологія» для магістрів факультету ветеринарної медицини Сумського національного аграрного університету та магістрів Хенанського інституту науки і технологій (HIST).

Ключові слова: *S. Pullorum*, специфічний збудник, ідентифікація бактеріальної культури, тест на чутливість до препаратів, *citE2*, інтервальна послідовність, мультиплексна ПЛР, чутливість і специфічність, *steE* , клітини HD-11, кури, вірулентність, колонізація, запальна реакція, цитокіни Th1/Th2, STAT3/SOCS3, NF-κB P65.

LIST OF WORKS PUBLISHED ON THE THEME OF THE DISSERTATION

Scientific works in which the main scientific results of the dissertation are published:

Articles in scientific professional publications of Ukraine

1. **Zhike, L.,** Fotina, T., Petrov, R., Klishchova, Z., & Fotin, A. (2021). Isolation, identification and analysis of drug resistance of *Salmonella* Pullorum. Ukrainian Journal of Veterinary and Agricultural Sciences, 4(1), 33-38. https://doi.org/10.32718/ujvas4-1.07. https://ujvas.com.ua/index.php/journal/article/view/79 (The applicant participated in research, analysis of the results and writing the article).

2. **Liu, Z.,** Fotina, T. I., Petrov, R. V., Fotin, A. I., & Ma, J. (2022). Construction and characterization of *steE* deletion mutant of *Salmonella* Pullorum. Bulletin of Sumy National Agrarian University. The Series: Veterinary Medicine, 2(57), 9-15. https://doi.org/10.32845/bsnau.vet. 2022.2.2. https://www.snaubulletin.com.ua/index.php/vm/article /view/665. (The applicant participated in research, analysis of the results and writing the article).

3. **Liu, Z.,** Fotin, A., Petrov, R., Ma, J., & Fotina, T. (2023). SteE enhances the colonization of *Salmonella* Pullorum in chickens. Ukrainian Journal of Veterinary and Agricultural Sciences, 6(1), 45-50. https://doi.org/10.32718/ujvas6-1.07. https://ujvas.com.ua/index.php/journal/article/view/145 (The applicant participated in research, analysis of the results and writing the article).

Articles in scopus journals

4. **Liu, Z.,** Yu, Y., Fotina, T., Petrov, R., Klishchova, Z., Fotin, A., Ma, J. (2022). Multiplex PCR assay based on the *citE2* gene and intergenic sequence for

the rapid detection of *Salmonella* Pullorum in chickens. Poult Sci, 101(8), 101981. doi: 10.1016/j.psj.2022.101981. https://www.ncbi.nlm.nih.gov/pmc/articles/PMC9264022/pdf/main.pdf. (The applicant participated in research, analysis of the results and writing the article).

5. **Liu, Z.,** Wang, L., Yu, Y., Fotin, A., Wang, Q., Gao, P., Zhang, Y., Fotina, T., & Ma, J. (2022). SteE enhances the virulence of *Salmonella* Pullorum in chickens by regulating the inflammation response. Front Vet Sci, 9, 926505. doi: 10.3389/fvets.2022.926505. https://www.ncbi.nlm .nih.gov/pmc/articles/PMC9330158/pdf/fvets-09-926505.pdf. (The applicant participated in research, analysis of the results and writing the article).

Theses of scientific reports

6. **Liu, Z.,** Fotina T., Petrov R., Kleshova J. (2021). Isolation, identification and drug resistance analysis of *Salmonella* Pullorum. BTRP Ukraine 2021 International BioThreat Reduction Symposium, (29 June - 2 July, 2021, Kyiv, Ukraine). (PhD participant in carrying out of experimental researches, processing of results, preparation of article for printing).

7. **Liu, Z.,** Yu, Y., Fotina, T., Petrov, R, Fotin, A., Ma, J. (2022). Multiplex PCR assay based on the *citE2* gene and intergenic sequence for the rapid detection of *Salmonella* Pullorum in chickens. Chinese Association of Animal Science and Veterinary Medicine, 2022 Academic Forum (14-16 August, 2022. Foshan, China). (PhD participant in carrying out of experimental researches, processing of results, preparation of article for printing).

8. **Liu, Z.,** Fotina, T., Fotin, A., Ma, J. (2022). *SteE* enhances the virulence of *Salmonella* Pullorum in chickens by regulating the inflammation response. Chinese Association of Animal Science and Veterinary Medicine, 2022 Academic Forum (14-16 August, 2022. Foshan, China). (PhD participant in carrying out of experimental researches, processing of results, preparation of article for printing).

9. **Liu, Z.,** Fotin, A., Fotina, T. (2023). The distribution of *Salmonella* Pullorum in different organs of chicken using in situ. The III Scientific and Practical

International Distance Conference «Microbiological and Immunological Research in Modern Medicine», (24 March, 2023, Kharkiv, Ukraine). (PhD participant in carrying out of experimental researches, processing of results, preparation of article for printing).

10. **Liu, Z.,** Fotin, A., Petrov, R., Fotina, T. (2023). SteE regulates Th1/Th2 cytokine expression in chickens during *Salmonella* Pullorum infection. The III Scientific and Practical International Distance Conference «Microbiological and Immunological Research in Modern Medicine», (24 March, 2023, Kharkiv, Ukraine). (PhD participant in carrying out of experimental researches, processing of results, preparation of article for printing).

11. **Liu, Z.,** Fotin, A., Ma, J., Tetiana Fotina. (2023). *Salmonella* Pullorum effector SteE regulates Th1/Th2 balance by triggering the STAT33/SOCS3 axis that suppresses NF-κB activation. The III Scientific and Practical International Distance Conference «Microbiological and Immunological Research in Modern Medicine», (24 March, 2023, Kharkiv, Ukraine). (PhD participant in carrying out of experimental researches, processing of results, preparation of article for printing).

12. **Liu, Z.,** Fotina, T. (2023). Construction and characterization of *steE* deletion mutant of *Salmonella* Pullorum. The XI International Scientific and Practical Conference «Problems of the development of science and the view of society», (21-24 March, 2023, Graz, Austria). (PhD participant in carrying out of experimental researches, processing of results, preparation of article for printing).

13. **Liu, Z.,** Tetiana Fotina, T. (2023). SteE induces the colonization of *Salmonella* Pullorum in chickens.The XI International Scientific and Practical Conference «Problems of the development of science and the view of society», (21-24 March, 2023, Graz, Austria). (PhD participant in carrying out of experimental researches, processing of results, preparation of article for printing).

14. **Liu, Z.,** Fotin, A., Tetiana Fotina. (2023). *Salmonella* Pullorum effector SteE inhibits NF-κB activity by STAT3-mediated upregulation of SOCS3. Chinese

Association of Animal Science and Veterinary Medicine, 2023 Academic Forum (12-15 May, 2023. Yangzhou, China). (PhD participant in carrying out of experimental researches, processing of results, preparation of article for printing).

CONTENT

LIST OF CONDITIONAL ABBREVIATIONS

APS - Ammonium persulphate

ATCC - American Type Culture Collection

BLAST - Basic Local Alignment Search Tool

BPW - buffered peptone water

BSA - Bovine serum albumin

CFU - Colony-forming unit

CI - Competitive index

CVCC - China Veterinary Culture Collection

DAPI - 4',6-diamidino-2-phenylindole

DDW - Double-distilled water

DMEM - Dulbecco's Modified Eagle Medium

dpi - Days post-infection

EDTA- Ethylene Diamine Tetraacetic Acid

HE - Hektoen enteric agar

hpi - Hour post-infection

IHC - Immunohistochemistry

JNK - Jun N-terminal kinase

LB - Luria-Bertani

LD_{50} - Half-lethal dose

LPS - lipopolysaccharide

LRR - Leucine-rich repeat

MAC - Macconkey agar

MOI - Multiplicity of infection

MR - Methyl red

NADPH - Nicotinamide adenine dinucleotide phosphate

NCBI - National Center for Biotechnology Information

NF-κB - Nuclear factor-κB

OD - Optical density

ONPG - O-Nitrophenyl-β-D-Galactopyranoside

PBS - Phosphate-buffered saline

PKN1 - Protein kinase N1

RNI - Reactive nitrogen intermediates

ROD - Region of difference

ROIs - Reactive oxygen intermediates

S. Dublin - *Salmonella* Dublin

S. Enteritidis - *Salmonella* Enteritidis

S. Gallinarum - *Salmonella* Gallinarum

S. Pullorum - *Salmonella* Pullorum

S. Typhimurium - *Salmonella* Typhimurium

SCV - *Salmonella*-containing vacuole

SOCS3 - Suppressors of cytokine signaling 3

SPI-1 - *Salmonella* pathogenic island 1

SPI-2 - *Salmonella* pathogenic island 2

SS - *Salmonella Shigella* agar

SS-*Salmonella–Shigella* Agar

STAT3 - Signal transducer and activator of transcription 3

T3SS - Type III secretion system

Th1 - T helper type 1

Th2 - T helper type 2

TNF-α- Tumor necrosis factor alpha

VP -Voges and Proskauer

XLD -Xylose lysine deoxycholate agar

INTRODUCTION

Justification of the choice of research topic. *S.* Pullorum is an important host-specific pathogen that causes white diarrhea with high mortality rates in chicken within 2-3 weeks old. Infected adult chicken present reproductive tract abnormalities without severe clinical symptoms, and can be transmitted vertically to offspring through ovary. *S.* Pullorum has been basically purified in developed countries, but it is still widely distributed in most developing countries, thereby causing serious economic losses to chicken farms. The current effective measures to the prevention and control of *S.* Pullorum that mainly to eliminate the diseased chickens with suspected *S.* Pullorum, monitor the healthy chickens, and cut off the route of transmission. However, there is still a lack of related epidemiologic data of *S.* Pullorum, which is the first step of formulating effective control strategies. Therefore, a rapid and accurate method is urgently needed to identify *S.* Pullorum and help us make corresponding prevention and control measures.

Persistent *Salmonella* infection establishes an infection-permissive state by regulating host inflammatory response. More and more evidence showed that *Salmonella* can escape the host immune system via special effectors, thereby enhancing its intracellular survival and growth. SteE as an anti-inflammatory effector is involved to the system infection of *Salmonella*. However, the mechanism which *steE* regulates inflammatory response and enhances the persistent infection of *S.* Pullorum remains elusive.

Therefore, the purpose of this experiment is to reveal the main pathogenic bacteria species from the diseased chickens with suspected *S.* Pullorum and its drug susceptibility, establish a multiplex PCR method for the accurate detection of *S.* Pullorum, and clarify the mechanism via which *steE* inhibits the host inflammatory response in the case of *Salmonella* infection. So as to provide a scientific theoretical evidence for the prevention and treatment of *S.* Pullorum, and could be a novel therapeutic strategy against salmonellosis in chicken farms.

Relationship with academic programs, plans, themes. Work carried out in according with the main directions of scientific research of the National Natural Science Foundation of China-Henan Joint Fund (Grant Number U1904117), Key Science and Technology Program of Henan Province (Grant Number: 21210210100 and 212102110009), Sumy National Agrarian University and Henan Institute of Science and Technology within the framework of scientific programs of research work. The materials of the dissertation work are part of comprehensive scientific research of the Department of Veterinary Expertise, Microbiology, Zoohygiene and Safety and Quality of Livestock Products of the Sumy National Agrarian University according to the following thematic plans of research works: "System of monitoring methods of control and veterinary and sanitary measures, regarding the quality and safety of livestock products in diseases of infectious etiology" (state registration No. 0114U005551, 2014-2019); "Forecasting the risks of cross-border introduction and spread of particularly dangerous animal diseases and the development of scientifically based disinfection systems based on innovative import-substitutable highly effective means" (state registration No. 0115U001342, 2018-2023).

The purpose and objectives of the study. To accurately isolate *S.* Pullorum from the diseased chickens with suspected *S.* Pullorum and analyze its drug susceptibility, and to establish a multiplex PCR approach for the early diagnosis of *S.* Pullorum in clinical samples. Finally, the roles of *S.* Pullorum effector SteE in pathogenicity and immunity were analyzed, as well as the mechanism by which *steE* regulates host inflammation responses in chickens, which laying a foundation to develop attenuated *S.* Pullorum vaccine, it could be a novel therapeutic strategy for salmonellosis in chickens.

For the purpose were assigned the following tasks. The purpose of the dissertation work is that development and scientific justification of the prevention and accurate detection of *S.* Pullorum, and clarify the mechanism of persistent *S.* Pullorum infection in chickens. In order to achieve the main research goal, it was necessary to solve a number of interrelated tasks:

1. Confirm the pathogen of the diseased chickens with suspected *S*. Pullorum, and its drug susceptibility test.

2. Establish a multiplex PCR method by targeting the region of difference of *citE2* and intergenic sequence f the accurate and rapid detection of *S*. Pullorum.

3. The analysis of the association of the T3SS2 effector SteE with *S*. Pullorum virulence.

4. Evaluate the role of *steE* in *S*. Pullorum-induced inflammation, and clarify the molecular mechanism of persistent *S*. Pullorum infection in chickens.

Object of study – The main pathogenic bacteria of pullorum disease and its drug susceptibility, the rapid and sensitive multiplex PCR method of *S*. Pullorum, the role of *steE* on the pathogenicity of *S*. Pullorum, clarify the mechanism of *steE* regulates the balance of Th1/Th2-related cytokines.

Subject of study – The diseased chickens with suspected *S*. Pullorum, the *citE2* gene and intergenic sequence of *S*. Pullorum, the multiplex PCR method, the effects of *steE* on the virulence of *S*. Pullorum, the role of the regulatory network of *steE*, STAT3/SOCS3, and NF-κB pathways in *S*. Pullorum-induced Th1/Th2 balance.

Research methods – The microbiological method (isolation and purification, biochemical identification), drug susceptibility test, PCR, analysis of clinical symptoms and autopsy, λ-Red recombination system, prokaryotic expression vector method, transfection, flow cytometry, histopathology method, immunofluorescence staining, immunohistochemistry, qRT-PCR, western blotting, statistical analysis.

Scientific novelty of the obtained results. This thesis established the theoretical basis of prevention and treatment of *S*. Pullorum in chickens. This is the first multiplex PCR method based on the *citE2* gene and the intergenic sequence of SPS4_00301–SPS4_00311 was established for the accurate detection of *S*. Pullorum in clinical and food samples. Confirmed the pathogenicity associated with *steE* in *Salmonella* Pullorum. These results dissecting the molecular mechanism of *steE* in regulated the balance of Th1/Th2 cytokines during *S*.

Pullorum infection for the first time.

The practical significance of the results. Based on the results of theoretical and experimental studies provide a scientific reference for the prevention and accurate detection of *S.* Pullorum in chicken farmers. The developed multiplex PCR system had high sensitivity and specificity, and could be a valuable tool for the clinical diagnosis of *S.* Pullorum, which is an important pathogen in chickens. In addition, *steE* was associated with the persistent infection of *S.* Pullorum, which modulated Th1/Th2-related immune responses by STAT3/SOCS3 and NF-κB axis and could be a unique drug candidate for targeting salmonellosis.

The main provisions of the PhD thesis were included in the guidelines according to prevention and detection of *Salmonella* and the mechanism via which *steE* inhibits the host inflammatory response by STAT3/SOCS3 and NF-κB axis, approved by the Academic Council of SNAU (Protocol № 5, dated 29.12.2019).

The dissertanion materials are included in the syllabus, work program of courses "Veterinary microbiology", "Veterinary medicine" for masters of the Faculty of Veterinary Medicine of Sumy National Agrarian University, and are used in distance learning of students based on the platform «Moodle».

And for the courses "Veterinary microbiology" and "Veterinary medicine" for masters of the Henan Institute of Science and Technology (HIST).

Personal contribution of PhD. The author took part in the implementation of scientific programs based on PhD thesis, and conceived and designined experiments. Setting objectives, discussing the results, forming conclusions were conducted together with tutors. PhD student analyzed the data as well as interpretation of the data on the topic of the dissertation, and conducted experimental research using modern methods and softwares with co-authors of scientific papers. The applicant wrote dissertation and published articles in wich the main material of the PhD thesis. The author thanks all participants in the manuscript for kindly help.

Testing the results of the thesis. The main provisions of the dissertation were reported and discussed and approved at a meeting of: BTRP Ukraine 2021

International BioThreat Reduction Symposium, (29 June - 2 July, 2021, Kyiv, Ukraine); Chinese Association of Animal Science and Veterinary Medicine, 2022 Academic Forum (14-16 August, 2022. Foshan, China); The III Scientific and Practical International Distance Conference «Microbiological and Immunological Research in Modern Medicine», (March 24, 2023, Kharkiv, Ukraine); The XI International Scientific and Practical Conference «Problems of the development of science and the view of society», (March 21-24, 2023, Graz, Austria); Chinese Association of Animal Science and Veterinary Medicine, 2023 Academic Forum (12-15 May, 2023. Yangzhou, China).

Publications. According to the results of research, 14 scientific papers were published, including: 3 articles in professional editions of Ukraine, 2 articles in Web of Science or Scopus scientific-metric publication, and 9 abstracts of reports at scientific and practical international conferences.

Structure and scope of the thesis. The dissertation is set out on 133 pages of computer text. It consists of an annotation, introduction, 4 chapters, conclusions, a list of sources used and 2 annexes. The main body of the dissertation contains 7 tables, 45 figures. The list of references includes the name of 294 sources.

CHAPTER 1

LITERATURE REVIEW ON THE TOPIC AND CHOICE OF RESEARCH DIRECTIONS

1.1 Overview of persistent *Salmonella* infection

Salmonella is an important intracellular pathogen and can cause a severe systemic disease, such as typhoid fever in humans, diarrhea in chickens, paratyphoid fever in pigs and cattle [1, 2]. *Salmonella* enters the digestive tract by the oral infection of contaminated food [3]. Once *Salmonella* reach the small intestine and colon, a large number of *Salmonella* attach to the intestinal mucosal epithelial cells, invade the submucosal tissue through the M cells, and then engulfed by immune cells like dendritic cells, macrophages and neutrophils, which can help the spread of *Salmonella* to systemic tissues, such as liver and spleen [4, 5, 6]. In addition, *Salmonella* has flagellin and lipopolysaccharide (LPS) on the surface of bacteria [7]. At the same time, it also has a variety of effectors that are secreted into host cells though the type III secretion systems (T3SSs), and control different cellular functions to maintain a infection-permissive state [8]. These effectors of *Salmonella* interfere with cell signaling cascades through a variety of mechanisms, and enhanced their intracellular proliferation and survival in host cells [9]. NF-κB pathway is an important signaling pathway that affects the host immune response in *Salmonella* infection [10]. This article reviews the mechanism of *Salmonella* infection based on the latest research results about the interplay of *Salmonella* effectors and NF-κB signaling pathway, and will provide new ideas for the pathogenesis of *Salmonella*.

1.2 Detection of persistent *Salmonella* infection

At present, the traditional serological detection of *Salmonella* identifies O and H antigens by agglutination reaction between the specific antibody and *Salmonella* granular antigen, and the serotype of *Salmonella* is determined in accordance with

the White–Kauffmann–Le Minor scheme [11]. Additionally, *S.* Pullorum has no motility and has the same O antigen in etiology [12], and ornithine decarboxylation is only the main difference in biochemical characteristics [13]. Normally, these methods are time-consuming, laborious, and ineffective in distinguishing some serotypes or biotypes of *Salmonella* especially *S.* Pullorum. However, DNA-based molecular techniques that have already been developed for *Salmonella*, such as PCR [14], multiplex oligonucleotide ligation-PCR [15], solid-phase PCR [16], loop-mediated isothermal amplification combined with lateral flow dipstick [17, 18], repetitive sequence-based PCR [19], and PCR-restriction fragment length polymorphism [20], PCR-high-resolution melting analysis [21]. In addition, enterobacterial repeated intergenic consensus-PCR is also used to identify the serotypes of *S.* Pullorum/Gallinarum [22]. The main bottlenecks of the conventional PCR detection of *S.* Pullorum are due to serotypes of *Salmonella* and production of false-negative results. Given the inherent limitations of these methods, the combination of a variety of diagnostic techniques, repeated operation, and high cost are often needed to obtain results in a timely fashion. Thus, the conventional PCR method is not suitable for the routine clinical diagnosis of *Salmonella*. By contrast, the developed multiplex PCR method constitutes a highly efficient, systematic, economical, and simple tool for the detection of *Salmonella* species [23, 24].

1.3 Persistent *Salmonella* infection in animal hosts

Persistent infection of *Salmonella* is the most common foodborne bacterial pathogen in a wide range of animals, including poultry and domestic animals and domestic pets [25, 26]. These poultry and livestock are usually the source of foodborne outbreaks of non-typhoid *Salmonella* [27]. Poultry is one of the most important hosts of various *Salmonella* serotypes, and can be infected by host-specific *Salmonella* [28]. However, *S.* Pullorum can cause systemic diseases or prolonged carriage of this pathogen without clinical symptoms to adult chicken [29]. There are more than 20 *Salmonella* serotypes associated with poultry [30].

The most common serotypes are *S*. Pullorum, *S*. Typhimurium and *S*. Enteritidis. Research shows that *S*. Pullorum can continuously infect macrophages in chicken spleen and intestine [31].

1.3.1 *Salmonella* infection process

Salmonella is classically intracellular pathogen, which can lead to serious disease after infecting animals [32]. *Salmonella* has a strong viability, but the optimum temperature of *Salmonella* replication is 37 °C [33]. *Salmonella* mainly causes human poisoning and even death disseminated by animal food sources such as poultry meat, eggs, milk, and dairy products [34, 35]. It is generally believed that *Salmonella* infection caused endotoxin release by the synergy of a large number of live bacteria [36]. The mechanism of *Salmonella* pathogenicity is briefly described as follows: First, *Salmonella* contaminates the food, replicates in the contaminated food, and then host being ingested with contaminated food through the oral route [4]. After *Salmonella* reach the small intestine and colon, a large number of *Salmonella* attach to the intestinal mucosal epithelial cells, and invade the submucosal tissue through the M cells or intestinal mucosal epithelial cells that lead to the inflammatory responses. Subsequently, *Salmonella* is engulfed by macrophages or subcutaneous lymphoid tissue that can rapidly replicate and propagates within host cells by T3SS2 [5]. Ultimately, *Salmonella* enter the blood circulation through the lymphatic system, and causes systemic infection (Fig. 1.1).

Salmonella can invade the intestinal mucosal barrier and release toxins inside the target cells to gain the purpose of infecting cells [37]. At present, there are different reports about the way of *S*. Enteritidis-infected cells [38, 39, 40]. Some studies have shown that dendritic cells can open the tight connection between cells, and directly swallow *S*. Enteritidis from the surface of intestinal mucosa [4, 41]. When bacteria invade cells, it firstly inserted the host cell cytoplasm, and then combined with actin to rearrange the cytoskeleton, so as to facilitate promote intracellular survival of *Salmonella* [42]. After *Salmonella* Enteritidis attaches to intestinal epithelial cells, and then form *Salmonella*-containing vacuoles within the cytoplasm [43]. The mature of *Salmonella* vesicles will be transported to the Golgi

body and located around the nucleus, and begin to replicate in the *Salmonella* vesicles [44]. At this stage, a tubular vesicle structure of *Salmonella* can be formed, which is called *Salmonella*-induced microfilament [45]. Most of the infected *Salmonella* still remain in the intestinal macrophages and stimulates the inflammatory response of the host, lead to diarrhea and decreased animal immunity [46]. *Salmonella* can disseminate from intestine to the liver, spleen and even all tissues of the host through the circulation of blood and lymph system [47].

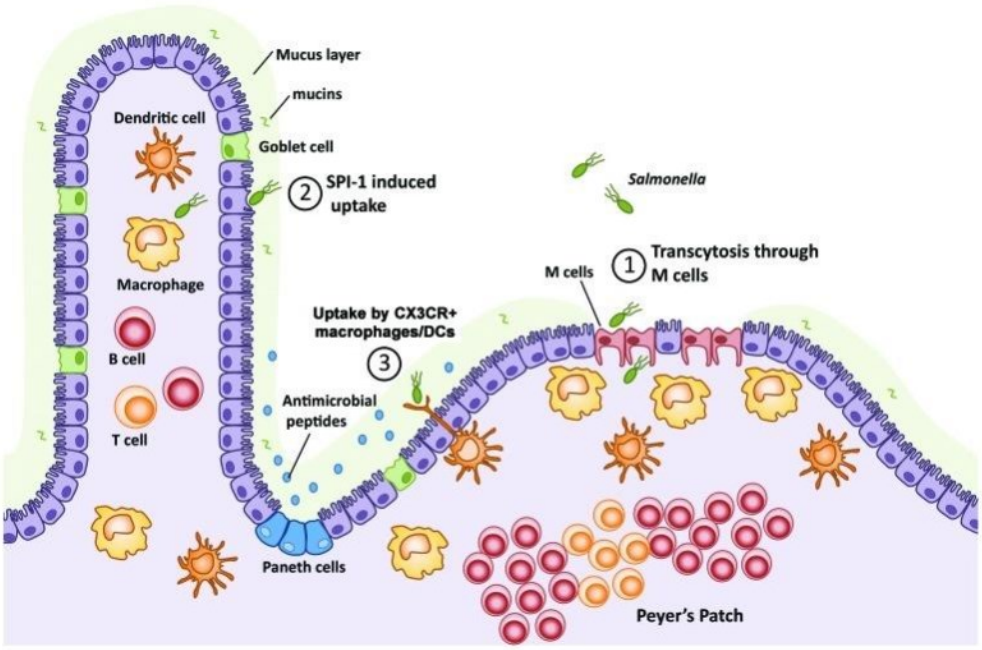

Fig. 1.1. Schematic representation shows the different routes of *Salmonella* invades the intestinal mucosa [4].

(1) The major pathway of invasion is macropinocytosis through M cells at the Peyer's patches; (2) Another route of invasion is to directly invade the intestinal epithelial cells surrounding the M cells; (3) This additional route of invasion requires the injection of *Salmonella* effector proteins by theT3SS1 that induce cell invasion.

1.3.2 *Salmonella* Type III secretion system and effectors

The key step of *Salmonella* infection is to invade intestinal epithelial cells [48]. This intracellular environment is conducive to escape the host's immune response [49]. The pathogenicity of *Salmonella* is mainly related to the *Salmonella* pathogenicity islands (SPIs), which can regulate and secrete virulence factors [50].

Among the SPI1-5, the type III secretory system (T3SS) encoded by SPI1 and SPI2 are closely related to bacterial pathogenicity, and can inject some effector proteins into the host cell cytoplasm, lead to increase *Salmonella* survives and replicates in host cells [51].

The device of *Salmonella* type III secretion system is similar to the needle-shaped supramolecular structure, which is composed of two distinct structural domains, a needle-shaped structure protruding from the surface of the cell and a cylindrical base anchored on the inner and outer membrane structure [52]. The T3SSs may be used as a bridge between the bacteria and the host cells, so that the effectors can be translocated into the host cells [8]. The secretory signal of effectors comes from both T3SSs device and the coding region of the N-terminal gene from the flagella specific secretory device [53]. *Salmonella* T3SSs can release a variety of effector proteins, and stimulate the signal transduction pathway of host cells, lead to a series of cellular effects such as the rearrangement of cytoskeleton, activation of transcription factors, and stimulation of ion channels [54]. This delicate process is regulated by an unusually complex transcription mechanism and post-transcription mechanism [55]. This regulatory mechanism is mainly limited by time (growth stage) and space (inside and outside of host cell), and this function of T3SSs must also be performed by the secretion and transfer of effectors [56].

The genome size of *Salmonella* is similar to that of *Escherichia coli*, with only 10% difference in sequence [57]. The virulence factors of *Salmonella* pathogenicity are mainly located on its pathogenicity island [58]. The intracellular survival and proliferation of *Salmonella* rely on the T3SS effectors encoded by SPI-1 and SPI-2, which can inject some effector proteins into the cytoplasm to promote *Salmonella* invasion and dissemination [59]. However, *Salmonella* T3SS effectors can stimulate the signal transduction pathways of host cells, leading to a series of cellular effects such as the rearrangement of cytoskeleton, activation of transcription factors, and stimulation of ion channels *in vivo* and *in vitro* [8, 60]. These effectors expression of SPI-1 and SPI-2 are strictly regulated in host cells and are essential for assembled T3SS at different infection phases [8].

1.4 Location of persistent *Salmonella* infection

The persistent infection of *Salmonella* is required to establish extraintestinal infection in a specific location of host [61]. Invasive *Salmonella* can enter into the gallbladder, the biliary tract and gallbladder, which are the main persistent infection location of *S.* Typhimurium [62]. As mentioned above, gallstones and chronic inflammation of the gallbladder (cholecystitis) are conducive to the persistent infection of *Salmonella* [63]. About 90% of chronic infection carriers have gallstones [64]. Some reports show that *Salmonella* can adhere to cholesterol and form biofilm, and cholesterol is the main component of gallstones [65]. In the acute phase of the disease, *S.* Typhimurium within macrophages can spread to all tissues of the host [66]. The infection of biliary tract and gallbladder may be caused by liver transmission. In the model of chronic infection *in vivo*, the main location of long-term pathogen persistence was gallbladder cavity and epithelial tissue during *S.* Typhimurium infection [67]. Due to numerous *Salmonella* serotypes, different serotypes have different infection patterns, and the genetic differences of various hosts are large, so the infection mechanism of *Salmonella* may also have great differences [68]. For example, *S.* Typhimurium can persists exist in macrophage of mesentery; *S.* Dublin can persist exist in the gallbladder and then form biofilm; *S.* Pullorum can persist exist in the spleen and reproductive tract of poultry [69].

1.5 Genes associated with persistent *Salmonella* infection

In various animal models, some *Salmonella* virulence genes have been found to enhance the persistent infection of *Salmonella* [1]. The persistence of *Salmonella* requires the participation of multiple genes, which needs adapt to various environmental conditions of the host, including complex immune response and microbiota [70]. In particular, fimbriae and adhesin have a major role in the adhesion and colonization of *Salmonella* [71]. The study found that different fimbriae operons (*lpf*, *bcf*, *stb*, *stc*, *std* and *sth*) contribute to the persistent infection of *Salmonella* in the intestine of genetically resistant mice, while another group of

fimbriae operons (*stc*, *bcf* and *sth*) also contribute to the prolonged carriage of *Salmonella* [1]. However, OmpV, as an adhesin protein of *S*. Typhimurium play a vital role in the pathogenicity of *Salmonella* [72]. The two genes *shdA* and *ratB* carried by *S*. Typhimurium pathogenic island cs54, which contribute to the intestinal persistence of *Salmonella* in host cells [73]. Similarly, *Salmonella ratB* mutant has defects in the colonization of caecum in an avian host [74].

Hosts have evolved strategies to promote *Salmonella* survival and escape host immune response by resistance and tolerance [75]. Similarly, the adhesin (*misL*) encoded by SPI-3, and also contributes to the persistent infection and colonization of *S*. Typhimurium in the mouse intestine model [76]. At the same time, LPS has also been proved to be the key factor for the persistent infection of *S*. Typhimurium *in vivo* model [77]. Iron is an essential nutrient for the survival and metabolism of *Salmonella* [78]. *Salmonella* have also evolved a unique survival countermeasure to transport iron. The main iron metabolism-related proteins of *Salmonella* are transferrin receptor, bivalent metal ion transporter 1 and membrane iron transporter [79]. These three systems are necessary to *Salmonella* escape macrophage phagocytosis and establish persistent infection or asymptomatic carriage in mouse [80]. However, it is still unclear how the persistence of *Salmonella* in host cells through iron metabolism.

1.6 Host immune response and NF-κB signaling pathway

In order to cope with the infection of *Salmonella*, the host has formed various defense mechanisms such as innate immunity and adaptive immunity [81]. The innate immune system are initiated through a series of pattern recognition receptors, which recognize the relatively conservative and key structural components of pathogenic microorganisms, thereby control the invading pathogen [82]. Normally, pathogen-associated molecular patterns are usually composed of bacterial surface components, such as LPS, flagellin, peptidoglycan, lipoteichoic acid, and cell wall lipoproteins [83, 84]. Furthermore, the pattern recognition receptors of the innate immune responses were involved include Toll-like receptors

(TLR), nucleotide oligomerizaton domain-like receptor (NLR), cytoplasmic RNA receptors, and cytoplasmic DNA-related receptors [85]. NF-κB transcription factor is the regulatory center of host inflammatory response that controls DNA transcription [86]. NF-κB is a homo- and hetero- dimers in mammals whose subunit consists of five members, such as c-Rel, p50 (NF-κB1), RelA (p65), p52 (NF-κB2), and RelB [87]. These members contain the Rel homologous domain with conserved DNA binding activity, and have the ability to regulate the protein dimerization and nuclear localization signals. Inactivation of NF-κB and inhibition of IκB protein phosphorylation are located within the cytoplasm [88]. When host is infected by pathogenic bacteria such as *Salmonella*, and TLRs signaling pathways are activated, resulting in initiate antigen presentation functions, thereby the NF-κB dimers rapidly dissociates from the cytoplasm to the nucleus, which triggers the proinflammatory-related gene expression [7, 89]. However, some *Salmonella* effectors target NF-κB signaling pathway to facilitate *Salmonella* invasion and dissemination within host cells at different stages of infection.

1.7 Activation of NF-κB signaling pathway by effectors

There are many microorganisms in the intestines of humans and animals [90]. In order to avoid unnecessary immune reactions, the NF-κB signaling pathway is suppressed in intestinal cells [91]. Pathogens induce NF-κB activity through a variety of mechanisms, which is crucial to promote its intracellular replication and virulence in their host [92]. Inflammation aggravates the accumulation of nutrients to the growth of *Salmonella* at an early stage of infection [93]. Furthermore, numerous intracellular effectors can drive the host's immune response to produce the electron acceptor tetrathionate in the respiratory chain [94], which can enable *Salmonella* to more efficiently gain host nutrients when compared with other bacterial pathogens, leading to promote intracellular replication in the host [95].

TLR5 is a receptor for *Salmonella* flagella, which in turn activates MyD88-NF-κB signaling pathway, but some effectors can activate NF-κB signaling pathway by other some ways [96]. SipA is a virulent effector of *Salmonella*, and

translocated into the host cells by T3SS-1, which enables *Salmonella* invasion [97]. Studies have found that NF-κB activity is trigged by SipA that is not dependent on the invasion of *Salmonella*, but it is requires for complete T3SS [98]. Furthermore, the heterologous expression of SipA affects NF-κB activity, but this signal does not depend on MyD88. Conceivably, the intracellular SipA and intracellular receptor NOD1 form a complex that can activate NOD1/NOD2, which lead to the invasion of epithelial cells and NF-κB activity within host cells [99].

T3SS1-related effectors can induce activation of Rho-family GTPases such as Rac1 and Cdc42, and contribute to *Salmonella* internalization by activating Rac-1 and inflammation by activating Cdc42, respectively [100]. These two Rho GTP enzymes are components of the host signaling pathway and participate in the rearrangement of the actin cytoskeleton structure [101]. Several effectors, SopE, SopE2, and SopB within the SPI1 all are associated with the stimulating MAP kinase and NF-κB signaling pathway by activate Rho-family GTPases [102]. SopE and SopE2 are guanine nucleotide exchange factors of Rac1 and Cdc42 that induces rapid membrane ruffling in host cells, which promotes *Salmonella* invasion and systemic infection [103]. SopB is a phosphoinositide phosphatase and has the ability to activate the Rho-family GTPases, such as Rac1 and Cdc42 [104]. These three effectors are secreted into host cells by T3SS1 that is required for *Salmonella* invasion. Therefore, the activated Rho-family GTPase significantly increases detected by NOD1, and subsequent induces inflammatory responses by activating NOD1-RIP2-NF-κB signaling pathway in host cell [102]. Studies have found that intracellular SopE forms complexes with Rac1, Cdc42, NOD1, and heat shock protein 90, indicating that SopE-dependent Rac1 and Cdc42 activation is required for the proteasome-mediated pathway, which in turn activates NF-κB signaling pathway through NOD1 [105]. Therefore, this multi-factorial and multi-channel activation mechanism strongly ensures NF-κB activity that is central to the system infection of *Salmonella* [106]. This phenomenon indicates that the activation of the immune response is greatly beneficial to *Salmonella* invasion in the case of *S*. Pullorum infection. However, the underlying mechanism of these

effectors between innate immune signal and innate immune receptors remains obscure.

1.8 Inhibition of NF-κB signaling pathway by effectors

Although the activation of host inflammatory response plays an important role in resisting the invasion of *Salmonella*, some effectors are secreted into host cells by T3SSs that have the ability to inhibit excessive immune response. However, the specific mechanism by which *Salmonella* effectors interface with NF-κB signaling pathway remains poorly understood.

1.8.1 AvrA

AvrA is a virulent effector of *Salmonella* within SPI-1, and its code size is 33kDa [107]. AvrA has the activity of serine/threonine acetyltransferase and ubiquitin hydrolase, and play a pivotal role in suppression of host's innate immune response, thereby contribution to *Salmonella* dissemination and intracellular carriage [108]. AvrA decreases IκBα degradation and stabilizes β-catenin, and inhibit NF-κB activity through ubiquitin-proteasome degradation pathway *in vivo* and *in vitro* [109]. AvrA is a deubiquitinase that can inhibit MAPK activity by downregulating p-MEK/p-ERK in *Salmonella*-infected HeLa cells, leading to facilitate *Salmonella* invasion [110]. AvrA as a key regulator of immune responses, which can control both the inflammatory and apoptotic signaling in infected macrophages [111]. Studies have shown that the *avrA*-deficient strain increased apoptosis in caspase-3-stimulated cells [112].

1.8.2 SseL

SseL is one of the *Salmonella* effectors secreted through T3SS2, and has the activity of the deubiquitinase [113]. The function of effector SseL was performed by the two-component regulatory system SsrA/SsrB, and can induce cytotoxicity in infected macrophages [114]. However, SseL has no effect to the intracellular replication of *Salmonella* within *Salmonella*-containing vacuoles (SCV), but it participates in the regulation of cytotoxicity [115]. SseL inhibit NF-κB activity by deubiquitinating of IkBa in primary murine bone-marrow-derived macrophages,

but the following study proposed that SseL does not affect the degradation of IκBα and inflammatory response [116]. However, some *in vitro* experiments shown that SseL protein directly targets the K63-polyubiquitin chain in the host cell, and regulate the intracellular signal activation of host cells degraded by the ubiquitin proteasome pathway [117]. In addition, SseL also represents a member of the deubiquitinate, but the regulatory effect of this protein *in vivo* is not fully understood.

1.8.3 SptP

SptP is a GTPase activating protein encoded by T3SS1 [118], and inhibit NF-κB activity by limiting the activation of Rac1, Cdc42, and Rho in host cells [119]. The SptP translocation can interfere with the actin cytoskeleton reorganization and c-Jun N-terminal kinase (JNK) activation with the ability to inhibit MAP kinases, thus causing the secretion of pro-inflammatory factors [120, 121]. SptP can increase the function of host cytoskeleton to recover homeostasis by preventing the activation of Cdc42, and contribute to the intracellular replication and dissemination of *Salmonella* [122]. SptP is composed of two different effector protein regions, and the existence of the amino terminal domain of SptP protein makes it have the characteristics of activating target protein, while its carboxyl terminal domain endows the protein with potential tyrosine phosphatase activity [104]. Some studies showed that SptP protein exerts its tyrosine phosphatase activity when *Salmonella* entry into host cells, thus causing systemic infection [119].

1.8.4 SspH1

SspH1 is encoded by T3SS-1 and/or T3SS-2, and inhibits inflammatory reactions and NF-κB signaling pathway in the mammalian nucleus [123]. SspH1 has the activity of E3 ubiquitin ligase contains a leucine-rich repeat (LRR) [124]. It is well documented that serine/threonine protein kinase N1 (PKN1) is the physiological substrate of SspH1 [125]. Based on the structure of SspH1-PKN1 complex, LRR domain of SspH1 protein interacts with human PKN1 in mammalian cells 123]. It can form the catalytic domain of LRR and activate the

catalytic function of SspH1 protein [126]. Interestingly, SspH1 does not depend on its catalytic function to the inhibition of NF-κB signaling pathway. Even if it does not interact with PKN1, SspH1 still can inhibit NF-κB activity [124]. Therefore, except PKN1, SspH1 protein may also interact with other substrates with the ability to modulate host immune response. Later work suggested that SspH1-mediated degradation of PKN1 is not required for inhibiting NF-κB activation.

1.8.5. GogB

GogB is the first open reading frame on Gifsy-1 prophage of *S*. Typhimurium [127]. GogB is translocated into the cytoplasm of host cells by T3SS2, which are essential for cell-to-cell spread in *Salmonella* infection [74]. GogB is regulated by the transcription activating factor SsrB, which contributes to the virulence of *Salmonella* [128]. GogB is a chimeric protein with the characteristics of E3 ubiquitin linking enzyme and can inhibit degradation of IκBα [58]. GogB interacts with FBXO22 protein of F-box family in host cells, which is beneficial for synergy with other effectors [129]. More importantly, GogB can inhibit NF-κB activity by suppressing ubiquitination and degradation of IκBα in infected macrophages [58]. In addition, the *Salmonella gogB* mutant-infected mice will induce more inflammatory response, tissue damage, intestinal colonization and chronic infection than that in the wild-type *Salmonella* strain-infected group [129]. As one of the anti-inflammatory effector, GogB is required and is conducive to promote the colonization of *Salmonella* by limiting tissue damage during *Salmonella* infection.

1.8.6 SpvB and SpvC

Spv gene is an important pathogenic factor on the *Salmonella* virulence plasmid and secreted by T3SS2 [130]. *Spv* contains three essential genes: positive transcriptional regulation gene *spvR* and two structural genes (*spvB* and *spvC*) [131]. Like SpvC protein is encoded by *spvC* that have phosphothreonine lyase activity, which can dephosphorylates Erk (pErk), p38, and JNK, all of which contribute to inhibit pyroptosis and intestinal inflammation by interfering with the MAPK pathway during systemic infection [103]. In case of *Salmonella* infection,

both SpvB and SpvC were translocated into the cytoplasm of host cells by T3SS2 to promote *Salmonella* virulence, which can induce more cell apoptosis by depolymerizing actin [58]. During the transport of NADPH oxidase to cell membrane, NADPH oxidase was strongly associated with the function of actin cytoskeleton [132]. Therefore, SpvB-mediated depolymerization of actin may inhibit the recruitment of NADPH oxidase to phagosomes, leading to reduce the oxidative killing effect of *Salmonella*. Some studies have shown that SpvB and SpvC can prevent the synthesis of anti-apoptotic factors and induce macrophage apoptosis [58]. Surprisingly, the enzyme activity of SpvC decreases the expression of pro-inflammatory factors (IL-8 and TNF-α) and neutrophil infiltration at an early stage of infection [133]. Thereby, SpvC is required to *Salmonella* dissemination in the systemic infection. Recent evidence suggests that SpvC can also cooperate with SpvB to prevent the recruitment of NADPH oxidase to phagocytosis, promote cell apoptosis, block NF-κB activity and inhibit the differentiation of macrophages [58].

1.8.7 IpaJ

IpaJ as an invasive plasmid gene of *Shigella flexneri*, was initially identified and its code size is 27kDa [134]. However, IpaJ is a specific effector of *S.* Pullorum encoded by T3SS1 that can present fragmentation state to Golgi body, and can attenuate NF-κB activity induced by TNF-α, LPS and IL-1 in HeLa cells [135]. It has been suggested that the transcription of IpaJ is regulated by ItrA with a novel DeoR family regulator to inhibit MAPK activation in *Salmonella*-infected HeLa cells [136]. At the same time, IpaJ has the function to inhibit the activation of NF-κB signaling pathway by suppressing the ubiquitination degradation of IκBα during *Salmonella* infection [135]. In addition, the absence of *SPI-1* and *SPI-2* does not affect the protein expression of NF-κB p65 showed that IpaJ is not regulated by T3SS1 and T3SS2 [136].

1.8.8 Other effectors

Previous study reported that T3SS1 and/or T3SS2 effectors GtgA, GogA, and PipA all contain two histidine residues, and have metalloprotease activity to

control *Salmonella* replication [103]. These zinc metalloproteases redundantly target the NF-κB subunits p65, RelB, and c-Rel, whereas GogA and GtgA only inhibit NF-κB-dependent gene transcription [137]. T3SS2 effectors SseK1, SseK2, and SseK3 all are death domain-containing proteins with the characteristics of N-linked glycosyl transferase, which can inhibit NF-κB activity by suppressing the phosphorylation of IκBα in 293ET cells treated with TNF-α [58]. Among them, SseK1 and SseK3 also inhibit *Salmonella*-induced NF-κB activity in macrophages [138]. Another report showed that SseK3-mediated inhibition of NF-B signaling pathway is not required for the E3-ubiquitin ligase tripartite motif-containing protein 32 [139]. In addition, the SPI-2 T3SS effector SpvD inhibit NF-κB activity by preventing nuclear translocation of p65 through interactions with the Exportin-2, but it does not affect the degradation of IκBα, which finally lead to the system grow of *Salmonella* [140].

Salmonella interact with host cells by using T3SSs to inject some effectors into the host cells. These effectors, like SopE, SopE2, and SopB all trigger NF-κB signaling pathway by activating Rho family small G proteins, while SptP has the activity of GTPase activating protein that can inhibit activation of G proteins. However, activation of NF-κB signaling pathway by SipA needs the mediation of NOD1/NOD2. Some effectors, including SspH1, AvrA, IpaJ, and SseL all suppressed NF-κB activity by blocking IκBα degradation. Furthermore, the enzymatic activity of these effectors is closely associated with their function in the regulation of NF-κB signaling pathway during *Salmonella* infection. These results suggesting that both T3SS1- and T3SS2-encode these effectors are translocated into the host cell, and contribute to downregulation of the inflammatory response and the persistent infection of *Salmonella* by targeting NF-κB signaling pathway when *Salmonella* invade target cells (Fig. 1.2).

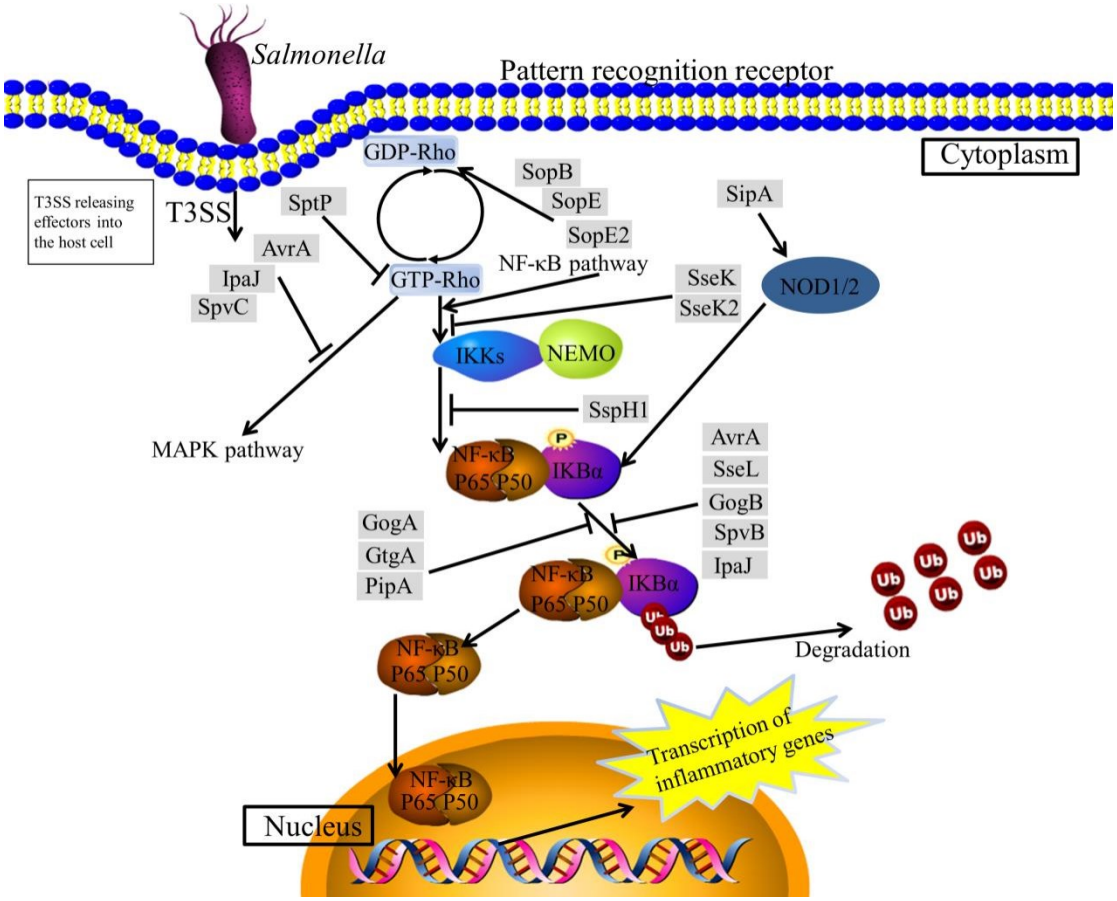

Fig. 1.2. *Salmonella* effectors regulate the NF-κB signaling pathway in host cells.

1.9 Resistance to cationic antimicrobial peptides

Cationic antimicrobial peptide is a positively charged polypeptide that exists in epithelial cells, bone marrow cells, neutrophils and macrophages [141]. It has a killing effect to the pathogenic bacteria, and is involved in innate immunity against various infections [142]. Pathogenic bacteria must resist these cationic antimicrobial peptides in order to cope with the attack of innate immunity [143]. Similar to the mechanism of antibiotic resistance, some pathogenic bacteria can change the surface structure of host cells to reduce the involvement of ionic peptides, code the transport system to discharge the involved cationic peptides, and even degrade the cationic antimicrobial peptides [144]. Macrophages and neutrophils can produce a variety of cationic antimicrobial peptides to kill the intracellular *Salmonella* [145]. *Salmonella* can change the structure of lipid A via

deacylation and palmitoylation [146]. On the one hand, *Salmonella* can decrease the negative charge of cell membrane to eliminate the involvement of cationic antimicrobial peptides. On the other hand, *Salmonella* can also attenuate the recognition of TLR-4, leading to reduce the inflammatory response [147].

1.10 *Salmonella* survives in macrophages

Macrophages are immune cells with diverse functions, which play an important role in the process of phagocytosis of pathogens and antigen presentation [148]. When the pathogen is swallowed by macrophages, the macrophage is activated to produce a variety of sterilization media, including oxidative killing mechanism (reactive oxygen species and reactive nitrogen intermediates) and non-oxidative killing mechanism (cationic antimicrobial peptides and lysosomal degradation) [149]. However, the *Salmonella* PhoP/PhoQ regulatory system can induce macrophage phagocytosis [150]. When *Salmonella* is swallowed by macrophages, it can replicate and survive within the SCV [151]. At least 20 effector proteins are translocated into the host cell cytoplasm through T3SS2 [152]. These effectors resisted various harmful environmental factors by regulating vacuoles and intracellular biochemical reactions, and promoted the survival and replication of *Salmonella* within the SCV in host cells [153]. *Salmonella* can survive in macrophages to avoid the phagocytic killing of neutrophils, because *Salmonella* has ability to resist the phagocytic killing of neutrophils.

1.10.1 *Salmonella* resistance to oxidative killing

Phagocytes undergo the oxidative burst catalyzed by NADPH oxidase after infection, and produce a large number of reactive oxygen intermediates (ROIs) such as superoxide anion radical and H_2O_2, which can be converted into strong oxidants and then quickly kill *Salmonella* [154]. However, *Salmonella* can rely on SPI-2 to escape host inflammatory response. In addition, *Salmonella* can use catalase, antioxidant protein and superoxide dismutase to resist the oxidative killing effect of ROI [155]. Reactive nitrogen intermediates (RNI) include nitric oxide and its derivatives such as nitrogen peroxide [156]. RNI can kill *Salmonella*

through a number of special mechanisms, such as causing DNA damage, preventing SPI-2 transcription, and inhibiting PhoP/PhoQ acid-resistant regulatory system 157]. However, *Salmonella* can also resist the damage of RNI used by NO_2 operating system and nitrate reductase [158].

1.10.2 *Salmonella* resistance to lysosomal degradation

The lysozyme contains a variety of hydrolases in the phagocyte [159]. Escaping lysozyme degradation is an important strategy for the survival of intracellular bacteria [160]. In fact, pathogens have evolved a variety of mechanisms to cope with the killing of phagocytes: blocking the phagocytosis of phagocytes, dissolve the vacuolar membrane and escape from cytoplasmic phagocytosis, prevent the fusion of phagosomes and lysosomes, resist the degradation of lysosomes [161]. Many studies have shown that *Salmonella* can prevent the fusion of SCV by protease and lysosome pathways [162, 163]. However, it has also been reported that SCV can fuse with lysosomes, which may be caused by different criteria for judging the fusion of phagosomes and lysosomes [163]. In fact, *Salmonella* has the ability to resist lysosomal degradation. Early studies showed that *Salmonella* can fuse with other phagosomes in macrophages to form wide phagosomes [164]. Compared with normal phagosomes, the wide phagosomes play the role in diluting the bactericidal medium [165]. The host cells need secrete more bactericidal media to kill the pathogens. Recently, Li and other researchers found that most SCVs contain only one bacterium in macrophages, which is due to the division of SCV [151, 97]. After *Salmonella* replication within the SCV, and then splits into multiple SCVs that this way is benefits for the intracellular survival of *Salmonella* [152]. This may be that the host cell is much more difficult to cope with multiple SCVs than that of a single SCV, because it needs to synthesize more bactericidal media. In addition, a bacterium occupying a single SCV will reduce the competition for nutrition, and can more effectively secrete some effectors into the host cell cytoplasm to the spread of *Salmonella* [166].

1.11 T cell response to the persistent infection of *Salmonella*

Different studies have shown that the chronic infection of various bacteria, viruses, parasites and other pathogens involves the conversion from T helper 1 (Th1) cells to T helper 2 (Th2) cells [167, 168, 169]. The establishment of persistent infection contributes to the activity of Th2 immune response. At the early stage of *Salmonella* infection, the strong Th1 and low Th2 immune response can inhibit the growth of the invading pathogen in host cell. This stage mainly induce the expression of TNF-α、 IL-12、 IFN-γ and IL-18, which is necessary for the host to control the growth of *Salmonella*. In the second stage of infection, the immune response of host tends to be Th2 immune responses, while the levels of Th1 immune responses are low, and finally restore the balance of Th1/Th2 responses [170]. This new balance is necessary to maintain the immune state and long-term pathogen persistence in host cells. Th2 cytokine (IL-10) inhibits the production of reactive oxygen, nitrogen, TNF-α, and IL-12 in activated macrophages. The increase of IL-10 expression level leads to the decrease of IFN-γ expression level that will affect the clearance of macrophage to *Salmonella*.

1.11.1 Th1 response

IFN-γ produced by T lymphocytes that is called Th1 response. Th1 cells can drive M1 classical polarization of macrophages induced by IFN-γ [171]. These cells can release a large number of pro-inflammatory cytokines (IL-12, IL-23 and TNF-α), reactive nitrogen intermediates and reactive oxygen intermediates, and the high expression of major histocompatibility complex class II and costimulatory molecules, which can carry out efficient antigen presentation and mediate bactericidal or tumor killing activities [172]. Importantly, M1 macrophages are part of the Th1 response, and can promote intracellular pathogen clearance [173]. Indeed, M1 macrophages can also drive the polarization and recruitment of Th1 cells induced by cytokines and chemokines (IL-12, CXCLi2 and CXCL10), and then amplify the Th1 immune response [174]. In addition, M1 macrophages change iron homeostasis by inhibiting iron transporters and inducing H-ferritin,

which is conducive to iron chelation and sterilization [175].

1.11.2 Th2 response

IL-4 and IL-10 are related to Th2 immune response. IL-4 will stimulate the production of antibodies [176]. IL-4 and IL-13 derived from Th2 cells that can directly affect the M2 polarization of macrophages such as worm infection [177]. The macrophages treated with IL-4 have low expression of IL-12 and high expression of IL-10, which have many characteristics of M2 macrophages, whereas M2 polarization are activated by Th2-related cytokines and contribute to tissue repair responses and remodeling [178]. At the same time, IL-4-activated macrophages can induce the expression of chemokine (CCL17, CCL22 and CCL24), and the corresponding chemokine receptors (CCR4 and CCR3), which were present on Treg cells, Th2 cells, eosinophils and basophils [179, 180]. Therefore, the release of these chemokines leads to the recruitment of corresponding cells. And, the recruitment of Th2 cells further amplifies the Th2 immune response. M2 macrophages promote the release of iron and cell proliferation by up-regulating iron transporter, down-regulating H-ferritin and heme oxygenase-1 [181]. The expression of folate receptor and folate uptake was also characteristics of M2 macrophages [182]. In general, M2 macrophages can limit inflammatory reaction and I type adaptive immunity, remove residues, promote angiogenesis, and tissue repair [183]. Therefore, the precise regulation of macrophage polarization is very important to maintain the health of the host.

1.12 Prospect

Host-*Salmonella* interactions are a very complex process during persistent infection. The host's immune system has the ability to identify and clear the pathogens, which manipulate cell signaling cascades through a variety of pattern recognition receptors to facilitate bacterial invasion and its intracellular replication. But, the genome of *S.* Pullorum is always evolving to long-term survive in host cells. However, there is still a lack of related epidemiologic data of *S.* Pullorum, which is the first step of formulating effective control strategies. Therefore, the

accurate and rapid method is significant for the prevention and control of *S.* Pullorum.

As known, pathogens escaped the elimination of the immune system and avoided causing excessive damage to the host, which were the two main elements for pathogens to maintain systemic infection. The activation or inhibition of NF-κB signaling pathway was involved by effectors associated with the initiation of the inflammatory response, which is beneficial to the persistent infection of *Salmonella*. As this review advances, the mechanism by which *Salmonella* induces host inflammatory responses by T3SSs-realted effectors are well clear now. In order to cope with the elimination of the host immune system, *Salmonella* mainly adopts the escape host attack rather than destroying the immune system. Of course, the reason is not determined by the unilateral factors of the pathogen for the persistent infection of *Salmonella*. These findings illustrated that *Salmonella* pathogenicity and its host immune defense are a process of dynamic balance within the host cells. When *Salmonella* invasion and the immune clearance of the host reach a balance state, *Salmonella* will cannot replication within the SCV. When the host immunity is low, chronic infection of *Salmonella* may become acute infection. But how *Salmonella* and its host reprogram this metabolic state to establish a long-term systemic infection remains obscure. In addition, various hosts have significant genetic differences, and their immune defense could also have great differences in *Salmonella* infection. Future studies also need to be illuminated the interplay between the different host and *Salmonella* effectors.

1.13 Conclusion in chapter 1

In summary, the main objective of this review shows that a rapid, simple, and accurate diagnosis method is of great significance for the epidemiological investigation and rapid clinical diagnosis of *S.* Pullorum. *Salmonella* have evolved complex strategy to evade host immune defense, and utilizes T3SSs to deliver some effectors into target cells by regulating NF-κB signaling pathway, so as to promote its survival and replication within host cells. In addition, persistent

infection of *Salmonella* modulate host immune response by the balance Th1/Th2 cells, which affect the polarization and function of macrophages. Altogether, *Salmonella* effectors and NF-κB signaling pathway can provide new ideas and countermeasures for the prevention and treatment of salmonellosis.

CHAPTER 2
OBJECTS AND METHODS

2.1 Research materials

The dissertation work is carried out in accordance with the programs of research work of Sumy National Agrarian University: "System of monitoring methods of control and veterinary and sanitary measures, regarding the quality and safety of livestock products in diseases of infectious etiology" (State registration No. 0114U005551, 2014-2019); "Forecasting the risks of cross-border introduction and spread of particularly dangerous animal diseases and the development of scientifically based disinfection systems based on innovative importsubstitutable highly effective means" (State registration No. 0115U001342, 2018-2023). The dissertation is a fragment of scientific programs of research work of the National Natural Science Foundation of China-Henan Joint Fund (Grant number U1904117), Key Science and Technology Program of Henan Province (Grant number 21210210100 and 212102110009). The work was carried out for the period from 2019 to 2023 at the departments of microbiologyof Sumy National Agrarian University. In addition, conduct relevant experimental research in Henan Institute of Science and Technology, Xinxiang, China.

The work was carried out for the period from 2019 to 2023 at the departments of veterinary examination, microbiology, zooghygiene and safety and quality of animal products, the department of epizootology and parazitology and the department of virology, pathanatomy and bird diseases of Sumy National Agrarian University. In addition, veterinary studies were conducted at Henan, China.

Object of study – The main pathogenic bacteria of pullorum disease and its drug susceptibility, the rapid and sensitive multiplex PCR method of *S.* Pullorum, the role of *steE* on the pathogenicity of *S.* Pullorum and host-pathogen interactions, clarify the mechanism of *steE* regulates the balance of Th1/Th2-related cytokines.

Subject of study – The diseased chickens with suspected *S.* Pullorum, the

citE2 gene and intergenic sequence of *S.* Pullorum, the multiplex PCR method, the effects of *steE* on the virulence of *S.* Pullorum, the role of the regulatory network of *steE*, STAT3/SOCS3, and NF-κB pathways in *S.* Pullorum-induced Th1/Th2 balance.

2.2 Research methods

During the study following methods were used: Isolation, purification and biochemical identification of bacteria, PCR, analysis of clinical symptoms and autopsy, drug susceptibility test, λ-Red recombination system, prokaryotic expression vector method, DNA and RNA extraction, construction of eukaryotic expression vector, plate agglutination test, transfection, flow cytometry, histopathology method, hematoxylin and eosin staining, immunofluorescence staining, immunohistochemistry, qRT-PCR, western blotting, statistical analysis.

Consumables – Gloves, syringes and needles, cotton wool, methyl alcohol, 6-well plates, 12-well plates, squirrel cage, disposable petri dishes, *Salmonella* biochemical identification tube (Haibo, China), TIANamp Bacteria DNAKit (Tiangen-Biotech, China), ES Taq MasterMix (No: RR902; TakaRa, China), pKD4, pKD46, pCP20, pBR322 and pBBR1MCS2-Tac-mCherry plasmids, TRIzol reagent (Invitrogen, USA), PrimeScript RT reagent Kit (TakaRa, China), SYBR Premix Ex Taq™ II (TakaRa, China), Dulbecco's Modified Eagle Medium (Hyclone, USA), Fetal bovine serum (Invigentech, USA), penicillin-streptomycin (Solarbio, China), *Xho*I and *Bam*HI (TakaRa, China), Lipofectamine™ 2000 reagent (Invitrogen, USA), Bovine serum albumin (Sangon Biotech, China), rabbit anti-phospho-P65 antibody (Cat# bs-0982R; Bioss, China), goat anti-rabbit IgG H & L/Alexa Fluor 594 (Cat# bs-0295G-AF594; Bioss, China), 4′-6-diamidino-2-phenylindole (DAPI), anti-phospho-p65 antibody (bs-0982R; Bioss, China), anti-P65 (Cat# bs-0465R; Bioss, China); anti-phospho-P65 (Cat# bs-0982R; Bioss, China), anti-SOCS3 (Cat# 14025-1-AP; Sanying, China), anti-STAT3 (Cat## 4904; Cell Signaling Technology, USA), anti-phospho-STAT3 (Cat# 9131; Cell Signaling

Technology, USA), anti-GAPDH (Cat# MB001H; Bioworld Technology, China), chemiluminescence reagent (Cat# P0018S; Beyotime Biotech, China).

Equipment. 1. Clean workbeanch (JinJing, China); 2. Gradient thermal cycler (PCR) (SensoQuest GmbH, Germany); 3. Spectrophotometer (BioDrop, England); 4. Biological safety cabinet (BIOBASE , China); 5. Incubator (BIOBASE , China); 6. Shaker (CIMO, China); 7. SPF isolator (KANGWAY MEDICAL, China); 8. Dehydrator (DANJIER, China); 9. Paraffin embedding machine (WHJJ, China); 10. Pathology slicer (Leica, Germany); 11. Imaging system (Nikon, Japan); 12. DM 3000 microscope (PHASE CONTRAST, Japan); 13. Laser confocal microscope (Zeiss GmbH, Germany); 14. Gel Image System (Tanon, China); 15. Luminescent image analyzer (Cytiva, Japan); 16. MicroPulser Electroporator (Bio-Rad, USA); 17. 0.1 cm electrode gap (Bio-Rad, USA); 18. Centrifuge (Eppendorf, Germany); Flow cytometry (BD, USA); 19. Nanopure water purifier (Millipore, USA); 20. Constant-temperature CO_2 incubator (RSBiotech, England); 21. Ultra low temperature freezer (Haier Biomedical, China); 22. QuantStudio 5 detector system (Thermo Scientific, Singapore).

Chemicals and solvents. 1. Methanol (HengXing, China); 2. Ethylene Diamine Tetraacetic Acid (MACKLIN , China); 3. TAE buffer (HengXing, China); 4. Ethanol (XinHua, China); 5. DMSO (Solarbio, China); 6. Bovine serum albumin (Solarbio, China); 7. Tris and Tris-Hcl (Solarbio, China); 8. *Salmonella Shigella* (SS) agar (Hopebio Biol-Technology, China); 9. Xylene (LingFeng, China); 10. Trisodium citrate and citric acid (Servicebio, China); 11. Spontaneouss fluorescence quenching reagent (Sangon Biotech, China); 12. Glycine and SDS (Sangon Biotech, China); 13. Trisodium citrate and Citric acid (Sangon Biotech, China); 14. Hektoen enteric (HE) agar (Hopebio Biol-Technology, China); 15. Drug sensitive tablets (ChiCheng, China); 16. Gram staining solution (Solarbio, China); 17. *S.* Pullorum/Gallinarum serum plate agglutination test polyvalent antigen (ZhongHai Biotech, China); 18. Macconkey (MAC) agar (Hopebio Biol-Technology, China); 19. M-broth medium (Hopebio Biol-Technology, China); 20.

Xylose lysine deoxycholatev (XLD) agar (Hopebio Biol-Technology, China); 21. Peptone; 22. Sodium chloride and Agar (Sangon Biotech, China); 23. Ampicillin (Sangon Biotech, China); 24. Kanamycin (Sangon Biotech, China); 25. Ammonium persulphate (APS) (Solarbio, China).

Solid LB medium: Weigh and took 1 g peptone, 0.5 g yeast, 1 g sodium chloride, 1.5 g agar using an electronic balance, added 100mL sterile distilled water and stirred evenly to dissolve, put it in a pressure cooker at 120 °C for 20 min, and waited until the temperature was reduced to 60 °C and took it out.

Liquid LB medium: Weigh and took 1 g peptone, 0.5 g yeast, 1 g sodium chloride using an electronic balance, added 200 mL sterile distilled water and stirred evenly to dissolve, put it in a pressure cooker at 120 °C for 20 min, and waited until the temperature was reduced to 60 °C and took it out.

100 mg/mL Ampicillin: Weigh and took 5 g Ampicillin using an electronic balance and added 20 mL deionized water, stirred to dissolve, diluted to 50 mL, and then filtered and removed bacteria using a 0.22 μm filter, subpackaged, and then stored -20 °C.

50 mg/mL Kanamycin: Weigh and took 2.5 g Ampicillin using an electronic balance and added 20 mL deionized water, stirred to dissolve, diluted to 50 mL, and then filtered and removed bacteria using a 0.22 μm filter, subpackaged, and then stored -20 °C.

Tris-Glycine Buffer: Weigh and took 3.02 g Tris, 18.8 g Glycine, and SDS 1.0 g using an electronic balance, added 800 mL deionized water, stirred to dissolve, diluted to 1000 mL, and then stored at room temperature.

0.01 mol/L Citrate antigen retrieval solution (pH 6.0): Weigh and took 3 g Trisodium citrate, and 0.4 g Citric acid using an electronic balance, added 200 mL deionized water, stirred to dissolve, diluted to 1000 mL, adjusted pH value to 6.0, and then stored at room temperature.

10% APS: Weigh and took 1 g APS using an electronic balance, added 10 mL of water, stir to dissolve, and stored -20 °C.

TBST buffer: Use an electronic balance to weigh and took 8.8 g of sodium

chloride, measure 20 mL of Tris-Hcl (pH = 8.0) in a graduated cylinder, add ddH2O to a constant volume of 1000 mL, added 0.05% Tween-20, mixed, and then stored at room temperature.

Transfer buffer: Weigh and took 1.45 g Glycine, 2.91 g Tris, and 0.185 g SDS using an electronic balance, added 400 mL of water, stirred to dissolve, added 100 mL of methanol, and stored at room temperature.

2.2.1 Ethics statement

Two hundred Hy-line brown laying hens (one-day-old) were purchased from the Animal Center of Zhengzhou University (No. 41003100024648). Animal experiments were reviewed and approved by the Laboratory Animal Care and Ethics Committee of Henan Institute of Science and Technology (Permit Number: 2020HIST016), in accordance with international law.

2.2.2 Primer design and synthesis

For PCR detection of *S.* Pullorum, according to the conserved nucleotide sequence of *S.* Pullorum *invA* gene (Accession number: NC003197.1) published by GenBank, a pair of primers was designed by using preimer 5.0 software analysis system. The sequences of the primers were *invA*-F, 5'-TCCTCCGCCCTGTCTACTT-3', *invA*-R, 5'-CCCTTTGCGAATAACATCCT-3'.

For the establishment of multiple PCR methods, all aligned target sequences in the NCBI GenBank must be present. Two pairs of specific primers for the *citE2* gene and intergenic sequence of SPS4_00301–SPS4_00311 were designed using the Primer Premier 5.0 software (Premier Biosoft, USA). The nucleotide sequences of two primer pairs used for multiplex PCR were as follows: *citE2*-F, 5′-TCGACATCGCCACCTCCAG-3′; *citE2*-R, 5′-CGGCAATCACCTCA TACAT-5′; SPS4_00301–SPS4_00311-F, 5′-GCACGCGACGTTCAAA TCTG-3′; and SPS4_00301–SPS4_00311-R, 5′-GACGGTCACACCAA ATAAGC-3′.

For the construction of *steE* deletion mutant of *S.* Pullorum and its complementary strains, the sequence of the kanamycin resistance cassette (Kan^R) was amplified from pKD4 plasmid, including 46-bp homology extensions at the 5′

and 3′ ends of the *steE* gene. According to the published sequence of *S.* Pullorum (GenBank: LK931482.1), the primers were designed to amplify the gene from the *S.* Pullorum using PCR method (Table 2.1). The above primers were synthesized in the study by Sangon Biotech Co., Ltd (Shanghai, China).

Table 2.1

The primers used for the construction of *steE* deletion mutant of *S.* Pullorum and its complementary strains.

Primer	Sequences (5′-3′) F /R	Size (bp)
P1	CGGGTGGCGATTTTAACGCCAGTGCGACGTTAGTCG TGGATTACCAgtgtaggctggagctgcttc	1567
P2	AACATTACGCCTCCGATCAAATGCCCGGCAGTTTGA AAAATACGGTcatatgaatatcctccttag	
CX1/ CX2	ATTCAGGGAACCACCACCAT/ACGCCAATCGCAAAA CCACT	1089/683 /2169*
N1/N2	ACGGTGAAATGCTGGAGGTC/CGTGCCGTTCTGTTGA AGTT	224
steE	GA**GTCGAC**[1]ATGATGGAGAGATTCATAGTG/CG**GGAT CC**[2]AGACCATTGGTAATCCACCTGTAACG	508

Small letter: Kan^{R} cassette amplification; *A 1089/683/2169 bp fragment was obtained by PCR method from WT, Δ*steE* and Δ*steE*::kan strains, respectively; [1]Underlined nucleotides denote the *Sal* I restriction site; [2]Underlined nucleotides denote the *Bam*H I restriction site.

2.2.3 Analysis of clinical symptoms and autopsy

The diseased chickens (21-day-old) with suspected *S.* Pullorum from a large-scale chicken farms in Xinxiang, China. Under sterile conditions, the morphological features of liver, kidney, heart, spleen, lung and cecum were observed immediately.

2.2.4 Isolation and identification of *S.* Pullorum

The livers of chicken were punctured aseptically with inoculating ring and

inoculated on MAC medium, XLD medium, HE agar and SS medium. The suspected *S*. Pullorum colonies were selected and purified by scribing, and shaked on the M-broth medium at 37 °C. The purified bacteria were stained with Gram staining.

2.2.5 Biochemical identification

The biochemical tube was cut with gear in the ultra clean worktable, and the purified bacteria were aseptically inoculated into the biochemical tubes such as sucrose, maltose and mannitol. The reaction state of bacteria was observed and recorded in the fermentation tube at 37 °C for 24-48 h.

2.2.6 Plate agglutination test

According to the instructions of *S*. Pullorum multivalent staining plate agglutination, the plate agglutination test was carried out to the blood samples from the diseased chickens with suspected *S*. Pullorum, and normal saline was used as negative control. After 2 min, the agglutination reaction was observed.

2.2.7 PCR assay

The PCR amplifications were set up in a total reaction volume of 25 μL. The PCR system contained 12.5 μL 2×Taq Master Mix, 1 μL of 10 μM *invA* primers, 2 μL DNA from the isolated bacteria, and 9.5 μL of sterile doube-distilled water (DDW). The optimized multiplex PCR conditions were performed: initial denaturation at 95 °C for 5 min, followed by 30 cycles of 95 °C for 40 s, annealing at 59 °C for 30 s, and extension step at 72 °C for 1 min 30 s, followed by a final extension step of 72 °C for 10 min. After PCR amplification, the amplified products (10 μL) were analyzed by 1.5% agarose gel electrophoresis.

2.2.8 Drug susceptibility test of *S*. Pullorum

According to the National Committee of Clinical Laboratories Standards for Clinical and Laboratory Standards Institute [184], the antimicrobial activity of *S*. Pullorum was analyzed. Briefly, the isolated *S.* Pullorum was purified and cultured, take 100 μL *S*. Pullorum solutions and add to the nutrient agar plate. The liquid was slightly dry and completely absorbed in the plate. Under sterile environment, the drugs sensitivity paper tablets were clipped and attached to the culture medium

with sterile tweezers, and then use tweezers gently pressed them. All plates were wrapped upside down in an incubator at 37 °C for 16–18 h, and the formation of S. Pullorum-susceptible zone was observed and calculated.

2.2.9 *Salmonella* and cell culture

A collection of 46 bacterial strains, including 6 strains of *S.* Pullorum, 27 strains of non-*S.* Pullorum, and 13 strains of non-*Salmonella enterica* subsp. *enterica*, were used (Table 2.2). The pBBR1MCS2-Tac-mCherry plasmid carrying the mCherry gene was transformed into the WT and Δ*steE* strains to provide the red fluorescence in *S.* Pullorum, respectively. All *Salmonella* strains were cultivated in Luria-Bertani (LB) broth at 37 °C for 12–14 h with shaking at 180 rpm. All non-*Salmonella enterica* subsp. enterica strains were routinely cultured overnight under suitable conditions and medium. All glycerol strains were stored at −80°C in a refrigerator until use.

Table 2.2

List of the bacteria strains used in this study and the results of the multiplex PCR system.

No.	Analyte	Source	Serogroup	the multiplex PCR results (333 bp/257 bp/167 bp)[e]		
				citE2	*citE2* ROD	SPS4_00301-SPS4_00311
Salmonella						
1	*S.* Pullorum	CVCC 530[a]	D	−	+	+
2	*S.* Pullorum	CVCC 1791	D	−	+	+
3	*S.* Pullorum	CVCC 1799	D	−	+	+
4	*S.* Pullorum	CVCC 535	D	−	+	+
5	*S.* Pullorum	ATCC 9120[b]	D	−	+	+
6	*S.* Gallinarum	CICC 21510[c]	D1	−	+	+
7	*S.* Enteritidis	ATCC 4931	D1	+	−	+
8	*S.* Typhimurium	ATCC 13311	B	+	−	+
9	*S.* Typhimurium	CMCC 50115[d]	B	+	−	+
10	*S.* Typhimurium	CVCC 541	B	+	−	+
11	*S.* Paratyphi	Laboratory stock	B	+	−	+
12	*S.* Kentucky	Laboratory stock	/	+	−	+
13	*S.* Paratyphoid	Laboratory stock	B	+	−	+
14	*S.* Heidelberg	Laboratory stock	/	+	−	+
15	*S.* Enteritidis	ATCC 13076	D	+	−	+
16	*S.* Choleraesuis	ATCC 10708	D	+	−	+
17	*S.* Enteritidis	ATCC 4931	D	+	−	+
18	*S.* Enteritidis	Laboratory stock	D	+	−	+

Continuation tabl.2.2

19	*S.* Choleraesuis	ATCC 10708	C1	+	−	+
20	*S.* Dublin	Laboratory stock	D1	+	−	+
21	*S.* Indiana	ATCC 51959	/	+	−	+
22	*S.* Oranienburg	ATCC 9239	B	+	−	+
23	*S.* Hadar	ATCC 51956	E	+	−	+
24	*S.* Newport	ATCC 6962	C2	+	−	+
25	*S.* Paratyphi A	ATCC 9150	/	+	−	+
26	*S.* Madelia	Laboratory stock	/	+	−	+
27	*S.* Kaapstad	Laboratory stock	/	+	−	+
28	*S.* Kentucky	Laboratory stock	/	+	−	+
29	*S.* Dublin	Laboratory stock	/	+	−	+
30	*S.* Enteritidis	Laboratory stock	/	+	−	+
31	*S.* Westhampton	ATCC 9712	/	+	−	+
32	*S.* Saintpaul	ATCC 19430	/	+	−	+
33	*S.* Typhi	Laboratory stock	D	+	−	+
Non-*Salmonella*						
1	*Escherichia coli* O157:H7	Laboratory stock	/	−	−	−
2	*Escherichia coli* O157:H7	CMCC 44828	/	−	−	−
3	*Listeria monocytogenes*	ATCC 19111	/	−	−	−
4	*Shigella flexneri*	ATCC 13932	/	−	−	−
5	*Staphylococcus aureus*	ATCC 25931	/	−	−	−
6	*Aeromonas hydrophila*	CMCC 26001	/	−	−	−
7	*Bacillus subtilis*	ATTC 9372	/	−	−	−
8	*Campylobacter jejuni*	ATCC 63501	/	−	−	−
9	*Pseudomonas aeruginosa*	ATCC 27853	/	−	−	−
10	*Escherichia coli*	CICC 10783	/	−	−	−
11	*Staphylococcus aureus*	ATCC 6538	/	−	−	−
12	*Enterococcus faecalis*	ATCC 29212	/	−	−	−
13	*Yersinia pseudotuberculosis*	ATCC 908	/	−	−	−

[a] CVCC: China Veterinary Culture Collection Center, China;

[b] ATCC: American Type Culture Collection, USA;

c CICC: China Center of Industrial Culture Collection, China;

[d] CMCC: National Center for Medical Culture Collections, China;

[e] +, positive; −, negative.

Avian HD-11 cells were cultured in Dulbecco's Modified Eagle Medium (DMEM) (Hyclone, UT, USA) with 10% fetal bovine serum (FBS; Invigentech, CA, USA) and 1% penicillin-streptomycin (Solarbio, Beijing, China). Cells were incubated at 37 °C in an incubator with 5% CO_2. Antibiotic-free media was used for 24 h before infection and transfection.

2.2.10 Bacterial DNA extraction

The overnight culture medium of the indicated bacteria (5 mL) was centrifuged at 10,000 rpm for 1 min, and the supernatant was removed as much as possible. Then, the genomic DNA from the indicated bacteria was extracted via the

TIANamp Bacteria DNAKit (Tiangen-Biotech, China). The DNA of *Salmonella* was extracted through the boiling method as template. The concentration and purity of DNA were quantified using the $A_{260/280}$ obtained by spectrophotometer (BioDrop, England). The DNA solution was subsequently packed and stored at −20 °C prior to use.

2.2.11 Bioinformatics analysis

To the detect *S.* Pullorum and non-*S.* Pullorum by the multiplex PCR assay, we compared the differences of genome sequences. The *citE2* gene and intergenic sequence between SPS4_00301 and SPS4_00311 of *S.* Pullorum (GenBank accession No: LK931482.1) were each analysed between *S.* Pullorum and *Salmonella* from the National Center for Biotechnology Information (NCBI). The *citE2* gene and the intergenic sequence between SPS4_00301 and SPS4_00311 were evaluated individually in the search database nucleotide collection (nr/nt) by using the Megablast from the Basic Local Alignment Search Tool (BLAST).

2.2.12 Multiplex PCR assay

Different annealing temperatures (52.5 °C–61.5 °C) and ratios of two primer pairs (*citE2*: SPS4_00301–SPS4_00311; 0.2:1, 0.4:1, 0.8:1, 1:1, 1:0.2, 1:0.4, and 1:0.8) were used to optimize and establish the multiplex PCR system. The multiplex PCR amplifications were set up using a total volume of 25 μL containing 12.5 μL 2× ES Taq MasterMix (No: RR902; TakaRa, China), 0.5 μL of 10 μM *citE2* F/R primers, 0.5 μL of 10 μM SPS4_00301–SPS4_00311 F/R primers, 1.0 μL genomic DNA, and 10.5 μL of DDW. The multiplex PCR conditions in the assay were performed as follows: initial denaturation at 95 °C for 5 min followed by 30 cycles of 95 °C for 40 s, annealing at 58 °C for 30 s, and extension step at 72 °C for 30 s. The final extension was at 72 °C for 10 min. The amplified products were separated with 1.5% agarose gel electrophoresis for 25 min and observed under ultraviolet light, and repeated three times.

Genomic DNA was extracted as described above to confirm whether the signal of the multiplex PCR could be detected for cross-reaction among different combinations of primer pairs (*citE2* and SPS4_00301–SPS4_00311) and templates

of *Salmonella* cells (*S.* Pullorum and *S.* Enteritidis). The PCR system and conditions were conducted in accordance with the PCR protocol. Bacterial tests were performed and repeated three times.

2.2.13 Sensitivity and specificity of the multiplex PCR assay

The genomic DNA of *S.* Pullorum was diluted 10 times serially from 62.5 ng/μL to 6.25 fg/μL with sterile DDW. The overnight culture of *S.* Pullorum was washed three times with sterile DDW, and the final concentrations of *S.* Pullorum cells were adjusted from 4×10^6 CFU/mL to 5×10^3 CFU/mL with sterile DDW The sensitivity of multiplex PCR was evaluated under the optimized reaction conditions. Finally, 1 μL of each dilution was used as template for the multiplex PCR detection. All experiments were repeated three times.

The specificity of the multiplex PCR assay based on the *citE2* and SPS4_00301–SPS4_00311 primers were conducted using genomic DNA from 33 *Salmonella* and 13 non-*Salmonella enterica* subsp. *enterica* strains. Cultures were adjusted to 10^6 CFU/mL and confirmed using plate counts six times. The DNA template was obtained by direct boiling method and subjected to simple centrifugation for 3 min at 5,000 rpm. The supernatant (1 μL) was analyzed for the multiplex PCR assay, and DDW was used as blank control. These experiments were independently repeated in triplicate.

2.2.14 Analytical characteristics of multiplex PCR assay in artificially contaminated egg samples

A total of 100 fresh eggs were purchased from a local supermarket (Xinxiang, China) and used to evaluate whether the multiplex PCR detection of *S.* Pullorum (CVCC 530) *and S.* Enteritidis (ATCC 4931) artificially contaminated eggs. All eggs were checked to ensure the *Salmonella*-free according to the standard culture method (GB/T4789.4–2016) depicted in Fig. 2.1 (China National Food Safety Standard, 2016) [185].

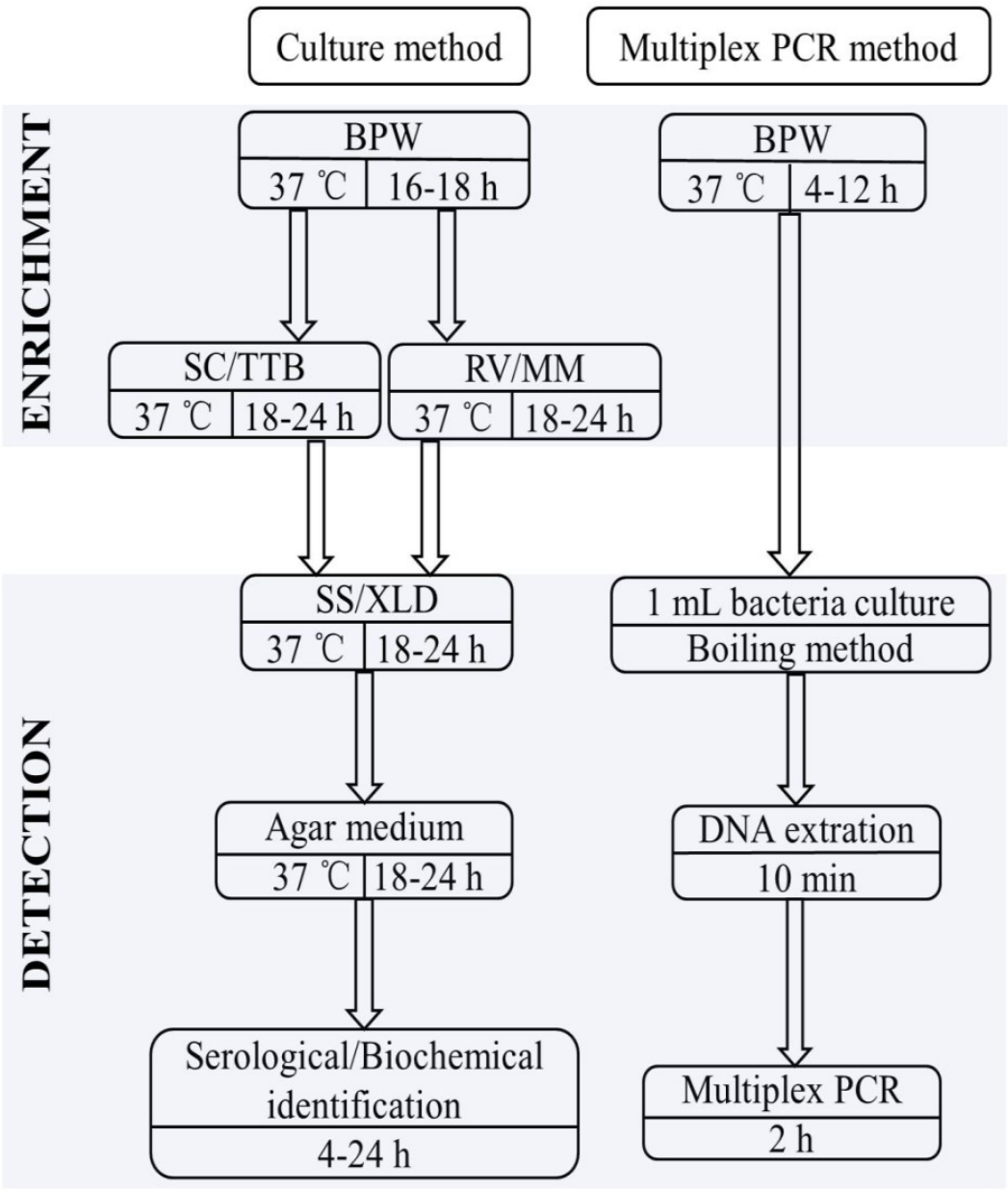

Fig. 2.1. Comparison of the culture method and multiplex PCR for *Salmonella* spp. detection in a fecal sample.

Briefly, take three eggs, each egg was placed into a homogeniser and stirred into the homogenate to ensure uncontaminated samples of target bacteria. Then, the homogenate (25 mL) was added into 225 mL buffered peptone water (BPW; Hopebio Biol-Technology, China) to obtain 1:10 as the culture medium of *Salmonella*. After the OD_{600} value of *S.* Pullorum culture was adjusted to 1, its serial 10-fold dilutions with DDW were from 10^6 CFU/mL to 10^0 CFU/mL. Simultaneously, each dilution was carried out using XLD agar (Hopebio Biol-Technology, China) plates through the plate count method to determine the actual

concentration of *S.* Pullorum. Ten fold serial dilutions (1 mL) were thoroughly added into 9 mL culture medium of *Salmonella* and incubated at 37 °C with shaking at 180 rpm for 0, 2, 6, 10, and 12 h, respectively. Thereafter, 1 mL enrichment culture of each dilution was collected by centrifugation at 10,000 rpm for 1 min. DNA was extracted by using the boiling method, and 1 μL of each supernatant was used using the multiplex PCR under the same conditions. These results of the multiplex PCR assay of all samples were compared with those of the culture method. Non-inoculated egg with *Salmonella* was tested as the negative template. All experiments were independently repeated in triple times.

2.2.15 Application of the multiplex PCR assay

To ensure the effect of the multiplex PCR assay, we tested the genomic DNA of 69 clinical samples from the feces of naturally contaminated chicken farms and 3 negative samples of smears from chickens (from which *Salmonella* was not isolated) in Xinjiang Province, China. Chickens were preliminary screened by *S.* Pullorum/Gallinarum serum plate agglutination test polyvalent antigen (Zhonghai Biotech, China). Finally, 69 chicken anal swab samples were identified as *S.* Pullorum strains by using the culture method (GB/T4789.4–2016) [185]. All clinical samples were tested using the multiplex PCR assay described above after 12 h enrichment at 37 °C in BPW. The results of multiplex PCR for known *S.* Pullorum strains were compared with those of the culture method in this assay. All assays were repeated independently three times.

2.2.16 Generation of the *steE*-deficient *S.* Pullorum and its complementation strain

The *steE* deletion mutant of *S.* Pullorum was constructed by λ-Red recombination system as previously described [186]. Briefly, the kanamycin resistance cassette (Kan^R) was amplified from pKD4 plasmid using the primers P1/P2. The PCR products were purified and transferred into *S.* Pullorum containing pKD46 plasmid by electroporation. The *steE* gene was replaced to construct the *S.*

Pullorum Δ*steE*::kan strain, and then the Δ*steE* strain was obtained through FLP recombinase expressed by pCP20 plasmid. The Δ*steE* strain was comfirmed by PCR method using the primers CX1/CX2 or N1/N2. The *steE* gene fragment was amplified by PCR method using primers *steE*-F/*steE*-R, and then cloned into pBR322 plasmid to construct the pBR322-*steE* vector. The pBR322-*steE* recombinant plasmid was then transformed into the Δ*steE* strain to construct its complementation (Δ*steE*+*steE*) strain by using prokaryotic expression vector method. The Δ*steE*+*steE* strain was confirmed by PCR method using primers CX1/CX2 or N1/N2.

2.2.17 Identification of growth curve and biochemical characteristics of the Δ*steE* strain

The WT, Δ*steE* and Δ*steE*+*steE* strains were inoculated into LB broth at 37 °C with shaking at 180 r/min for 15 h and subcultured 1:100 into LB broth as previously described [187]. At a starting time point (0 h), the optical density was measured to achieve an approximate concentration (OD_{600} = 0.01). The OD_{600} nm value of the bacterial cultures was measured at 2 h interval for 14 h by the Biodrop spectrophotometer (BioDrop, England). Biochemical characteristics of the WT, Δ*steE* and Δ*steE*+*steE* strains were performed, following the manufacturer's protocol, including glucose, lysine decarboxylase, sucrose, mannose, mannitol, sorbitol, lactose, maltose, malonate, ornithine decarboxylase, urease, arabinose and hydrogen sulfide.

2.2.18 HD-11 cells infection assay

HD-11 cells were kindly provided by Professor Heng-mi Cui of the Yangzhou University, China. HD-11 cells were used for the cell infection assay as described previously [188]. Cells were plated at 2×10^5 cells per well on a six-well plate and cultured overnight until 80%–90% confluency was obtained.

For the bacterial adhesion, invasion and proliferation assays, HD-11 cells were infected with overnight cultures of the WT, Δ*steE* and Δ*steE* + *steE* strains at a multiplicity of infection (MOI) of 10:1. Subsequently, the inoculated six-well plate was centrifuged at 500 × *g* for 10 min to promote the interaction of the cells with *Salmonella*. After 1 h incubation at 37 °C, the cells were lysed with 1 mL of 0.1% of Triton X-100 (Sangon Biotech, China) for 10 min. The cell lysates of the WT and Δ*steE* strains were serially diluted 10-fold using phosphate-buffered saline (PBS) and the dilutions were spread on LB agar before incubation at 37 °C for 12–16 h to analyze the adhesive ability of bacteria. For the bacterial invasion assay, at 1 h after infection, HD-11 cells were washed three times with PBS and incubated for another 1 h in DMEM with 10% FBS and 100 μg/mL gentamicin (Solarbio, China) to kill extracellular bacteria. HD-11 cells were subsequently lysed with 1 mL of 0.1% Triton X-100 for 10 min and plated to calculate the number of colonies. For the bacterial proliferation assay, the infected host cells were washed with PBS and incubated in DMEM supplemented with 10% FBS and 10 μg/mL gentamicin; this step was set as the 0 h time point. At 0, 3, 6, 9, 15, and 20 h time-points, HD-11 cells from each well were lysed with 1 mL of 0.1% Triton X-100 for 10 min. The cell lysates at 10-fold serial dilutions were plated for CFU analysis. The number of intracellular bacteria was calculated and presented as the fold-change at the indicated time points compared to the initial numbers present at 0 h.

For identification of effector genes and inflammation cytokines, HD-11 cells were infected with overnight cultures of the WT, Δ*steE* and Δ*steE*+*steE* strains at multiplicities of infection (MOI) of 5, 10, 20, and 40 for 1 h. After washing with PBS, the cells were cultured in DMEM (Solarbio, China) supplemented with 10% fetal bovine serum (FBS) (Invitrogen, USA) and 100 μg/mL gentamicin for 1 h to kill extracellular bacteria. At 2 h post-infection (hpi), the indicated cells were then washed twice with PBS and maintained in DMEM with 10% FBS and 10 μg/mL gentamicin. Infected HD-11 cells were incubated in DMEM with 10% FBS (10 μg/mL gentamicin). Finally, the HD-11 cells were fixed and harvested at the indicated time points after infection for further analysis, as required. HD-11 cells

stimulated with LPS (10 μg/mL) (Sigma, USA) were used as the positive reference group for mRNA expression analysis.

2.2.19 Cellular apoptosis assay

HD-11 cells were seeded on 6-well plates at a density of 1 × 10^5 cells/well and cultured for 18-20 h and reached 80%-90% confluence as previously described [189]. Briefly, the overnight cultured of mCherry-WT and mCherry-Δ*steE* strains in LB broth with kanamycin (50 mg/mL) were washed with PBS for 3 times to adjust the concentration of bacteria. HD-11 cells were infected with the indicated *S.* Pullorum at a multiplicity of infection (MOI) of 10:1. The cells were incubated for 3 h at 37 °C and then were fixed in 4% paraformaldehyde, and were stained with 4',6-diamidino-2-phenylindole (DAPI) staining. Staining was assessed by laser scanning confocal microscopy.

2.2.20 Chickens infection assay

Hy-line brown laying hens (one-day-old) obtained from the Animal Center of Zhengzhou University, China (No. 41003100024648). For the half-lethal dose (LD_{50}) of *S.* Pullorum assay, *S.* Pullorum and *S.* Pullorum Δ*steE* strains were inoculated respectively in LB broth for 12 h. The bacteria cultures were washed three times with PBS and suspended to adjust the bacterial concentration. One hundred Hy-line brown laying hens were randomly divided into 10 groups. Each group were infected orally with 10-fold serial dilutions of *S.* Pullorum or *S.* Pullorum Δ*steE* strain (1 ×10^6、1 ×10^7、1 ×10^8、1 × 10^9、1 ×10^{10} CFU or 1 ×10^7、1 ×10^8、1 × 10^9、 1 ×10^{10}、1 ×10^{11} CFU). Ten chickens received 100 μL of PBS as control group. Deaths were recorded until 14 days, and the LD_{50} of each strain was calculated to evaluate the virulence of the strain to chickens using the Karber's method. The clinical symptoms and morbidity of the chicks were observed every day after *S.* Pullorum or *S.* Pullorum Δ*steE* strain infection, and recorded and photographed.

For *in vivo* competition assays, twenty Hy-line brown laying hens were randomly assigned to two groups (10 chickens in each group). The chickens were infected orally with 2×10^8 CFUs of a 1:1 mixture of WT and Δ*steE*::Kan strains prepared in 100 μL PBS [187], and the chickens were sampled from each group at 3 days post-infection (dpi). Liver, spleen, and bursa tissues were collected from each chicken as described above. After weighing, tissues from six chickens in each group were homogenized mechanically. Appropriate dilutions were plated on XLD/XLD (Kan^R) agar and incubated at 37 °C for 14–16 h to calculate the total number of bacteria. The competitive index (CI) was defined using the following formula: the ratio of Δ*steE*/WT strains in the output divided by the ratio of Δ*steE*/WT strains in the input [190].

For the colonization of *Salmonella* and mRNA expression of cytokines assays, eighty Hy-line brown laying hens were randomly assigned to three groups, with each group containing 20 chickens. The chickens in the experimental groups were orally infected with the WT or Δ*steE* strains (1×10^9 CFU/chicken) in 100 μL PBS, according to the LD_{50} assay as mentioned previously. Twenty chickens were infected orally with 100 μL of PBS as control group. Chickens were deprived of food and water for 12 h before and after chicken immunization. At 12 h, 24 h, 36 h, 2 d, 3 d, 4 d, and 7 d post-infection (hpi or dpi), the liver, spleen, bursa, cecum, and heart tissues of each chicken from each group was collected and stored at -80 °C for further analysis.

For the *S.* Pullorum virulence assay, thirty Hy-line brown laying hens were randomly assigned to three groups (10 chickens per group). The chickens in the experimental groups were orally infected with 1×10^9 CFU of the WT or Δ*steE* strain in 100 μL PBS. Additionally, chickens in the control group were infected orally with 100 μL of PBS [151]. Death was monitored daily for 20 dpi, and the survival curves were analyzed to evaluate the differences in virulence between the two strains. In addition, the livers and spleens were fixed with 10% formalin for 48 h, embedded in paraffin, and cut into 4 μm sections with a paraffin slicer (Leica,

Germany) for histological analysis. The hematoxylin and eosin stained sections were visualized under a light microscope.

2.2.21 Colonization of *S.* Pullorum in chickens

The infected organs of chicks were were harvested from each chicken, according to experimental requirements. After weighing, the liver, spleen, bursa, cecum, and heart tissues of each chicken from each group were homogenized mechanically, and diluted serially of the subsequent cultivation on XLD agar plates at 37 °C for 12−16 h, respectively. The bacterial number was counted and displayed as log10 CFU/g. The dynamic distribution of *S.* Pullorum and *S.* Pullorum Δ*steE* strains in various organs were analyzed by plating on XLD agar. The bacterial number was counted and expressed as log10 CFU/g at 12 h, 24 h, 36 h, 2 d, 3 d, 4 d, and 7 d.

2.2.22 Overexpression plasmid and siRNA transfection assay

The coding sequences of *steE* (GenBank: LK931482.1) and *SOCS3* (GenBank: AF424806.1) were digested with *Xho*I and *Bam*HI and then inserted into the pEGFP-N1 vector to generate pEGFP-*steE* or pEGFP-*socs3*, respectively. HD-11 cells (60–80% confluent) were transfected with either overexpression plasmids (pEGFP-*steE* or pEGFP-*socs3*) or empty plasmids using the Lipofectamine^{TM} 2000 reagent (Invitrogen, USA), according to the manufacturer's protocols. At 48 h post-transfection, the transfected cells were infected with the indicated *S.* Pullorum strains at an MOI of 10 for 2 h, followed by treatment with LPS (10 μg/mL) for 30 min. Chicken siRNA sequences targeting STAT3 or SOCS3 were synthesized by GenePharma (Suzhou, China). The siRNA was used to silence STAT3 or SOCS3, respectively. HD-11 cells (60–80% confluent) were transfected with either targeting siRNAs (siSTAT3 and siSOCS3) or non-targeting siRNA (siNT) using the LipofectamineTM 2000 reagent. At 48 h post-transfection, the transfected cells were infected with the indicated S. Pullorum strains at an MOI of 10 for 2 h. The transfection efficiency of siRNAs was determined using quantitative reverse

transcription-polymerase chain reaction (qRT-PCR) and western blotting. For co-transfection of plasmid DNA and siRNA assay, HD-11 cells (60–80% confluent) were simultaneously transfected with overexpression plasmids (pEGFP-*steE* and pEGFP-*socs3*) and targeting siRNAs (siSTAT3 and siSOCS3), or corresponding controls using the LipofectamineTM 2000 reagent, according to the manufacturer's protocols. After 48 h, transfected cells were collected and lysed in a lysis buffer for further analysis. The sequences of all the primers and siRNAs are listed in Table 2.3.

Table 2.3

The primers used for overexpression plasmid and siRNA transfection assay.

Primer	Sequences (5′-3′) F /R	Size (bp)
steE	C**CTCGAG**[1]ATGATGGAGAGATTCATAGTG/CG**GGATCC**[2]AGACCATTGGTAATCCACCTGTAACG	507
SOCS3	C**CTCGAG**[1]GCCACCATGGTCACCCACAGCAAGTTCC/CG**GGATCC**[2]TAGAGGGGGGCATCGTACTGGTC	646
siNT	UUCUCCGAACGUGUCACGUTT/ACGUGACACGUUCGGAGAATT	
siSTAT3-2	GGUCCCGGAAGUUUAACAUTT/AUGUUAAACUUCCGGGACCTT	
siSTAT3-3	GGCUGGACAAUAUCAUUGATT/UCAAUGAUAUUGUCCAGCCTT	
siSOCS3-1	CGGCUUGAGAACUGGAUAATT/UUAUCCAGUUCUCAAGCCGTT	
siSOCS3-2	CUCAAGACGUUCAGCUCUATT/UAGAGCUGAACGUCUUGAGTT	
siSOCS3-3	CGCACCUACUACAUUUACUTT/AGUAAAUGUAGUAGGUGCGTT	

[1]Underlined nucleotides denote the *Xho* I restriction site; [2]Underlined nucleotides

denote the *Bam*H I restriction site.

2.2.23 Immunofluorescence staining assay

Phosphorylated P65 (p-P65) expression was detected using immunofluorescence staining as previously described [191]. Briefly, *Salmonella*-infected HD-11 cells were fixed using 4% paraformaldehyde (Solarbio, China) for 1 h and blocked with 3% bovine serum albumin (BSA) to eliminate non-specific targets. Then, 0.1% Triton X-100 was used to increase permeability at room temperature for 10 min. Subsequently, the cells were incubated with the primary rabbit anti-phospho-P65 antibody (Cat# bs-0982R, 1:100; Bioss, China) overnight at 4 °C, followed by incubation with goat anti-rabbit IgG H & L/Alexa Fluor 594 (Cat# bs-0295G-AF594, 1:300; Bioss, China) at room temperature for 1 h. Nuclei were stained with 4′-6-diamidino-2-phenylindole (DAPI). Finally, cell fluorescence was observed using a laser confocal microscope (Zeiss GmbH, Germany).

2.2.24 Immunohistochemistry assay

The IHC assay was performed as previously described [192]. Briefly, the paraffin-embedded spleen sections were deparaffinized and then rehydrated using graded ethanol. After the above-treated spleen sections were subjected to antigen retrieval with citrate antigen retrieval solution buffer at 93–97 °C for 14 min and endogenous peroxidase ablation with 3% H_2O_2 solution in darkness for 25 min, they were blocked with 5% normal goat serum for 30 min. The processed sections were then covered with anti-phospho-p65 antibody (bs-0982R, 1:200; Bioss, China) overnight at 4 °C, followed by incubation with horseradish peroxidase-conjugated goat anti-rabbit IgG for 2 h. Subsequently, the sections were counterstained with hematoxylin for 2 min. IHC staining of p-P65 was quantified using the ImageJ software (Bethesda, USA) by a veterinarian pathologist. The percentage of p-P65-positive cells was calculated as p-P65-stained cell

number/total cell number for each section.

2.2.25 RNA extrations

Total RNA was isolated from infected spleens or cells using TRIzol (Invitrogen, USA), and cDNA from 500 ng total RNA was synthesized using the PrimeScript RT reagent kit (TakaRa, China) according to the manufacturer's instructions. The extracted cDNA was stored at –80 °C until qRT-PCR analysis.

2.2.26 qRT-PCR

The cDNA was prepared from infected HD-11 cells and the organs of chickens, as described above. The qRT-PCR was performed using the QuantStudio 5 detector system (Thermo Scientific, Singapore) with the 2 × SYBR Premix Ex Taq II (TakaRa, China) for analyzing the mRNA expression of effector genes and cytokines (Table 2.4). The PCR reaction program was set to 95 °C for 30 s followed by 40 cycles of denaturation at 95 °C for 5 s, annealing at 59 °C for 30 s and extension at 72 °C for 30 s. The *β-actin* for HD-11 cells or *gmk* for *S.* Pullorum was used as the internal control [193]. The threshold cycle (Ct) values were evaluated to calculate the relative expression levels using the $2^{-\Delta\Delta Ct}$ method [194] (4). All qRT-PCR reactions were analyzed in triplicate for each sample.

Table 2.4

The primers used for qRT-PCR assay.

Primer	Sequences (5′-3′) F /R	Size (bp)
IL-1β	ATGTCGTGTGTGATGAGCGGC/AGGCGGTAGAAGATGAAGCGG	107
IL-6	AAATCCCTCCTCGCCAATCTG/CCTCACGGTCTTCTCCATAAACG	105
TNF-α	TGTCTGCTCCTAGTGGCTTTCC/TTGGCATAGGCTGTCCTGAGT	165
iNOS	TGGTAACAGCGGAAGGAGACA/TTCCAGGACCTCCAGGATGTT	110
TGF-β1	TCCAATGTAGCCACCACCAA/ACAGGGACAAGACGCAAACC	121
IL-12	TGCCTTACTTTCATTACTTTCCTTTG/TTTAGCTGGTGTCTCATCGTTCC	109
IFN-γ	TCCTGATGGCGTGAAGAAGG/TCGGAGGATCCACCAGCTTC	128

Cont. tabl.2.4

IL-4	TGCCTTACTTTCATTACTTTCCTTTG/TTTAGCTGGTGTCTCATCGTTCC	172
IL-10	CGCTGTCACCGCTTCTTCAC/GGCTCACTTCCTCCTCCTCATC	99
IL-18	CATTCACTGTTACAAAACCACCGC/AACTCTTATCTTCTACCTGGACGCTG	77
P65	CAGCCCATCTATGACAACCG/TCAGCCCAGAAACGAACCTC	152
STAT3	TGCCTATTAGCCTCCGATTG/CAGAGCCACTCACTGTCCCT	281
SOCS3	CGGCACTTCTTCACCCTCAG/ACCAGCTTCAGCACGCAGTC	143
β-actin	TATTGCTGCGCTCGTTGTTGAC/GATACCTCTTTTGCTCTGGGCTTC	181
gmK	CTTCTTCGCTATCTTGCCCG/ACCATTGAGCAAGTGCTGGC	172
spiC	CCATCCGCTGTGAGCTGTAT/CCGAAGGTAATAGCCGATCC	199
sefC	GCCAATTGACATGGCAAGCA/TGAGCAATCACCCCACCAGA	172
sspH2	TCCACTCCCTGAACTCGCTT/AAAGGTCAGAACGCTGGCTC	197
sseJ	CTTATCGGCGTGTTCCTGTG/GCAGAGGCGCTCGAATGTAT	156
ssaT	TTGAGCGGCATTGAGAGGAA/AGGCAGAGTGGAGAACGCTT	145
sseF	TTTGTTCAGGCGTAAGCAGC/TTCCGTCAGCGGCAAGTAAT	138
pipB	ACCCGTTGACATCCTCCAGA/CACGCGGTATACTGGAATGG	171
sseC	AGCCTCCTCTGCCATCTCATT/TTGGCGAGGAAGTGGTTGAG	158
sipA	CTTTCGGATGAAGCGTTGGT/CGACTACGCATCAAACGGAG	127
hilA	ACGGACAGGGCTATCGGTTT/TCTTCGTAATGGTCACCGGC	201
sseG	GGAGACGGCTTTAGCAATCG/GCGGATGTCGCCTGTCTTAT	138
ssaV	GCGATAATGATACCGCCGAT/GATTTGCGTGCCGGAGTTAT	173
sifB	GGCGGCTTTTCTTTCCTGTT/GCTTGTTCCCTGAGCGGTTA	143
sipC	GCAACGGCACTGGAAGACAT/GTCACGACTAAAGCGAATGAGG	104
steA	GTATCGGTAATGGCACGCTG/GTCAGTCTTCATCAGCGCGA	182
prgH	CGCAAACTGCACATAGCGTC/CAGGCGTTACCTTATTCCCG	147
steB	AAGTTTAGCGGGCAGCACAC/CTTCCGACATCCGCAATCAC	126
steE	ACGGTGAAATGCTGGAGGTC/CATCGCGAAAGCTGCTGTC	114

2.2.27 Western blot assay

Western blotting was performed as previously described [195]. Briefly, spleen tissues and cells from different groups were lysed using 100 μL

radioimmunoprecipitation assay buffer (Solarbio, China) containing phosphatase inhibitor complex I (Sangon Biotech, China), and proteins were quantified using a bicinchoninic acid protein assay kit (TakaRa, China). All target proteins from whole spleen or HD-11 cells lysates were immediately separated on 10−12% sodium dodecyl sulfate polyacrylamide gel and transferred onto polyvinylidene difluoride membranes (Millipore, USA). Subsequently, the membranes were blocked with 5% BSA to eliminate binding to non-specific sites and incubated overnight with the following primary antibodies: anti-P65 (Cat# bs-0465R, 1:2000; Bioss, China), anti-phospho-P65 (Cat# bs-0982R, 1:2000; Bioss, China), anti-SOCS3 (Cat# 14025-1-AP, 1:3000; Sanying, China), anti-STAT3 (Cat## 4904, 1:2000; Cell Signaling Technology, USA), anti-phospho-STAT3 (Cat# 9131, 1:1000, Cell Signaling Technology), and anti-GAPDH (Cat# MB001H, 1:5000; Bioworld Technology, China) at 4 °C. The blots were then incubated with horseradish peroxidase-labeled secondary antibodies for 1 h. Subsequently, the strips were incubated with enhanced chemiluminescent substrate (Beyotime Biotech, China). Finally, the intensity of the target bands was measured using the ImageJ software.

2.2.28 Statistical analysis

All data are presented as the mean values ± standard errors. One-way analysis of variance and Student's t-test were performed for statistical analysis using the GraphPad Prism 5 software (GraphPad Software, USA). Data from at least three biological replicates of each experiment are shown as required. Statistical significance was considered at * $P < 0.05$, ** $P < 0.01$.

2.2.29 Conclusions in chapter 2

1. Methodological approaches adopted in the dissertation work that include theoretical research, analysis of clinical symptoms and autopsy, antimicrobial susceptibility test, bioinformatics analysis, cells and chickens infection assay,

histopathology assay, transfection assay, qRT-PCR, western blot assay, and its subordinate research methods, which solved the scientific problems of this dissertation.

2. The object of research of dissertation work is determined the pathogenic bacteria species from the diseased chickens with suspected *S*. Pullorum and its drug susceptibility, the developed multiplex PCR system, the role of *steE* on the pathogenicity of *S*. Pullorum, and clarify the mechanism of *steE* regulates the balance of Th1/Th2-related cytokines..

3. Research items are the diseased chickens with suspected *S*. Pullorum, molecular marker of *S*. Pullorum, and the function of *steE*.

4. The selected set of methods allows you to comprehensively fulfill the isolation, identification, drug resistance analysis, developed multiplex PCR system of *S*. Pullorum, and evaluate the role of the regulatory network of *steE*, STAT3/SOCS3, and NF-κB pathways in *S.* Pullorum-induced Th1/Th2 balance.

CHAPTER 3

RESULTS OF RESEARCH

3.1 Isolation, identification and drug resistance analysis of *S.* Pullorum

In this study, the pathogen of the diseased chickens with suspected *S.* Pullorum from a large-scale chicken farms was isolated and identified. The results showed that the isolated *S.* Pullorum was the main pathogenic bacteria of chickens. Antibacterial drugs sensitivity test confirmed that the isolated *S.* Pullorum were resistant to amoxicillin, sulfamethazine, tetracycline and ciprofloxacin, but sensitive to ceftriaxone, ceftiofur and kanamycin.

3.1.1 *S.* Pullorum isolation and culture results

The isolated bacteria were colorless, transparent to light orange, round, transparent and needle size colonies on MAC medium. The colony morphology of bacteria were pink or with black center, round, with neat edge and smooth surface on XLD medium (Fig. 3.1A) . M-broth medium can be seen in the uniform turbidity of floccules, gently shaking into white sediment. On HE agar, there were colorless and translucent blue-green colonies, a few yellow colonies with a diameter of 2 mm, and most of the colonies showed black luster. The isolated bacteria were colorless, transparent or small colonies with black center with the diameter of 2–3 mm on SS medium (Fig. 3.1B) . The Gram staining assay was negative. Under the microscope, the bacteria was red and straight rod-shaped with blunt round ends, with the size of 0.8–1.6 μm × 1.9–4.5μm (Fig. 3.1C) .

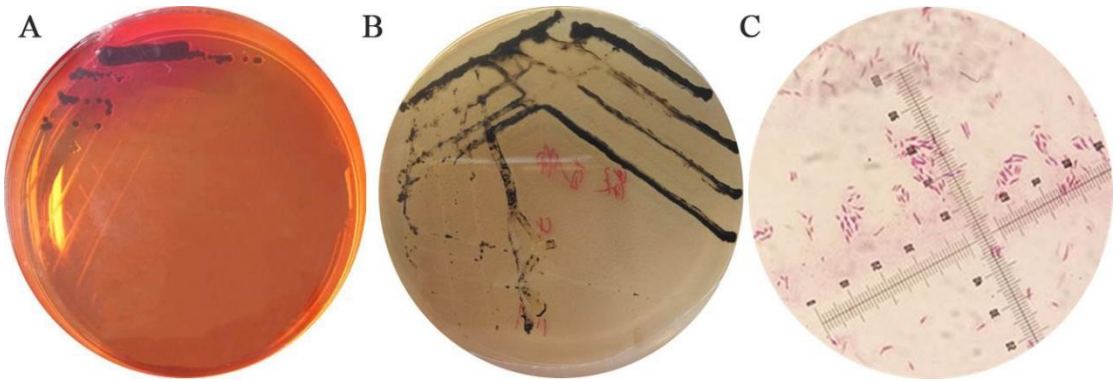

Fig. 3.1 Colony morphology and gram staining identification of the isolated bacteria.

(A) XLD medium; (B) SS medium; (C) Gram staining assay （100 ×）.

3.1.2 Biochemical characteristics results

The isolated bacteria were inoculated into the *Salmonella* biochemical identification tube according to the manufacturer's instructions. The biochemical reaction characteristics of bacteria were shown in Table 3.1. It can be seen that the isolate bacteria did not liquefy gelatin, can ferment glucose and produce gas on trisaccharide iron agar, and can not metabolize lactose, can ferment sorbitol and glucose, did not produce indole. Amino acid decarboxylase, tartrate and MR tests were positive. VP and ONPG tests were negative. These features of the isolated bacteria were consistent with the characteristics of *S.* Pullorum.

Table 3.1

Biochemical identification results of the isolated bacteria.

Items	Isolates	Model strain	Test items	Isolates	Model strain
Salicin	-	-	ONPG	-	-
Glucose	+	+	H_2S	+	+
Urease	-	-	Tartrate	+	+
Amino acid decarboxylase	+	+	Sorbitol	+	+
Indole test	-	-	Lysine	+	+
Potassium cyanide	-	-	Gelatin	-	-
VP	-	-	MR	+	+

Note: “+” means positive; “-”" means negative.

3.1.3 Plate agglutination assay results

Through the plate agglutination test, the isolated bacteria had agglutination, while the negative control did not agglutination.

3.1.4 Autopsy assay results

The surface of liver was densely covered with small gray miliary necrotic foci

(Fig. 3.2A). The heart was severely deformed with round appearance, punctate hemorrhage and large granuloma (Fig. 2B). There was yellow effusion in the abdominal cavity, and the kidney was swollen and congested (Fig. 3.2C). The spleen was swollen and necrotic with brittle texture and gray white nodules on the surface (Fig. 3.2D). Hemorrhagic catarrhal inflammation of the small intestine, gray white protuberant nodules on the mucosal surface of the colon, and the cecum and cecal tonsils were enlarged with bleeding spots and small ulcers, and the contents were caseous (Fig. 3.2E). There was gray tumor like necrosis in the lung. The cysts are large with bleeding points (Fig. 3.2F).

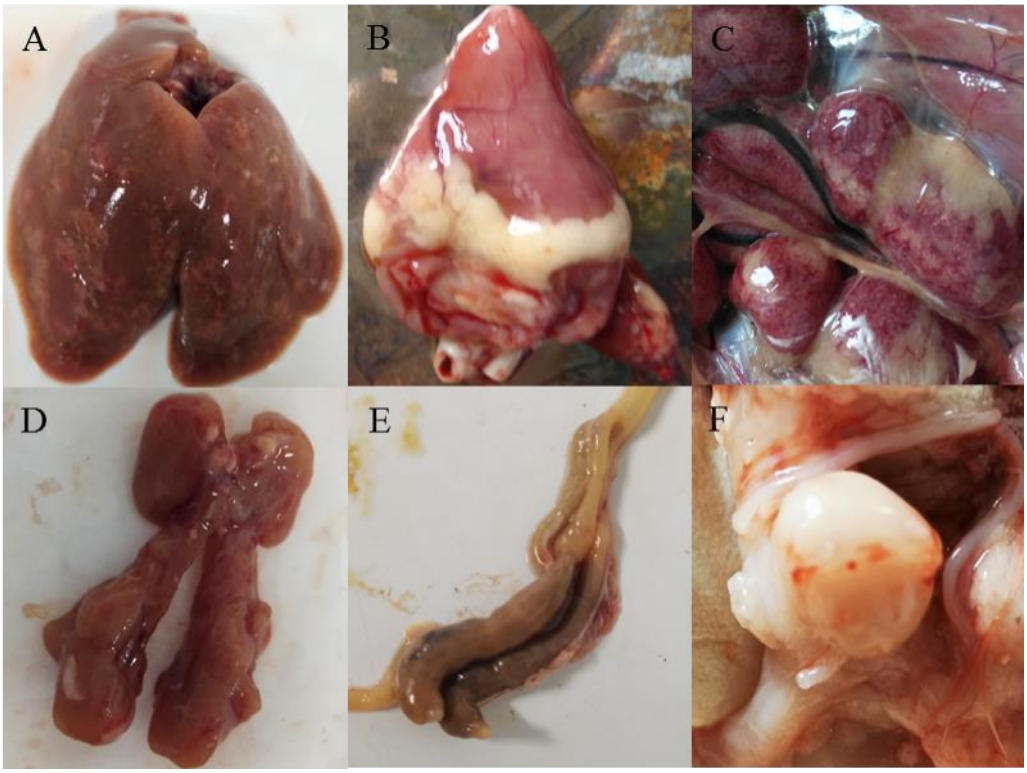

Fig. 3.2 Anatomical symptoms of diarrhea chickens

(A) Liver enlargement and necrosis; (B) Granuloma on the surface of pericardium; (C) The kidney was swollen and congested; (D) The spleen was swollen, necrotic and brittle; (E) Cecal enlargement; (F) Massive hemorrhage of bursa.

3.1.5 PCR results

The amplicon lengths of the isolated bacteria were 1143 bp, while the negative control did not have the specific band (Fig. 3.3).

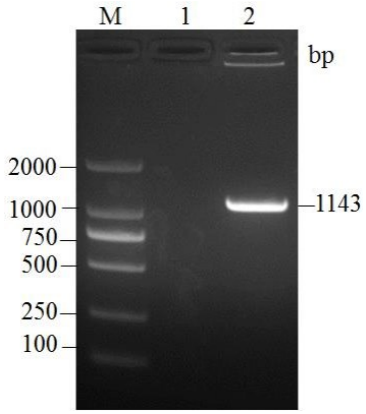

Fig. 3.3 PCR amplification of *S*.Pullorum *invA* gene

Lane M: DL2000 DNA Marker; Lane 1: Negative control; Lane 2: DNA of the suspected *S*. Pullorum. The PCR product size was 1143 bp.

3.1.6 Drug susceptibility testing results

Drug sensitivity test of the isolated *S*. Pullorum was determined by the drug sensitivity paper tablets method. The results showed (Table 3.2) that the isolated *S*. Pullorum were severely resistant to amoxicillin, sulfamethazine, tetracycline and ciprofloxacin, but sensitive to ceftriaxone, ceftiofur and kanamycin.

Table 3.2

The results of drug susceptibility test of isolated *S*. Pullorum to 16 different antibiotics.

Drugs	Judgment standard R I S	Diameter of bacteriostatic zone/mm	Sensitivity
Amoxicillin	≤14 15-20 ≥21	0	R
Polymyxin	≤10 11-15 ≥16	16	S
Sulfamethazine	≤14 15-19 ≥20	6	R
Tetracycline	≤14 15-18 ≥19	7	R
Cefatriaxone	≤13 14-20 ≥21	36	S
Gentamicin	≤12 13-14 ≥15	28	R
Neomycin	≤12 13-16 ≥17	15	I
Mezlocillin	≤17 18-20 ≥21	33	S
Ciprofloxacin	≤18 19-21 ≥22	6	R
Ceftiofur	≤14 15-17 ≥18	24	S
Fudaxin	≤14 15-17 ≥18	20	S
Neomycin	≤12 13-16 ≥17	29	R
Sulfamethoxazole	≤23 24-32 ≥33	9	R
Kanamycin	≤13 14-17 ≥18	22	S
Streptomycin	≤13 14-16 ≥17	9	R

3.1.7 Conclusions in chapter 3.1

The pathogen of chicken with diarrhea was identified as *S*. Pullorum, which have potentially pathogenic. The isolated *S*. Pullorum was severely resistant to amoxicillin, sulfamethazine, tetracycline and ciprofloxacin, but sensitive to ceftriaxone, ceftiofur and kanamycin.

3.2 Multiplex PCR assay based on *citE2* gene and intergenic sequence for the rapid *S*. Pullorum in chickens

This study aimed to establish a multiplex PCR approach for the accurate detection of *S*. Pullorum. The *citE2* gene and interval sequence of SPS4_00301–SPS4_00311 existed in *Salmonella enterica* subsp. *enterica* by genomic comparison. By contrast, a 76 bp deletion in *citE2* was found only in *S*. Pullorum. Two pairs of special primers designed from *citE2* and interval sequence were used to establish the multiplex PCR system. The optimized multiplex PCR system could distinguish *S*. Pullorum and non-*S*. Pullorum. The sensitivity of the optimized multiplex PCR system could be as low as 6.25 pg/μL and 10^4 CFU/mL for genomic DNA and *S*. Pullorum cells, respectively. The developed multiplex PCR assay distinguished *S*. Pullorum from 33 different *Salmonella* serotypes and 13 non-target species. The detection of egg samples artificially contaminated with *S*. Pullorum, *S*. Enteritidis and naturally contaminated 69 anal swab samples showed that results were consistent with the culture method.

3.2.1 Sequence alignment analysis and *S*. Pullorum detection of the multiplex PCR

Bioinformatics analysis showed that *citE2* was conserved, repeatable, and existed in *Salmonella enterica* subsp. *enterica* after searching in the BLASTn program of Web BLAST (Supplementary Fig. 3.1). The *citE2* sequence comparison showed that the 76 bp fragment of the *citE2* gene in all *S*. Pullorum strains might be absent compared with that in non-*S*. Pullorum. The intergenic sequence between SPS4_00301 *and* SPS4_00311 had 100% homology with *Salmonella enterica* subsp. *enterica* after searching in the BLASTn program of

Web BLAST (Supplementary Fig. 3.2). In this study, the specific primer from the *citE2* gene was designed for *S.* Pullorum, and the intergenic sequence primer of SPS4_00301–SPS4_00311 was designed as a molecular marker for the identification of *Salmonella enterica* subsp. *enterica* (Fig. 3.4A). The fragment sizes of multiplex PCR were 167 and 257 bp for *S.* Pullorum and 167 and 333 bp for *S.* Enteritidis (Fig. 3.4B).

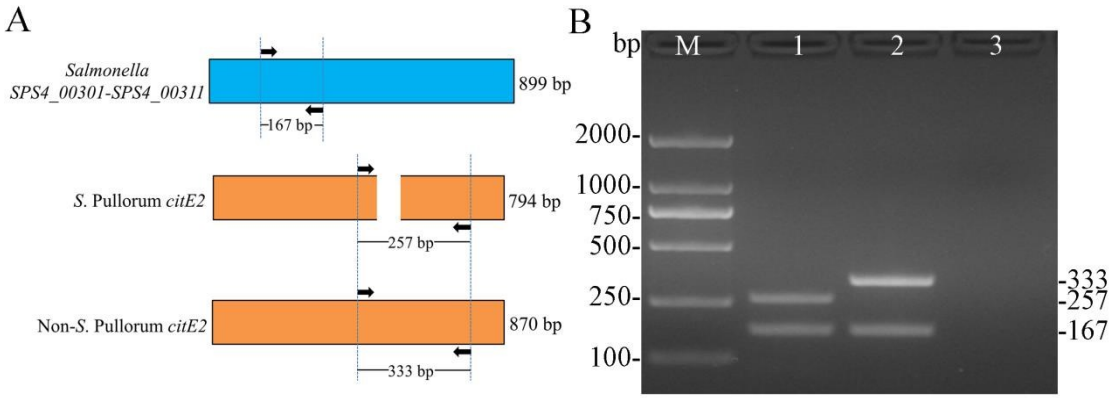

Fig. 3.4. Overview of the multiplex PCR assay for the detection of *S.* Pullorum.

(A) Intergenic sequence between SPS4_00301 and SPS4_00311 and *citE2* gene existing in *Salmonella enterica* subsp. *enterica* and highly conserved ROD of the *citE2* of *S.* Pullorum among *Salmonella* serovars. The intergenic sequence and *citE2* were applied to design primers, and black arrows show the size of the amplified fragment; (B) Multiplex PCR results using genomic DNA from *Salmonella* strains. M: DL2000 DNA marker (No: 3427A; TakaRa, China); Lane 1: *S.* Pullorum; Lane 2: *S.* Enteritidis; Lane 3: Negative control (DDW).

3.2.2 Optimization and effect of the multiplex PCR assay

After the multiplex PCR system was generated, the annealing temperature and the combination ratio of two pairs of primers were optimized. As shown in Fig 3.5A and 3.5B, no significant difference was observed in the annealing temperature of *citE2* and SPS4_00301–SPS4_00311 primers at 52.5 °C-61.5 °C. Fig 3.5C demonstrates that the different annealing temperatures of multiplex PCR were 55.3 °C, 56.4 °C, 57.6 °C, 58.7 °C, 59.8 °C, and 60.7 °C and that the electrophoretic bands were relatively bright and had no significant difference. Thus, the optimal

conditions of multiplex PCR were as follows: annealing temperature of 60 °C and ratio of two pairs of primers (*citE2* primers: SPS4_00301–SPS4_00311 primers) of 1:1 (Fig. 3.5D). These conditions were applied to amplify the simplex and multiple templates of *Salmonella* (*S.* Pullorum and *S.* Enteritidis, respectively) to verify whether single and mixed primer pairs, respectively, could be used in a multiplex PCR system. The results of agarose gel electrophoresis showed that the amplified fragments of 167, 257, and 333 bp were obtained from *S.* Pullorum and *S.* Enteritidis. The amplicon lengths of *S.* Pullorum were 167 and 257 bp, and the product sizes of *S.* Enteritidis were 167 and 333 bp (Fig. 3.6). Results showed that the mixed primer pairs could be specifically and effectively applied to the detection system of *S.* Pullorum and non-*S.* Pullorum. The results indicated that SPS4_00301–SPS4_00311 exists in *Salmonella enterica* subsp. *enterica* serotypes, which could be designed to identify *Salmonella* from other *Salmonella enterica* subsp. *enterica* serovars and non-*Salmonella enterica* subsp. *enterica* pathogens.

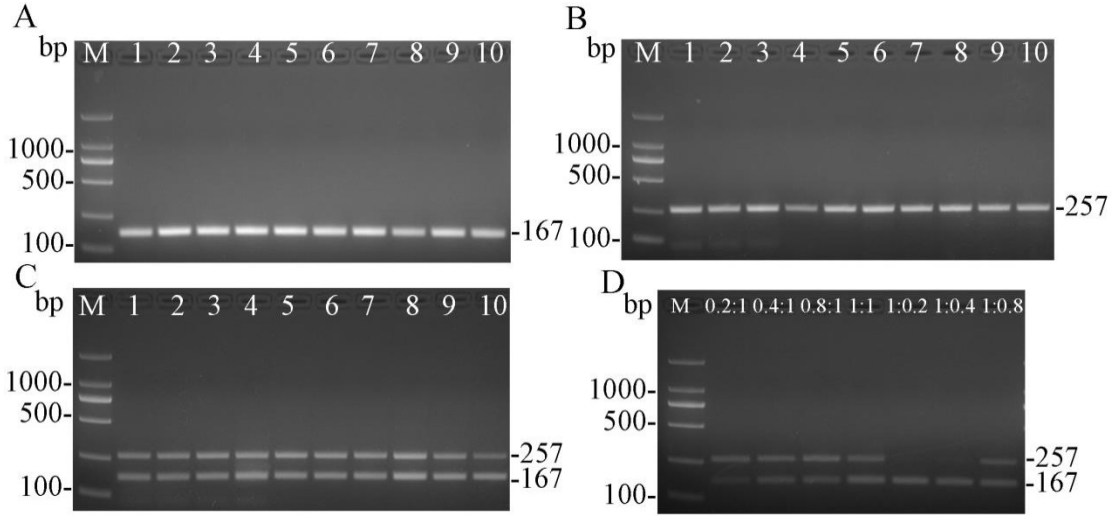

Fig. 3.5 Optimal temperature and combination ratio of two pairs of primers for the multiplex PCR.

Lane M: DL2000 DNA marker; Lanes 1–10: 52.5 °C, 53.3 °C, 54.2 °C, 55.3 °C, 56.4 °C, 57.6 °C, 58.7 °C, 59.8 °C, 60.7 °C, and 61.5 °C, respectively; (A) Annealing temperature optimization results of SPS4_00301–SPS4_00311 primers; (B) Annealing temperature optimization results of *citE2* primers; (C) Annealing temperature optimization results of SPS4_00301–SPS4_00311 and *citE2* primers;

(D) Volume ratio of two sets of primers ($V_{SPS4\_00301–SPS4\_00311}$:$V_{citE2}$).

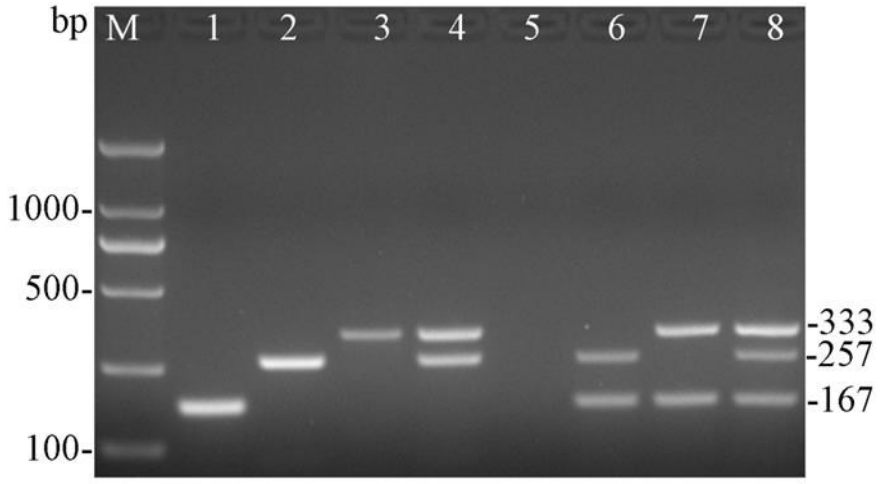

Fig. 3.6 Effect of PCR and multiplex PCR assays for detecting *S*.Pullorum.

Lane M: DL2000 DNA marker. Lane 1: *S*. Pullorum with SPS4_00301–SPS4_00311 primers; Lane 2: *S*. Pullorum with *citE2* primers; Lane 3: *S*. Enteritidis with *citE2* primers; Lane 4: Two target bacteria with *citE2* primers; Lane 5: Negative template (DDW) with mixed primer pairs; Lane 6: *S*. Pullorum with mixed primer pairs; Lane 7: *S*. Enteritidis with mixed primer pairs, and Lane 8: Two target bacteria with mixed primer pairs.

3.2.3 Specificity of the multiplex PCR

A total of 33 strains of *Salmonella* and 13 strains of non-*Salmonella enterica* subsp. *enterica* were tested to determine the specificity of the multiplex PCR assay. The amplicons of 167 and 257 bp size fragments were clearly generated on 1.5% agarose gels for *S.* Pullorum, and two bands with sizes of 167 and 333 bp were observed in 1.5% agarose gels for other *Salmonella* (Fig. 3.7 and Table 3.1). By contrast, non-*Salmonella enterica* subsp. *enterica* species and blank control did not have the specific band, indicating no cross amplification with other primers. Overall, we speculated that the multiplex PCR showed excellent specificity for the detection of *S.* Pullorum and non-*Salmonella*.

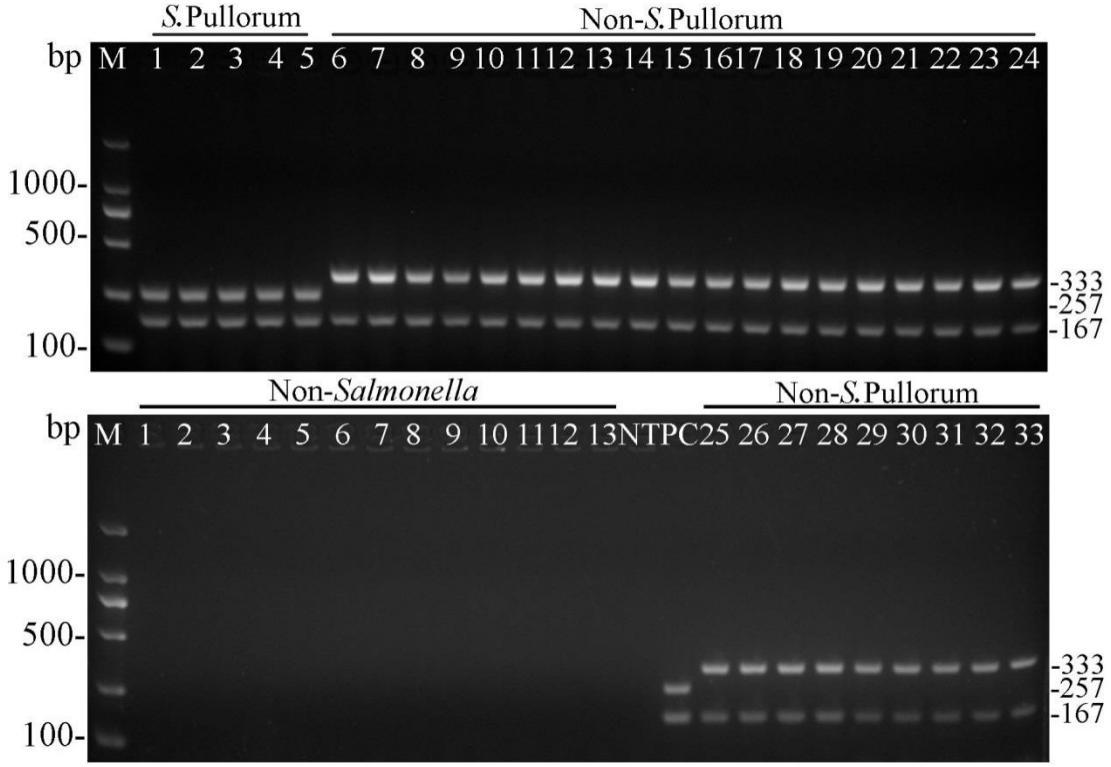

Fig. 3.7 Specificity of a multiplex PCR assay for the detection of *S.* Pullorum.

Lane M: DL2000 DNA marker; NT: Negative template (DDW); PC: Positive control (*S.* Pullorum CVCC 530); Non-*Salmonella*: Non-*Salmonella enterica* subsp. *enterica*. All strain details are shown in Table 3.1.

3.2.4 Sensitivity of the multiplex PCR assay

The genomic DNA concentration of *S.* Pullorum was aseptically diluted 10-fold from 62.5 ng/μL to 6.25 fg/μL as a template and tested using the multiplex PCR assay to assess the diagnostic sensitivity of the multiplex PCR system. The detection limit of the PCR method could reach at least 6.25 pg/μL genomic DNA (Fig. 3.8A). Pure *S.* Pullorum cells were diluted from 4×10^6 CFU/mL to 5×10^3 CFU/mL. Results showed that the purpose fragment (as low as 10 CFU per reaction) was still detected (Fig. 3.8B).

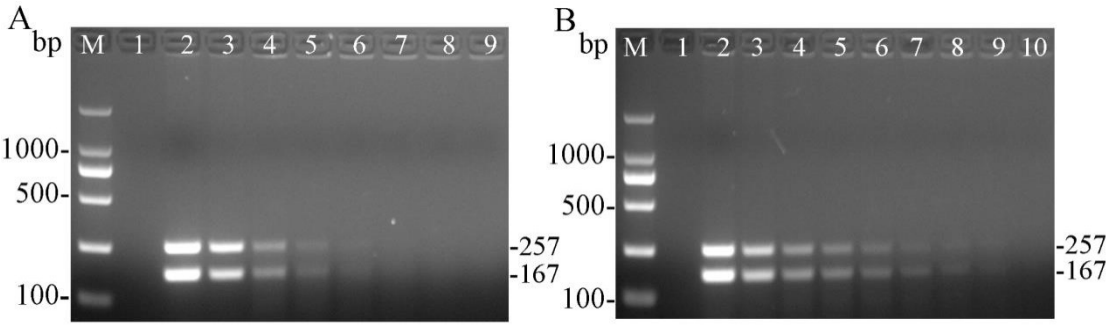

Fig. 3.8 Limit of detection of multiplex PCR assays for *S.* Pullorum.

Lane M: DL2000 DNA marker, Lane 1: Negative template (DDW); (A) PCR for the detection of *Salmonella* DNA samples. Lanes 2–9: 62.5 ng/μL, 6.25 ng/μL, 625 pg/μL, 62.5 pg/μL, 6.25 pg/μL, 625 fg/μL, 62.5 fg/μL, and 6.25 fg/μL, respectively; (B) PCR for the detection of S. Pullorum. Lanes 2–10: 4×10^6, 2×10^6, 1×10^6, 1×10^5, 8×10^4, 4×10^4, 2×10^4, 1×10^4, and 5×10^3 CFU/mL, respectively.

Table 3.2

List of nucleic acid-based assays for the determination of *S.* Pullorum/Gallinarum.

Methods	Target	Comment	Linear range	Sensitivity	References
Multiple PCR	*S.* Pullorum/Gallinarum	*cigR*	4×10^5 - 2×10^4 CFU/mL	2×10^4 CFU/mL	[23]
One-step PCR	*S.* Pullorum/Gallinarum	*flhB*	2×10^6 - 2×10^3 CFU/mL	2×10^3 CFU/mL	[196]
flgE-PCR	*S.* Pullorum/Gallinarum	*flgE*	10^9 - 10^5 CFU/mL	10^5 CFU/mL	[197]
LFNAA	*S.* Pullorum	*SEEP*	10 - 5×10^{-3} ng/ uL	5×10^{-3} ng/ uL	[198]
LP-LAMP	*S.* Pullorum	*rfbS*	49.2 ng/μL - 4.92 pg/μL	4.92 pg/μL	[199]
EA-probe	*S.* Pullorum	*rfbS*	4.53 pg/mL - 45.3 ng/μL	4.53 pg/μL	[200]
Multiplex qPCR	*S.* Pullorum/Gallinarum	*pSGP/pSG/pSP*	10^8 - 10^1 CFU/mL	10^1 CFU/mL	[201]

Continuation tabl.3.2

Multiplex PCR	*S.* Pullorum/Gallinarum	*tcpS*	2×10^7 - 2×10^4 CFU/mL	2×10^4 CFU/mL	[202]
PCR	*S.* Pullorum/Gallinarum	*ipaJ*	10^{10} - 10^5 CFU/mL	10^5 CFU/mL	[203]
CACA	*S.* Pullorum	*rfbS*	3.98×10^3 - 3.98 pg/μL	3.98 pg/μL	[204]
PCR	*S.* Pullorum	*SPUL 2693*	6.24×10^8 - 6×10^3 CFU/mL	6×10^3 CFU/mL	[205]
LAMP	*S.* Gallinarum	*sefA*	2×10^8 - 2×10^5 CFU/mL	2×10^5 CFU/mL	206]
Multiplex PCR	*S.* Pullorum/Gallinarum	*citE2*	4×10^6 - 10^4 CFU/mL	10^4 CFU/mL	in this study

3.2.5 Multiplex PCR assay evaluation in artificially contaminated egg samples

The different concentrations of *S.* Pullorum and *S.* Enteritidis from 10^6 CFU/mL to 10^0 CFU/mL were used to examine the detection sensitivity of the multiplex PCR assay for artificially contaminated egg samples. As shown in Fig. 3.9, the results of multiplex PCR with different enrichment time points corresponding to different concentrations of *S.* Pullorum and *S.* Enteritidis were detected. At initial inoculation concentrations of 10^6 and 10^5 CFU/mL per reaction, positive signals could be identified without enrichment. The limits of detection of the multiplex PCR assay in egg were 10^4 CFU/mL after 2 h enrichment, 10^1 CFU/mL after 6 h enrichment, and 10^0 CFU/mL after 10 h and 12 h enrichment, respectively. In addition, the detection limits of *S.* Pullorum and *S.* Enteritidis were similar to that of 10^4 CFU/mL viable *S.* Pullorum pure cells in this multiplex PCR assay. Results indicated that the multiplex PCR was experimentally sufficient for the target pathogen in artificially contaminated egg samples.

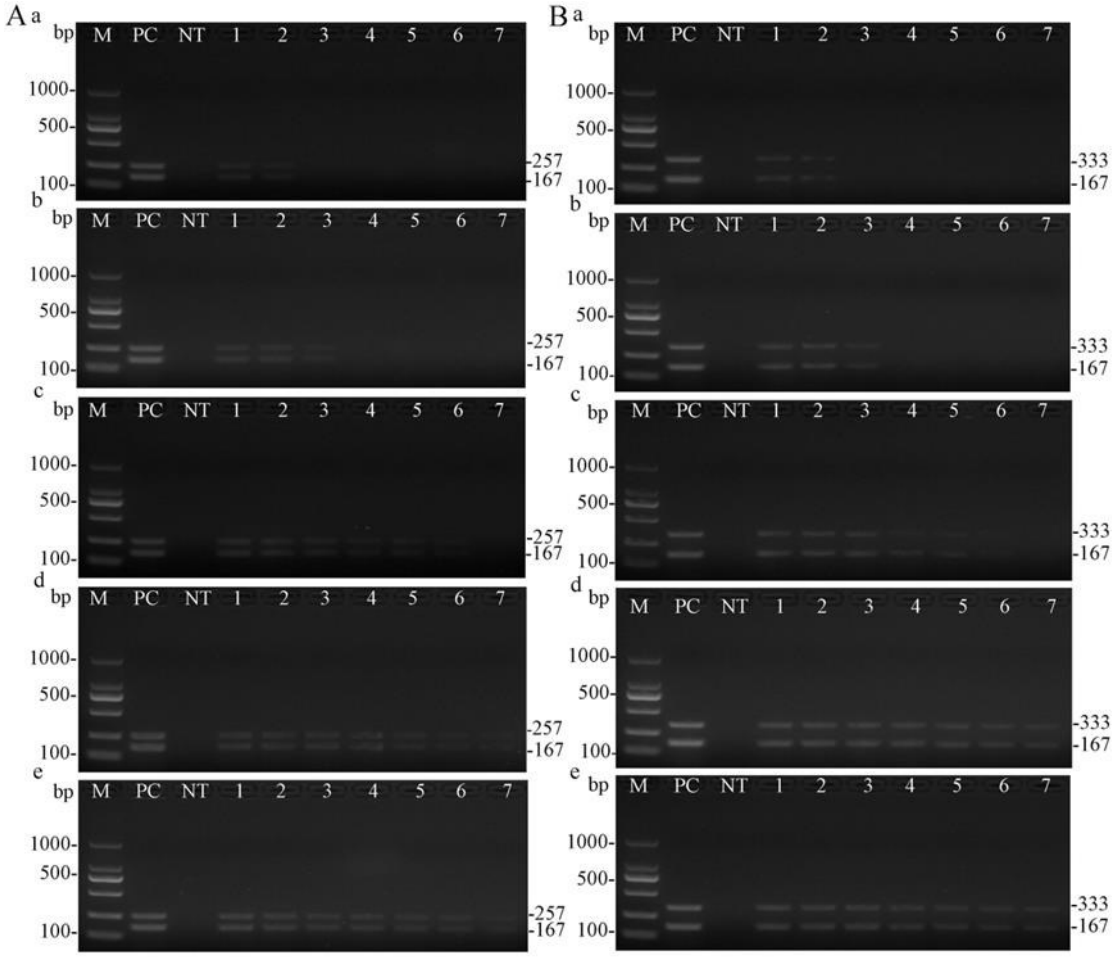

Fig. 3.9 Evaluation of multiplex PCR assay by using artificially contaminated egg samples.

(A) *S.* Pullorum and (B) *S.* Enteritidis. (a) 0, (b) 2, (c) 6, (d) 10, and (e) 12 h enrichment. Lane 1–7: 10^6 CFU/mL, 10^5 CFU/mL, 10^4 CFU/mL, 10^3 CFU/mL, 10^2 CFU/mL, 10^1 CFU/mL, 10^0 CFU/Ml; Lane M: DL2000 DNA marker; PC: Positive control (*S.* Pullorum CVCC 530 or *S.* Enteritidis ATCC 4931); NT: Negative template (DDW).

3.2.6 Application of the multiplex PCR assay in fecal samples

A total of 69 typical anal swab samples from chicken farms were simultaneously subjected to the multiplex PCR assay to test the diagnostic efficiency of this assay for the detection of *S.* Pullorum. As shown in Fig. 3.10, results demonstrated that 69 bacterial samples amplified two expected bands of 167 and 257 bp for *S.* Pullorum, and no PCR product was observed for 3 negative samples.The multiplex PCR method was excellent and consistent with the culture

method, indicating that the assay could be used for the clinical diagnosis of *S.* Pullorum.

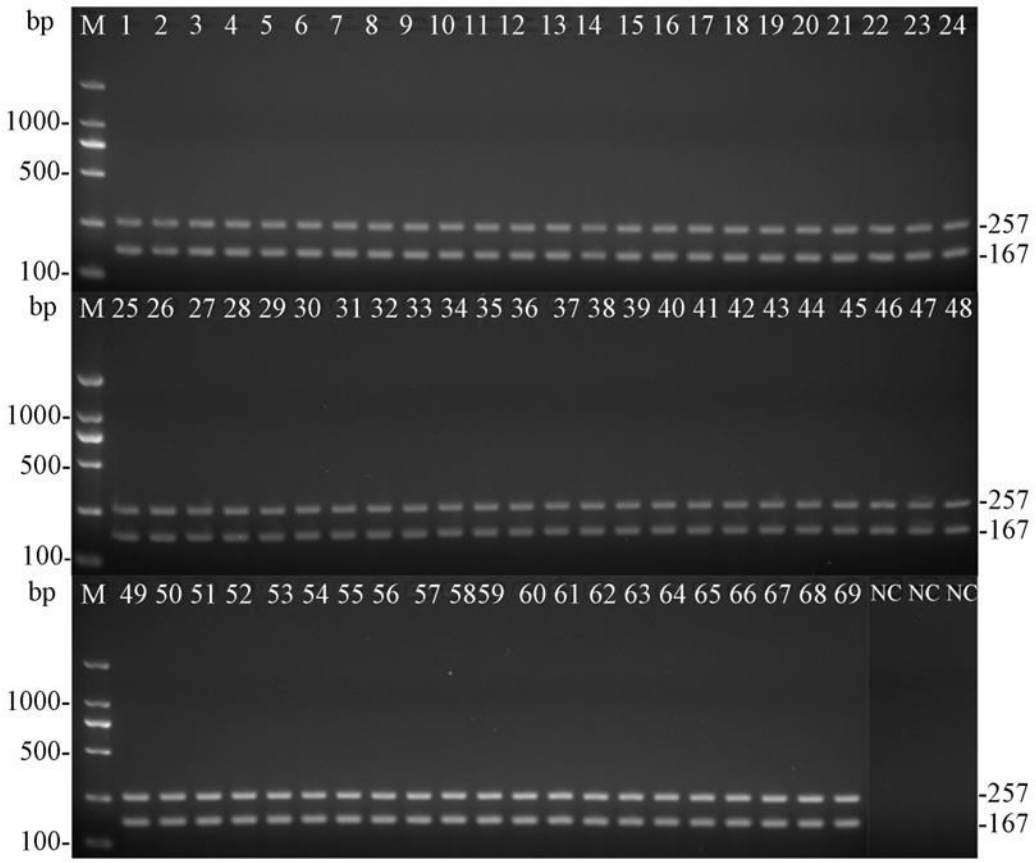

Fig. 3.10 Multiplex PCR assay for the detection of *S.* Pullorum from chicken anal swab samples.

Lane M: DL2000 DNA marker; Lanes 1–69: 69 wild strains of *S.* Pullorum from chicken farms; NC: Negative control (*Salmonella*-free).

3.2.7 Conclusions in chapter 3.2

The 76 bp fragment of the *citE2* gene in all *S.* Pullorum was absent compared with that in non-*S.* Pullorum. The intergenic sequence between SPS4_00301 and SPS4_00311 had 100% homology with all *Salmonella*. The sensitivity of the developed multiplex PCR system was 6.25 pg/μL and 10^4 CFU/mL for genomic DNA and *Salmonella* Pullorum cells, respectively. The multiplex PCR was a highly efficient and practical method to distinguish *S.* Pullorum of natural chicken anal swab and egg samples artificially contaminated with *S.* Pullorum and *S.* Enteritidis.

3.3 Construction and characterization of *steE* deletion mutant of *S.* Pullorum and its complementary strain

In order to define the role of *steE* in *S.* Pullorum virulence, the *steE* deletion mutant of *S.* Pullorum and its complemented strain were successfully constructed by λ-Red recombination technology and prokaryotic expression vector method, respectively, and then its characterization were analyzed. The biological characteristics of Δ*steE* strain were consistent with those of WT and its complementary (Δ*steE*+*steE*) strains. In addition, *steE* enhanced *S.* Pullorum invasion in HD-11 cells.

3.3.1 Construction and confirmation of the Δ*steE* strain

To identify the roles of *steE* in *S.* Pullorum, the *steE* deletion mutant of *S.* Pullorum was correctly constructed. The gene environment of *steE* is shown in Fig. 3.11A. *SteE* is the second open reading frame located in the Gifsy-1 in *Salmonella* chromosomal DNA, indicating horizontal transmission. A schematic diagram depicting the deletion strategy for Δ*steE* strain generation using λ-Red recombination system is shown in Fig. 3.11B.

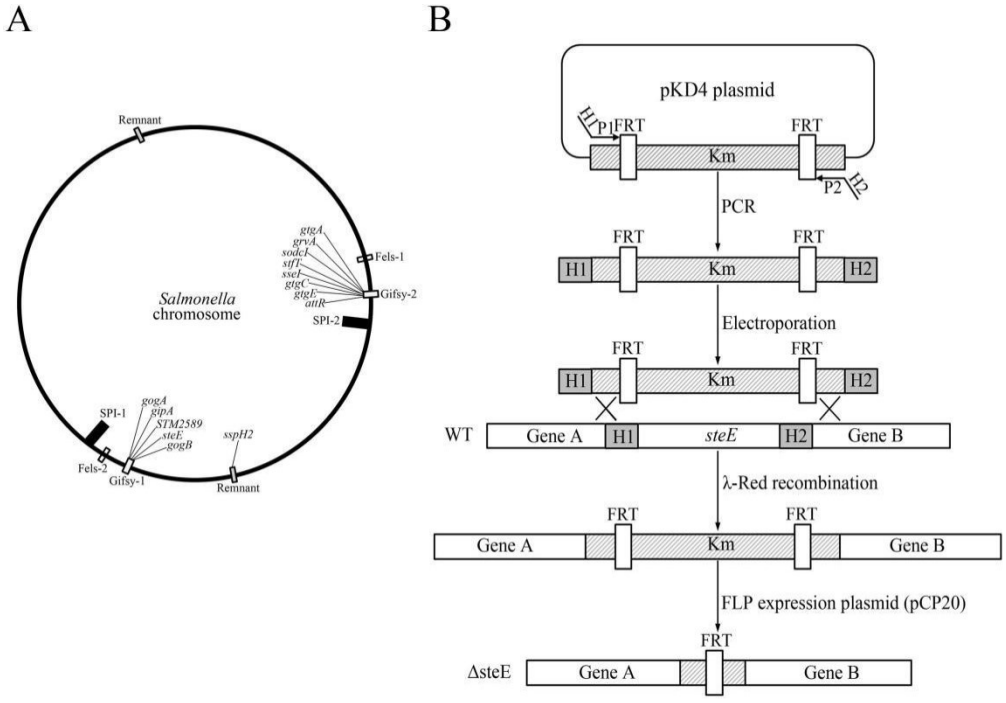

Fig. 3.11 Schematic diagrams for the location and construction of the Δ*steE* strain.

The upstream and downstream homologous arms of the *steE* gene and Kan gene with fragment size of 1567 bp were obtained from pKD46 plasmid by PCR method using primers P1/P2 (Fig. 3.12A). The Δ*steE*::kan strain had a length of 2169 bp by PCR method using primers CX1/CX2 (Fig. 3.12B). The Δ*steE* strain was verified by PCR using primers CX1/CX2 or N1/N2 to generate a 1089 bp or 224 bp fragment (Fig. 3.12C). These results indicated that the Δ*steE* strain was successfully constructed. (A) The location of *steE* in *Salmonella* chromosome DNA was indicated. The map was depicted from Coombes et al and Klumpp et al [128, 207]; (B) Construction of the Δ*steE* strain with λ-Red recombination system.

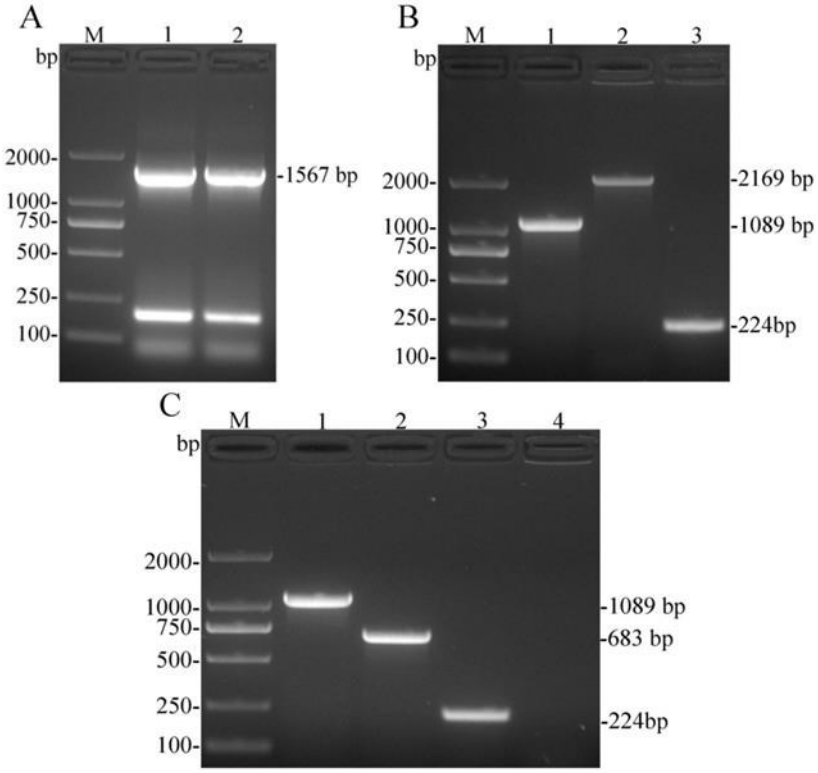

Fig. 3.12 Identification of the Δ*steE* strain by PCR method

M: DL 2000 DNA marker. (A) PCR identification of pKD4 plasmid with primers P1/P2; 1, 2: PCR products from pKD4 plasmid; (B) PCR identification of the Δ*steE*::kan strain with primers CX1/CX2 or N1/N2; 1: WT; 2, 3: Δ*steE*::kan; (C) PCR identification of the Δ*steE* strain with primers CX1/CX2 or N1/N2; 1: WT strain; 2, 3: Δ*steE* strain; 4: Negative control.

3.3.2 Confirmation of the Δ*steE*+*steE* strain

The Δ*steE*+*steE* strain was verified by PCR method using primers CX1/CX2

or N1/N2. As shown in Fig. 3.13, the WT and Δ*steE* strains have a length of 1089 bp or 683 bp by PCR method using primers CX1/CX2, respectively. In addition, the WT and Δ*steE*+*steE* strains have a length of 224 bp by PCR method using N1/N2 primers. These results indicated that the Δ*steE*+*steE* strain were successfully constructed.

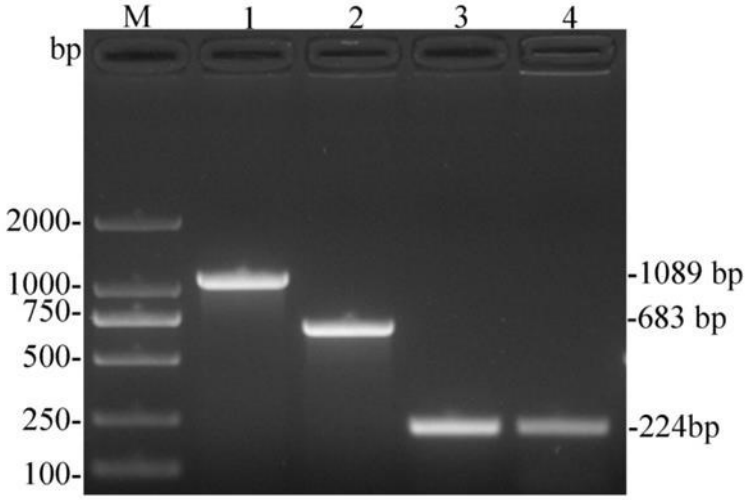

Fig. 3.13. PCR identification of the Δ*steE*+*steE* strain.

PCR identification of the Δ*steE*+*steE* strain with primers CX1/CX2 or N1/N2. M: DL 2000 DNA marker; 1, 3: WT strain; 2: Δ*steE* strain; 4: Δ*steE*+*steE* strain.

3.3.3 The growth curve and biochemical characteristics of the Δ*steE* strain

The growth curve analysis revealed no significant differences among the WT, Δ*steE* and Δ*steE*+*steE* strains cultured in LB broth at different time points at 37 °C (Fig. 3.14). Similar to the WT and Δ*steE* strains, the Δ*steE* strain was able to ferment mannitol, glucose, arabinose, ornithine, mannose, decarboxylase and lysine decarboxylase activity, but could not utilize sucrose, hydrogen sulfide, maltose, sorbitol, lactose, malonate and urease. It shows that the deletion of *steE* gene in *S.* Pullorum does not affect the biochemical characteristics of the WT strain.

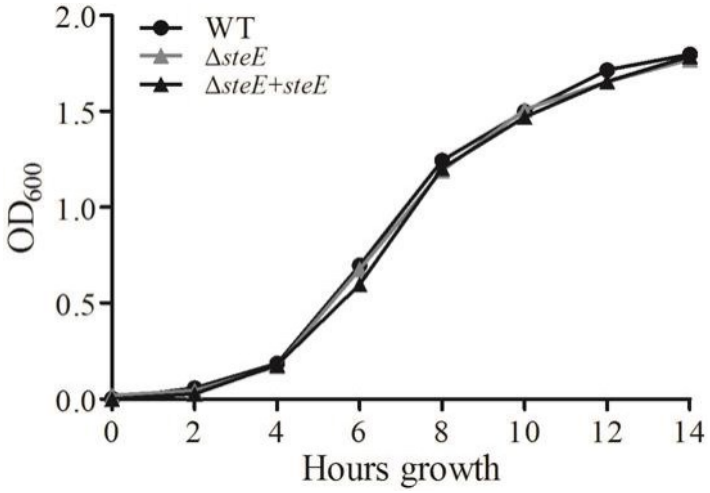

Fig. 3.14 Growth curves of the WT, Δ*steE* and Δ*steE* +*steE* strains in LB broth.

The OD600 values of WT, Δ*steE* and Δ*steE* +*steE* strains cultures were determined in 2 h intervals by spectrophotometry, respectively.

3.3.4 *SteE* promoted *S.* Pullorum invasion in HD-11 cells

To evaluate the effect of *steE* for *S.* Pullorum invasion, HD-11 cells was infected with mCherry-*S.* Pullorum, DAPI staining was observed by laser scanning confocal microscopy. The result showed a large number of *S.* Pullorum within the HD-11 cells were observed in WT or Δ*steE* +*steE* strain infected group compared to that of the cells infected with the Δ*steE* strain (Fig. 3.15).

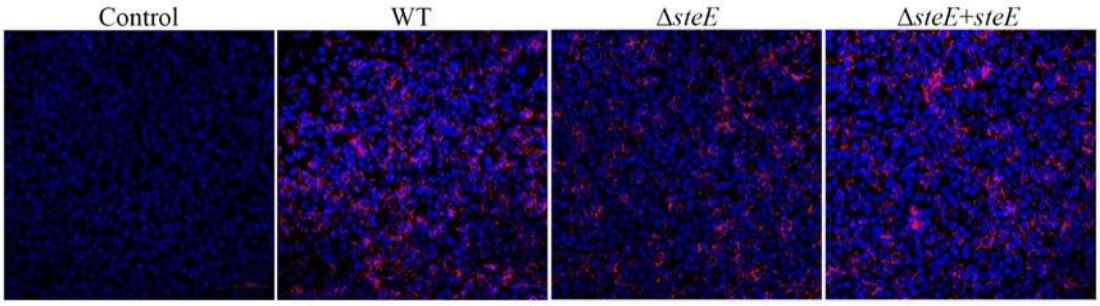

Fig. 3.15. S*teE* promotes *S.* Pullorum invasion in HD-11 cells.

HD-11 cells were infected with mCheery-*S.* Pullorum strain at a MOI of 10:1 at 3 hpi, and the red fluorescence was observed by confocal laser scanning microscopy (20 ×).

3.3.5 Conclusions in chapter 3.3

The *steE* deletion mutant of *S.* Pullorum and its complemented strain were successfully constructed by λ-Red recombination technology and prokaryotic

expression vector method, respectively. The deletion of *steE* in *S.* Pullorum had no effect the growth and biochemical characteristics, but its invasion ability decreased significantly in HD-11 cells.

3.4 *SteE* enhances the colonization of *S.* Pullorum in chickens

In order to investigate the role of *steE* on the colonization of *S.* Pullorum in the main organs of chicken, we used WT and Δ*steE* strains infected chickens, respectively. The results of virulence assay showed that the LD_{50} of Δ*steE* was 22.8 times higher than that of WT in chickens. The colonization experiment of *S.* Pullorum showed that the overall change trend of the number of WT and Δ*steE* strains were similar in chicken livers, spleens, hearts, bursas, and cecums, which increased first and then decreased. Therefore, *steE* caused significantly increased colonization of *S.* Pullorum in a chicken infection model.

3.4.1 *SteE* reduces the virulence of *S.* Pullorum in chickens

The virulence of WT and Δ*steE* strains was analyzed in chickens, respectively. As shown in Table 3.3, the LD_{50} of WT strain was 9.14×10^7 CFU, but LD_{50} of the Δ*steE* strain was 2.08×10^9 CFU. The LD_{50} of Δ*steE* strain was 22.8 times higher than that of WT strain. The result showed that *steE* can increased the virulence of *S.* Pullorum.

Table 3.3

LD_{50} of the WT and Δ*steE* strains.

Strain	Challenge doses	Dead counts/Chicken counts	LD_{50}/CFU
WT	1×10^{10}	10/10	9.14×10^7
	1×10^9	10/10	
	1×10^8	6/10	
	1×10^7	2/10	
	1×10^6	0/10	
Δ*steE*	1×10^{11}	10/10	2.08×10^9
	1×10^{10}	9/10	
	1×10^9	3/10	
	1×10^8	0/10	
	1×10^7	0/10	

3.4.2 Clinical symptoms and changes of autopsy

The chickens were infected with WT or Δ*steE* strain. At 3 day after infection, the chickens were depressed and had a poor appetite, accompanied by the phenomenon of gathering together. Some chicks could not stand steadily, discharged white sticky feces, and the feathers around the anus were covered with feces. As shown in Fig. 3.16, the pathological change of chicken organs infected with WT strain were more serious than that of the Δ*steE* strain and control groups as follows: there were dark red needle tips and large bleeding spots at the edge of the liver, splenomegaly, dark red in color, bursal enlargement, the cecum has puffing and bleeding, heart congestion, swelling with blood filaments.

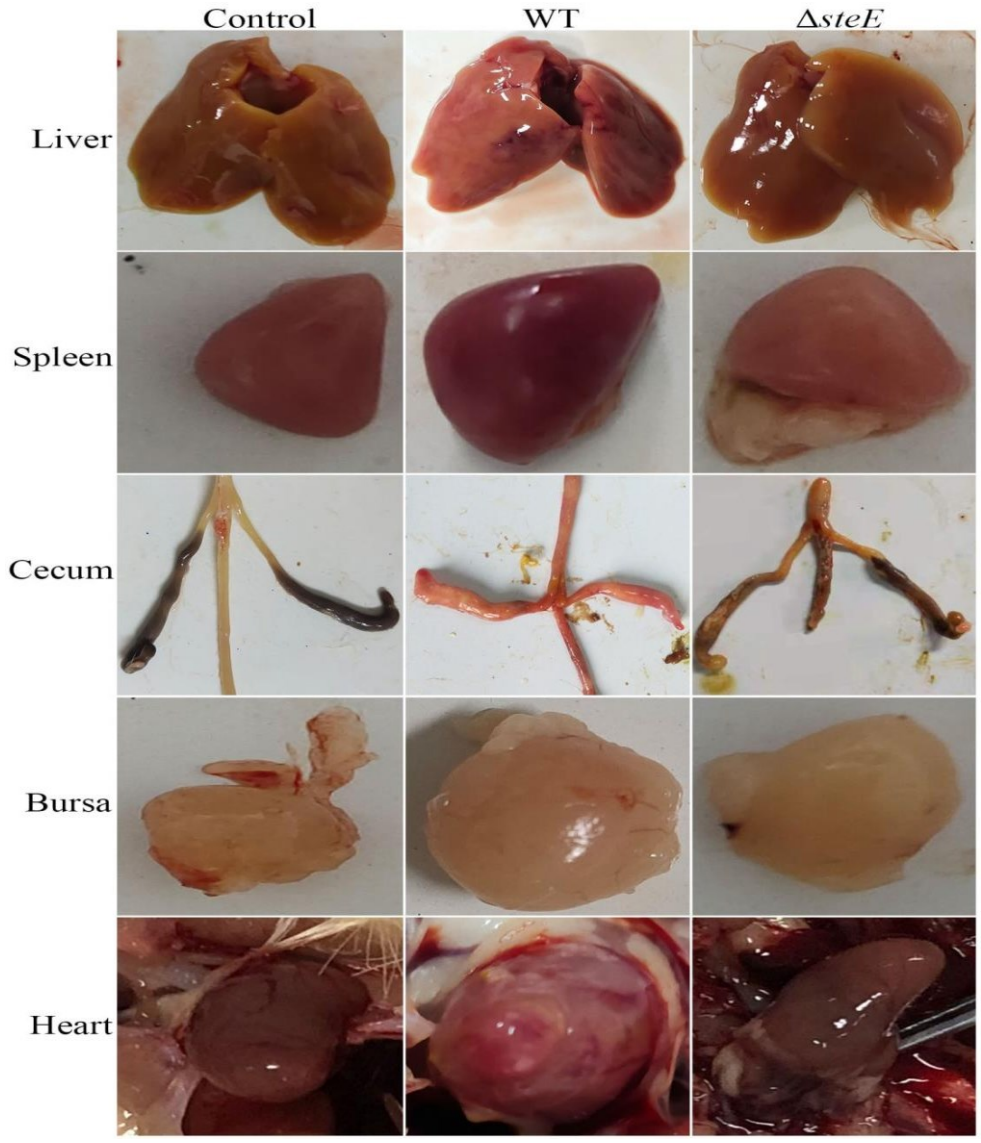

Fig. 3.16. Anatomical symptoms of chickens infected with WT and Δ*steE* strains.

3.4.3 *SteE* enhances the colonization of *S.* Pullorum in chicken cecums

The results of bacterial colonization showed that the number of WT and Δ*steE* strains in chicken cecums were increased from 12 h to 3 d, but decreased from 3 d to 7 d (Fig. 3.17). At 3 days after infection, the colonization of WT and Δ*steE* stains reached the peak in chicken cecums, and the settlement amount of WT and Δ*steE* strains reached the lowest at 7 d. The change trend of WT and Δ*steE* strains were increased at first and then decreased in the whole process of the infection, but the settled quantity of Δ*steE* strain was always lower than that of WT strain in chicken cecums.

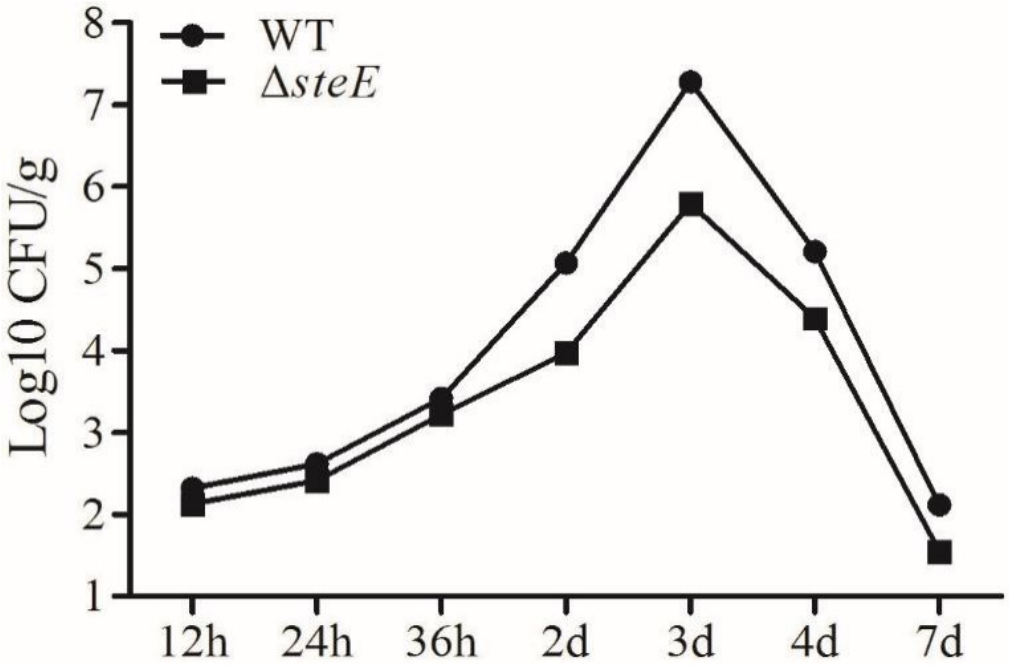

Fig. 3.18 The change of *S.* Pullorum colonization in chicken cecums.

3.4.4 *SteE* enhances the colonization of *S.* Pullorum in chicken livers

The results of bacterial colonization showed that the number of WT and Δ*steE* strains in chicken livers were increased from 12 h to 4 d in the whole process of the infection, and decreased significantly from 4 d to 7 d (Fig. 3.19). The total amount of Δ*steE* strain was increased from 12 h to 3 d after infection, and decreased from 4 d to 7 d. The colonization of WT and Δ*steE* strains reached the peak about 4 d in chicken lives after infection. The change trend of WT and Δ*steE* strains increased first and then decreased in the whole experiment process, but the settled quantity of Δ*steE* strain was always lower than that of WT strain in chicken lives.

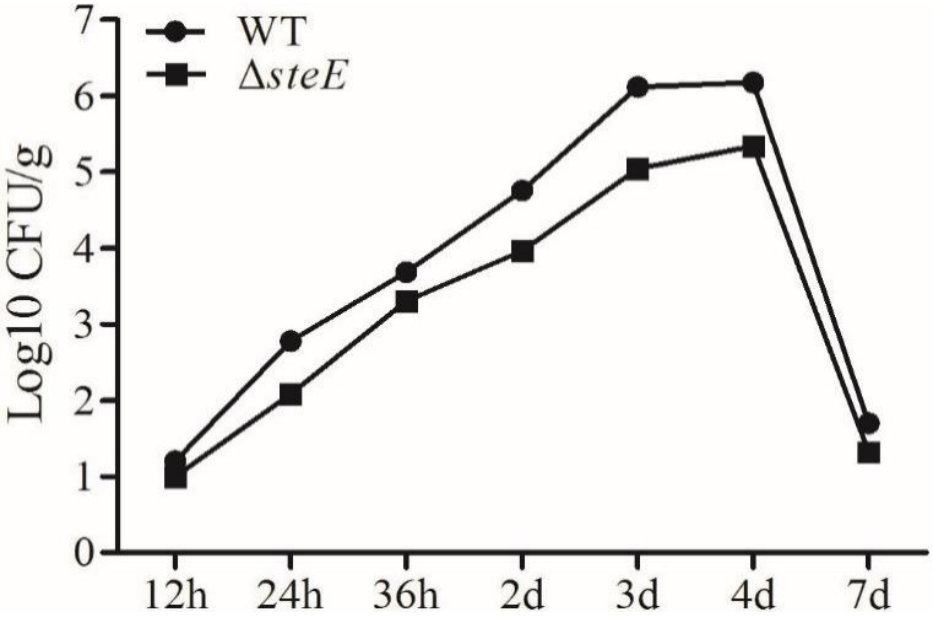

Fig. 3.19 The change of *S.* Pullorum colonization in chicken livers.

3.4.5 *SteE* enhances the colonization of *S.* Pullorum in chicken spleens

The colonization of WT and Δ*steE* strains were increased from 12 h to 3 d after chicken infection, and decreased significantly from 3 d to 7 d in chicken spleens (Fig. 3.20). The colonization of WT and Δ*steE* strains reached the peak about 3 d in chicken spleens after infection. The change trend of WT and Δ*steE* strains increased at first and then decreased in the whole process of the infection, but the settled quantity of Δ*steE* strain was always lower than that of WT strain in chicken spleens.

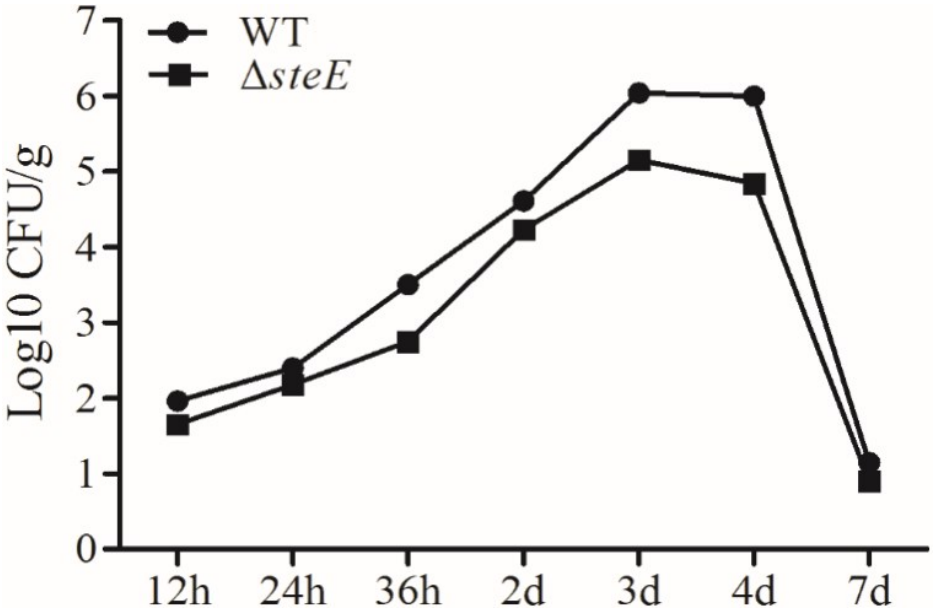

Fig. 3.20. The change of *S.* Pullorum colonization in chicken spleens.

3.4.6 *SteE* enhances the colonization of *S.* Pullorum in chicken bursas

The colonization of WT strain was increased from 12 h to 3 d in chicken bursa, increased slowly at 36 h, and decreased from 3 d to 7 d. The results showed that WT strain reached the peak about 3 d in chicken bursas after infection (Fig. 3.21). The change trend of Δ*steE* strain in chicken bursas is basically consistent with that of *S.* Pullorum, while the settled number of Δ*steE* strain was always lower than that of WT strain in chicken bursas.

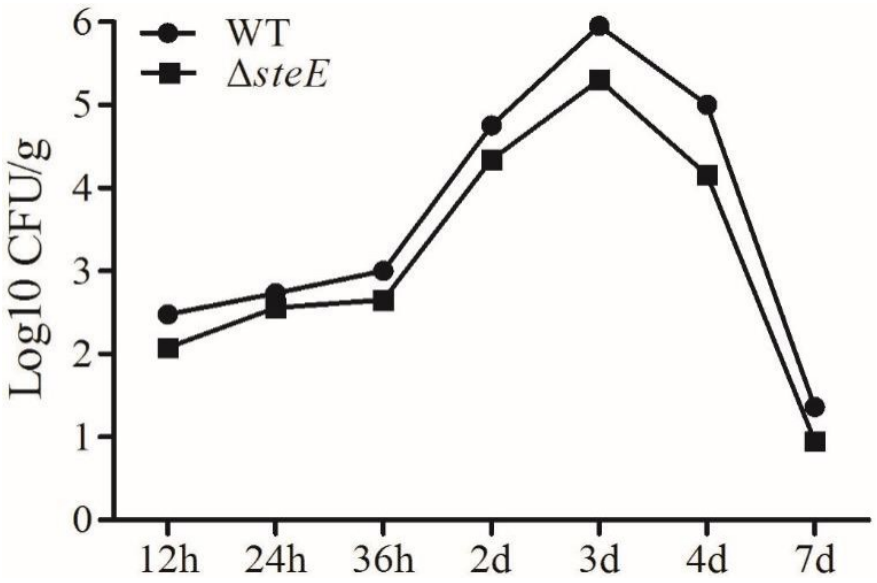

Fig. 3.21 The change of *S.* Pullorum colonization in chicken bursas.

3.4.7 *SteE* enhances the colonization of *S.* Pullorum in chicken hearts

The colonization of WT and Δ*steE* strains were increased from 12 h to 4 d in hearts after chicken infection, and decreased from 4 d to 7 d. As shown in Fig. 3.22, the bacterial number of WT and Δ*steE* stains reached the peak about 4 days in chicken hearts after chicken infection, the settlement amount of WT and Δ*steE* strains reached the lowest at 7 d. The change trend of WT and Δ*steE* strains were increased at first and then decreased in the whole process of the infection, but the settled quantity of Δ*steE* strain was always lower than that of WT strain in chicken hearts.

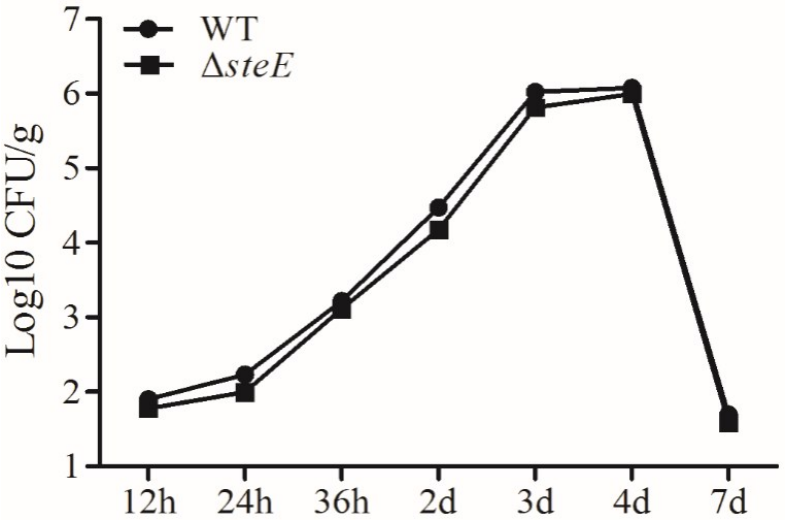

Fig. 3.22. The change of *S.* Pullorum colonization in chicken hearts.

3.4.8 Conclusions in chapter 3.4

The deletion of *steE* caused significantly decreased the virulence of *S.* Pullorum, and its pathogenicity and colonization were also significantly reduced compared with *S.* Pullorum in chickens.

3.5 *SteE* enhances the virulence of *S.* Pullorum in chickens by regulating the inflammation response

To elucidate the functions of *steE* in *S.* Pullorum, Δ*steE* strain was constructed using the λ-Red recombination technology. Compared to that in the wild-type, the deletion of *steE* in *S.* Pullorum reduced bacterial invasion, proliferation, and late apoptosis in the infected HD-11 cells. In addition, we analyzed the mRNA expression levels of effector genes and cytokines by qRT-PCR. *SteE* was associated with the regulation of various effector genes and inflammatory cytokines in HD-11 cells during *S.* Pullorum infection. Effector steE promoted the expression of anti-inflammatory cytokines (*IL-4* and *IL-10*) and reduced that of pro-inflammatory cytokines (*IL-1β*, *IL-6* and *IL-12*) compared to that in the Δ*steE*-infected HD-11 cells and chicken spleens. Results from the chicken infection model showed that the deletion of *steE* resulted in significantly decreased colonization and long-term survival of the bacteria and alleviated pathological lesions compared to those in the wild-type. Further, *steE* increased the virulence of *S.* Pullorum in chickens by regulating the expression of inflammatory cytokines.

3.5.1 Role of *steE* in the adhesive, invasive, and proliferative abilities of *S.* Pullorum in HD-11 cells

The adhesive, invasive, and proliferative abilities of the WT and Δ*steE* strains were examined in HD-11 cells. The Δ*steE* strain had no significant effect on *S.* Pullorum adhesion to HD-11 cells (Fig. 3.23A). However, the invasive ability of Δ*steE* strain was significantly reduced compared to that of the WT strain. Additionally, lower proliferation levels were observed with Δ*steE* compared to the WT, and a significant difference was observed at 3, 15, and 20 h in HD-11 cells (Fig. 3.23B). In addition, the intracellular replication of the WT strain showed an increase from 0 to 6 h hpi and subsequently decreased from 6 to 20 hpi. These results indicated that deletion of *steE* reduced the colonization and survival of the bacteria *in vitro*.

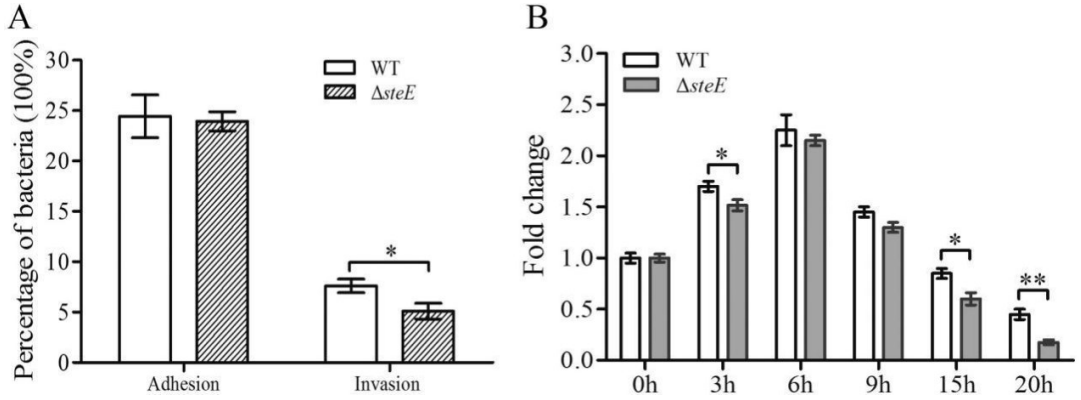

Fig. 3.23. Adhesive, invasive, and proliferative abilities of the WT and Δ*steE* strains in HD-11 cells.

(A) The percent adhesion and invasion were calculated by comparing bacterial recovery from the primary inoculum at 1 and 2 hour post-infection (hpi);

(B) (B) Proliferation of the WT or Δ*steE* strains within HD-11 cells. It denotes the number of bacteria invading HD-11 cells after a 1 h incubation with 10% FBS and 10 μg/mL gentamicin, which was set as 1 and shown as 0 h time point in the figure. The fold-change is the number of intracellular bacteria at 0, 3, 6, 9, 15, and 20 h/the initial intracellular bacteria present (0 h). $^{*}p < 0.05$; $^{**}p < 0.01$.

3.5.2 Effector gene expression in HD-11 cells infected with WT and Δ*steE* strains

To identify the effects of *steE* deletion on *S*. Pullorum effector genes, mRNA expression levels of the genes were evaluated at 3, 8, and 16 h via qRT-PCR. The transcriptional level of *steE* was not detected in the Δ*steE* strain-infected HD-11 cells, confirming its successful deletion in *S.* Pullorum (Fig. 3.24B). The T3SS1 and T3SS2 effector genes showed differential expression in the WT strain-infected cells. Transcription levels of *sipA*, *sipC*, and *prgH* were significantly decreased in cells infected with the WT compared to Δ*steE*-infected cells at 3 and 8 hpi, but no significant difference was observed at 16 hpi (Fig. 3.24A). However, the deletion of *steE* significantly reduced the transcriptional levels of *sefC*, *ssaV*, and *hilA* in HD-11 cells compared to those in the WT at 8 hpi, but the mRNA levels of *ssaT*, *sseC*, and *spiC* did not significantly differ between the two infected groups at 3, 8, and 16 hpi. The mRNA transcription levels of *sspH2*, *sseG*, *steA*, and *steB* were significantly decreased in cells infected with WT compared to those in the Δ*steE*-infected cells at 3 and 8 hpi, and a significant decrease was detected in *sifB* and *pipB* mRNA levels between strains at 8 hpi (Fig. 3.24B). In addition, *sseJ* showed lower levels at three different time points in the Δ*steE* strain-infected HD-11 cells as compared to those in WT, and *sseF* expression was significantly decreased at 8 and 16 hpi (Fig. 3.24B). These results indicated that *steE* reduces the expression of T3SS2 effector genes and few T3SS1 effector genes.

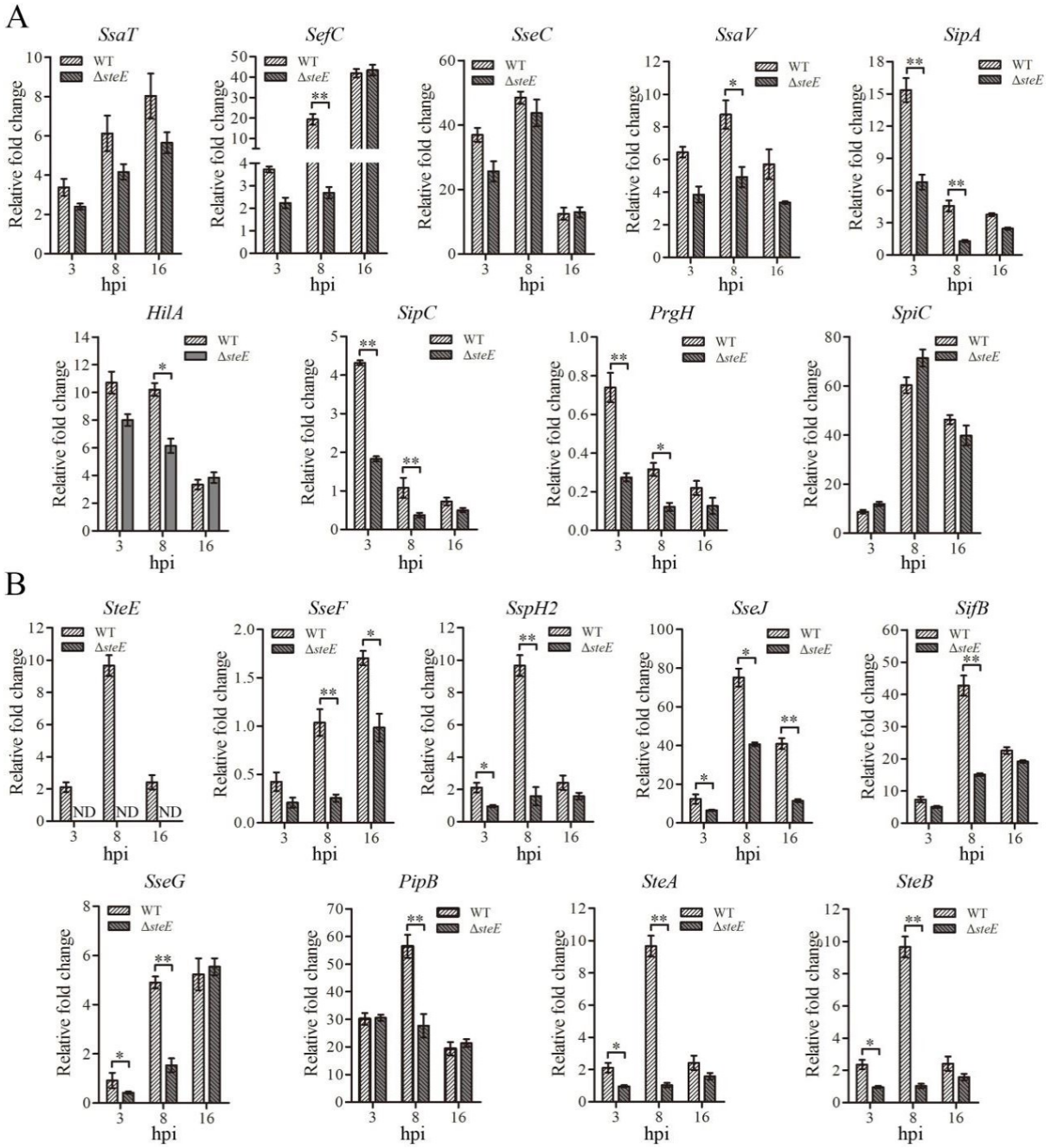

Fig. 3.24 Relative expression levels of effector genes in HD-11 cells infected with the WT and Δ*steE* strains.

The expression levels of T3SS1 effector genes *ssaT, sefC*, *sseC*, *ssaV*, *sipA*, *hilA*, *sipC*, *prgH*, and *spiC* (A) and the T3SS2 effector genes *steE*, *sseF*, *sspH2*, *sseJ*, *sseG*, *sifB*, *pipB*, *steA*, and *steB* (B) in HD-11 cells infected WT and Δ*steE* strains were evaluated via qRT-PCR at 3, 8, and 16 hpi compared to those with the WT strain at 1.5 hpi. *Gmk* was used as an internal control to analyze the relative mRNA levels of effector genes. ND indicates not detected. $^{*}p < 0.05$; $^{**}p < 0.01$.

3.5.3 *SteE* promotes apoptosis in HD-11 cells

To assess the effect of *steE* deletion on apoptosis in HD-11 cells, annexin V-FITC/PI analysis was performed. Deletion of *steE* significantly reduced late apoptosis in HD-11 cells as compared to WT strain, although no significant difference was detected for early apoptosis (Fig. 3.25). These results suggest that infection with Δ*steE* significantly reduces late apoptosis in HD-11 cells relative to infection with the WT strain.

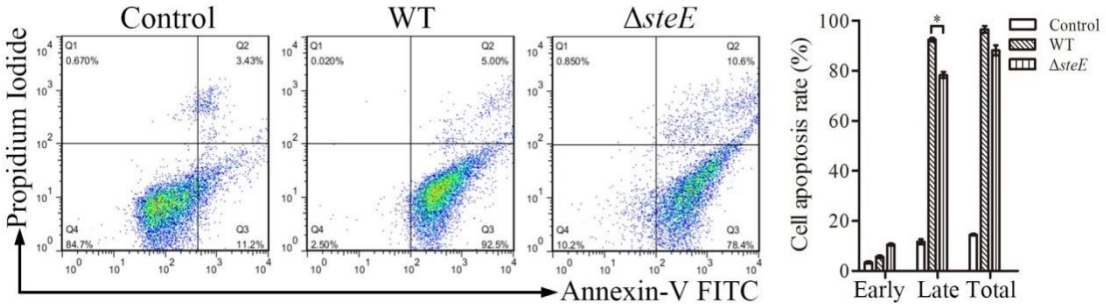

Fig. 3.25. HD-11 cells infected with WT strain promote apoptosis as compared to the Δ*steE* strain.

The apoptosis rates were analyzed using flow cytometry. HD-11 cells were collected to analyze total apoptosis (early + late) at 3 hpi. Representative images and the statistical histogram are shown in the left and right panels, respectively. The scatter diagram shows the early (Q2) and late (Q3) apoptosis rates.

3.5.4 *SteE* is required for WT strain-induced cytokine expression in HD-11 cells

To investigate the effect of *steE* on the immune response *in vitro*, the expression levels of several cytokines were examined using HD-11 cells infected with WT and Δ*steE* strains via qRT-PCR at 4, 8, and 16 hpi. *IL-12* expression was strongly increased in Δ*steE* strain-infected HD-11 cells at 8 hpi (Fig. 3.26), but the difference was not significant between the two groups at 4 and 16 hpi. *IL-6* expression was higher in the Δ*steE* vs. WT strain-infected group at 8 hpi. However, the expression levels of *iNOS* and *IL-1β* were strongly increased in HD-11 cells infected with the Δ*steE* strain compared to those in the WT at 16 hpi.

TNF-α expression was similar between the two groups at 4, 8, and 16 hpi. In addition, Δ*steE* strain significantly reduced the expression of the anti-inflammatory cytokine IL-10 in infected HD-11 cells at 8 and 16 hpi; however, *IL-4* and *TGF-β1* mRNA level differences were significantly lower in HD-11 cells infected with the Δ*steE* strain than in the WT at 16 hpi. These results illustrated the anti-inflammatory effects of *steE* in cells infected with *S.* Pullorum.

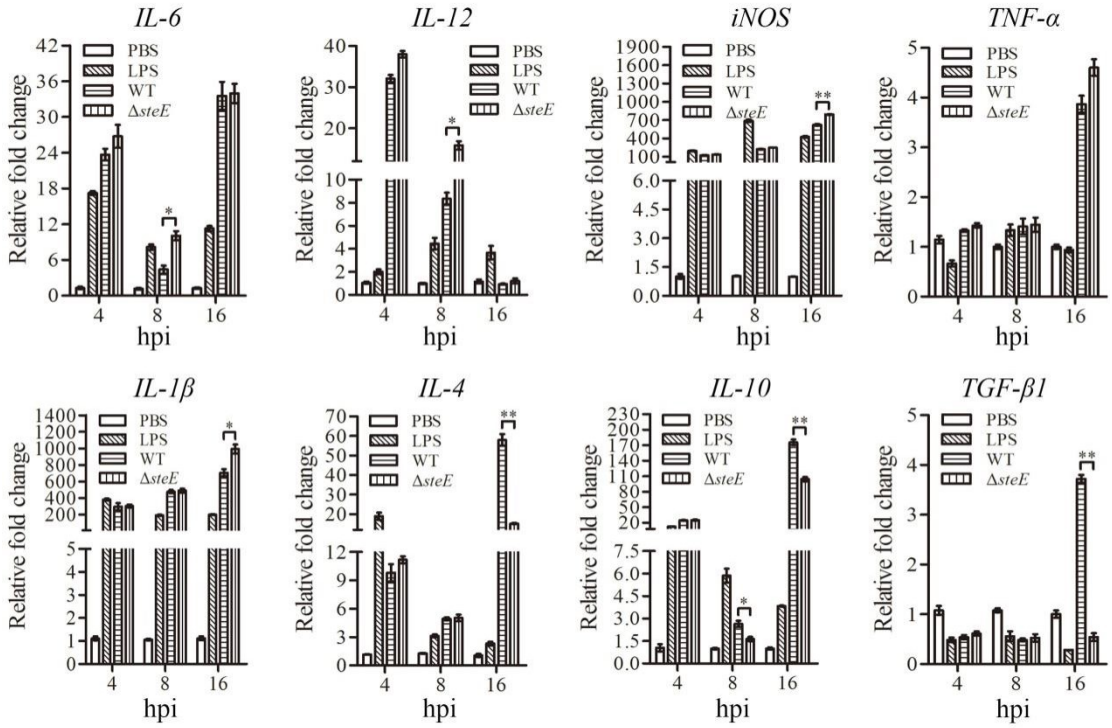

Fig. 3.26. *SteE* is integral for *S.* Pullorum-induced cytokine expression in HD-11 cells.

Relative expression levels of *IL-6*, *IL-12*, *iNOS*, *TNF-α*, *IL-1β*, *IL-4*, *IL-10*, and *TGF-β1* were evaluated via qRT-PCR at 4, 8, and 16 hpi. The mRNA levels of cytokines were evaluated relative to *β-actin* expression. $^{*}p < 0.05$; $^{**}p < 0.01$.

3.5.5 *SteE* regulates the expression of inflammatory cytokines in chicken spleens

To test the effect of *steE* on inflammatory responses *in vivo*, cytokines from the spleen of chickens infected with WT and Δ*steE* strains were analyzed via qRT-PCR. *IL-6* expression was significantly higher in the Δ*steE* strain group than that

in the WT strain group at 3 dpi, but no difference was detected in *iNOS* production between the two groups at 1, 3, and 7 dpi (Fig. 3.27). The expression levels of *IL-1β* and *TNF-α* were strongly increased in Δ*steE* vs. WT strain group at 3 dpi, but no difference was detected between strains at 1 and 7 dpi. In addition, the expression levels of *TGF-β1* was decreased significantly in the Δ*steE* strain infected group than that in the WT strain group at 1 and 3 dpi. The data showed that *steE* was closely associated with the expression of anti-inflammatory and pro-inflammatory cytokines *in vivo*.

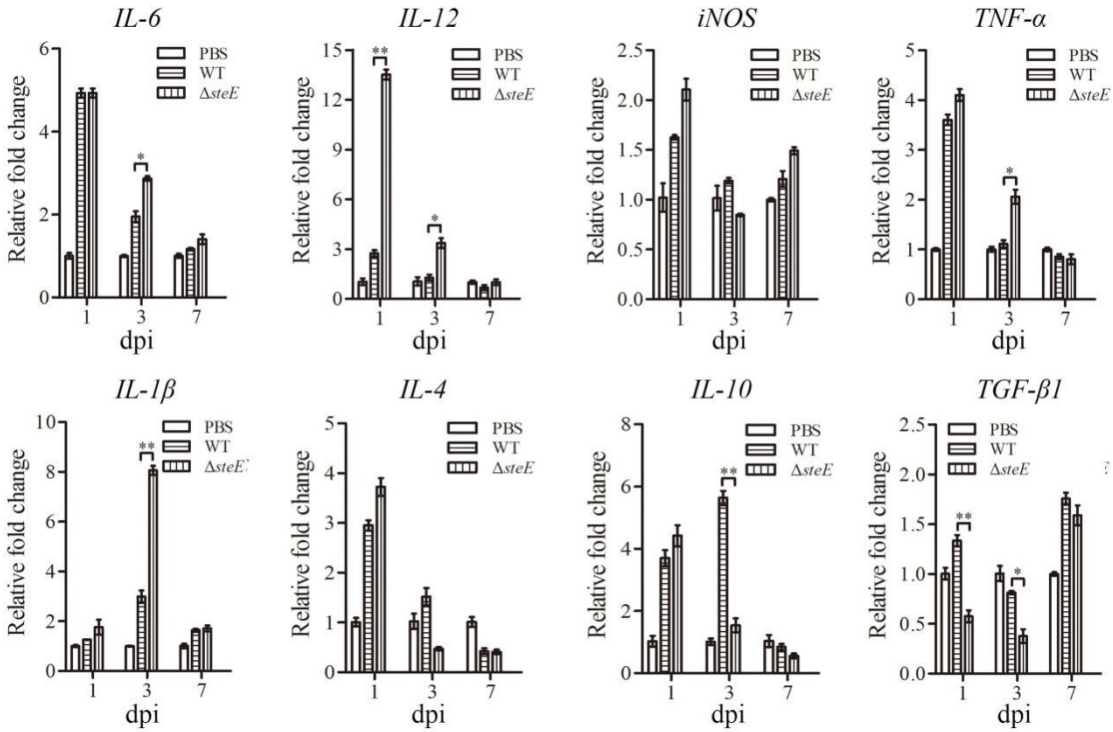

Fig. 3.27. *SteE* regulates the expression of inflammatory cytokines in chicken spleens.

The expression levels of *IL-6*, *IL-12*, *iNOS*, *TNF-α*, *IL-1β*, *IL-4*, *IL-10*, and *TGF-β1* in chicken spleens infected with WT and Δ*steE* strains were analyzed via qRT-PCR at 1, 3, and 7 dpi. The mRNA levels of cytokines were analyzed relative to *β-actin* expression. $^{*}p < 0.05$; $^{**}p < 0.01$.

3.5.6 *SteE* enhances the virulence of *S.* Pullorum in chickens

To further investigate the effects of *steE* on colonization ability, we evaluated the bacterial load and long-term survival ability of the strains in chickens. Results

showed that *steE* deletion decreased the colonization ability of *S.* Pullorum in the liver, spleen, and bursa of chickens at 3 dpi. The total number of bacteria recovered from the liver and spleen of the WT strain-infected chickens was significantly greater than those infected with Δ*steE* (Fig. 3.28A). The competition index (CI) were <1, indicating that the deletion of *steE* reduced colonization, sustainability, and fitness of *S.* Pullorum relative to the WT strain in chickens (Fig. 3.28B). Similar to the competitive index assays, the equivalent bacterial burden analysis showed that chicken inoculated orally with the Δ*steE* strain had a moderately long-term survival (Fig. 3.28C).

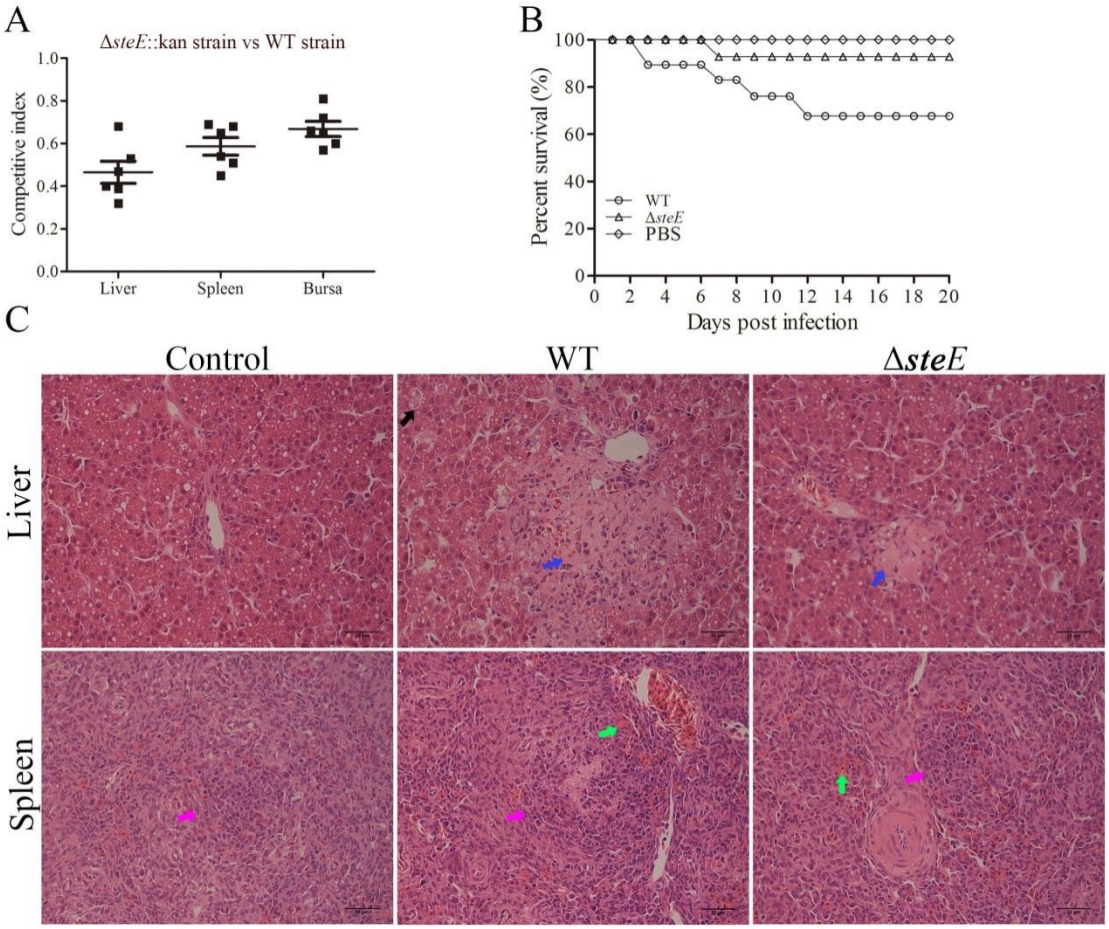

Fig. 3.28. *S.* Pullorum Δ*steE* reduces virulence in chickens.

To examine the effect of *steE* deletion on the virulence of *S.* Pullorum, we compared the histopathological lesions induced by the WT and Δ*steE* strains in chickens. As shown in Fig. 3.28D, the histopathological analysis showed a marked difference between chickens infected with the WT and Δ*steE* strains. The chickens infected with the Δ*steE* strain showed weak pathological lesions in the liver and

spleen, including exudative nodules (black arrow), granular degeneration (blue arrow) of liver cells, splenic corpuscles (pink arrow) and congestion (green arrow). No significant damages were observed in the control group. Overall, the results from the chicken infection model suggest that *steE* is essential for virulence.

(A) *SteE* contributes to WT strain growth in chickens. Chickens were infected orally with 2×10^8 CFU of a mixture of the Δ*steE*::Kan and WT strains prepared at a ratio of 1:1, and CFUs were evaluated from the liver, spleen, and bursa at 3 dpi using the plating assay; (B) *SteE* contributes to WT virulence in chickens. The experimental groups were infected orally with 10^9 CFU of the WT or Δ*steE* strain, and the control group was administered PBS. The chickens were monitored daily for 20 dpi to evaluate the survival rate; (C) Histopathology of the liver and spleen tissues from chickens infected with the strains. Chickens were infected orally with 10^9 CFU of the strains, and the liver and spleen samples were collected at 3 dpi for histological analysis. Hematoxylin and eosin staining analysis showed the pathological changes in the infected livers and spleens (400 ×; scale bar: 25 μm).

3.5.7 Conclusions in chapter 3.5

SteE was required for *S.* Pullorum invasion and proliferation and increased late apoptosis in HD-11 cells. *SteE* reduces the expression of T3SS2 effector genes and few T3SS1 effector genes in HD-11 cells. *SteE* had the anti-inflammatory effects in cells infected with *S.* Pullorum. Furthermore, the Δ*steE* strain significantly decreased pathological lesions and virulence of *S.* Pullorum in chickens by regulating the inflammation response.

3.6 *SteE* regulates Th1/Th2 cytokine expression in chickens during *S.* Pullorum infection

In this study, chickens were artificially infected with WT, Δ*steE*, and Δ*steE*+*steE* strains, respectively, and then the mRNA levels of inflammatory genes in tissues were analyzed by using qRT-PCR at 3 days post-infection. Compared with those of the WT or Δ*steE*+*steE* strain-infected group, the mRNA transcript

levels of *IL-12* and *IFN-γ* were significantly higher, whereas the *IL-10* mRNA expression was significant decreased in the Δ*steE* strain-infected liver and bursa; the *IL-4* displayed dramatically decreased transcriptional level in the Δ*steE* strain-spleen, cecum, and heart; the *IL-10* mRNA expression was significantly lower in the Δ*steE* strain-infected spleen and cecum.

3.6.1 *SteE* changes the mRNA levels of inflammatory cytokines in the liver of *S.* Pullorum infected-chickens

As shown in Fig. 3.29, the mRNA levels of *IL-12* and *IFN-γ* were significantly higher in the spleen of the Δ*steE* group than that in the WT or Δ*steE*+*steE* group at 3 dpi. The mRNA level of *IL-10* was significantly lower in the spleen of the Δ*steE* group than that in the WT or Δ*steE*+*steE* group, whereas the mRNA level of *IL-4* was not significant difference.

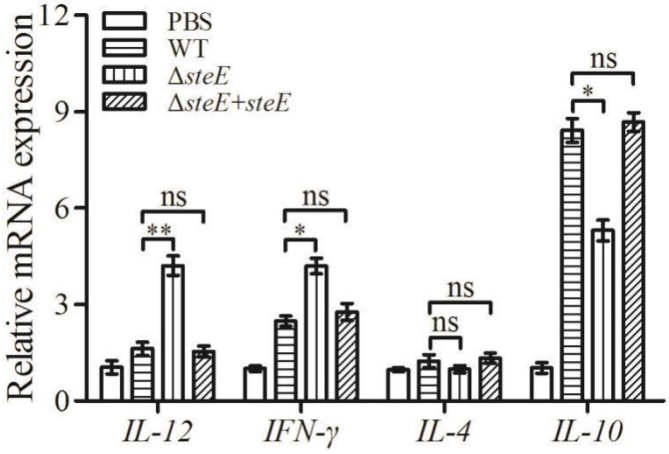

Fig. 3.29 *SteE* changes the mRNA levels of inflammatory cytokines in the liver of chickens during *S.* Pullorum infection.

3.6.2 *SteE* changes the mRNA levels of inflammatory cytokines in the spleen of *S.* Pullorum infected-chickens

To identify whether *steE* can influence the mRNA levels of inflammatory cytokines in spleen from chickens infected with *Salmonella*, the mRNA levels of *IL-12*, *IFN-γ*, *IL-4*, and *IL-10* were examined by qRT-PCR. As shown in Fig. 3.30, the mRNA level of *IL-12* was significantly higher in the spleen of the Δ*steE* group

than that in the WT or Δ*steE*+*steE* strain group at 3 dpi. As to the mRNA levels of anti-inflammatory cytokines, the *IL-4* and *IL-10* were dramatically decreased in the spleen of the Δ*steE* group compared to the WT or Δ*steE*+*steE* group, whereas the mRNA level of *IFN-γ* was not significant difference.

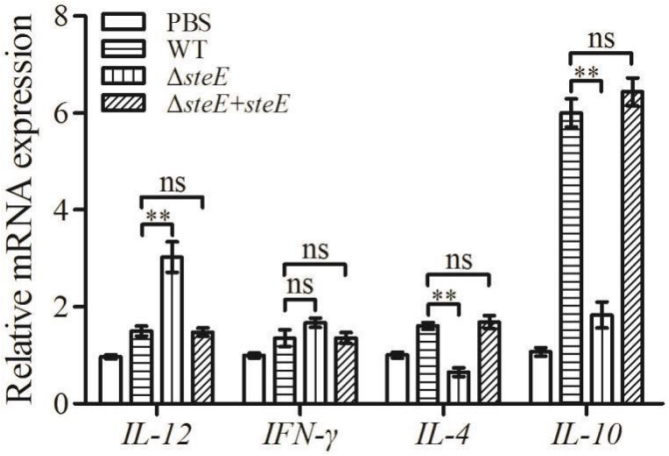

Fig. 3.30 *SteE* changes the mRNA levels of inflammatory cytokine in the spleen of chickens during *S.* Pullorum infection.

3.6.3 *SteE* changes the mRNA levels of inflammatory cytokines in bursa of *S.* Pullorum infected-chickens

As shown in Fig. 3.31, the mRNA levels of *IL-12* and *IFN-γ* were significantly higher, but no difference was detected in *IL-4* in the spleen of the Δ*steE* group than that in the WT or Δ*steE*+*steE* group at 3 dpi. The mRNA level of *IL-10* was significantly lower in the spleen of the **Δ***steE* group than that in the WT or Δ*steE*+*steE* group.

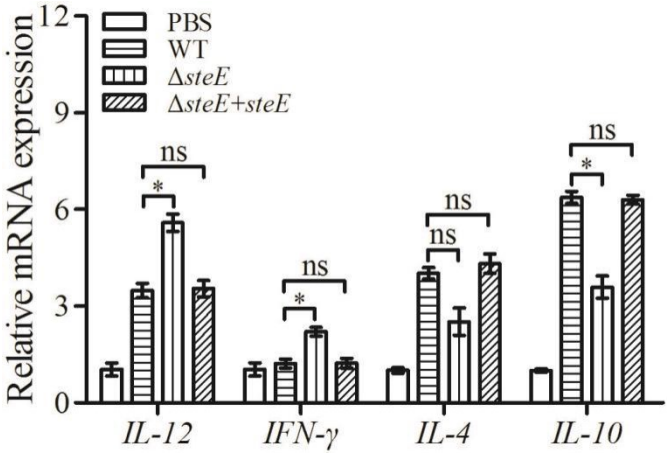

Fig. 3.31 *SteE* changes the mRNA levels of inflammatory cytokines in the bursa of chickens during *S.* Pullorum infection.

3.6.4 *SteE* changes the mRNA levelss of inflammatory cytokines in cecum of *S.* Pullorum infected-chickens

As shown in Fig. 3.32, the mRNA levels *IL-12* and *IFN-γ* were not significantly difference in in the spleen of the Δ*steE* group than that in the WT or Δ*steE*+*steE* group at 3 dpi. The mRNA levels of *IL-4* and *IL-10* were significantly lower in the spleen of the Δ*steE* group than that in the WT or Δ*steE*+*steE* group.

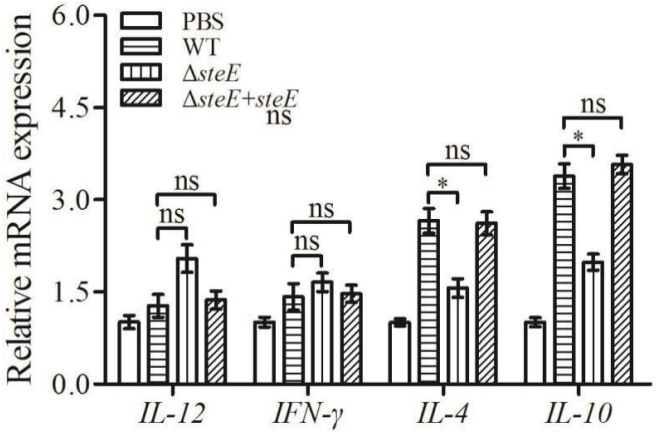

Fig. 3.32 *SteE* changes the mRNA levels of inflammatory cytokines in cecum of chickens during *S.* Pullorum infection.

3.6.5 *SteE* changes the mRNA levels of inflammatory cytokines in the heart of *S.* Pullorum infected-chickens

As shown in Fig. 3.33, the mRNA levels of *IL-12*, *IFN-γ*, and *IL-10* were not significantly difference in in the heart of the **Δ***steE* group than that in the WT or Δ*steE*+*steE* group at 3 dpi. The mRNA level of *IL-4* was significantly lower in the spleen of the Δ*steE* group than that in the WT or Δ*steE*+*steE* group.

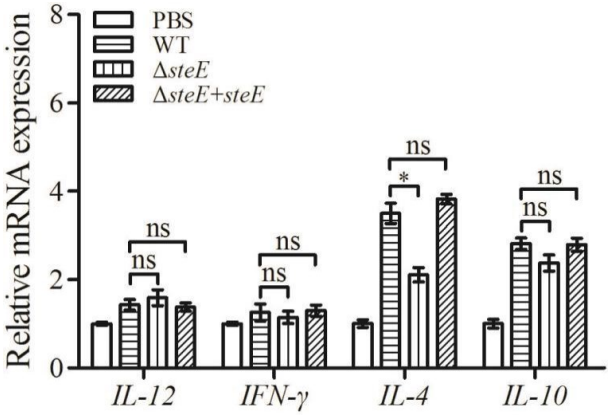

Fig. 3.33 *SteE* changes the mRNA levels of inflammatory cytokines in the heart of chickens during *S.* Pullorum infection.

3.6.6 Conclusions in chapter 3.6

SteE can regulate the balance of Th1/Th2 cytokine response in *S.* Pullorum-infected chicken. And *steE* increased the anti-inflammation response induced by strong Th2 immune response.

3.7 *S.* Pullorum effector SteE regulates Th1/Th2 cytokine expression by triggering the STAT3/SOCS3 pathway that suppresses NF-κB activation

In this study, our aim was to evaluate, for the first time, the effects of *steE* on the Th1/Th2 balance, STAT3/SOCS3 pathway and NF-κB P65 activation in *S.* Pullorum-infected HD-11 cells and chicken models. We demonstrated that *steE* diminished the expression of Th1-related cytokines (*IFN-γ* and *IL-12*) and promoted the expression of Th2-related cytokines (*IL-4* and *IL-10*) in HD-11 cells and chicken models of S. Pullorum infection. SOCS3 silencing suppressed the function of *steE* in HD-11 cells, led to the imbalance of Th1/Th2-related cytokines. *SteE* promoted SOCS3 expression by activating STAT3 in HD-11 cells. Moreover, *steE* inhibited NF-κB P65 expression and blocked its translocation to the nucleus by promoting SOCS3 expression.

3.7.1 *SteE* regulates Th1/Th2-related cytokines during *S.* Pullorum infection

We determined whether *steE* modulated the mRNA levels of inflammatory Th1/Th2-related cytokines in HD-11 cells and chicken models of S. Pullorum infection using qRT-PCR. As shown in Fig. 3.34, the mRNA levels of *IFN-γ* were higher in the Δ*steE* strain-infected HD-11 cells than in the WT or Δ*steE* + *steE*-infected HD-11 cells, while *IL-10* mRNA levels were significantly lower in the Δ*steE* strain-infected HD-11 cells than that in the WT or Δ*steE* + *steE*-infected HD-11 cells at 1, 2, 3, and 4 hpi. The WT or Δ*steE* + *steE*-infected HD-11 cells significantly decreased the *IL-12* mRNA levels but increased the *IL-4* mRNA levels as compared to Δ*steE* strain-infected HD-11 cells at 2 and 3 hpi. However, *IL-12* and *IL-4* mRNA levels showed no significant differences between WT or Δ*steE* + *steE*-infected HD-11 cells and Δ*steE*-infected HD-11 cells at 4 hpi. These

results suggest that *steE* regulated the mRNA levels of Th1/Th2-related cytokines in *S.* Pullorum-infected HD-11 cells.

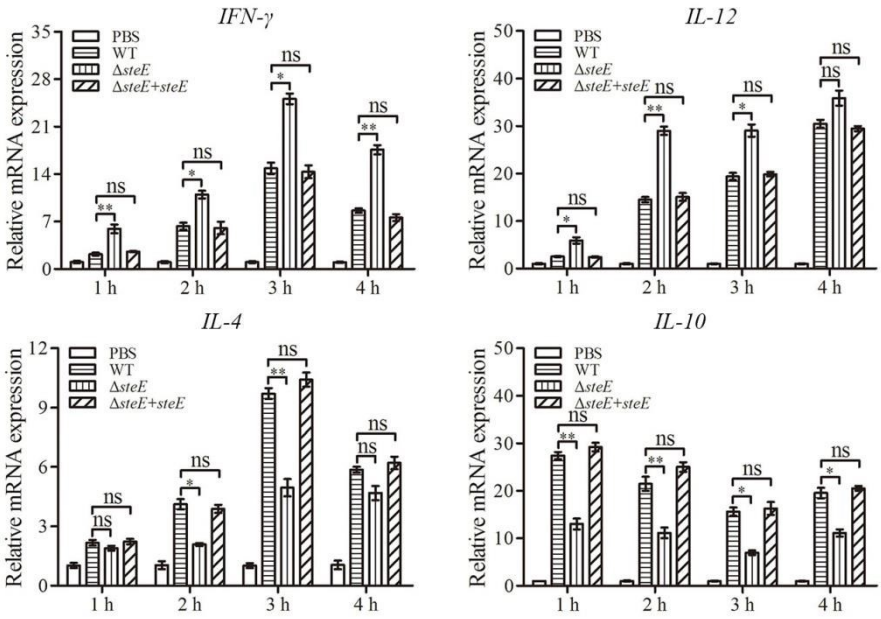

Fig. 3.34. *SteE* regulates Th1/Th2-related cytokines in HD-11 cells and chickens during *S.* Pullorum infection.

HD-11 cells were infected with the WT, Δ*steE* or Δ*steE* + *steE* strain at MOI of 10 for 1, 2, 3, and 4 h, and *IFN-γ*, *IL-12*, *IL-4*, and *IL-10* mRNA levels were determined using qRT-PCR. The experiments were performed in three biological replicates for each target gene. *P < 0.05, **P < 0.01.

3.7.2 *SteE* regulates Th1/Th2-related cytokines by targeting SOCS3

To determine whether *steE* enhanced the transcription of SOCS3, HD-11 cells were infected with the WT, Δ*steE*, or Δ*steE* + *steE* strain. *SOCS3* mRNA levels were reduced in the Δ*steE*-infected HD-11 cells than in the WT or Δ*steE* + *steE* strain at 2, 3, and 4 h (Fig. 3.35A), which suggests that *steE* enhanced the transcription of *SOCS3* in *S.* Pullorum-infected HD-11 cells. To determine whether SOCS3 was involved in the regulation of inflammatory responses, we overexpressed *socs3* in HD-11 cells, which was confirmed using western blotting, where SOCS3 level was significantly increased in *socs3*-overexpressing HD-11 cells (Fig. 3.35B). *SOCS3* overexpression in HD-11 cells significantly decreased *IFN-γ* and *IL-12* mRNA levels but increased *IL10* mRNA levels, whereas *IL-4* mRNA levels did not significantly difference (Fig. 3.35C).

Next, we confirmed whether *steE* regulated inflammatory responses in the *socs3*-silenced HD-11 cells model. qRT-PCR showed that *IFN-γ* and *IL-12* mRNA levels were significantly higher in the Δ*steE*-infected siNT-treated cells than in the WT or Δ*steE* + *steE* -infected siNT-treated cells, whereas the mRNA levels of *IL-4* and *IL-10* were significantly reduced in the Δ*steE*-infected siNT-treated cells. However, *IFN-γ*, *IL-12*, *IL-4*, and *IL-10* mRNA levels did not significantly difference between Δ*steE*-infected siSOCS3-treated cells and WT or Δ*steE* + *steE*-infected siSOCS3-treated cells (Fig. 3.35D). In contrast to the pEGFP-N1 plasmid and siNT group, the downregulation of *IFN-γ* and *IL-12* mRNA levels were induced by co-transfection with the *steE* overexpression plasmid and siNT group, whereas *IL-4* and *IL-10* mRNA levels were upregulated. After SOCS3 knockdown, *IFN-γ*, *IL-12*, *IL-4*, and *IL-10* mRNA levels did not significantly difference in HD-11 cells co-transfected with the *steE* overexpression plasmid and siSOCS3 group compared to that of the pEGFP-N1 plasmid and siSTAT3 group (Fig. 3.35E). Collectively, these data demonstrate that SOCS3 was involved in regulating the balance of Th1/Th2-related cytokines in HD-11 cells induced by *steE*.

(A) HD-11 cells were infected with the WT, Δ*steE*, or Δ*steE* + *steE* strain at MOI of 10 for 1, 2, 3, and 4 h. The *SOCS3* mRNA level was determined using qRT-PCR; (B, C) HD-11 cells were transfected with pEGFP-N1 or pEGFP-*socs3* for 48 h*;* (B) The SOCS3 protein level was determined using western blotting; (C) *IFN-γ*, *IL-12*, *IL-4*, and *IL-10* mRNA levels were assessed using qRT-PCR; (D) HD-11 cells were transfected with siNT or siSOCS3; after 48 h, they were then infected with the WT, Δ*steE* or Δ*steE* + *steE* strain at MOI of 10 for 2 h. *IFN-γ*, *IL-12*, *IL-4*, and *IL-10* mRNA levels were determined using qRT-PCR; (E) HD-11 cells were co-transfected with siSOCS3 and pEGFP-*steE* and incubated for 48 h. The mRNA levels of *IFN-γ*, *IL-12*, *IL-4*, and *IL-10* were determined using qRT-PCR. The experiments were performed in triplicate for each target gene. *$P < 0.05$, **$P < 0.01$.

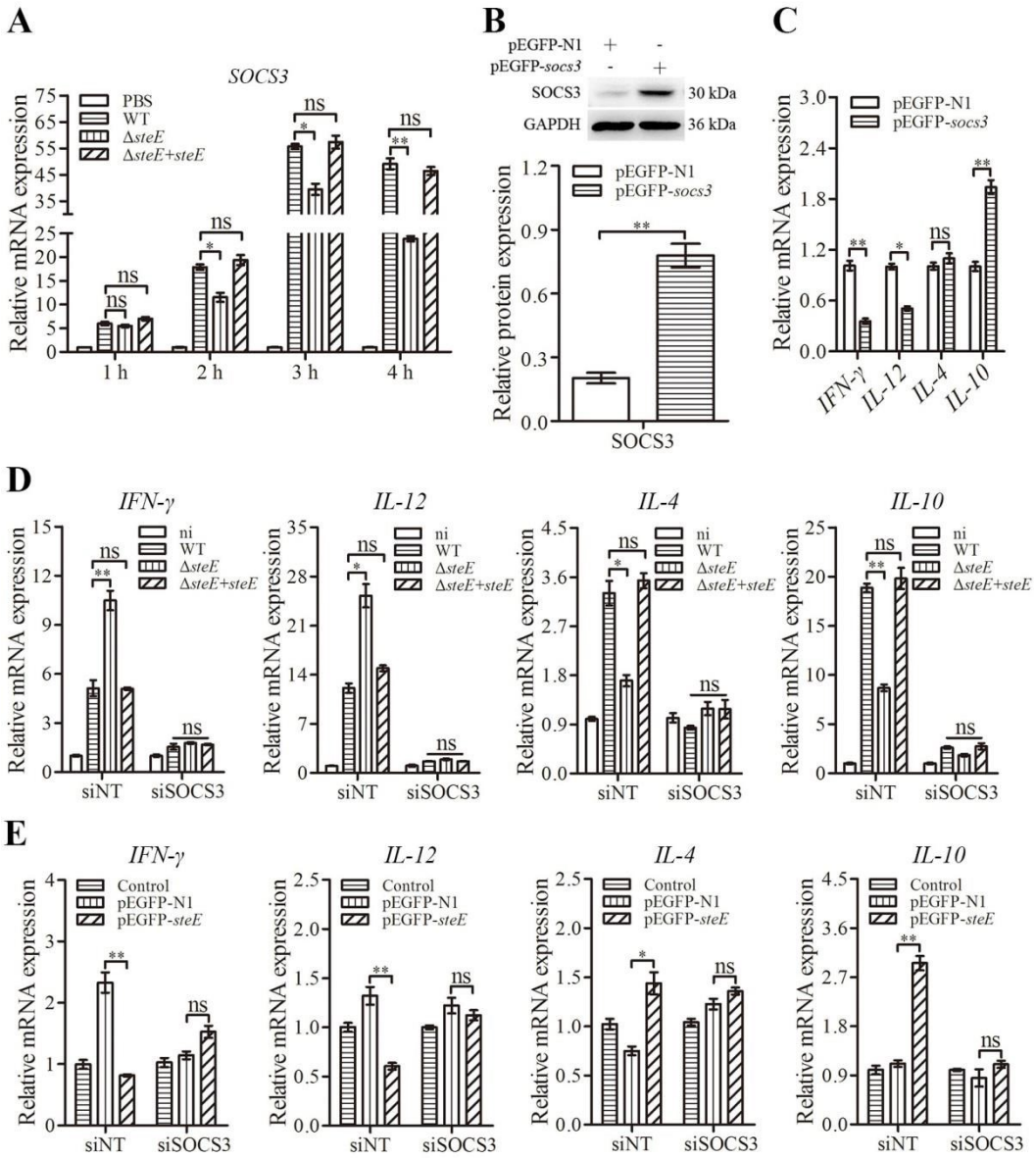

Fig. 3.35. *SteE* regulates Th1/Th2-related cytokines in HD-11 cells by targeting SOCS3.

3.7.3 *SteE* promotes SOCS3 expression by activating STAT3

To determine whether *steE* enhanced STAT3 and SOCS3 expression, HD-11 cells were infected with the WT, Δ*steE*, or Δ*steE* + *steE* strains. We observed that *STAT3* mRNA level and p-STAT3/STAT3 ratio were significantly lower in the Δ*steE*-infected HD-11 cells than in the WT or Δ*steE* + *steE*-infected HD-11 cells at 1, 2, 3, and 4 h (Fig. 3.36A, B). Additionally, SOCS3 protein level was notably lower in the Δ*steE*-infected HD-11 cells than in the WT or Δ*steE*+*steE*-infected HD-11 cells at 1, 2, 3, and 4 h (Fig. 3.36B). *SteE* overexpression in HD-11 cells

significantly upregulated *STAT3* and *SOCS3* mRNA levels as compared to those transfected with the control vector pEGFP-N1 with or without LPS stimulation (Fig. 3.36C). As expected, when transfected HD-11 cells with LPS stimulation, we found that p-STAT3/STAT3 ratio and SOCS3 protein level were still higher in *steE*-overexpressing HD-11 cells than that of the control vector pEGFP-N1 (Fig. 3.36D). These results indicate that *steE* promoted STAT3 and SOCS3 expression in HD-11 cells.

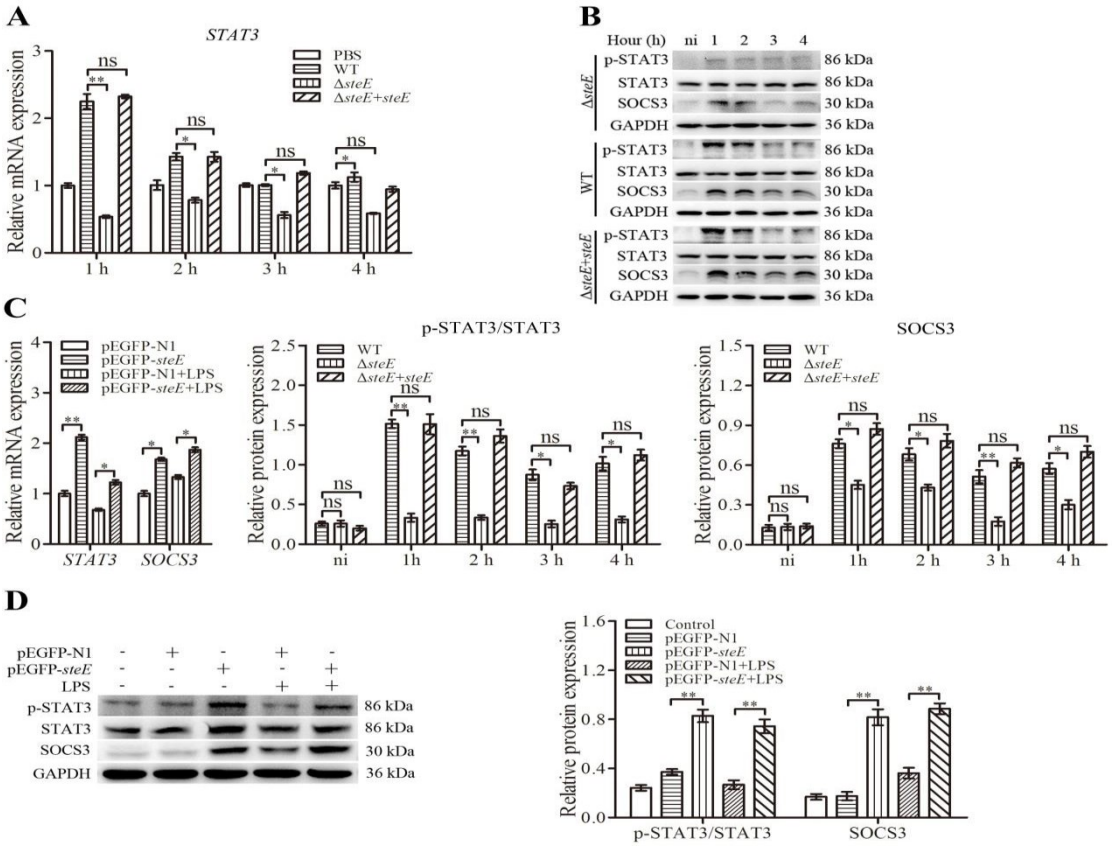

Fig. 3.36. *SteE* promotes the expression of STAT3 and SOCS3 in HD-11 cells.

HD-11 cells were infected with the WT, Δ*steE,* or Δ*steE* + *steE* strains at MOI of 10 for 1 h, 2 h, 3 h, and 4 h. (A) The *STAT3* mRNA level was determined using qRT-PCR**.** (B) The p-STAT3/STAT3 ratio and SOCS3 protein level were determined using western blotting. HD-11 cells were transfected with pEGFP-N1 or pEGFP-*steE* and then treated with or without LPS (10 μg/mL) 48 h post transfection for 30 min. (C) *STAT3* and *SOCS3* mRNA level were determined using qRT-PCR**.** (D) The p-STAT3/STAT3 ratio and SOCS3 protein level were

determined using western blotting. SOCS3 protein level was normalized to GAPDH protein level. Three biological replicates were used for each target gene. *P < 0.05, **P < 0.01.

To evaluate the efficiency of siSTAT3-1, siSTAT3-2, or siSTAT3-3 transfection, *STAT3* mRNA and STAT3 protein level were determined using qRT-PCR and western blot assays 48 h after transfection (Fig. 3.37A, B). To investigate the effect of STAT3 on *steE*-mediated SOCS3 expression, we assessed the expression of SOCS3 in STAT3-silenced cells. In the siNT-treated HD-11 cells, WT or Δ*steE* + *steE* strain significantly increased SOCS3 expression compared to that of the Δ*steE* strain. In contrast, SOCS3 expression showed no significant difference between WT or Δ*steE*+*steE*-infected siSTAT3-treated HD-11 cells and Δ*steE*-infected siSTAT3-treated HD-11 cells (Fig. 3.37C, D). Compared with the pEGFP-N1 and siNT group, the pEGFP-*steE* and siNT group significantly increased SOCS3 expression. After STAT3 knockdown, SOCS3 expression did not significantly difference in HD-11 cells co-transfected with the *steE* overexpression plasmid and siSTAT3 group compared to that of the pEGFP-N1 plasmid and siSTAT3 group (Fig. 3.37E, F).

(A) HD-11 cells were transfected with siNT, siSTAT3-1, siSTAT3-2 or siSTAT3-3 for 48 h, and *STAT3* mRNA level was determined using qRT-PCR; (B) STAT3 protein level was assessed using western blotting. HD-11 cells were transfected with siNT or siSTAT3 and infected with the WT, Δ*steE*, or Δ*steE*+*steE* strains 48 h post transfection at MOI of 10 for 2 h; (C) *SOCS3* mRNA level was determined using qRT-PCR**.** (D) SOCS3 protein level was determined using western blotting; (E) HD-11 cells were co-transfected with siSTAT3 and pEGFP-*steE* and incubated for 48 h, and *SOCS3* mRNA level was determined using qRT-PCR; (F) SOCS3 protein level was determined using western blotting. SOCS3 protein level was normalized to GAPDH protein level. Three biological replicates were used for each target gene. *P < 0.05, **P < 0.01.

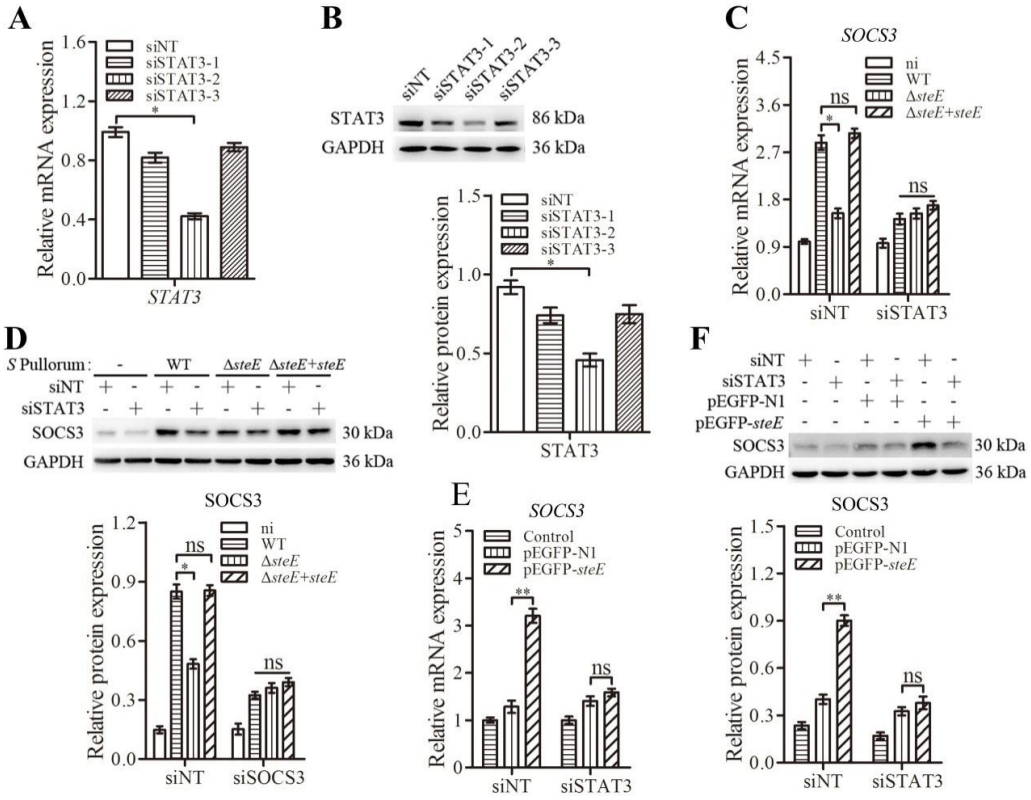

Fig.3.37. *SteE* inhibits the expression of SOCS3 in STAT3-silenced HD-11 cells.

Finally, we determined whether *steE* enhanced the expression of STAT3 and SOCS3 in spleen of chickens. To this end, chickens were infected with the WT, Δ*steE* or Δ*steE*+*steE* strains. *STAT3* mRNA level and p-STAT3/STAT3 ratio were obviously lower in the Δ*steE*-infected chickens than in the WT or Δ*steE* + *steE*-infected chickens (Fig. 3.38A, B). Moreover, SOCS3 expression was notably lower in the Δ*steE*-infected chickens than in the WT or Δ*steE*+*steE*-infected chickens. Taken together, these data suggested that *steE* enhanced SOCS3 expression via STAT3 activation.

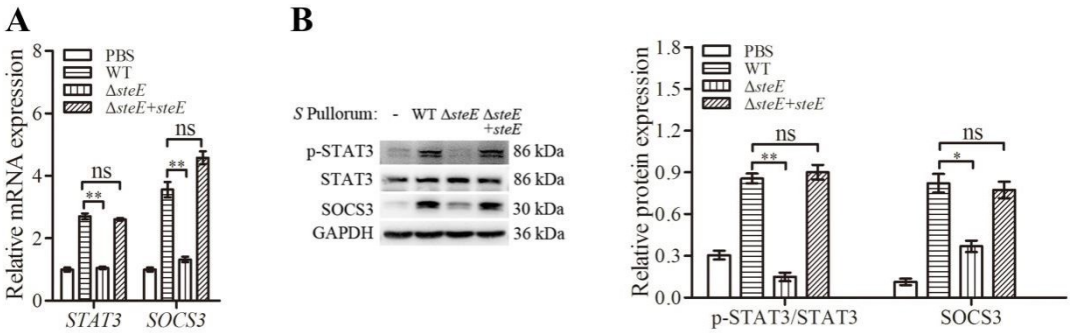

Fig.3.38. *SteE* enhances the expression of STAT3 and SOCS3 in spleen of chickens.

Chickens were infected with the WT, Δ*steE,* or Δ*steE* + *steE* strains (10^9 CFU). At 3 dpi, (A) *STAT3* and *SOCS3* mRNA level were determined using qRT-PCR. (B) The p-STAT3/STAT3 ratio and SOCS3 protein level were measured using western blotting. SOCS3 protein level was normalized to GAPDH protein level. Three biological replicates were used for each target gene. *P < 0.05, **P < 0.01.

3.7.4 *SteE* inhibits the expression of P65 in HD-11 cells

We further evaluated whether *steE* inhibited P65 expression during *S.* Pullorum infection. As shown in Fig. 3.39A, *P65* mRNA level significantly increased in the Δ*steE*-infected HD-11 cells as compared to WT or Δ*steE*+*steE*-infected HD-11 cells from 1 to 3 hpi. Additionally, *P65* mRNA level was significantly higher in the Δ*steE*-infected HD-11 cells than in the WT or Δ*steE* + *steE*-infected HD-11 cells at MOI of 10, 20, and 40 (Fig. 3.39B). Western blotting indicated that the p-P65/P65 ratio was significantly upregulated in Δ*steE*-infected HD-11 cells as compared to WT or Δ*steE*+*steE*-infected HD-11 cells at 2, 3, and 4 hpi (Fig. 3.39C). In addition, the p-P65/P65 ratio was also significantly higher in Δ*steE*-infected HD-11 cells than in the WT or Δ*steE* + *steE*-infected HD-11 cells at MOI of 10, 20, and 40 (Fig. 3.39D). Similar to the results observed in immunofluorescence assays, *steE* blocked p-P65 translocation to the nucleus (Fig. 3.39E). These results suggest that *steE* reduced NF-κB p65 expression at both mRNA and protein levels in *S.* Pullorum-infected HD-11 cells.

HD-11 cells were infected with the WT, Δ*steE*, or Δ*steE*+*steE* strains at MOI of 10 for 1, 2, 3, and 4 h or at different MOI of 5, 10, 20, and 40 for 2 h. (A, B) *P65* mRNA level was determined using qRT-PCR**;** (C, D) The p-P65/P65 ratio was measured using western blotting; (E) HD-11 cells were infected with the WT, Δ*steE*, or Δ*steE*+*steE* strain at MOI of 10 for 2 h, followed by immunofluorescence staining of p-P65 (red) and nuclei (blue) (scale bar: 25 μm). Three biological replicates were used for each target gene. *P < 0.05, **P < 0.01.

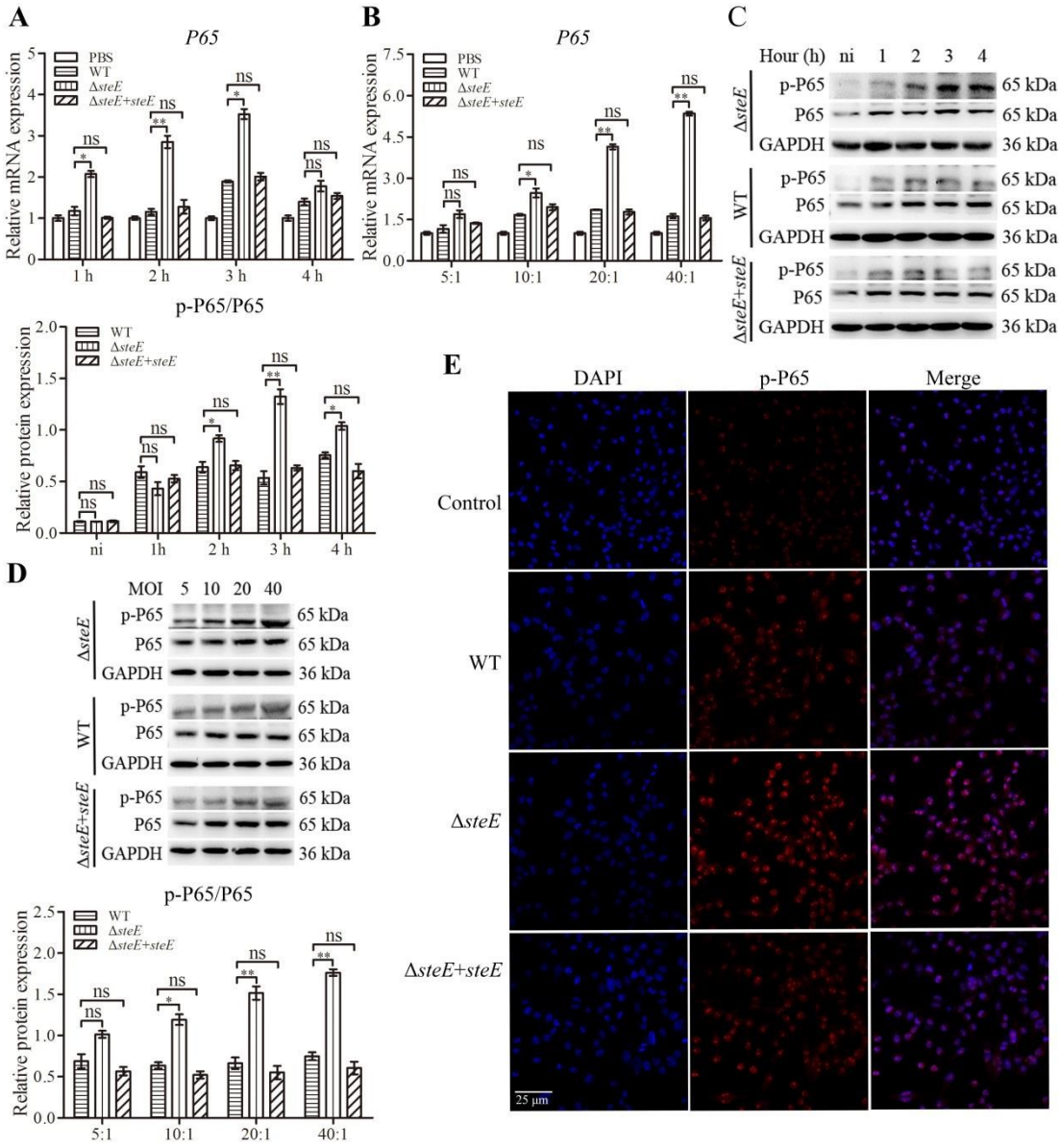

Fig. 3.39. *SteE* inhibits the expression of P65 in HD-11 cells during *S.* Pullorum infection.

3.7.5 *SteE* overexpression decreases the expression of Th1-related cytokines and P65 toward a Th2-related cytokines expression in HD-11 cells triggered by LPS

To further confirm whether *steE* regulated LPS-producing Th1 response and P65 expression toward a Th2 response, HD-11 cells were transfected with pEGFP-N1 or pEGFP-*steE* and then treated with or without LPS. As shown in Fig. 3.40A, *steE* overexpression in HD-11 cells significantly decreased *IFN-γ* and *IL-12* mRNA levels but increased *IL-4* and *IL-10* mRNA levels compared with that of the empty

vector with or without LPS stimulation. In addition, when transfected HD-11 cells with LPS stimulation, we found that *P65* mRNA level and the p-P65/P65 ratio were still lower in *steE*-overexpressing HD-11 cells than those transfected with the empty vector (Fig. 3.40B, C). These data indicate that *steE* overexpression decreased the expression of Th1-related cytokines and P65 but upregulated Th2-related cytokines in HD-11 cells triggered by LPS.

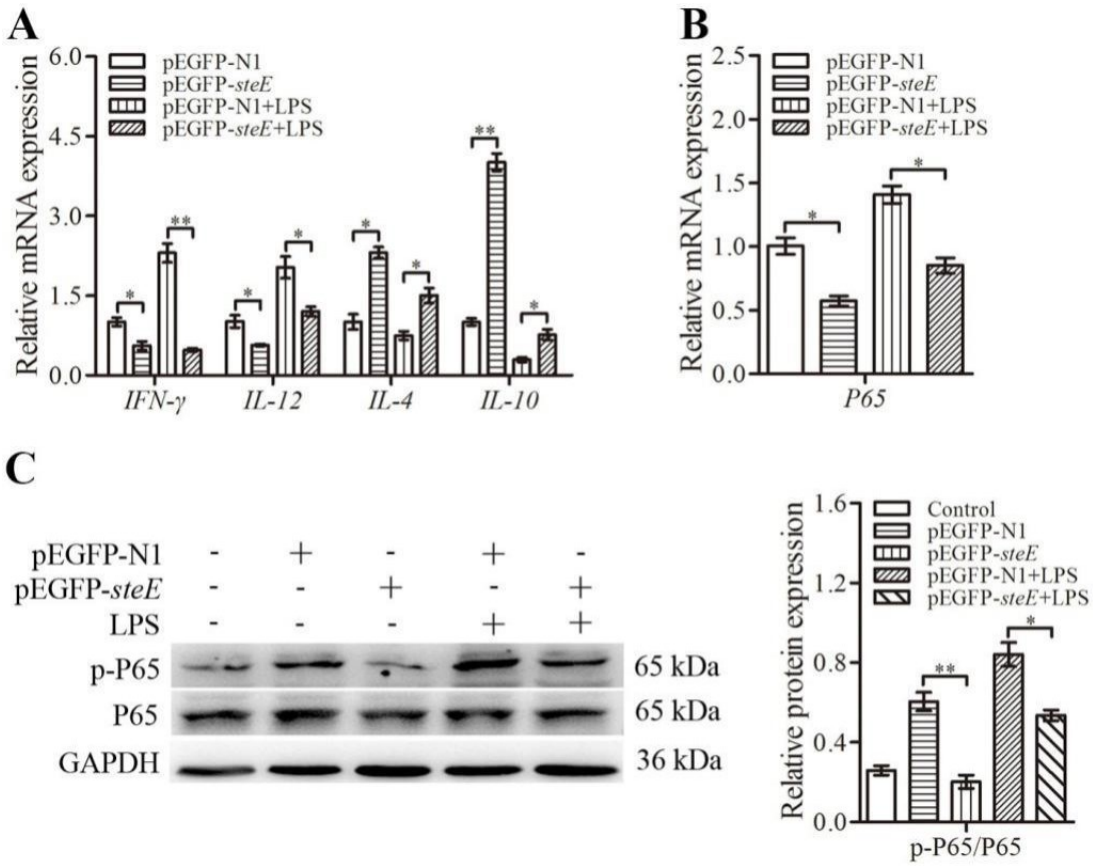

Fig. 3.40. Overexpression of *steE* decreases the expression of Th1-related cytokines and P65 but upregulated Th2-related cytokines in HD-11 cells triggered by LPS.

HD-11 cells were transfected with pEGFP-N1 or pEGFP-*steE* and incubated for 48 h, and treated with or without 10 μg/mL LPS for an additional 30 min. (A) *IFN-γ*, *IL-12*, *IL-4*, and *IL-10* mRNA levels were assessed using qRT-PCR; (B) *P65* mRNA level was assessed using qRT-PCR**;** (C) The p-P65/P65 ratio was measured using western blotting. Three biological replicates were used for each target gene. *P < 0.05, **P < 0.01.

3.7.6 *SteE* inhibits the expression of P65 in chickens

We evaluated *P65* transcription and expression in *S.* Pullorum-infected chickens using qRT-PCR and western blot assays. Fig. 3.41A and B shows that *P65* mRNA level and the p-P65/P65 ratio were significantly higher in Δ*steE*-infected chickens than in the WT or Δ*steE*+*steE*-infected chickens. Moreover, the results of IHC showed that the p-P65-positive area in the nucleus was significantly lower in the spleen of WT or Δ*steE*+*steE*-infected chickens than in the Δ*steE*-infected chickens at 3 dpi (Fig. 3.41C, D). Taken together, these results suggest that *steE* inhibited P65 expression in chickens during *S.* Pullorum infection.

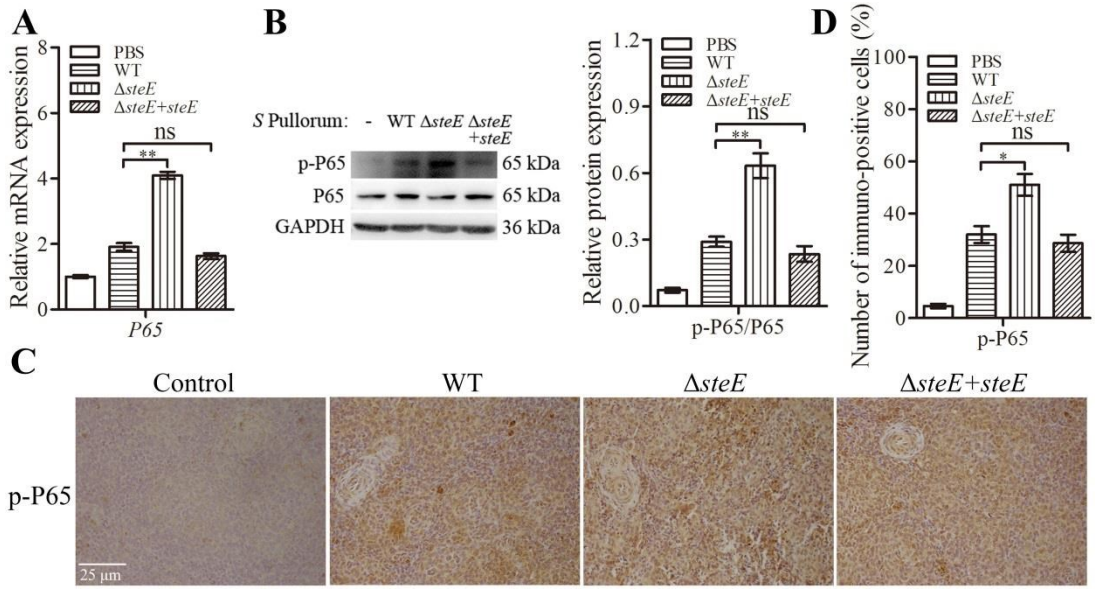

Fig. 3.41. *SteE* inhibits the expression of P65 in chickens during *S*.Pullorum infection.

(A) Chickens were infected with the WT, Δ*steE*, or Δ*steE*+*steE* strain (10^9 CFU); (B) At 3 dpi, *P65* mRNA level was measured using qRT-PCR, the p-P65/P65 ratio was determined using western blotting; (C) Immunohistochemical analysis of p-P65 expression (brownish yellow) in the spleen of chickens (scale bar: 25 μm); (D) Percentage of the p-P65-positive cells shown was calculated from the total cell population in the nucleus. Three biological replicates were used for each target gene. *P < 0.05, **P < 0.01

3.7.7 *SteE* inhibits P65 expression by targeting SOCS3 in HD-11 cells

To assess whether *steE* affected the expression of P65 by targeting SOCS3,

P65 mRNA levels, and the p-P65/P65 ratio were determined in *steE*/*socs3*-overexpressing HD-11 cells. As shown in Fig. 3.42A, B, *P65* mRNA level and the p-P65/P65 ratio were lower in HD-11 cells transfected with pEGFP-*steE* or pEGFP-*socs3* than those transfected with the pEGFP-N1. Moreover, *P65* mRNA level and the p-P65/P65 ratio were also significantly lower in HD-11 cells co-transfected with pEGFP-*steE* and pEGFP-*socs3* than those transfected with pEGFP-*socs3*. The transfection efficiency of siSOCS3-1, siSOCS3-2, or siSOCS3-3-silenced HD-11 cells was analyzed by assessing the expression of SOCS3 using qRT-PCR and western blotting after 48 h (Fig. 3.42C, D). Next, we transfected siSOCS3 into HD-11 cells and infected them with the WT, Δ*steE* or Δ*steE*+*steE* strains.

In the siNT-treated HD-11 cells, WT or Δ*steE*+*steE* strain significantly decreased *P65* mRNA level and the p-P65/P65 ratio compared to that of the Δ*steE* strain. In contrast, WT or Δ*steE*+*steE* strain did not significantly decrease *P65* mRNA level and the p-P65/P65 ratio in siSOCS3-treated HD-11 cells (Fig. 3.42E, F). Furthermore, *P65* mRNA level and the p-P65/P65 ratio were notably lower in HD-11 cells co-transfected with *steE* overexpression plasmid and siNT group than that of co-transfected with pEGFP-N1 plasmid and siNT group (Fig. 3.42G, H). After SOCS3 knockdown, *P65* mRNA level and the p-P65/P65 ratio did not significantly difference in HD-11 cells co-transfected with the *steE* overexpression plasmid and siSOCS3 group than those co-transfected with pEGFP-N1 plasmid and siSOCS3 group. Altogether, these data indicate that *steE* dampened p65 expression via the upregulation of SOCS3. (A) HD-11 cells were transfected or co-transfected with pEGFP-*steE* and pEGFP-*socs3*; 48 h post transfection, the *P65* mRNA level was determined using qRT-PCR; (B) The p-P65/P65 ratio was determined using western blotting; (C) HD-11 cells were transfected with siNT, siSOCS3-1, siSOCS3-2, or siSOCS3-3 for 48 h, following which *SOCS3* mRNA level was determined using qRT-PCR; (D) SOCS3 protein level was determined using western blotting; (E) HD-11 cells were transfected with siNT or siSOCS3; 48 h post transfection, they were infected with the WT, Δ*steE* or Δ*steE*+*steE* strain at

MOI of 10 for 2 h, *P65* mRNA level was determined using qRT-PCR; (F) The p-P65/P65 ratio was determined using western blotting; (G) HD-11 cells were co-transfected with siSOCS3 and pEGFP-*steE*; 48 h post transfection, the *P65* mRNA level was determined using qRT-PCR; (H) The p-P65/P65 ratio was determined using western blotting. SOCS3 protein level was normalized to GAPDH protein level. Three biological replicates were performed for each target gene. *P < 0.05, **P < 0.01.

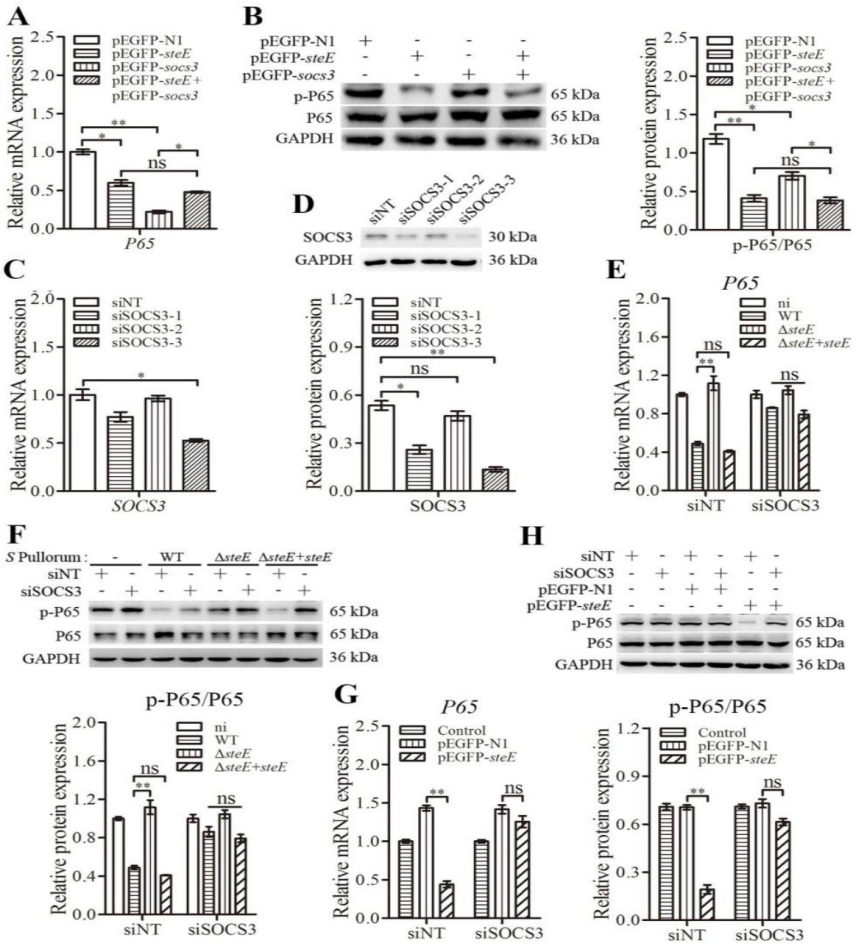

Fig. 3.42. *SteE* inhibits P65 expression via the upregulation of SOCS3 in HD-11 cells.

3.7.8 Conclusions in chapter 3.8

SteE regulated the mRNA levels of Th1/Th2-related cytokines in *S.* Pullorum-infected HD-11 cells and chickens. SOCS3 was involved in regulating the balance of Th1/Th2-related cytokines in HD-11 cells induced by STAT3. *SteE* reduced NF-

κB p65 expression at both mRNA and protein levels via the upregulation of SOCS3 in *S.* Pullorum-infected HD-11 cells. *SteE* regulate Th1/Th2-related cytokine expression by modulating the STAT3/SOCS3 and NF-κB axis that might be associated with the Th1/Th2 cells differentiation in HD-11 cells and chickens during *S.* Pullorum infection.

CHAPTER 4

SUMMARY AND ANALYSIS OF RESULTS

Salmonella is an intracellular pathogen that causes great harm to human and livestock health worldwide, which has complex and diverse antigenicity and serotypes [208]. Among the prevalent serotypes, *S*. Pullorum causes systemic fatal diseases with high mortality among chickens within 2–3 weeks [209]. Infected adult chicken presents reproductive tract abnormalities without severe clinical symptoms, lead to chronic or recessive infection [210]. Pullorum disease causes significant economic losses to the chicken farms worldwide, especially in developing countries [211, 212]. Therefore, it is of great significance to control the spread of *S*. Pullorum in chicken farms.

S. Pullorum was the main pathogenic bacteria of the diseased chickens with suspected *S*. Pullorum from a large-scale chicken farms. At the same time, antimicrobial susceptibility test showed that the isolated *S*. Pullorum was resistant to amoxicillin, sulfamethazine, tetracycline and ciprofloxacin, but sensitive to ceftriaxone, ceftiofur and kanamycin, which was basically consistent with the results of a previous report [213]. Previous studies have shown that *Salmonella* multidrug resistance is considered closely related to its serotype [214, 215, 216].

According to clinical needs, different drugs administered in different ways to ensure the effect of drugs in host [217, 218].

Even previous studies demonstrate that probiotics can inhibit the proliferative ability of *Salmonella* in the intestine, which have great clinical value in the early prevention and treatment of *Salmonella* [219, 220, 221]. So, the combined application of bacterial culture identification and drug susceptibility test can accurately confirm the distribution and drug resistance of pathogenic bacteria, and provide effective reference for the clinical rational use of antibiotics. Additionally, attenuated and inactivated vaccines can also against *Salmonella* infection in

chickens, and reduced the harm of *Salmonella* to human and livestock health [222, 223].

S. Pullorum can spread horizontally and vertically to offspring, which can hardly be eliminated [17]. Therefore, the accurate and rapid diagnosis of pathogens is significant for the control and eradication of *S.* Pullorum. At present, the detection of pathogenic bacteria depends on culture-based techniques and biochemical identification, which are time consuming, have long detection cycle and low sensitivity, and cannot meet the needs of social development [224]. Thus, the accurate and simple detection method should be developed for the serotype diagnosis of *S.* Pullorum.

The conventional PCR assay has been successfully established for the diagnosis and identification of *Salmonella*. At the same time, these techniques did still need to develop an improved method for the identification and detection of target bacteria [225, 226]. Many studies reported that multiplex PCR is widely used to control microorganisms spread, due to the advantages of high efficiency, system, economy, and simplicity [23, 227, 228]. Strikingly, the design and quantity of multiplex PCR primers are important for the effective amplification of the target gene sequence. Herein, our assay was applied successfully to improve this problem by designing two sets of primers with different target sequences derived from *S.* Pullorum. The PCR method can remarkably improve the detection specificity and eliminate false-positive results. This design may extend the application of PCR for genotyping, evolutionary history of host adaptation, and bacterial biology [229, 230, 231].

Our established multiplex PCR method could successfully solve the difficulties on the basis of the diagnostic marker of the *citE2* gene and intergenic sequence between SPS4_00301 and SPS4_00311 for *S.* Pullorum. A previous study indicated that *citE2* is a subunit of bacterial citrate lyase in bacterial energy metabolism and has been demonstrated as a robust drug target for the physiology and virulence of *Mycobacterium tuberculosis* [232]. The sequence alignment of the *citE2* gene was present in *Salmonella enterica* subsp. *enterica* strains, but *S.*

Pullorum strains had a 76 bp deletion in *citE2*. The intergenic sequence between SPS4_00301 and SPS4_00311 existed in *Salmonella enterica* subsp. *enterica* and was the first to be reported as a diagnostic marker of *Salmonella*. Recent studiy have reported that multiple PCR-based on the 42 bp–deficient region of *cigR*, and has excellent effectivity and suitability for detection of S. Pullorum/Gallinarum [23]. The conserved ROD represents a potential marker for the specific identification of *S.* Pullorum/Gallinarum [196, 233]. Similarly, the intergenic sequence between two genes in *Salmonella* is conservative in the process of evolution and has important biological functions [234]. In epidemiologic investigation and transmission of *S.* Pullorum/Gallinarum, increased specific genes are explored to determine *Salmonella* serovars for PCRs [235]. For example, the *fliC* and *fljB* genes present in *S*. Typhimurium are not highly conservative to discriminate clinical mutants [236]. The multiplex real-time PCR assay reduces the problems of atypical strains or false-negative results [237].

The conservation status of *citE2* ROD and the intergenic sequence of SPS4_00301–SPS4_00311 were exploited as target sequences to design *S*. Pullorum primers. In this study, our multiplex PCR assay produced the two expected bands for 6 strains of *S.* Pullorum and 27 strains of non-*S.* Pullorum individually, but 13 strains of non-*Salmonella enterica* subsp. *enterica* did not have a band (Fig. 4). Detection limits for the multiplex PCR could be analyzed at the 6.25 pg/μL for the genomic DNA of *S*. Pullorum and 10^4 CFU/mL for pure *S*. Pullorum cells in a single tube. As shown in Table 3.2, our method exhibited a sensitivity that was comparable with other earlier reported data for the detection of *S*. Pullorum/Gallinarum [238].

From the results of the spiked eggs with two of the individual target bacteria, a 10-fold enrichment could be observed to detect 10^0 CFU/mL viable *S*. Pullorum and *S*. Enteritidis. A recent study has reported that a real-time fluorescent quantitative PCR to detect *Salmonella* spp and *S*. Enteritidis in food samples, and 10 CFU in BPW could be detected by applying this quantitative PCR [239]. A total of 69 chicken anal swab samples from chicken farms were detected using the

multiplex PCR system, which was also identical with the culture method, to verify the clinical application of this method. Cumulatively, the specificity and sensitivity of two special primer pairs were effectively sufficient to construct a multiplex PCR system for the identification and diagnosis of *S.* Pullorum. Our results indicated that the proposed PCR method could provide a valuable tool to identify *S.* Pullorum in laboratory and real samples efficiently.

Salmonella can form *Salmonella*-containing vacuole (SCV) in the host cell, which is very important for the disseminate of *S.* Pullorum [151, 240]. *Salmonella* pathogenesis are two T3SSs encoded in *Salmonella* pathogenicity islands 1 and 2 (SPI-1 and SPI-2) that are responsible for the secretion and translocation of a set of bacterial proteins termed effectors into host cells with the intention of altering host cell physiology for bacterial entry and survival.

The maintenance of SCV function is inseparable from the participation of a series of *Salmonella* virulence factors, in which the T3SS2 encoded by SPI-2 and its secreted effector protein [241]. As a potential virulence protein of T3SS2, *steE* was found to regulate macrophage activation and host immune response. Some studies have found that *Salmonella* can be colonized in the intestine and spleen, and directly take macrophages as target cells [113, 242].

After *S.* Pullorum infection, the bacterium can not only avoid the killing of intracellular active substances, but also proliferate and spread in macrophages [243]. *SteE* is necessary for the replication and virulence of *Salmonella* in macrophages [244]. Therefore, we speculated that the pathogenic mechanism of *S.* Pullorum infection in chickens may be the same as that in HD-11 cells.

In this study, *steE* was selected as the research gene based on λ-Red recombination system to construct the *S.* Pullorum Δ*steE* strain. The results showed that the growth and biochemical characteristics of *S.* Pullorum and *S.* Pullorum Δ*steE* strains are similar, which is consistent with the previous result, but *steE* is not necessary for the growth and metabolism of *S.* Pullorum [245]. The results showed that *steE* would reduce the colonization ability and virulence of *S.* Pullorum in HD-11 cells. *S.* Pullorum induced apoptosis of HD-11 cells is a special

virulence mechanism, which could promote the spread of bacteria between cells. Recent studies have shown that the deletion of *S.* Pullorum SPI-2 significantly reduced the pathogenicity of chicks, which is consistent with *steE* belonging to SPI-2 effector protein [246, 247, 248]. In addition, Pham et al [245] reported that *steE* can drive macrophages to polarize to M2 type and increased the ability of *Salmonella* infection-permissive state. Therefore, we suspected that *steE* may be related to the virulence of *Salmonella*. The results of *S.* Pullorum infecting HD-11 cells also showed that *steE* enhanced the intracellular viability of *S.* Pullorum and promoted the apoptosis of HD-11 cells.

The results of virulence assay showed that the deletion of *steE* caused decreased in the pathogenicity of *S.* Pullorum in chickens, which proved the important role of *steE* in the virulence of *S.* Pullorum (Fig. 3.16). At the same time, the colonization of bacteria in chicken organs showed that the overall change trend of *S.* Pullorum was similar to that of Δ*steE* strain. The colonization of WT and Δ*steE* strains in cecum, spleen, and bursa of chickens reached the peak at 3 d, while the number of WT and Δ*steE* strains in liver of chickens reached the peak at 4 d. From the whole process of infection, the number of Δ*steE* in various organs at the initial infection stage after after *Salmonella* infection in chickens that first increased, reached the peak at the middle infection stage, and decreased at the later infection stage. At the same time, the number of Δ*steE* strain in chicken organs was always significantly lower than that of WT strain. In addition, the colonization number of Δ*steE* strain in chicken organs was always lower than that of WT strain. These results show that *steE* can promote the colonization of *S.* Pullorum in chicken organs and contribute to the virulence of *S.* Pullorum.

Recent studies demonstrated that the deletion of *SPI-2* reduced the virulence of *Salmonella*, which was related to that SPI-2 is a DNA fragment obtained by the external level in the process of *Salmonella* evolution. Some reported that the deletion of *steE* significantly attenuated colonization of mouse spleens, and caused decreased the virulence of *S.* Typhimurium [246].

SteE had been considered as an important effector in host organs for persistent

Salmonella infection [245]. SteE was encoded by *Salmonella* Gifsy-1 prophage [244, 249, 250], that reported to activate the signal transducer and activator of transcription 3 signaling pathway and then produce anti-inflammatory cytokine IL-10, thereby promoting *Salmonella* replication in cells and increasing bacterial colonization *in vivo* [195]. In this study, there were many factors that affect the accuracy of the final results. On the one hand, the interval between organ collections was relatively long, and the accurate time of bacteria invading various organs can't be well determined. On the other hand, only by reducing the interval between collecting organs that we can determine the time when bacteria settle in organs from chickens to reach the peak. In addition, there were also other factors affecting the number of *S.* Pullorum in the test process, such as equipment, reagents, the cleanliness of petri dish, and the errors caused by the operation and so on.

Inflammatory cytokines are one of the most important regulators of host-cell interaction in acute systemic disease [251]. After *S.* Pullorum infection in chickens, the cells of the host will secrete Th1/Th2 cytokines, which regulate the balance of the internal environment and resist the damage of external harmful substances [170]. *SteE* increased the bacterial virulence, translocated into the cytoplasm of the host cell through T3SS-2, and caused the severe disseminated infection of other extra-intestinal tissues, such as the spleen and liver in mouse infected with *Salmonella* [245]. Here, we found that *steE* regulated positively the balance of Th1/Th2-related cytokines in tissues of chicken infected with *S.* Pullorum.

Salmonella can regulate host immune response via T cell activation [252]. IL-12 is a pro-inflammatory cytokine that plays an important role in the host's defense against intracellular pathogen infection [253]. IFN-γ production by Th1 cells and initiated by IL-12 and IL-18, induced the oxidative effect and improved the ability to suppress intracellular bacteria growth [254]. A previous study showed that *sspH2* significantly decreased the mRNA expression of Th1-related cytokines (IL-12 and IFN-γ) in tissues of mice infected with *S.* Enteritidis [255]. Furthermore, *S.* Pullorum decreased the mRNA expression levels of pro-inflammation cytokine

(IL-12, IL-18, and IFN-γ) compared with *S*. Enteritidis in infected macrophages [31]. In the current study, *steE* increased the Th1-related cytokines expression (*IL-12* and *IFN-γ*) in the chicken tissues infected with *S.* Pullorum, which was consistent with the previous report. We speculated that *steE* might be involved in Th1-mediated tissue injury and elimination of pathogen during *S.* Pullorum infection. Anti-inflammatory cytokines are mainly related to clear pathogens and tissue repair after *Salmonella* infection. IL-10, as an important anti-inflammatory medium, can inhibit the expression of various pro-inflammatory factors induced by Th1 cell, and also participate in Th2 cell-mediated anti-inflammatory response [256]. Recent studies have found that *steE* can induce the production of anti-inflammatory cytokine IL-10 in the spleen of mouse infected with *Salmonella*, but it has no relevant data in other tissues [195]. Moreover, the persistent infection of *Mycobacterium tuberculosis* needs the participation of IL-10, which indicates that IL-10 contribute to long-term systemic infection of intracellular bacteria [257]. Another study found that the persistent infection of *Salmonella* needs the support of IL-10, which is associated with the Th1/Th2 balance [195, 258]. Induced the expression of IL-10 contributed to limit the Th1 cytokines and escape the immune response of host cells [259]. In the present study, *steE* obviously increased the IL-10 mRNA transcript level during the infection phase. Therefore, *steE* may be more conducive to the repair of damaged tissues by promoting the anti-inflammatory or Th2 cytokines expression during early stages of infection.

The imbalance of Th1/Th2 cytokine is an important indicator of pathogens invasion [251]. Recent studies show that *S.* Pullorum was inclined to regulate host immunity toward a Th2-like immune response in poultry [31]. In this study, our results demonstrated that *steE* inhibited the Th1 immune response, but promoted the Th2 immune response. Furthermore, *steE* activity promoted anti-inflammatory M2 phenotype and facilitated *Salmonella* invasion into host cells, leading to increased pathogen persistence [195]. *SteE* have the function of immune response of transforming different types, which is beneficial to intracellular survival of *Salmonella* [249]. Our study previously showed that *steE* can also increase the

virulence of *S.* Pullorum and aggravate the outcome of host infection [260].

Thus, we speculate that *steE*-inhibited inflammatory response could be related to M2 phenotype, which was beneficial to evade immunity and persistent infection of *S.* Pullorum. However, how *steE* regulates the cytokine balance of Th1/Th2 in *S.* Pullorum-infected chicken needs to be further confirmed.

To date, more than 40 different effector proteins of the T3SSs encoded by SPI have been identified, which are involved in host-pathogen interaction. However, the effect of most effector proteins on the immune response of chicken macrophages and the pathogenicity of *S.* Pullorum is unclear [151]. In this study, we showed that the effector protein SteE can enhance invasiveness and proliferation of *S.* Pullorum, which are required for bacterial survivability in host cells. Defensive responses can evolve in *Salmonella* to maintain a dynamic balance within the host, and these responses mediate the long-term survival and persistent infection of pathogens [261, 262]. The findings of this study contributed to understanding the pathogenicity-related role of SteE during *S.* Pullorum infection, thus provided important clues for further studies.

The invasion and proliferation phenotypes of *Salmonella* are closely associated with bacterial virulence in macrophages [151]. The T3SS2 is required for the intramacrophage replication of *S.* Typhimurium [115]. Furthermore, the *steE* does not affect the invasion of *S.* Typhimurium in LCLs cells but result in its increased replication [195]. In the present study, we found that *steE* increased the invasion and replication of *S.* Pullorum in HD-11 cells. Our results were not completely consistent with a previous report, with differences resulting due to the different cell lines used, MOI, or serotypes of *Salmonella* [195, 263].

Other intracellular bacteria, including *Mycobacterium tuberculosis*, *Brucella*, and *Francisella tularensis*, also affect the number of macrophages and promote bacterial survival during infection [264, 265, 266].

Therefore, we hypothesized that the effector protein SteE, as a potential virulence factor, may contribute to invasiveness and proliferation.

Previous studies demonstrated that *SPI-2* deletion significantly affected the

expression of T3SS2-related effector [187]. In this study, deletion of *steE* significantly reduced the expression of selective T3SS virulence genes in *S.* Pullorum-infected HD-11 cells (Fig. 3.24). We hypothesized that *steE* was closely related to the T3SS2-dependent virulence of *S.* Pullorum in HD-11 cells. Recent studies have evaluated the mechanisms underlying *steE*-mediated regulation of macrophage polarization and have provided insights into chronic infection with *Salmonella* [267, 268].

Furthermore, SPI-2 effector mutants (*ssaV* and *steE*) in *S.* Typhimurium infected macrophages with significantly decreased IL-4 expression levels [244]. Thus, *steE* may induce a competitive balance between the host microbiota and inflammation. Several studies have shown that *steE* can promote IL-10 production via the activation of STAT3 signaling and metabolic and physiological environment reprogramming for *Salmonella* in B cells, changing it from an anti-inflammatory to an infection state [195, 244, 249]. In addition, the SteE effector increased the polarization of M2 macrophages in granulomas [245]. Recently, Brodsky et al. [268] obtained similar results that SteE promotes *Salmonella* replication within tissue granulomas to induce M2 polarization. Furthermore, the *steE*-driven M2 granuloma macrophages polarization reduced iNOS mRNA expression compared to M1 granuloma macrophages, but the mRNA levels of IL-4 were significantly high [245, 249].

The Δ*steE* strain induced a reduction in IL-10 levels in mice relative to *S.* Typhimurium [195]. Our results confirmed that effector *steE* promoted the production of anti-inflammatory cytokines (*IL-4* and *IL-10*) in HD-11 and chicken spleens while reducing that of the pro-inflammatory cytokine *iNOS* in HD-11 cells (Fig. 3.26), indicating that *steE* may provide a more permissive noninflammatory environment for *S.* Pullorum infection *in vivo* and *in vitro*.

The interaction between bacteriophages was also an important factor in bacterial virulence (Fig. 3.23A). The functional prophages Gifsy-1 (*steE*, *gogB*, and *gipA*) and Gifsy-2 (*gtgE*, *sodCI*, and *gtgA*) of *Salmonella* affect the virulence of the pathogen and play a critical role in infecting host cells [128, 129, 269]. *SteE*

is encoded within pathogenicity islands (Gifsy-1), which contributes to overcome host restriction during *Salmonella* infection [270]. Our study confirmed that deletion of *steE* in *S.* Pullorum caused the increased virulence to Jinghong laying hens. GogB can interfere with NF-κB activation and reduce the host inflammatory response [162]. GipA play an important role in replication of *S.* typhimurium within macrophages [207].The deletion of *gtgA* can significantly increase the virulence of *S.* Typhimurium in mice, indicating that a few effector proteins may play variable roles in different animal infection models that are conducive to *Salmonella* infection and cell survival [137]. After animals are infected with *Salmonella*, the pathogen can spread through the epithelial cells or lymphoid tissues in the intestine. Infected phagocytes and free bacteria can translocate to the liver, spleen, and other organs and show aggregation and infiltration, resulting in systemic infection [270]. Reportedly, *steE* significantly increased colonization of *S.* Typhimurium in mouse tissues [246, 270]). In this study, deletion of *steE* attenuated the colonization of *S.* Pullorum to chickens. At the same time, the competition index and survival assays showed that the deletion of *steE* could reduce the fitness and persistence of *S.* Pullorum in chicken organs (Fig. 3.28). Furthermore, *Salmonella*-containing vacuoles are formed in host cells, which provide a beneficial environment for the proliferation of *Salmonella*, whereas *steE*-deficient *S.* Typhimurium reduced virulence in the BALB/c mice model [43, 50]. From the results of our study, deletion of *steE* alleviated tissue injury and reduced the virulence of *S.* Pullorum in chickens, and these findings were consistent with *steE*-dependent regulation of inflammatory response *in vivo*. In future studies, we aimed to include an analysis of the specific signaling pathways and mechanisms to improve our understanding of the interaction between the *S.* Pullorum effector SteE and host immune response.

Changes of inflammatory cytokine levels are the main markers of the shift in the polarization of Th1/Th2 cells, which underscores the importance of inflammatory activities in host anti-infection processes [271, 272]. IL-4 and IL-10 are the hallmark Th2 cytokine that can stimulate M2 macrophage polarization and

inhibit Th1 immune response [273]. Infection of chickens with *S.* Pullorum was found to drive M2 macrophage polarization activated by Th2-related cytokines and inhibited the expression of IFN-γ and IL-12, which ultimately led to systemic infection [31]. In the present study, we observed decreased mRNA levels of Th1-related cytokines (*IFN-γ* and *IL-12*) in the WT or Δ*steE* + *steE*-infected HD-11 cells and chickens, but increased mRNA levels of Th2-related cytokines (*IL-4* and *IL-10*) when compared with Δ*steE* group (Fig. 3.34). Previous studies have also shown that effector SteE promotes IL-10 expression in LCLs (GM19154), and drives M2 macrophage phenotype [195, 244]. IL-10 is an important regulator of T cells activation that maintains the Th1/Th2 balance via regulation of macrophage activity while avoiding excessive immune response [274].

These results indicated that *steE* was positively associated with the Th2 immune response, and that a pathogen-persistent state was generated in the host as a result of the competitive response of these inflammatory activities [75, 244]. In this study, we found that *steE* can regulate Th1/Th2-related cytokines expression in *S.* Pullorum-infected HD-11 cells and chicken models. This suggests that *steE* may play an indispensable role in modulating the balance of both Th1 and Th2 immune response to *S.* Pullorum infection. In this case, the permissive anti-inflammatory state induced by *steE* could be more advantageous for *Salmonella* to manipulate the intracellular environment.

Previous studies have demonstrated that SOCS3 can inhibit inflammatory cytokine expression associated with the NF-κB activity during disease occurrence, which can be used as a diagnostic marker and molecular target for diagnosing and treating specific diseases [276, 277]. Moreover, SOCS3 is an anti-inflammatory mediator and involved in regulating Th1/Th2 cells differentiation [278, 279]. Similarly, our study showed that SOCS3 inhibited *P65* mRNA level and the p-P65/P65 ratio, and increased Th2-related cytokines development in HD-11 cells and chickens. The regulation of the STAT3 pathway in immune responses mainly depends on its upstream activators; for example, IL-6 exerts a pro-inflammatory effect, while IL-10 exerts an anti-inflammatory effect [280]. Furthermore, IL-10

binds to the IL-10 receptor, which activates STAT3 and then promotes SOCS3 expression, leading to enhancement of anti-inflammatory function and risk of developing immunosuppression in host cells [281, 282]. In our study, *steE* induced SOCS3 expression, which is in line with previous findings [248]. In particular, the s*teE*-induced IL-10 is a natural and continuous state, which can reduce inflammation in autoimmunity and cancer [195]. Importantly, when SOCS3 was silenced in HD-11 cells, *steE* did not affect the expression of pro-inflammatory cytokines. These results suggest that s*teE* could affect the Th1/Th2 cells differentiation via the upregulation of SOCS3 in HD-11 cells. However, the mechanism via which SOCS3 exerts anti-inflammatory effects via the regulation of P65 phosphorylation after *steE* induction requires further investigation.

Infection with *Salmonella* induces the phosphorylation of STAT3 in macrophages [129]. *SteE* has been found to manipulate host cell physiology during *Salmonella* infection, in which it induces activation of anti-inflammatory pathways such as the STAT3 pathway [195]. Evidence has shown that STAT3 phosphorylation can regulate the gene expression patterns of host cells and promote the persistence of *Salmonella* in the development of salmonellosis [268]. SOCS3 positively regulates STAT3 phosphorylation and decreases the levels of pro-inflammatory cytokines during infection by many pathogens, such as *Salmonella* and *Mycobacterium tuberculosis* [277, 283, 284].

In this study, *steE* promoted prolonged STAT3 activation and SOCS3 expression in HD-11 cells and chickens (Fig. 3.36 and 3.38). We also found that STAT3 silencing diminished the production of SOCS3 in HD-11 cells, suggesting that *steE* could promote the expression of SOCS3 by directly activating STAT3 phosphorylation, which was consistent with the results of previous studies [195, 248]. Therefore, we speculate that anti-inflammatory signals in host cells are positively involved in *steE*-induced STAT3 activation in *S.* Pullorum infection. Nevertheless, the role of the regulatory network of *steE*, STAT3/SOCS3, and NF-κB pathways in *S.* Pullorum-induced Th1/Th2 balance warrants further investigation.

Previous studies have shown that mild inflammation associated with Th-1-dominated responses contributes to the clearance of infection and repair of injured tissue in the host [31, 285, 286].

Additionally, aberrant activation of NF-κB usually increases the immune disorder and inflammation, which are associated with Th1 cells differentiation, but many immune cells such as T cells and macrophages, and can control this abnormal activation by reducing P65 expression [287, 288, 289]. *Salmonella* effectors, such as AvrA, SseL and SpvB, interfered with the activation of NF-κB by inhibiting P65 expression, and contributed to the elimination of excessive and prolonged inflammatory reactions caused by *Salmonella* infection [113, 191, 290]. A recent study has reported that *steE* attenuated the activation of the NF-κB pathway induced by TNF-α in HeLa cells [137]. Our findings demonstrated that *steE* inhibited phosphorylation of P65, and blocked its translocation to the nucleus in HD-11 cells and chickens during infection (Fig. 3.39), which might drive anti-inflammatory activities by enhancing SOCS3 expression.

One study suggested that inhibition of NF-κB P65 expression is possibly attributed to the SOCS3-reduced pro-inflammatory effects in inflammation-related diseases [279]. In addition, over-expressed SOCS3 suppressed the phosphorylation of P65 in macrophages and FHC cells [291, 292, 293].

In our study, we investigated whether *steE* inhibited P65 expression via SOCS3 in *S.* Pullorum-induced inflammation in HD-11 cells. Interestingly, we found that P65 mRNA expression and phosphorylation were downregulated upon overexpression of SOCS3 in HD-11 cells (Fig. 3.42). Moreover, our data suggest that *steE* inhibited the expression of Th1-related cytokines and P65 that was dependent on SOCS3 in HD-11 cells. Similarly, upregulation of SOCS3 expression blocked NF-κB activation by STAT3 phosphorylation in macrophages [293, 294]. Overall, these results illustrate that *steE* increased the expression of Th2-related cytokine but downregulated Th2-related cytokines via STAT3/SOCS3 activity that suppresses NF-κB activation.

CONCLUSION

In the dissertation work, the pathogen of the diseased chickens with suspected *S*. Pullorum was isolated and its antimicrobial susceptibility testing was analyzed, and a multiplex PCR system was established for the detection of *S.* Pullorum. Finally, this study confirmed that SteE as anti-inflammatory effector contributed to the persistent infection of *S.* Pullorum by regulating the host's innate immune response though modulate the STAT3/SOCS3 and NF-κB axis, which provided a novel therapeutic strategy for salmonellosis. Based on the overall research results, the following conclusions are justified:

1. The isolated *S.* Pullorum was the main pathogenic bacteria of the diseased chickens that was sensitive to ceftriaxone, ceftiofur and kanamycin, and has a certain application value for the prevention and treatment of *S.* Pullorum.

2. The multiplex PCR based on the *citE2* gene and intergenic sequence was a highly efficient and practical method to distinguish *S.* Pullorum of natural chicken anal swab and egg samples artificially contaminated with *S*. Pullorum and *S*. Enteritidis. Presumably, the present approach may be a valuable strategy for the early diagnosis and epidemiological investigation of *S.* Pullorum.

3. *SteE* was required for *S*. Pullorum invasion and proliferation, and increased late apoptosis of HD-11 cells in *S*. Pullorum infection. Furthermore, the deletion of *steE* significantly decreased colonization, pathological lesions, virulence, and long-term survival of *S*. Pullorum in chickens by regulating the inflammation response.

4. *SteE* increased the anti-inflammation response, and regulated Th1/Th2-related cytokine expression by modulating the STAT3/SOCS3 and NF-κB axis that may be associated with the Th1/Th2 cells differentiation in HD-11 cells and chickens during *S*. Pullorum infection.

PRODUCTION PROPOSALS

1. On the basis of our recearsh Methodological Recommendations «Construction of multiplex PCR assay based on the *citE2* gene to identity *Salmonella* Pullorum and its effector SteE in pathogenicity and immunity», for laboratory, practical classes and independent work for master's students of veterinary department from disciplines "Veterinary Microbiology"and «Veterinary Zoohygiene», specialties: 211 "Veterinary Medicine", 212 "Veterinary Hygiene, Sanitation and Expertise" was development. (Approved by the Scientific Council of SNAU, protocol No. 5, dated December 29, 2022)

2. We recommend using the materials of the dissertation work when studying the courses "Veterinary microbiology", "Veterinary pharmacology" for masters of the Faculty of Veterinary Medicine of Sumy NAU, and the courses "Veterinary microbiology" and "Veterinary pharmacology" for masters of the Henan Institute of Science and Technology (HIST).

3. We can recommend that the multiplex PCR assay based on the *citE2* gene and intergenic sequence can be used for the accurate detection of *Salmonella* Pullorum in clinical samples, and *steE*, an anti-inflammatory effector as a unique candidate for treating salmonellosis in the future.

REFERENCES

1. Gal-Mor, O. (2018). Persistent Infection and long-term carriage of typhoidal and nontyphoidal *Salmonellae*. Clin Microbiol Rev. 32(1):e00088-18. doi: 10.1128/CMR.00088-18.
2. Coburn, B., Grassl, G. A., and Finlay, B. B. (2007). *Salmonella*, the host and disease: a brief review. Immunol Cell Biol. 85(2):112-8. doi: 10.1038/sj.icb.7100007.
3. Ménard, S., Lacroix-Lamandé, S., Ehrhardt, K., Yan, J., Grassl, G. A., and Wiedemann, A. (2022). Cross-talk between the intestinal epithelium and *Salmonella* Typhimurium. Front Microbiol. 13:906238. doi: 10.3389/fmicb.2022.906238.
4. Broz, P., Ohlson, M. B., and Monack, D. M. (2012). Innate immune response to *Salmonella* Typhimurium, a model enteric pathogen. Gut Microbes. 3(2):62-70. doi: 10.4161/gmic.19141.
5. Xie, Z., Zhang, Y., and Huang, X. (2020). Evidence and speculation: the response of *Salmonella* confronted by autophagy in macrophages. Future Microbiol. 15:1277-1286. doi: 10.2217/fmb-2020-0125.
6. Krukonis, E. S., and Thomson, J. J. (2020). Complement evasion mechanisms of the systemic pathogens *Yersiniae* and *Salmonellae*. FEBS Lett. 594(16):2598-2620. doi: 10.1002/1873-3468.13771.
7. Liu, W., Zhuang, J., Jiang, Y., Sun, J., Prinz, R. A., Sun, J., Jiao, X., and Xu, X. (2019). Toll-like receptor signalling cross-activates the autophagic pathway to restrict *Salmonella* Typhimurium growth in macrophages. Cell Microbiol. 21(12):e13095. doi: 10.1111/cmi.13095.
8. Santos, A. M. P. D., Ferrari, R. G., and Conte-Junior, C. A. (2020). Type three secretion system in *Salmonella* Typhimurium: The key to infection. Genes Genomics. 42(5):495-506. doi: 10.1007/s13258-020-00918-8.
9. Walch, P., Selkrig, J., Knodler, L. A., Rettel, M., Stein, F., Fernandez, K.,

Viéitez, C., Potel, C. M., Scholzen, K., Geyer, M., Rottner, K., Steele-Mortimer, O., Savitski, M. M., Holden, D. W., and Typas, A. (2021). Global mapping of *Salmonella* enterica-host protein-protein interactions during infection. Cell Host Microbe. 29(8):1316-1332.e12. doi: 10.1016/j.chom.2021.06.004.

10. Sun, H., Kamanova, J., Lara-Tejero, M., and Galán, J. E. (2016). A family of *Salmonella* type III secretion effector proteins selectively targets the NF-κB signaling pathway to preserve host homeostasis. PLoS Pathog. 12(3):e1005484. doi: 10.1371/journal.ppat.1005484.
11. Issenhuth-Jeanjean, S., Roggentin, P., Mikoleit, M. L., Guibourdenche, M., de Pinna, E., Nair, S., Fields, P. I., and Weill, F. X. (2014). Supplement 2008-2010 (no. 48) to the white-kauffmann-le minor scheme. Res. Microbiol. 165(7):526–530. doi:10.1016/j.resmic.2014.07.004.
12. Guo, R., Li, Z., Jiao, Y., Geng, S., Pan, Z., Chen, X., Li, Q., and Jiao, X. (2017). O-polysaccharide is important for *Salmonella* Pullorum survival in egg albumen, and virulence and colonization in chicken embryos. Avian Pathol. 46(5):535–540. doi: 10.1080/03079457.2017.1324197.
13. Barrow, P. A., and Neto, O. C. F. (2011). Pullorum disease and fowl typhoid–new thoughts on old diseases: a review. Avian Pathol. 40(1):1–13. doi: 10.1080/03079457.2010.542575.
14. Kubo, I., Kajiya, M., Aramaki, N., and Furutani, S. (2020). Detection of *Salmonella* Enterica in egg yolk by PCR on a microfluidic disc device using immunomagnetic beads. Sensors. 20(4):1060. doi: 10.3390/s20041060.
15. Gand, M., Mattheus, W., Roosens, N. H. C., Dierick, K., Marchal, K., de Keersmaecker, S. C. J., and Bertrand, S. (2020). A multiplex oligonucleotide ligation-PCR method for the genoserotyping of common *Salmonella* using a liquid bead suspension assay. Food Microbiol. 87:103394. doi: 10.1016/j.fm.2019.103394.
16. Vinayaka, A. C., Ngo, T. A., Nguyen, T., Bang, D. D., and Wolff, A. (2020). Pathogen concentration combined solid-phase PCR on supercritical angle fluorescence microlens array for multiplexed detection of invasive nontyphoidal

Salmonella serovars. Anal Chem. 92(3):2706–2713. doi: 10.1021/acs.analchem.9b04863.

17. Liu, Z., Zhang, Q., Yang, N. N., Xu, M. G., Xu, J. F., Jing, M. L., Wu, W. X., Lu, Y. D., Shi, F., and Chen, C. F. (2019). Rapid and sensitive detection of *Salmonella* in chickens using loop-mediated isothermal amplification combined with a lateral flow dipstick. J Microbiol. Biotechnol. 29(3):454–464. doi: 10.4014/jmb.1712.12010.
18. Priya, G. B., Agrawal, R. K., Milton, A. A. P., Mishra, M., Mendiratta, S. K., Luke, A., Inbaraj, S., Sungh, B. R., Kumar, D., Kumar, G. R., and Rajkhowa, S. (2020). Rapid and visual detection of *Salmonella* in meat using invasin A (*invA*) gene-based loop-mediated isothermal amplification assay. LWT-Food Sci Technol. 126:109262. doi：10.1016/j.lwt.2020.109262.
19. Gogoi, P., Borah, P., Hussain, I., Das, L., Hazarika, G., Tamuly, S., and Barkalita, L. M. (2018). Efficacy of pulsed-field gel electrophoresis and repetitive element sequence-based PCR in typing of *Salmonella* isolates from Assam. India. J Clin Microbiol. 56(5):e02043–17. doi: 10.1128/JCM.02043-17.
20. Soler-García, A. A., De Jesús, A. J., Taylor, K., and Brown, E. W. (2014). Differentiation of *Salmonella* strains from the SARA, SARB and SARC reference collections by using three genes PCR-RFLP and the 2100 agilent bioanalyzer. Front Microbiol. 5:417. doi: 10.3389/fmicb.2014.00417.
21. Ren, X., Fu, Y., Xu, C., Feng, Z., Li, M., Zhang, L., Zhang, J., and Liao, M. (2017). High resolution melting (HRM) analysis as a new tool for rapid identification of *Salmonella enterica* serovar Gallinarum biovars Pullorum and Gallinarum. Poult Sci. 96(5):1088–1093. doi: 10.3382/ps/pew400.
22. Xu, Z., Wang, M., Zhou, C., Gu, G., Liang, J., Hou, X., Wang, M., and Wei, P. (2020). Prevalence and antimicrobial resistance of retail-meat-borne *Salmonella* in southern China during the years 2009-2016: the diversity of contamination and the resistance evolution of multidrug-resistant isolates. Int J Food Microbiol. 333:108790. doi: 10.1016/j.ijfoodmicro.2020.108790.

23. Zhou, Y., Kang, X., Meng, C., Xiong, D., Xu, Y., Geng, S., Pan, Z., and Jiao, X. (2020). Multiple PCR assay based on the *cigR* gene for detection of *Salmonella* spp. and *Salmonella* Pullorum/Gallinarum identification. Poult Sci. 99(11):5991–5998. doi: 10.1016/j.psj.2020.07.026.

24. Wilwet, L., Jeyashakila, R., Sivaraman, B., Nayak, B. B., Kumar, H. S., Jaiswar, A. K., Ratrey, V. P., and Jeyasekaran, G. (2021). In-house and on-field validation of the multiplex PCR assay developed for authentication of three commercially important shrimp species. LWT-Food Sci Technol. 148:111701. doi： 10.1016/j.lwt.2021.111701

25. McWhorter, A. R., and Chousalkar, K. K. (2018). A Long-Term Efficacy Trial of a Live, Attenuated *Salmonella* Typhimurium vaccine in layer hens. Front Microbiol. 9:1380. doi: 10.3389/fmicb.2018.01380.

26. Khalefa, H. S., Ahmed, Z. S., Abdel-Kader, F., Ismail, E. M., and Elshafiee, E. A. (2021). Sequencing and phylogenetic analysis of the stn gene of *Salmonella* species isolated from different environmental sources at lake qarun protectorate: The role of migratory birds and public health importance. Vet World. 14(10):2764-2772. doi: 10.14202/vetworld.2021.2764-2772.

27. Mthembu, T. P., Zishiri, O. T., and Zowalaty, M. E. E. (2021). Genomic characterization of antimicrobial resistance in food Chain and livestock-associated *Salmonella* species. Animals (Basel). 11(3):872. doi: 10.3390/ani11030872.

28. Huang, K., Herrero-Fresno, A., Thøfner, I., Skov, S., and Olsen, J. E. (2019). Interaction differences of the avian host-specific *Salmonella enterica* serovar Gallinarum, the host-generalist *S.* Typhimurium, and the cattle host-adapted *S.* Dublin with chicken primary macrophage. Infect Immun. 87(12):e00552-19. doi: 10.1128/IAI.00552-19.

29. Li, Q., Zhu, Y., Yin, K., Xu, L., Yin, C., Li, Y., Ren, J., Yuan, Y., and Jiao, X. (2019). Purification of recombinant IpaJ to develop an indirect ELISA-based method for detecting *Salmonella enterica* serovar Pullorum infections in

chickens. BMC Vet Res. 15(1):3. doi: 10.1186/s12917-018-1753-0.

30. Mohanapriya, K., Agri, H., Anbazhagan, S., Khawaskar, D., Jayakumar, V., Lalrinzuala, M. V., Himani, K. M., Sophia, I., Mariappan, A. K., Abhishek, Nagaleekar, V. K., Sinha, D. K., Chaudhuri, P., Chaturvedi, V. K., Singh, B. R., and Thomas, P. (2023). Development and validation of multiplex PCR based molecular serotyping of *Salmonella serovars* associated with poultry in India. J Microbiol Methods. 207:106710. doi: 10.1016/j.mimet.2023.106710.
31. Tang, Y., Foster, N., Jones, M. A., and Barrow, P. A. (2018). Model of Persistent *Salmonella* infection: *Salmonella enterica* serovar Pullorum modulates the immune response of the chicken from a Th17-Type response towards a Th2-type response. Infect Immun. 86(8):e00307-18. doi: 10.1128/IAI.00307-18.
32. Sedivy-Haley, K., Blimkie, T., Falsafi, R., Lee, A. H., and Hancock, R. E. W. (2022). A transcriptomic analysis of the effects of macrophage polarization and endotoxin tolerance on the response to *Salmonella*. PLoS One. 17(10):e0276010. doi: 10.1371/journal.pone.0276010.
33. Chen, C., Li, J., Zhang, H., Xie, Y., Xiong, L., Liu, H., and Wang, F. (2020). Effects of a probiotic on the growth performance, intestinal flora, and immune function of chicks infected with *Salmonella* pullorum. Poult Sci. 99(11):5316-5323. doi: 10.1016/j.psj.2020.07.017.
34. Bakhshandeh, B., Sorboni, S. G., Haghighi, D. M., Ahmadi, F., Dehghani, Z., and Badiei, A. (2022). New analytical methods using carbon-based nanomaterials for detection of *Salmonella* species as a major food poisoning organism in water and soil resources. Chemosphere. 287(Pt 3):132243. doi: 10.1016/j.chemosphere.2021.132243.
35. Salaheen, S., Sonnier, J., Kim, S. W., Haley, B. J., and Kessel, J. A. S. V. (2020). Interaction of *Salmonella enterica* with bovine epithelial cells demonstrates serovar-specific association and invasion patterns. Foodborne Pathog Dis. 17(10):608-610. doi: 10.1089/fpd.2019.2765.
36. Pacheco, M., Jurado-Sánchez, B., and Escarpa, A. (2018). Sensitive monitoring

of enterobacterial contamination of food using self-propelled janus microsensors. Anal Chem. 90(4):2912-2917. doi: 10.1021/acs.analchem.7b05209.

37. Al-Barazie, R. M., Bashir, G. H., Qureshi, M. M., Mohamed, Y. A., Al-Sbiei, A., Tariq, S., Lammers, W. J., Al-Ramadi, B. K., and Fernandez-Cabezudo, M. J. (2018). Cholinergic activation enhances resistance to oral *Salmonella* infection by modulating innate immune defense mechanisms at the intestinal barrier. Front Immunol. 9:551. doi: 10.3389/fimmu.2018.00551.
38. Moral-Anter, D., Campo-Sabariz, J., Ferrer, R., and Martín-Venegas, R. (2020). *Cyperus esculentus* L. Tubers (tiger nuts) protect epithelial barrier function in Caco-2 Cells infected by *Salmonella* Enteritidis and promote *Lactobacillus plantarum* growth. Nutrients. 13(1):71. doi: 10.3390/nu13010071.
39. Shi, S., Wu, S., Shen, Y., Zhang, S., Xiao, Y., He, X., Gong, J., Farnell, Y., Tang, Y., Huang, Y., and Gao, L. (2018). Iron oxide nanozyme suppresses intracellular *Salmonella* Enteritidis growth and alleviates infection in vivo. Theranostics. 8(22):6149-6162. doi: 10.7150/thno.29303.
40. Gupta, A., Bansal, M., Liyanage, R., Upadhyay, A., Rath, N., Donoghue, A., and Sun, X. (2021). Sodium butyrate modulates chicken macrophage proteins essential for *Salmonella* Enteritidis invasion. PLoS One. 16(4):e0250296. doi: 10.1371/journal.pone.0250296.
41. Aghamiri, S. S., Puniya, B. L., Amin, R., and Helikar, T. (2023). A multiscale mechanistic model of human dendritic cells for in-silico investigation of immune responses and novel therapeutics discovery. Front Immunol. 14:1112985. doi: 10.3389/fimmu.2023.1112985.
42. Park, D., Lara-Tejero, M., Waxham, M. N., Li, W., Hu, B., Galán, J. E., and Liu, J. (2018). Visualization of the type III secretion mediated *Salmonella*-host cell interface using cryo-electron tomography. Elife. 7:e39514. doi: 10.7554/eLife.39514.
43. Stévenin, V., Chang, Y. Y., Toquin, Y. L., Duchateau, M., Gianetto, Q. G., Luk, C. H., Salles, A., Sohst, V., Matondo, M., Reiling, N., and Enninga, J. (2019).

Dynamic growth and shrinkage of the *Salmonella*-containing vacuole determines the intracellular pathogen niche. Cell Rep. 29(12):3958-3973.e7. doi: 10.1016/j.celrep.2019.11.049.

44. Kriston-Vizi, J., Lenart, I., Iwawaki, T., Gould, K., Nesbeth, D., Powis, S. J., and Antoniou, A. N. (2022). *Salmonella* exhibit altered cellular localization in the presence of HLA-B27 and codistribute with endo-reticular membrane. J Immunol Res. 2022:9493019. doi: 10.1155/2022/9493019.
45. Heggie, A., Cerny, O., and Holden, D. W. (2021). SteC and the intracellular *Salmonella*-induced F-actin meshwork. Cell Microbiol. 23(4):e13315. doi: 10.1111/cmi.13315.
46. Kang, X., Huang, T., Shen, H., Meng, C., Jiao, X., and Pan Z. (2022). *Salmonella* Enteritidis subunit vaccine candidate based on SseB Protein co-delivered with simvastatin as adjuvant. Pathogens. 11(4):443. doi: 10.3390/pathogens11040443.
47. Li, Q. (2022). Mechanisms for the invasion and dissemination of *Salmonella*. Can J Infect Dis Med Microbiol. 2022:2655801. doi: 10.1155/2022/2655801.
48. Dong, K., Zhu, Y., Deng, Q., Sun, L., Yang, S., Huang, K., Cao, Y., Li, Y., Wu, S., and Huang, R. (2022). *Salmonella* pSLT-encoded effector SpvB promotes RIPK3-dependent necroptosis in intestinal epithelial cells. Cell Death Discov. 8(1):44. doi: 10.1038/s41420-022-00841-9.
49. Chandra, K., Chowdhury, A. R., Chatterjee, R., and Chakravortty, D. (2022). GH18 family glycoside hydrolase Chitinase A of *Salmonella* enhances virulence by facilitating invasion and modulating host immune responses. PLoS Pathog. 18(4):e1010407. doi: 10.1371/journal.ppat.1010407.
50. Johnson, R., Mylona, E., and Frankel, G. (2018). Typhoidal *Salmonella*: Distinctive virulence factors and pathogenesis. Cell Microbiol. 20(9):e12939. doi: 10.1111/cmi.12939.
51. Zhang, J., Liu, J., Chen, C., Wang, Y., Chen, X., Li, X., and Xu, F. (2022). Resistance and pathogenicity of *Salmonella* Thompson isolated from incubation end of a poultry farm. Vet Sci. 9(7):349. doi: 10.3390/vetsci9070349.

52. Miletic, S., Goessweiner-Mohr, N., and Marlovits, T. C. (2020). The structure of the type III secretion system needle complex. Curr Top Microbiol Immunol. 427:67-90. doi: 10.1007/82_2019_178.

53. Matthews-Palmer, T. R. S., Gonzalez-Rodriguez, N., Calcraft, T., Lagercrantz, S., Zachs, T., Yu, X. J., Grabe, G. J., Holden, D. W., Nans, A., Rosenthal, P. B., Rouse, S. L., and Beeby, M. (2021). Structure of the cytoplasmic domain of SctV (SsaV) from the *Salmonella* SPI-2 injectisome and implications for a pH sensing mechanism. J Struct Biol. 3(2):107729. doi: 10.1016/j.jsb.2021.107729.

54. Marchelletta, R. R., Gareau, M. G., McCole, D. F., Okamoto, S., Roel, E., Klinkenberg, R., Guiney, D. G., Fierer, J., and Barrett, K. E. (2013). Altered expression and localization of ion transporters contribute to diarrhea in mice with *Salmonella*-induced enteritis. Gastroenterology. 145(6):1358-1368.e1-4. doi: 10.1053/j.gastro.2013.08.054.

55. Plumbridge, J., Bossi, L., Oberto, J., Wade, J. T., and Figueroa-Bossi, N. (2014). Interplay of transcriptional and small RNA-dependent control mechanisms regulates chitosugar uptake in *Escherichia coli* and *Salmonella*. Mol Microbiol. 92(4):648-58. doi: 10.1111/mmi.12573.

56. De Nisco, N. J., Rivera-Cancel, G., and Orth, K. (2018). The Biochemistry of sensing: Enteric pathogens regulate type III secretion in response to environmental and host cues. mBio. 9(1):e02122-17. doi: 10.1128/mBio.02122-17.

57. de Jong, H. K., Parry, C. M., van der Poll, T., and Wiersinga, W. J. (2012). Host-pathogen interaction in invasive salmonellosis. PLoS Pathog, 8(10):e1002933. doi: 10.1371/journal.ppat.1002933.

58. Jennings, E., Thurston, T. L. M., and Holden, D. W. (2017). *Salmonella* SPI-2 type III secretion system effectors: Molecular mechanisms and physiological consequences. Cell Host Microbe 22(2):217-231. doi: 10.1016/j.chom.2017.07.009.

59. Brink, T., Leiss, V., Siegert, P., Jehle, D., Ebner, J. K., Schwan, C., Shymanets, A., Wiese, S., Nürnberg, B., Hensel, M., Aktories, K., and Orth, J. H. C. (2018).

Salmonella Typhimurium effector SseI inhibits chemotaxis and increases host cell survival by deamidation of heterotrimeric Gi proteins. PLoS Pathog, 14(8):e1007248. doi: 10.1371/journal.ppat.1007248.

60. Jia, H., Song, N., Ma, Y., Zhang, F., Yue, Y., Wang, W., Li, C., Li, H., Wang, Q., Gu, L., and Li, B. (2022). *Salmonella* facilitates iron acquisition through UMPylation of ferric uptake regulator. mBio, 13(3):e0020722. doi: 10.1128/mbio.00207-22.
61. Wheeler, N. E., Gardner, P. P., and Barquist, L. (2018). Machine learning identifies signatures of host adaptation in the bacterial pathogen *Salmonella* enterica. PLoS Genet. 14(5):e1007333. doi: 10.1371/journal.pgen.1007333.
62. Chin, K. C. J., Taylor, T. D., Hebrard, M., Anbalagan, K., Dashti, M. G., and Phua, K. K. (2017). Transcriptomic study of *Salmonella enterica* subspecies enterica serovar Typhi biofilm. BMC Genomics. 18(1):836. doi: 10.1186/s12864-017-4212-6.
63. Hoffman, S. A., Desai, S. N., Sikorski, M. J., Fatupaito, G., Tupua, S., Thomsen, R. E., Rambocus, S., Nimarota-Brown, S., Punimata, L. L., Sialeipata, M., Tuilagi, C. F., Han, J., Robins-Browne, R. M., Naseri, T. K., and Levine, M. M. (2022). Point-of-care ultrasound by nonexpert operators demonstrates high sensitivity and specificity in detecting gallstones: Data from the Samoa Typhoid fever control program. Am J Trop Med Hyg. 106(3):798-804. doi: 10.4269/ajtmh.21-0973.
64. Hoffman, S. A., Desai, S. N., Sikorski, M. J., Fatupaito, G., Tupua, S., Thomsen, R. E., Rambocus, S., Nimarota-Brown, S., Punimata, L. L., Sialeipata, M., Tuilagi, C. F., Han, J., Robins-Browne, R. M., Naseri, T. K., and Levine, M. M. (2022). Point-of-care ultrasound by nonexpert operators demonstrates high sensitivity and specificity in detecting gallstones: Data from the Samoa Typhoid fever control program. Am J Trop Med Hyg. 106(3):798-804. doi: 10.4269/ajtmh.21-0973.
65. Marshall, J. M., Flechtner, A. D., Perle, K. M. L., and Gunn, J. S. (2014). Visualization of extracellular matrix components within sectioned *Salmonella*

biofilms on the surface of human gallstones. PLoS One. 9(2):e89243. doi: 10.1371/journal.pone.0089243.

66. Richards, A. F., Torres-Velez, F. J., and Mantis, N. J. (2022). *Salmonella* uptake into gut-associated lymphoid tissues: Implications for targeted mucosal vaccine design and delivery. Methods Mol Biol. 2410:305-324. doi: 10.1007/978-1-0716-1884-4_15.

67. Sepe, L. P., Hartl, K., Iftekhar, A., Berger, H., Kumar, N., Goosmann, C., Chopra, S., Schmidt, S. C., Gurumurthy, R. K., Meyer, T. F., and Boccellato, F. (2020). Genotoxic effect of *Salmonella* Paratyphi a infection on human primary gallbladder cells. mBio. 11(5):e01911-20. doi: 10.1128/mBio.01911-20.

68. Savas, S., and Çetinkaya, S. (2020). Molecular typing of different *Salmonella* serotypes by multiple-locus analysis of tandem repeats. J Oleo Sci. 69(12):1585-1589. doi: 10.5650/jos.ess20231.

69. Foster, N., Tang, Y., Berchieri, A., Geng, S., Jiao, X., and Barrow, P. (2021). Revisiting persistent *Salmonella* infection and the carrier state: What do we know? Pathogens. 10(10):1299. doi: 10.3390/pathogens10101299.

70. Badie, F., Saffari, M., Moniri, R., Alani, B., Atoof, F., Khorshidi, A., and Shayestehpour, M. (2021). The combined effect of stressful factors (temperature and pH) on the expression of biofilm, stress, and virulence genes in *Salmonella enterica* ser. Enteritidis and Typhimurium. Arch Microbiol. 203(7):4475-4484. doi: 10.1007/s00203-021-02435-y.

71. Kuźmińska-Bajor, M., Grzymajło, K., and Ugorski, M. (2015). Type 1 fimbriae are important factors limiting the dissemination and colonization of mice by *Salmonella* Enteritidis and contribute to the induction of intestinal inflammation during *Salmonella* invasion. Front Microbiol. 6:276. doi: 10.3389/fmicb.2015.00276.

72. Kaur, D., Gandhi, S., and Mukhopadhaya, A. (2021). *Salmonella* Typhimurium adhesin OmpV activates host immunity to confer protection against systemic and gastrointestinal infection in mice. Infect Immun. 89(8):e0012121. doi: 10.1128/IAI.00121-21.

73. Pławińska-Czarnak, J., Wódz, K., Guzowska, M., Rosiak, E., Nowak, T., Strzałkowska, Z., Kwieciński, A., Kwieciński, P., and Anusz, K. (2023). Comparison of phenotype and genotype virulence and antimicrobial factors of *Salmonella* Typhimurium isolated from human milk. Int J Mol Sci. 24(6):5135. doi: 10.3390/ijms24065135.

74. Cohen, E., Azriel, S., Auster, O., Gal, A., Zitronblat, C., Mikhlin, S., Scharte, F., Hensel, M., Rahav, G., and Gal-Mor, O. (2021). Pathoadaptation of the passerine-associated *Salmonella enterica* serovar Typhimurium lineage to the avian host. PLoS Pathog. 17(3):e1009451. doi: 10.1371/journal.ppat.1009451.

75. Wang, M., Qazi, I. H., Wang, L., Zhou, G., and Han, H. (2020). *Salmonella* virulence and immune escape. Microorganisms. 8(3):407. doi: 10.3390/microorganisms8030407.

76. Elpers, L., Lüken, L., Lange, F., and Hensel, M. (2023). Factors required for adhesion of *Salmonella enterica* serovar Typhimurium to lactuca sativa (lettuce). Microbiol Spectr. 11(1):e0343622. doi: 10.1128/spectrum.03436-22.

77. Giordano, N. P., Mettlach, J. A., and Dalebroux, Z. D. (2022). Conserved tandem arginines for PbgA/YejM allow *Salmonella* Typhimurium to regulate LpxC and control lipopolysaccharide biogenesis during infection. Infect Immun. 90(2):e0049021. doi: 10.1128/IAI.00490-21.

78. Haschka, D., Tymoszuk, P., Petzer, V., Hilbe, R., Heeke, S., Dichtl, S., Skvortsov, S., Demetz, E., Berger, S., Seifert, M., Mitterstiller, A. M., Moser, P., Bumann, D., Nairz, M., Theurl, I., and Weiss, G. (2021). Ferritin H deficiency deteriorates cellular iron handling and worsens *Salmonella* Typhimurium infection by triggering hyperinflammation. JCI Insight. 6(13):e141760. doi: 10.1172/jci.insight.141760.

79. Domínguez-Acuña, L., and Portillo, F. G. (2022). Ferrous iron uptake is required for *Salmonella* to persist within vacuoles of host cells. Infect Immun. 90(6):e0014922. doi: 10.1128/iai.00149-22.

80. Amano, F. (2019). Interaction of *Salmonella* with macrophages-critical roles of *Salmonella* SEp22, a pathogenicity-related protein, and macrophage reactive-

oxygen intermediate species (ROIs) on the infection and survival of *Salmonella*. Yakugaku Zasshi. 139(4):617-627. doi: 10.1248/yakushi.18-00216.

81. Noster, J., Chao, T. C., Sander, N., Schulte, M., Reuter, T., Hansmeier, N., and Hensel, M. (2019). Proteomics of intracellular *Salmonella enterica* reveals roles of *Salmonella* pathogenicity island 2 in metabolism and antioxidant defense. PLoS Pathog. 15(4):e1007741. doi: 10.1371/journal.ppat.1007741.
82. Kogut, M. H., Lee, A., and Santin, E. (2020). Microbiome and pathogen interaction with the immune system. Poult Sci. 99(4):1906-1913. doi: 10.1016/j.psj.2019.12.011.
83. Potrykus, M., Czaja-Stolc, S., Stankiewicz, M., Kaska, Ł., and Małgorzewicz, S. (2021). Intestinal microbiota as a contributor to chronic inflammation and its potential modifications. Nutrients. 13(11):3839. doi: 10.3390/nu13113839.
84. Lu, X., Zhang, M., Yang, S., Deng, Y., and Jiao, Y. (2022). Transcriptome analysis reveals the diverse response of pearl oyster pinctada fucata martensii after different PAMP stimulation. Fish Shellfish Immunol. 131:881-890. doi: 10.1016/j.fsi.2022.10.058.
85. Liao, Z., and Su, J. (2021). Progresses on three pattern recognition receptor families (TLRs, RLRs and NLRs) in teleost. Dev Comp Immunol. 122:104131. doi: 10.1016/j.dci.2021.104131.
86. Stormberg, T., Filliaux, S., Baughman, H. E. R., Komives, E. A., and Lyubchenko, Y. L. (2021). Transcription factor NF-κB unravels nucleosomes. Biochim Biophys Acta Gen Subj. 1865(9):129934. doi: 10.1016/j.bbagen.2021.129934.
87. Hayden, M. S., and Ghosh, S. (2008). Shared principles in NF-kappaB signaling. Cell. 132(3):344-62. doi: 10.1016/j.cell.2008.01.020.
88. Bariana, M., Cassella, E., Rateshwar, J., Ouk, S., Liou, H. C., Heller, C., Colorado, I., Feinman, R., Makhdoom, A., Siegel, D. S., Heller, G., Tuckett, A., Mondello P., and Zakrzewski, J. L. (2022). Inhibition of NF-κB DNA binding suppresses myeloma growth via intracellular redox and tumor microenvironment modulation. Mol Cancer Ther. 21(12):1798-1809. doi: 10.1158/1535-

7163.MCT-22-0257.

89. Li, R., Zhou, Y., Zhang, S., Li, J., Zheng, Y., and Fan, X. (2022). The natural (poly)phenols as modulators of microglia polarization via TLR4/NF-κB pathway exert anti-inflammatory activity in ischemic stroke. Eur J Pharmacol. 914:174660. doi: 10.1016/j.ejphar.2021.174660.

90. Markowiak, P., and Śliżewska, K. (2017). Effects of probiotics, prebiotics, and synbiotics on human health. Nutrients. 9(9):1021. doi: 10.3390/nu9091021.

91. Tao, H., Li, W., Zhang, W., Yang, C., Zhang, C., Liang, X., Yin, J., Bai, J., Ge, G., Zhang, H., Yang, X., Li, H., Xu, Y., Hao, Y., Liu, Y., and Geng, D. (2021). Urolithin A suppresses RANKL-induced osteoclastogenesis and postmenopausal osteoporosis by, suppresses inflammation and downstream NF-κB activated pyroptosis pathways. Pharmacol Res. 174:105967. doi: 10.1016/j.phrs.2021.105967.

92. Gómez-Chávez, F., Correa, D., Navarrete-Meneses, P., Cancino-Diaz, J. C., Cancino-Diaz, M. E., and Rodríguez-Martínez, S. (2021). NF-κB and its regulators during pregnancy. Front Immunol. 12:679106. doi: 10.3389/fimmu.2021.679106.

93. Sharma, A., Raman, V., Lee, J., and Forbes, N. S. (2022). Microbial imbalance induces inflammation by promoting *Salmonella* penetration through the mucosal barrier. ACS Infect Dis. 8(5):969-981. doi: 10.1021/acsinfecdis.1c00530.

94. Bliska, J. B., and van der Velden, A. W. M. (2012). *Salmonella* "sops" up a preferred electron receptor in the inflamed intestine. mBio. 3(4):e00226-12. doi: 10.1128/mBio.00226-12.

95. Lawrence, A. E., Abuaita, B. H., Berger, R. P., Hill, D. R., Huang, S., Yadagiri, V. K., Bons, B., Fields, C., Wobus, C. E., Spence, J. R., Young, V. B., and O'Riordan, M. X. (2021). *Salmonella enterica* serovar Typhimurium SPI-1 and SPI-2 shape the global transcriptional landscape in a human intestinal organoid model system. mBio. 12(3):e00399-21. doi: 10.1128/mBio.00399-21.

96. Jiang, Y., He, L., Ju, C., Pei, Y., Ji, M., Li, Y., Liao, L., Jang, S., Zhu, Z., and Wang, Y. (2015). Isolation and expression of grass carp toll-like receptor 5a

(CiTLR5a) and 5b (CiTLR5b) gene involved in the response to flagellin stimulation and grass carp reovirus infection. Fish Shellfish Immunol. 44(1):88-99. doi: 10.1016/j.fsi.2015.01.024.

97. Finn, C. E., Chong, A., Cooper, K. G., Starr, T., and Steele-Mortimer, O. (2017). A second wave of *Salmonella* T3SS1 activity prolongs the lifespan of infected epithelial cells. PLoS Pathog. 13(4):e1006354. doi: 10.1371/journal.ppat.1006354.

98. Li, D., Wang, X., Wang, L., and Zhou, D. (2013). The actin-polymerizing activity of SipA is not essential for *Salmonella* enterica serovar Typhimurium-induced mucosal inflammation. Infect Immun. 81(5):1541-9. doi: 10.1128/IAI.00337-12.

99. Keestra, A. M., Winter, M. G., Klein-Douwel, D., Xavier, M. N., Winter, S. E., Kim, A., Tsolis, R. M., and Bäumler, A. J. (2011). A *Salmonella* virulence factor activates the NOD1/NOD2 signaling pathway. mBio. 2(6):e00266-11. doi: 10.1128/mBio.00266-11.

100. Parween, F., Yadav, J., and Qadri, A. (2019). The virulence polysaccharide of *Salmonella* Typhi suppresses activation of Rho family GTPases to limit inflammatory responses from epithelial cells. Front Cell Infect Microbiol. 9:141. doi: 10.3389/fcimb.2019.00141.

101. Liu, Y., Dou, Y., Yan, L., Yang, X., He, B., Kong, L., and Smith, W. (2020). The role of Rho GTPases' substrates Rac and Cdc42 in osteoclastogenesis and relevant natural medicinal products study. Biosci Rep. 40(7): BSR20200407. doi: 10.1042/BSR20200407.

102. Bruno, V. M., Hannemann, S., Lara-Tejero, M., Flavell, R. A., Kleinstein, S. H., and Galán, J. E. (2009). *Salmonella* Typhimurium type III secretion effectors stimulate innate immune responses in cultured epithelial cells. PLoS Pathog. 5(8):e1000538. doi: 10.1371/journal.ppat.1000538.

103. Galán, J. E. (2021). *Salmonella* Typhimurium and inflammation: a pathogen-centric affair. Nat Rev Microbiol. 19(11):716-725. doi: 10.1038/s41579-021-00561-4.

104. Pinaud, L., Sansonetti, P. J., and Phalipon, A. (2018). Host cell targeting by enteropathogenic bacteria T3SS effectors. Trends Microbiol. 26(4):266-283. doi: 10.1016/j.tim.2018.01.010.

105. Keestra, A. M., Winter, M. G., Auburger, J. J., Frässle, S. P., Xavier, M. N., Winter, S. E., Kim, A., Poon, V., Ravesloot, M. M., Waldenmaier, J. F., Tsolis, R. M., Eigenheer, R. A., and Bäumler, A. J. (2013). Manipulation of small Rho GTPases is a pathogen-induced process detected by NOD1. Nature. 496(7444):233-7. doi: 10.1038/nature12025.

106. Cuadrado, A., Martín-Moldes, Z., Ye, J., and Lastres-Becker, I. (2014). Transcription factors NRF2 and NF-κB are coordinated effectors of the Rho family, GTP-binding protein RAC1 during inflammation. J Biol Chem. 289(22):15244-58. doi: 10.1074/jbc.M113.540633.

107. Lin, Z., Zhang, Y. G., Xia, Y., Xu, X., Jiao, X., and Sun, J. (2016). *Salmonella enteritidis* effector AvrA stabilizes intestinal tight junctions via the JNK pathway. J Biol Chem. 291(52):26837-26849. doi: 10.1074/jbc.M116.757393.

108. Zhang, Y., Wu, S., Ma, J., Xia, Y., Ai, X., and Sun, J. (2015). Bacterial protein AvrA stabilizes intestinal epithelial tight junctions via blockage of the C-Jun N-terminal kinase pathway. Tissue Barriers. 3(1-2):e972849. doi: 10.4161/21688362.2014.972849.

109. Ye, Z., Petrof, E. O., Boone, D., Claud, E. C., and Sun, J. (2007). *Salmonella* effector AvrA regulation of colonic epithelial cell inflammation by deubiquitination. Am J Pathol. 171(3):882-92. doi: 10.2353/ajpath.2007.070220.

110. Giogha, C., Lung, T. W., Pearson, J. S., and Hartland, E. L. (2014). Inhibition of death receptor signaling by bacterial gut pathogens. Cytokine Growth Factor Rev. 25(2):235-43. doi: 10.1016/j.cytogfr.2013.12.012.

111. Jiao, Y., Zhang, Y. G., Lin, Z., Lu, R., Xia, Y., Meng, C., Pan, Z., Xu, X., Jiao, X., and Sun, J. (2020). *Salmonella* Enteritidis effector AvrA suppresses autophagy by reducing beclin-1 protein. Front Immunol. 11:686. doi: 10.3389/fimmu.2020.00686.

112. Wu, H., Jones, R. M., and Neish, A, S. (2012). The *Salmonella* effector AvrA mediates bacterial intracellular survival during infection *in vivo*. Cell Microbiol. 14(1):28-39. doi: 10.1111/j.1462-5822.2011.01694.x.

113. Geng, S., Wang, Y., Xue, Y., Wang, H., Cai, Y., Zhang, J., Barrow, P., Pan, Z., and Jiao, X. (2019). The SseL protein inhibits the intracellular NF-κB pathway to enhance the virulence of *Salmonella* Pullorum in a chicken model. Microb Pathog. 129:1-6. doi: 10.1016/j.micpath.2019.01.035.

114. Rytkönen, A., Poh, J., Garmendia, J., Boyle, C., Thompson, A., Liu, M., Freemont, P., Hinton, J. C., and Holden, D. W. (2007). SseL, a *Salmonella* deubiquitinase required for macrophage killing and virulence. Proc Natl Acad Sci USA. 104(9):3502-7. doi: 10.1073/pnas.0610095104.

115. Figueira, R., Watson, K. G., Holden, D. W., and Helaine, S. (2013). Identification of *Salmonella* pathogenicity island-2 type III secretion system effectors involved in intramacrophage replication of *S. enterica* serovar Typhimurium: implications for rational vaccine design. mBio. 4(2):e00065. doi: 10.1128/mBio.00065-13.

116. Mesquita, F. S., Holden, D. W., and Rolhion, N. (2013). Lack of effect of the *Salmonella* deubiquitinase SseL on the NF-κB pathway. PLoS One. 8(1):e53064. doi: 10.1371/journal.pone.0053064.

117. LaRock, D. L., Chaudhary, A., and Miller, S. I. (2015). Salmonellae interactions with host processes. Nat Rev Microbiol. 13(4):191-205. doi: 10.1038/nrmicro3420.

118. Kubori, T., and Galán, J. E. (2003). Temporal regulation of *Salmonella* virulence effector function by proteasome-dependent protein degradation. Cell. 115(3):333-42. doi: 10.1016/s0092-8674(03)00849-3.

119. Johnson, R., Byrne, A., Berger, C. N., Klemm, E., Crepin, V. F., Dougan, G., and Frankel, G. (2017). The type III secretion system effector SptP of *Salmonella enterica* serovar typhi. J Bacteriol. 199(4):e00647-16. doi: 10.1128/JB.00647-16.

120. Cain, R. J., Hayward, R. D., and Koronakis, V. (2008). Deciphering interplay

between *Salmonella* invasion effectors. PLoS Pathog. 4(4):e1000037. doi: 10.1371/journal.ppat.1000037.

121. Lhocine, N., Arena, E. T., Bomme, P., Ubelmann, F., Prévost, M. C., Robine, S., and Sansonetti, P. J. (2015). Apical invasion of intestinal epithelial cells by *Salmonella* Typhimurium requires villin to remodel the brush border actin cytoskeleton. Cell Host Microbe. 17(2):164-77. doi: 10.1016/j.chom.2014.12.003.

122. Fu, Y., and Galán, J. E. (1999). A *Salmonella* protein antagonizes Rac-1 and Cdc42 to mediate host-cell recovery after bacterial invasion. Nature. 401(6750): 293-7. doi: 10.1038/45829.

123. Keszei, A. F., Tang, X., McCormick, C., Zeqiraj, E., Rohde, J. R., Tyers, M., and Sicheri, F. (2014). Structure of an SspH1-PKN1 complex reveals the basis for host substrate recognition and mechanism of activation for a bacterial E3 ubiquitin ligase. Mol Cell Biol. 34(3):362-73. doi: 10.1128/MCB.01360-13.

124. Cook, M., Delbecq, S. P., Schweppe, T. P., Guttman, M., Klevit, R. E., and Brzovic, P. S. (2019). The ubiquitin ligase SspH1 from *Salmonella* uses a modular and dynamic E3 domain to catalyze substrate ubiquitylation. J Biol Chem. 294(3):783-793. doi: 10.1074/jbc.RA118.004247.

125. Haraga, A., and Miller, S, I. (2006). A *Salmonella* type III secretion effector interacts with the mammalian serine/threonine protein kinase PKN1. Cell Microbiol. 8(5):837-46. doi: 10.1111/j.1462-5822.2005.00670.x.

126. Batkhishig, D., Bilguun, K., Enkhbayar, P., Miyashita, H., Kretsinger, R. H., and Matsushima, N. (2018). Super secondary structure consisting of a polyproline II helix and a β-turn in leucine rich repeats in bacterial type III secretion system effectors. Protein J. 37(3):223-236. doi: 10.1007/s10930-018-9767-9.

127. Svahn, A. J., Suster, C. J. E., Chang, S. L., Rockett, R. J., Sim, E. M., Cliff, O. M., Wang, Q., Arnott, A., Ramsperger, M., Sorrell, T. C., Sintchenko, V., and Prokopenko, M. (2023). Pangenome analysis of a *Salmonella* Enteritidis population links a major outbreak to a Gifsy-1-like prophage containing anti-

inflammatory gene *gogB*. Microbiol Spectr. 11(2):e0279122. doi: 10.1128/spectrum.02791-22.

128. Coombes, B. K., Wickham, M. E., Brown, N. F., Lemire, S., Bossi, L., Hsiao, W. W., Brinkman, F. S., and Finlay, B. B. (2005). Genetic and molecular analysis of GogB, a phage-encoded type III-secreted substrate in *Salmonella enterica* serovar Typhimurium with autonomous expression from its associated phage. J Mol Biol. 348(4):817-830. doi: 10.1016/j.jmb.2005.03.024.

129. Pilar, A. V., Reid-Yu, S. A., Cooper, C. A., Mulder, D. T., and Coombes, B. K. (2012). GogB is an anti-inflammatory effector that limits tissue damage during *Salmonella* infection through interaction with human FBXO22 and Skp1. PLoS Pathog. 8(6):e1002773. doi: 10.1371/journal.ppat.1002773.

130. Wang, L., Li, Y., Liu, Y., Zuo, L., Li, Y., Wu, S., and Huang, R. (2019). *Salmonella spv* locus affects type I interferon response and the chemotaxis of neutrophils via suppressing autophagy. Fish Shellfish Immunol. 87:721-729. doi: 10.1016/j.fsi.2019.02.009.

131. Passaris, I., Cambré, A., Govers, S. K., and Aertsen, A. (2018). Bimodal expression of the *Salmonella* Typhimurium *spv* operon. Genetics. 210(2): 621-635. doi: 10.1534/genetics.118.300822.

132. Stanley, A., Thompson, K., Hynes, A., Brakebusch, C., and Quondamatteo, F. (2014). NADPH oxidase complex-derived reactive oxygen species, the actin cytoskeleton, and Rho GTPases in cell migration. Antioxid Redox Signal. 20(13):2026-42. doi: 10.1089/ars.2013.5713.

133. Haneda, T., Ishii, Y., Shimizu, H., Ohshima, K., Iida, N., Danbara, H., and Okada, N. (2012). *Salmonella* type III effector SpvC, a phosphothreonine lyase, contributes to reduction in inflammatory response during intestinal phase of infection. Cell Microbiol. 14(4):485-99. doi: 10.1111/j.1462-5822.2011.01733.x.

134. Burnaevskiy, N., Fox, T. G., Plymire, D. A., Ertelt, J. M., Weigele, B. A., Selyunin, A. S., Way, S. S., Patrie, S. M., and Alto, N. M. (2013). Proteolytic elimination of N-myristoyl modifications by the *Shigella* virulence factor IpaJ.

Nature. 496(7443):106-9. doi: 10.1038/nature12004.

135. Li, Q., Xu, L., Yin, C., Liu, Z., Li, Y., Yuan, Y., Hu, Y., and Jiao, X. (2020). The invasion plasmid antigen J (IpaJ) from *Salmonella* inhibits NF-κB activation by suppressing IκBα ubiquitination. Infect Immun. 88(3):e00875-19. doi: 10.1128/IAI.00875-19.

136. Yin, C., Gu, J., Gu, D., Wang, Z., Ji, R., Jiao, X., and Li, Q. (2022). The *Salmonella* T3SS1 effector IpaJ is regulated by ItrA and inhibits the MAPK signaling pathway. PLoS Pathog. 18(12):e1011005. doi: 10.1371/journal.ppat.1011005.

137. Takemura, M., Haneda, T., Idei, H., Miki, T., and Okada, N. (2021). A *Salmonella* type III effector, PipA, works in a different manner than the PipA family effectors GogA and GtgA. PLoS One. 16(3):e0248975. doi: 10.1371/journal.pone.0248975.

138. Günster, R. A., Matthews, S. A., Holden, D. W., and Thurston, T. L. M. (2017). SseK1 and SseK3 type III secretion system effectors inhibit NF-κB signaling and necroptotic cell death in *Salmonella*-infected macrophages. Infect Immun. 85(3):e00010-17. doi: 10.1128/IAI.00010-17.

139. Yang, Z., Soderholm, A., Lung, T. W., Giogha, C., Hill, M. M., Brown, N. F., Hartland, E., and Teasdale, R. D. (2015). SseK3 is a *Salmonella* effector that binds TRIM32 and modulates the host's NF-κB signalling activity. PLoS One. 10(9), e0138529. doi: 10.1371/journal.pone.0138529.

140. Rolhion, N., Furniss, R. C., Grabe, G., Ryan, A., Liu, M., Matthews, S. A., and Holden, D. W. (2016). Inhibition of nuclear transport of NF-κB p65 by the *Salmonella* type III secretion system effector SpvD. PLoS Pathog. 12(5):e1005653. doi: 10.1371/journal.ppat.1005653.

141. Lashua, L. P., Melvin, J. A., Deslouches, B., Pilewski, J. M., Montelaro, R. C., and Bomberger, J. M. (2016). Engineered cationic antimicrobial peptide (eCAP) prevents *Pseudomonas aeruginosa* biofilm growth on airway epithelial cells. J Antimicrob Chemother. 71(8):2200-7. doi: 10.1093/jac/dkw143.

142. Mangmee, S., Reamtong, O., Kalambaheti, T., Roytrakul, S., and

Sonthayanon, P. (2021). Antimicrobial peptide modifications against clinically isolated antibiotic-resistant *Salmonella*. Molecules. 26(15):4654. doi: 10.3390/molecules26154654.

143. Baradaran, E., Moharramipour, S., Asgari, S., and Mehrabadi, M. (2019). Induction of DNA methyltransferase genes in Helicoverpa armigera following injection of pathogenic bacteria modulates expression of antimicrobial peptides and affects bacterial proliferation. J Insect Physiol. 118:103939. doi: 10.1016/j.jinsphys.2019.103939.
144. Matthias, J., Heink, S., Picard, F., Zeiträg, J., Kolz, A., Chao, Y. Y., Soll, D., de Almeida, G. P., Glasmacher, E., Jacobsen, I. D., Riedel, T., Peters, A., Floess, S., Huehn, J., Baumjohann, D., Huber, M., Korn, T., and Zielinski, C. E. (2020). Salt generates antiinflammatory Th17 cells but amplifies pathogenicity in proinflammatory cytokine microenvironments. J Clin Invest. 130(9):4587-4600. doi: 10.1172/JCI137786.
145. Hou, X., Zhang, X., Zhao, W., Zeng, C., Deng, B., McComb, D. W., Du, S., Zhang, C., Li, W., and Dong, Y. (2020). Vitamin lipid nanoparticles enable adoptive macrophage transfer for the treatment of multidrug-resistant bacterial sepsis. Nat Nanotechnol. 15(1):41-46. doi: 10.1038/s41565-019-0600-1.
146. Anandan, A., and Vrielink, A. (2020). Structure and function of lipid A-modifying enzymes. Ann N Y Acad Sci. 1459(1):19-37. doi: 10.1111/nyas.14244.
147. Renu, S., Markazi, A. D., Dhakal, S., Lakshmanappa, Y. S., Shanmugasundaram, R., Selvaraj, R. K., and Renukaradhya, G. J. (2020). Oral deliverable mucoadhesive chitosan-*Salmonella* subunit nanovaccine for layer chickens. Int J Nanomedicine. 15:761-777. doi: 10.2147/IJN.S238445.
148. Germic, N., Frangez, Z., Yousefi, S., and Simon, H. U. (2019). Regulation of the innate immune system by autophagy: monocytes, macrophages, dendritic cells and antigen presentation. Cell Death Differ. 26(4):715-727. doi: 10.1038/s41418-019-0297-6.
149. Ma, C., Wu, M., Ye, W., Huang, Z., Ma, X., Wang, W., Wang, W., Huang, Y.,

Pan, X., and Wu, C. (2021). Inhalable solid lipid nanoparticles for intracellular tuberculosis infection therapy: Macrophage-targeting and pH-sensitive properties. Drug Deliv Transl Res. 11(3):1218-1235. doi: 10.1007/s13346-020-00849-7.

150. Bruna, R. E., Casal, A., Bercovich, B., Gramajo, H., Rodríguez, E., and García Véscovi, E. (2022). A natural product from *Streptomyces* targets PhoP and exerts antivirulence action against *Salmonella enterica*. J Antimicrob Chemother. 77(11):3050-3063. doi: 10.1093/jac/dkac278.

151. Li, Q., Wang, X., Xia, J., Yuan, Y., Yin, C., Xu, L., Li, Y., and Jiao, X. (2018). *Salmonella*-containing vacuole development in avian cells and characteristic of cigR in *Salmonella enterica* serovar Pullorum replication within macrophages. Vet Microbiol. 223:65-71. doi: 10.1016/j.vetmic.2018.07.013.

152. Knuff-Janzen, K., Tupin, A., Yurist-Doutsch, S., Rowland, J. L., and Finlay, B. B. (2020). Multiple *Salmonella*-pathogenicity island 2 effectors are required to facilitate bacterial establishment of its intracellular niche and virulence. PLoS One. 15(6):e0235020. doi: 10.1371/journal.pone.0235020.

153. Walch, P., Selkrig, J., Knodler, L. A., Rettel, M., Stein, F., Fernandez, K., Viéitez, C., Potel, C. M., Scholzen, K., Geyer, M., Rottner, K., Steele-Mortimer, O., Savitski, M. M., Holden, D. W., and Typas, A. (2021). Global mapping of *Salmonella enterica*-host protein-protein interactions during infection. Cell Host Microbe. 29(8):1316-1332.e12. doi: 10.1016/j.chom.2021.06.004.

154. Cavinato, L., Genise, E., Luly, F. R., Domenico, E. G. D., Porto, P. D., and Ascenzioni, F. (2020). Escaping the phagocytic oxidative burst: The role of SODB in the survival of *Pseudomonas aeruginosa* within macrophages. Front Microbiol. 11:326. doi: 10.3389/fmicb.2020.00326. 155. Rhen, M. (2019). *Salmonella* and reactive oxygen species: A love-hate relationship. J Innate Immun. 11(3):216-226. doi: 10.1159/000496370.

156. Lapp, K., Vödisch, M., Kroll, K., Strassburger, M., Kniemeyer, O., Heinekamp, T., and Brakhage, A. A. (2014). Characterization of the *Aspergillus*

fumigatus detoxification systems for reactive nitrogen intermediates and their impact on virulence. Front Microbiol. 5:469. doi: 10.3389/fmicb.2014.00469.

157. Helm, J. S., and Rudel, R. A. (2020). Adverse outcome pathways for ionizing radiation and breast cancer involve direct and indirect DNA damage, oxidative stress, inflammation, genomic instability, and interaction with hormonal regulation of the breast. Arch Toxicol. 94(5):1511-1549. doi: 10.1007/s00204-020-02752-z.

158. Downs, D. M., and Ernst, D. C. (2015). From microbiology to cancer biology: The Rid protein family prevents cellular damage caused by endogenously generated reactive nitrogen species. Mol Microbiol. 96(2):211-9. doi: 10.1111/mmi.12945.

159. Zhang, L., and Yi, H. (2022). Potential antitumor and anti-inflammatory activities of an extracellular polymeric substance (EPS) from *Bacillus subtilis* isolated from a housefly. Sci Rep. 12(1):1383. doi: 10.1038/s41598-022-05143-9.

160. Bonnet, J., Durmort, C., Jacq, M., Mortier-Barrière, I., Campo, N., VanNieuwenhze, M. S., Brun, Y. V., Arthaud, C., Gallet, B., Moriscot, C., Morlot, C., Vernet, T., and Guilmi, A. M. D. (2017). Peptidoglycan O-acetylation is functionally related to cell wall biosynthesis and cell division in *Streptococcus pneumoniae*. Mol Microbiol. 106(5):832-846. doi: 10.1111/mmi.13849.

161. Chu, Y., Kang, Y., Yan, C., Yang, C., Zhang, T., Huo, H., and Liu, Y. (2021). LUBAC and OTULIN regulate autophagy initiation and maturation by mediating the linear ubiquitination and the stabilization of ATG13. Autophagy. 17(7):1684-1699. doi: 10.1080/15548627.2020.1781393.

162. Claviere, M., Lavedrine, A., Lamiral, G., Bonnet, M., Verlhac, P., Petkova, D. S., Espert, L., Duclaux-Loras, R., Lucifora, J., Rivoire, M., Boschetti, G., Nancey, S., Rozières, A., Viret, C., and Faure, M. (2023). Measles virus-imposed remodeling of the autophagy machinery determines the outcome of bacterial coinfection. Autophagy. 19(3):858-872. doi:

10.1080/15548627.2022.2107309.

163. Tuli, A., and Sharma, M. (2019). How to do business with lysosomes: *Salmonella* leads the way. Curr Opin Microbiol. 47:1-7. doi: 10.1016/j.mib.2018.10.003.

164. Gutiérrez, S., Wolke, M., Plum, G., and Robinson, N. (2017). Isolation of *Salmonella* Typhimurium-containing phagosomes from macrophages. J Vis Exp. 128(128):56514. doi: 10.3791/56514.

165. Giraud-Gatineau, A., Coya, J. M., Maure, A., Biton, A., Thomson, M., Bernard, E. M., Marrec, J., Gutierrez, M. G., Larrouy-Maumus, G., Brosch, R., Gicquel, B., and Tailleux, L. (2020). The antibiotic bedaquiline activates host macrophage innate immune resistance to bacterial infection. Elife. 9:e55692. doi: 10.7554/eLife.55692.

166. Liss, V., Swart, A. L., Kehl, A., Hermanns, N., Zhang, Y., Chikkaballi, D., Böhles, N., Deiwick, J., and Hensel, M. (2017). *Salmonella enterica* remodels the host cell endosomal system for efficient intravacuolar nutrition. Cell Host Microbe. 21(3):390-402. doi: 10.1016/j.chom.2017.02.005.

167. Wu, S. Y., Wang, L. D., Xu, G. M., Yang, S. D., Deng, Q. F., Li, Y. Y., and Huang, R. (2017). Spv locus aggravates *Salmonella* infection of zebrafish adult by inducing Th1/Th2 shift to Th2 polarization. Fish Shellfish Immunol. 67:684-691. doi: 10.1016/j.fsi.2017.06.057.

168. Essa, S., Siddique, I., Saad, M., and Raghupathy, R. (2021). Modulation of production of Th1/Th2 cytokines in peripheral blood mononuclear cells and neutrophils by Hepatitis C virus infection in chronically infected patients. Pathogens. 10(11):1519. doi: 10.3390/pathogens10111519.

169. Carneiro, M. B., Lopes, M. E., Hohman, L. S., Romano, A., David, B. A., Kratofil, R., Kubes, P., Workentine, M. L., Campos, A. C., Vieira, L. Q., and Peters, N. C. (2020). Th1-Th2 cross-regulation controls early *Leishmania* infection in the skin by modulating the size of the permissive monocytic host cell reservoir. Cell Host Microbe. 27(5):752-768.e7. doi: 10.1016/j.chom.2020.03.011.

170. Wu, Q. J., Zheng, X. C., Wang, T., and Zhang, T. Y. (2018). Effects of oridonin on immune cells, Th1/Th2 balance and the expression of BLys in the spleens of broiler chickens challenged with *Salmonella* pullorum. Res Vet Sci. 119:262-267. doi: 10.1016/j.rvsc.2018.07.008.

171. Wang, C., Cheng, W., Yu, Q., Xing, T., Chen, S., Liu, L., Yu, L., Du, J., Luo, Q., Shen, J., and Xu, Y. (2018). *Toxoplasma* Chinese 1 strain of WH3Δ*rop16I*/*III*/*gra15II* genetic background contributes to abnormal pregnant outcomes in murine model. Front Immunol. 9:1222. doi: 10.3389/fimmu.2018.01222.

172. Barrientos, L., Bignon, A., Gueguen, C., de Chaisemartin, L., Gorges, R., Sandré, C., Mascarell, L., Balabanian, K., Kerdine-Römer, S., Pallardy, M., Marin-Esteban, V., and Chollet-Martin, S. (2014). Neutrophil extracellular traps downregulate lipopolysaccharide-induced activation of monocyte-derived dendritic cells. J Immunol. 193(11):5689-98. doi: 10.4049/jimmunol.1400586.

173. Ho, T. T. B., Nasti, A., Seki, A., Komura, T., Inui, H., Kozaka, T., Kitamura, Y., Shiba, K., Yamashita, T., Yamashita, T., Mizukoshi, E., Kawaguchi, K., Wada, T., Honda, M., Kaneko, S., and Sakai, Y. (2020). Combination of gemcitabine and anti-PD-1 antibody enhances the anticancer effect of M1 macrophages and the Th1 response in a murine model of pancreatic cancer liver metastasis. J Immunother Cancer. 8(2):e001367. doi: 10.1136/jitc-2020-001367.

174. Antonelli, A., Fallahi, P., Elia, G., Ragusa, F., Paparo, S. R., Ruffilli, I., Patrizio, A., Gonnella, D., Giusti, C., Virili, C., Centanni, M., Shoenfeld, Y., and Ferrari, S. M. (2020). Graves' disease: Clinical manifestations, immune pathogenesis (cytokines and chemokines) and therapy. Best Pract Res Clin Endocrinol Metab. 34(1):101388. doi: 10.1016/j.beem.2020.101388.

175. Gan, Z. S., Wang, Q. Q., Li, J. H., Wang, X. L., Wang, Y. Z., and Du, H. H. (2017). Iron reduces M1 macrophage polarization in RAW264.7 macrophages associated with inhibition of STAT1. Mediators Inflamm. 2017:8570818. doi: 10.1155/2017/8570818.

176. Fan, L., Qi, Y., Qu, S., Chen, X., Li, A., Hendi, M., Xu, C., Wang, L., Hou, T., Si, J., and Chen, S. (2021). *B. adolescentis* ameliorates chronic colitis by regulating Treg/Th2 response and gut microbiota remodeling. Gut Microbes. 13(1):1-17. doi: 10.1080/19490976.2020.1826746.

177. Gonzalez, M. E., Volk-Draper, L., Bhattarai, N., Wilber, A., and Ran, S. (2022). Th2 Cytokines IL-4, IL-13, and IL-10 promote differentiation of pro-lymphatic progenitors derived from bone marrow myeloid precursors. Stem Cells Dev. 31(11-12):322-333. doi: 10.1089/scd.2022.0004.

178. Lv, R., Bao, Q., and Li, Y. (2017). Regulation of M1-type and M2-type macrophage polarization in RAW264.7 cells by Galectin-9. Mol Med Rep. 16: (6)9111-9119. doi: 10.3892/mmr.2017.7719.

179. Fan, C., Dai, Y., Zhang, L., Rui, C., Wang, X., Luan, T., Fan, Y., Dong, Z., Hou, W., Li, P., Liao, Q., and Zeng, X. (2021). Aerobic vaginitis induced by *Escherichia coli* infection during pregnancy can result in adverse pregnancy outcomes through the IL-4/JAK-1/STAT-6 pathway. Front Microbiol. 12:651426. doi: 10.3389/fmicb.2021.651426.

180. Rosshirt, N., Trauth, R., Platzer, H., Tripel, E., Nees, T. A., Lorenz, H. M., Tretter, T., and Moradi, B. (2021). Proinflammatory T cell polarization is already present in patients with early knee osteoarthritis. Arthritis Res Ther. 23(1):37. doi: 10.1186/s13075-020-02410-w.

181. Muraille, E., Leo, O., and Moser, M. (2014). TH1/TH2 paradigm extended: macrophage polarization as an unappreciated pathogen-driven escape mechanism? Front Immunol. 5:603. doi: 10.3389/fimmu.2014.00603.

182. Shen, J., Chelvam, V., Cresswell, G., and Low, P. S. (2013). Use of folate-conjugated imaging agents to target alternatively activated macrophages in a murine model of asthma. Mol Pharm. 10(5):1918-27. doi: 10.1021/mp3006962.

183. Gazzinelli-Guimaraes, P. H., Prado, R. D. Q., Ricciardi, A., Bonne-Année, S., Sciurba, J., Karmele, E. P., Fujiwara, R. T., and Nutman, T. B. (2019). Allergen presensitization drives an eosinophil-dependent arrest in lung-specific helminth

development. J Clin Invest. 12(9):3686-3701. doi: 10.1172/JCI127963.

184. de Sousa, E. S. O., Cortez, A. C. A., Melhem, M. D. S. C., Frickmann, H., and de Souza, J. V. B. (2020). Factors influencing susceptibility testing of antifungal drugs: a critical review of document M27-A4 from the Clinical and Laboratory Standards Institute (CLSI). Brazilian Journal of Microbiology. 51(4):1791-1800. doi: 10.1007/s42770-020-00354-6.

185. China National Food Safety Standard. 2016. Detection of Food Microorganisms-*Salmonella* spp. Ministry of Health of the People's Republic of China. National Food Safety Standard, China GB4789.4−2016

186. Ho, K., and Harshey, R. M. (2021). Goodbye PAM: Phage λ's Red recombination system cripples PAMs and helps dodge CRISPR attacks. Cell Host Microbe. 29(10):1469-1471. doi: 10.1016/j.chom.2021.09.011.

187. Yin, J., Xia, J., Tao, M., Xu, L., Li, Q., Geng, S., and Jiao, X. (2016). Construction and characterization of a *cigR* deletion mutant of *Salmonella enterica* serovar Pullorum. Avian Pathol. 45(5):569-575. doi: 10.1080/03079457.2016.1187708.

188. Mu, X., Huan, H., Xu, H., Gao, Q., Xiong, L., Gao, R., Gao, S., and Liu, X. (2013). The transfer-messenger RNA-small protein B system plays a role in avian pathogenic *Escherichia coli* pathogenicity. J Bacteriol. 195(22):5064–5071.

189. Wang, X. D., Li, C. Y., Jiang, M. M., Li, D., Wen, P., Song, X., Chen, J. D., Guo, L. X., Hu, X. P., Li, G. Q., Zhang, J., Wang, C. H., and He, Z. D. (2016). Induction of apoptosis in human leukemia cells through an intrinsic pathway by cathachunine, a unique alkaloid isolated from Catharanthus roseus. Phytomedicine. 23(6):641-653. doi: 10.1016/j.phymed.2016.03.003.

190. Shi, M., Li, N., Xue, Y., Zhong, Z., and Yang, M. (2020). The 58th cysteine of TcpP is essential for *Vibrio cholera* virulence factor production and pathogenesis. Front Microbiol. 11:118. doi: 10.3389/fmicb.2020.00118.

191. Yang, S., Deng, Q., Sun, L., Zhu, Y., Dong, K., Wu, S., Huang, R., and Li, Y. (2021). *Salmonella* effector SpvB inhibits NF-κB activity via KEAP1-mediated

downregulation of IKKβ. Front Cell Infect Microbiol. 11:641412. doi: 10.3389/fcimb.2021.641412.

192. Peng, L., Wen, L., Shi, Q. F., Gao, F., Huang, B., Meng, J., Hu, C. P., and Wang, C. M. (2020). Scutellarin ameliorates pulmonary fibrosis through inhibiting NF-κB/NLRP3-mediated epithelial-mesenchymal transition and inflammation. Cell Death Dis. 11(11):978. doi: 10.1038/s41419-020-03178-2.

193. Li, Q., Hu, Y., Chen, J., Liu, Z., Han, J., Sun, L., and Jiao, X. (2013). Identification of *Salmonella enterica* serovar pullorum antigenic determinants expressed in *vivo*. Infect Immun. 81(9):3119–3127. doi: 10.1128/IAI.00145-13.

194. Xian, H., Yuan, Y., Yin, C., Wang, Z., Ji, R., Chu, C., Jiao, X., and Li, Q. (2020). The SPI-19 encoded T6SS is required for *Salmonella* Pullorum survival within avian macrophages and initial colonization in chicken dependent on inhibition of host immune response. Vet Microbiol. 250:108867. doi: 10.1016/j.vetmic.2020.108867.

195. Jaslow, S. L., Gibbs, K. D., Fricke, W. F., Wang, L., Pittman, K. J., Mammel, M. K., Thaden, J. T., Fowler Jr, V. G., Hammer, G. E., Elfenbein, J. R., and Ko, D. C. (2018). *Salmonella* activation of STAT3 signaling by SarA effector promotes intracellular replication and production of IL-10. Cell Rep. 23(12):3525-3536. doi: 10.1016/j.celrep.2018.05.072.

196. Xiong, D., Song, L., Geng, S., Tao, J., An, S., Pan, Z., and Jiao, X. (2016). One-step PCR detection of *Salmonella* Pullorum/Gallinarum using a novel target: the flagellar biosynthesis gene *flhB*. Front. Microbiol. 7:1863. doi: 10.3389/fmicb.2016.01863.

197. Yang, Y., Wang, P., Xia, P., Yang, B., Dai, P., Hong, T., Li, J., Meng, X., Qaidi, S. E., and Zhu, G. (2020). Rapid detection of flagellated and non-flagellated *Salmonella* by targeting the common flagellar hook gene *flgE*. Appl Microbiol Biot. 104(22): 9719–9732. doi: 10.1007/s00253-020-10925-0.

198. Liu, R., Wang, Z., Liu, X., Chen, A., and Yang, S. (2020). Rapid on-site detection of *Salmonella* Pullorum based on lateral flow nucleic acid assay combined with recombinase polymerase amplification reaction. Poult Sci.

99(12):7225–7232. doi: 10.1016/j.psj.2020.10.020.

199. Shen, H., Wen, J., Liao, X., Lin, Q., Zhang, J., Chen, K., Wang, S., and Zhang, J. (2020). A sensitive, highly specific novel isothermal amplification method based on single-nucleotide polymorphism for the rapid detection of *Salmonella* Pullorum. Front Microbiol. 11:560791. doi: 10.3389/fmicb.2020.560791.

200. Wen, J., Gou, H., Liu, J., Zhou, H., Lin, Q., Qu, X., Chen, K., Wang, S., Shen, H., Liao, M., and Zhang, J. (2021a). A one-step closed-tube enzyme-activated blocked probe assay based on SNP for rapid detection of *Salmonella* Pullorum. Poult Sci. 100(2):1059-1067.

201. Rubio, M. D. S., Filho, R. A. C. P., Almeida, A. M. D., and Junior, A. B. (2017). Development of a multiplex qPCR in real time for quantification and differential diagnosis of *Salmonella* Gallinarum and *Salmonella* Pullorum. Avian Pathol 46(6):644–651. doi: 10.1080/03079457.2017.1339866.

202. Xiong, D., Song, L., Tao, J., Zheng, H., Zhou, Z., Geng, S., Pan, Z., and Jiao, X. (2017). An efficient multiplex PCR-based assay as a novel tool for accurate inter-serovar discrimination of *Salmonella* Enteritidis, *S*. Pullorum/Gallinarum and *S*. Dublin. Front Microbiol. 8:420. doi: 10.3389/fmicb.2017.00420.

203. Xu, L., Liu, Z., Li, Y., Yin, C., Hu, Y., Xie, X., Li, Q., and Jiao, X. (2018). A rapid method to identify *Salmonella enterica* serovar Gallinarum biovar Pullorum using a specific target gene *ipaJ*. Avian Pathol. 47(3):238-244. doi: 10.1080/03079457.2017.1412084.

204. Wen, J., Gou, H., Wang, S., Lin, Q., Chen, K., Wu, Y., Huang, X., Shen, H., Qu, X., Lin, J., Liao, M., and Zhang, J. (2021). Competitive activation cross amplification combined with smartphone-based quantification for point-of-care detection of single nucleotide polymorphism. Biosens Bioelectron. 183:113200. doi: 10.1016/j.bios.2021.113200.

205. Xu, Y., Hu, Y., Guo, Y., Zhou, Z., Xiong, D., Meng, C., Li, Q., Geng, S., Pan, Z., and Jiao, X. (2018). A new PCR assay based on the new gene-SPUL_2693 for rapid detection of *Salmonella enterica* subsp. *enterica* serovar Gallinarum

biovars Gallinarum and Pullorum. Poult Sci. 97(11):4000–4007. doi: 10.3382/ps/pey254.

206. Gong, J., Zhuang, L., Zhu, C., Shi, S., Zhang, D., Zhang, L., Yu, Y., Dou, X., Xu, B., and Wang, C. (2016). Loop-mediated isothermal amplification of the *sefA* gene for rapid detection of *Salmonella* Enteritidis and *Salmonella* Gallinarum in chickens. Foodborne Pathog Dis. 13(4):177–181. doi: 10.1089/fpd.2015.2082.

207. Klumpp, J., and Fuchs, T. M. (2007). Identification of novel genes in genomic islands that contribute to *Salmonella* Typhimurium replication in macrophages. Microbiology (Reading). 153(Pt 4):1207-1220. doi: 10.1099/mic.0.2006/004747-0.

208. Gut, A. M., Vasiljevic, T., Yeager, T., and Donkor, O. N. (2018). *Salmonella* infection-prevention and treatment by antibiotics and probiotic yeasts: A review. Microbiology. 164(11):1327-1344. doi: 10.1099/mic.0.000709.

209. Hu, Y., Wang, Z., Qiang, B., Xu, Y., Chen, X., Li, Q., and Jiao, X. (2019). Loss and gain in the evolution of the *Salmonella enterica* serovar Gallinarum biovar Pullorum genome. mSphere. 4(2):e00627-18. doi: 10.1128/mSphere.00627-18.

210. Salem, R. B., Abbassi, M. S., García, V., García-Fierro, R., Njoud, C., Messadi, L., and Rodicio, M. R. (2015). Detection and molecular characterization of *Salmonella enterica* serovar eppendorf circulating in chicken farms in Tunisia. Zoonoses & Public Health. 63(4):320-327. doi: 10.1111/zph.12234.

211. Wigley, P. (2017). *Salmonella enterica* serovar Gallinarum: addressing fundamental questions in bacteriology sixty years on from the 9R vaccine. Avian Pathology. 46(2):119-124. doi: 10.1080/03079457.2016.1240866.

212. Guo, R., Li, Z., Zhou, X., Huang, C., Hu, Y., Geng, S., Chen, X., Li, Q., Pan, Z., and Jiao, X. (2018). Induction of arthritis in chickens by infection with novel virulent *Salmonella* Pullorum strains. Vet Microbiol. 228:165-172. doi: 10.1016/j.vetmic.2018.11.032.

213. Akinola, S. A., Mwanza, M., and Ateba, C. N. (2019). Occurrence, genetic diversities and antibiotic resistance profiles of *Salmonella* serovars isolated from chickens. Infect Drug Resist. 12:3327-3342. doi: 10.2147/IDR.S217421.

214. Tamang, M. D., Gurung, M., Nam, H. M., Moon, D. C., Jang, G. C., Jung, S. C., and Lim, S. K. (2014). Antimicrobial susceptibility and virulence characteristics of *Salmonella* enterica Typhimurium isolates from healthy and diseased pigs in Korea. J Food Prot. 77(9):1481-1486. doi: 10.4315/0362-028X.JFP-14-084.

215. Ramirezhernandez, A., Carrascalcamacho, A. K., Brashears, M. M., and Sanchez-Plata, M. X. (2021). Genotypic characterization of antimicrobial resistant *Salmonella* spp. strains from three poultry processing plants in Colombia. Foods. 10(3):491-507. doi: 10.3390/foods10030491.

216. Parvin, M. S., Hasan, M. M., Ali, M. Y., Chowdhury, E. H., Rahman, M. T., and Islam, M. T. (2020). Prevalence and multidrug resistance pattern of *Salmonella* carrying extended-spectrum β-lactamase in frozen chicken meat in Bangladesh. J Food Prot. 83(12):2107-2121. doi: 10.4315/JFP-20-172.

217. Guo, X., Wang, H., Cheng, Y., Zhang, W., Luo, Q., Wen, G., Wang, G., Shao, H., Zhang, T., Zhang, W., Luo, Q., Wen, G., Wang, G., Shao, H., and Zhang, T. (2018). Quinolone resistance phenotype and genetic characterization of *Salmonella enterica* serovar Pullorum isolates in China, during 2011 to 2016. BMC Microbiol. 18(1):225-241. doi: 10.1186/s12866-018-1368-4.

218. Ahmed, A. O., Raji, M. A., Mamman, P. H., Kwanashie, C. N., Raufu, I. A., Aremu, A., and Akorede, G. J. (2019). Salmonellosis: Serotypes, prevalence and multi-drug resistant profiles of *Salmonella enterica* in selected poultry farms, Kwara State, North Central Nigeria. Onderstepoort J Vet Res. 86(1):e1-e8. doi: 10.4102/ojvr.v86i1.1667.

219. Gharieb, R. M., Tartor, Y. H., and Khedr, M. H. E. (2015). Non-Typhoidal *Salmonella*, in poultry meat and diarrhoeic patients: prevalence, antibiogram, virulotyping, molecular detection and sequencing of class I integrons in multidrug resistant strains. Gut Pathog. 7(1):1-11. doi: 10.1186/s13099-015-

0081-1.

220. Torres, A. C., Vannini, V., Bonacina, J., Font, G., Saavedra, L., and Taranto, M. P. (2016). Cobalamin production by *Lactobacillus* coryniformis: biochemical identification of the synthetized corrinoid and genomic analysis of the biosynthetic cluster. BMC Microbiol. 16(1):240-249. doi: 10.1186/s12866-016-0854-9.

221. Nhung, N. T., Chansiripornchai, N., and Carrique-Mas, J. J. (2017). Antimicrobial resistance in bacterial poultry pathogens: A review. Front Vet Sci. 4(126):1-17. doi: 10.3389/fvets.2017.00126.

222. Samykannu, G., Vijayababu, P., Antonyraj, C. B, Perumal, P., Narayanan, S., Ahamed, S. I. B., and Natarajan, J. (2019). In silico characterization of B cell and T cell epitopes for subunit vaccine design of *Salmonella* typhi PgtE: A molecular dynamics simulation approach. J Comput Biol. 26(2):105-116. doi: 10.1089/cmb.2018.0010.

223. Ahmed, N., Ali, Z., Riaz, M., Zeshan, B., Wattoo, J. I., and Aslam, M. N. (2020). Evaluation of antibiotic resistance and virulence genes among clinical isolates of *Pseudomonas aeruginosa* from cancer patients. Asian Pac J Cancer Prev. 21(5):1333-1338. doi: 10.31557/APJCP.2020.21.5.1333.

224. Blanco, G., and de Tuesta, J. A. D. (2018). Culture- and molecular-based detection of swine-adapted *Salmonella* shed by avian scavengers. Sci Total Environ. 634:1513–1518. doi: 10.1016/j.scitotenv.2018.04.089.

225. Park, S. H., Aydin, M., Khaiwara, A., Dolan, M. C., Gilmore, D. F., Bouldin, J. L., Ahn, S., and Ricke, S. C. (2014). Current and emerging technologies for rapid detection and characterization of *Salmonella* in poultry and poultry products. Food Microbiol. 38:250–262. doi: 10.1016/j.fm.2013.10.002.

226. Babu, U. S., Harrison, L. M., Patel, I. R., Mammel, M. K., Bigley 3rd, E., and Balan, K. V. (2021). Development and validation of an improved method for the detection of *Salmonella* in cinnamon bark and oregano leaves using the adsorbent beta zeolite in the pre-enrichment media. Food Microbiol. 100:103852. doi: 10.1016/j.fm.2021.103852.

227. Yang, Y., Xu, F., Xu, H., Aguilar, Z. P., Niu, R., Yuan, Y., Sun, J., You, X., Lai, W., Xiong, Y., Wan, C., and Wei, H. (2013). Magnetic nano-beads based separation combined with propidiummonoazide treatment and multiplex PCR assay for simultaneous detection of viable *Salmonella* Typhimurium, *Escherichia coli* O157:H7 and Listeria monocytogenes in food products. Food Microbiol. 34(2):418–424. doi: 10.1016/j.fm.2013.01.004.

228. Quick, J., Grubaugh, N. D., Pullan, S. T., Claro, I. M., Smith, A. D., Gangavarapu, K., Oliveira, G., Robles-Sikisaka, R., Rogers, T. F., Beutler, N. A., Burton, D. R., Lewis-Ximenez, L. L., de Jesus, J. G., Giovanetti, M., Hill, S. C., Black, A., Bedford, T., Carroll, M. W., Nunes, M., Alcantara Jr, L. C., Sabino, E. C., Baylis, S. A., Faria, N. R., Loose, M., Simpson, J. T., Pybus, O. G., Andersen, K. G., and Loman, N. J. (2017). Multiplex PCR method for MinION and Illumina sequencing of Zika and other virus genomes directly from clinical samples. Nat Protoc. 12(6):1261–1276. doi: 10.1038/nprot.2017.066.

229. Dobrindt, U., and Hacker, J. (2001). Whole genome plasticity in pathogenic bacteria. Curr Opin Microbiol. 4(5):550–557. doi: 10.1016/s1369-5274(00)00250-2.

230. Thomson, N. R., Clayton, D. J., Windhorst, D., Vernikos, G., Davidson, S., Churcher, C., Quail, M. A., Stevens, M., Jones, M. A., Watson, M., Barron, A., Layton, A., Pickard, D., Kingsley, R. A., Bignell, A., Clark, L., Harris, B., Ormongd, D., Abdellah, Z., Brooks, K., Cherevach, I., Chillingworth, T., Woodward, J., Norberczak, H., Lord, A., Arrowsmith, C., Jagels, K., Moule, S., Mungall, K., Sanders, M., Whitehead, S., Chabalgoity, J. A., Maskell, D., Humphrey, T., Roberts, M., Barrow, P. A., Dougan, G., and Parkhill, J. (2008). Comparative genome analysis of *Salmonella* Enteritidis PT4 and *Salmonella* Gallinarum 287/91 provides insights into evolutionary and host adaptation pathways. Genome Res. 18(10):1624–1637. doi: 10.1101/gr.077404.108.

231. Shen, H., Wen, J., Liao, X., Lin, Q., Zhang, J., Chen, K., Wang, S., and Zhang, J. (2020). A sensitive, highly specific novel isothermal amplification

method based on single-nucleotide polymorphism for the rapid detection of *Salmonella* Pullorum. Front Microbiol. 11:560791. doi: 10.3389/fmicb.2020.560791.

232. Arora, G., Chaudhary, D., Kidwai, S., Sharma, D., and Singh, R. (2018). CitE enzymes are essential for *Mycobacterium tuberculosis* to establish infection in macrophages and guinea pigs. Front Cell Infect Microbiol. 8:385. doi: 10.3389/fcimb.2018.00385.

233. Xiong, D., Song, L., Pan, Z., and Jiao, X. (2018). Identification and discrimination of *Salmonella enterica* serovar Gallinarum biovars Pullorum and Gallinarum based on a one-step multiplex PCR assay. Front Microbiol. 9:1718. doi: 10.3389/fmicb.2018.01718.

234. Tang, L., Zhu, S., Mastriani, E., Fang, X., Zhou, Y. J., Li, Y. G., Johnston, R. N., Guo, Z., Liu, G. R., and Liu, S. L. (2017). Conserved intergenic sequences revealed by CTAG-profiling in *Salmonella*: thermodynamic modeling for function prediction. Sci Rep. 7:43565. doi: 10.1038/srep43565.

235. Batista, D. F. A., de Freitas Neto, O. C., de Almeida, A. M., Maboni, G., de Carvalho, T. F., de Carvalho, T. P., Barrow, P. A., and Junior, A. B. (2018). Evaluation of pathogenicity of *Salmonella* Gallinarum strains harbouring deletions in genes whose orthologues are conserved pseudogenes in *S.* Pullorum. PLoS One. 13(7):e0200585. doi: 10.1371/journal.pone.0200585.

236. Khaltabadi, R. F., Shahrokhi, N., Ebrahimi-Rad, M., and Ehsani, P. (2019). *Salmonella* Typhimurium in Iran: Contribution of molecular and IS200 PCR methods in variants detection. PLoS One. 14(3):e0213726. doi: 10.1371/journal.pone.0213726.

237. Naberhaus, S. A., Krull, A. C., Bradner, L. K., Harmon, K. M., Arruda, P., Arruda, B. L., Sahin, O., Burrough, E. R., Schwartz, K. J., and Kreuder, A. J. (2019). Emergence of *Salmonella enterica* serovar 4,[5],12:i:-as the primary serovar identified from swine clinical samples and development of a multiplex real-time PCR for improved *Salmonella* serovar-level identification. J Vet Diagn Invest. 31(6):818–827. doi: 10.1177/1040638719883843.

238. Sahu, B., Singh, S. D., Behera, B. K., Panda, S. K., Das, A., and Parida, P. K. (2019). Rapid detection of *Salmonella* contamination in seafoods using multiplex PCR. Braz J Microbiol. 50(3):807–816. doi: 10.1007/s42770-019-00072-8.

239. Wan, J., Zheng, L., Kong, L., Lu, Z., Tao, Y., Feng, Z., Lv, H., Meng, F., and Bie, X. (2021). Development of a rapid detection method for real-time fluorescent quantitative PCR of *Salmonella* spp. and *Salmonella* Enteritidis in ready-to-eat fruits and vegetables. LWT-Food Sci Technol. 149: 111837. doi：10.1016/j.lwt.2021.111837.

240. Yu, X. J., Liu, M., and Holden, D. W. (2016). *Salmonella* effectors SseF and SseG Interact with mammalian protein ACBD3 (GCP60) to anchor *Salmonella*-containing vacuoles at the golgi network. mBio. 7(4):e00474-16. doi: 10.1128/mBio.00474-16.

241. Kodama, T., Hiyoshi, H., Okada, R., Matsuda, S., Gotoh, K., and Iida, T. (2015). Regulation of vibrio parahaemolyticus T3SS2 gene expression and function of T3SS2 effectors that modulate actin cytoskeleton. Cell Microbiol. 17(2):183-190. doi: 10.1111/cmi.12408.

242. Lin, Z., Tang, P., Jiao, Y., Kang, X., Li, Q., Xu, X., Sun, J., Pan, Z., and Jiao, X. (2017). Immunogenicity and protective efficacy of a *Salmonella* Enteritidis *sptP* mutant as a live attenuated vaccine candidate. BMC Vet Res. 13(1):194-203. doi: 10.1186/s12917-017-1115-3.

243. Gulati, A., Shukla, R., and Mukhopadhaya, A. (2019). *Salmonella* effector SteA suppresses proinflammatory responses of the host by interfering with IκB degradation. Front Immunol. 10:2822. doi: 10.3389/fimmu.2019.02822.

244. Stapels, D. A. C., Hill, P. W. S., Westermann, A. J., Fisher, R. A., Thurston, T. L., Saliba, A. E., Blommestein, I., Voge, J., and Helaine, S. (2018). *Salmonella* persisters undermine host immune defenses during antibiotic treatment. Science. 362(6419):1156–1160. doi: 10.1126/science.aat7148.

245. Pham, T. H. M., Brewer, S. M., Thurston, T., Massis, L. M., Honeycutt, J.,

Lugo, K., Jacobson, A. R., Vilches-Moure, J. G., Hamblin, M., Helaine, S., and Monack, D. M. (2019). *Salmonella*-driven polarization of granuloma macrophages antagonizes TNF-mediated pathogen restriction during persistent infection. Cell Host Microbe. 27(1):54–67. doi: 10.1016/j.chom.2019.11.011.

246. Niemann, G. S., Brown, R. N., Gustin, J. K., Stufkens, A., Shaikh-Kidwai, A. S., Li, J., McDermott, J. E., Brewer, H. M., Schepmoes, A., Smith, R. D., Adkins, J. N., and Heffron, F. (2011). Discovery of novel secreted virulence factors from *Salmonella enterica serovar* Typhimurium by proteomic analysis of culture supernatants. Infect Immun. 79(1):33-43. doi: 10.1128/IAI.00771-10.

247. Lawley, T. D., Chan, K., Thompson, L. J., Kim, C. C., Govoni, G. R., and Monack, D. M. (2006). Genome-wide screen for *Salmonella* genes required for long-term systemic infection of the mouse. PLoS Pathog. 2(2):e11. doi: 10.1371/journal.ppat.0020011.

248. Gibbs, K. D., Washington, E. J., Jaslow, S. L., Bourgeois, J. S., Foster, M, W., Guo, R., Brennan, R. G., and Ko, D. C. (2019). The *Salmonella* secreted effector SarA/SteE mimics cytokine receptor signaling to activate STAT3. Cell Host Microbe. 27(1):129-139.e4. doi: 10.1016/j.chom.2019.11.012.

249. Panagi, I., Jennings, E., Zeng, J., Günster, R. A., Stones, C. D., Mak, H., Jin, E., Stapels, D. A. C, Subari, N. Z., Pham, T. H. M., Brewer, S. M., Ong, S. Y. Q., Monack, D. M., Helaine, S., and Thurston, T. L. M. (2020). *Salmonella* effector SteE converts the mammalian serine/threonine kinase GSK3 into a tyrosine kinase to direct macrophage polarization. Cell Host Microbe. 27(1):41–53. doi: 10.1016/j.chom.2019.11.002.

250. Ruan, H. H., Zhang, Z., Wang, S. Y., Nickels, L. M., Tian, L., Qiao, J. J., and Zhu, J. (2017). Tumor necrosis factor receptor-associated factor 6 (TRAF6) mediates ubiquitination-dependent STAT3 activation upon *Salmonella enterica* serovar Typhimurium infection. Infect Immun. 85(8):e00081-17. doi: 10.1128/IAI.00081-17.

251. Abebe, F. (2019). Synergy between Th1 and Th2 responses during *Mycobacterium tuberculosis* infection: A review of current understanding. Int

Rev Immunol. 38(4):172-179. doi: 10.1080/08830185.2019.1632842. 30.

252. Cerny, O., and Holden, D. W. (2019). *Salmonella* SPI-2 type III secretion system-dependent inhibition of antigen presentation and T cell function. Immunol Lett. 215:35-39. doi: 10.1016/j.imlet.2019.01.006.

253. Yang, R., Yang, E., Shen, L., Modlin, R. L., Shen, H., and Chen, Z. W. (2018). IL-12+IL-18 cosignaling in human macrophages and lung epithelial cells activates cathelicidin and autophagy, inhibiting intracellular *Mycobacterial* growth. J Immunol. 200(7):2405-2417. doi: 10.4049/jimmunol.1701073.

254. Withanage, G. S., Wigley, P., Kaiser, P., Mastroeni, P., Brooks, H., Powers, C., Beal, R., Barrow, P., Maskell, D., and McConnell, I. (2005). Cytokine and chemokine responses associated with clearance of a primary *Salmonella enterica* serovar Typhimurium infection in the chicken and in protective immunity to rechallenge. Infect Immun. 73(8):5173-82. doi: 10.1128/IAI.73.8.5173-5182.2005.

255. Shappo, M. O. E., Li, Q., Lin, Z., Hu, M., Ren, J., Xu, Z., Pan, Z., and Jiao, X. (2020). SspH2 as anti-inflammatory candidate effector and its contribution in *Salmonella* Enteritidis virulence. Microb Pathog. 142:104041. doi: 10.1016/j.micpath.2020.104041.

256. Rasquinha, M. T., Sur, M., Lasrado, N., and Reddy, J. (2021). IL-10 as a Th2 cytokine: differences between mice and humans. J Immunol. 207(9):2205-2215. doi: 10.4049/jimmunol.2100565.

257. Park, H. S., Back, Y. W., Jang, I. T., Lee, K. I., Son, Y. J., Choi, H. G., Dang, T. B., and Kim, H. J. (2021). *Mycobacterium tuberculosis* Rv2145c promotes intracellular survival by STAT3 and IL-10 receptor signaling. Front Immunol. 12:666293. doi: 10.3389/fimmu.2021.666293.

258. Liu, Q. Q., Zhong, D., Zhang, X., and Li, G. Z. (2018). IL-10 targets Th1/Th2 balance in vascular dementia. Eur Rev Med Pharmacol Sci. 22(17):5614-5619. doi: 10.26355/eurrev_201809_15826.

259. Webster, H. C., Gamino, V., Andrusaite, A. T., Ridgewell, O. J., McCowan, J., Shergold, A. L., Heieis G. A., Milling S. W. F., Maizels R. M., and Perona-

Wright, G. (2022). Tissue-based IL-10 signalling in helminth infection limits IFNγ expression and promotes the intestinal Th2 response. Mucosal Immunol. 15(6):1257-1269. doi: 10.1038/s41385-022-00513-y.

260. Liu, Z., Wang, L., Yu, Y., Fotin, A., Wang, Q., Gao, P., Zhang, Y., Fotina, T., and Ma, J. (2022). SteE enhances the virulence of *Salmonella* Pullorum in chickens by regulating the inflammation response. Front Vet Sci. 9:926505. doi: 10.3389/fvets.2022.926505.

261. Lawley, T. D., Chan, K., Thompson, L. J., Kim, C. C., Govoni, G. R., and Monack, D. M., (2006). Genome-wide screen for *Salmonella* genes required for long-term systemic infection of the mouse. PLoS Pathog. 2(2):e11. doi: 10.1371/journal.ppat.0020011

262. Hannemann, S., Gao, B., and Galán, J. E., (2013). *Salmonella* modulation of host cell gene expression promotes its intracellular growth. PLoS Pathog. 9(10):e1003668. doi: 10.1371/journal.ppat.1003668

263. Zhou, L., Li, Y., Gao, S., Yuan, H., Zuo, L., Wu, C., Huang, R., and Wu, S. (2021). *Salmonella spvC* gene inhibits autophagy of host cells and suppresses NLRP3 as well as NLRC4. Front Immunol. 12:639019. doi: 10.3389/fimmu.2021.639019.

264. Kerrinnes, T., Winter, M. G., Young, B. M., Diaz-Ochoa, V. E., Winter, S. E., and Tsolis, R. M. (2018). Utilization of host polyamines in alternatively activated macrophages promotes chronic infection by brucella abortus. Infect Immun. 86(3):e00458–17. doi: 10.1128/IAI.00458-17.

265. Refai, A., Gritli, S., Barbouche, M. R., and Essafi, M. (2018). *Mycobacterium tuberculosis* virulent factor ESAT-6 drives macrophage differentiation toward the pro-inflammatory M1 phenotype and subsequently switches it to the anti-inflammatory M2 phenotype. Front Cell Infect Microbiol. 8:327–340. doi: 10.3389/fcimb.2018.00327.

266. Jiang, L., Wang, P., Song, X., Zhang, H., Ma, S., Wang, J., Li W., Lv, R., Liu, X., Ma, S., Yan, J., Zhou, H., Huang, D., Cheng, Z., Yang, C., Feng, L., and Wang, L. (2021). *Salmonella* Typhimurium reprograms macrophage

metabolism via T3SS effector SopE2 to promote intracellular replication and virulence. Nat Commun. 12(1):879. doi: 10.1038/s41467-021-21186-4.

267. Eisele, N. A., Ruby, T., Jacobson, A., Manzanillo, P. S., Cox, J. S., Lam, L., Mukundan, L., Chawla, A., and Monack, D. M. (2013). *Salmonella* require the fatty acid regulator PPARδ for the establishment of a metabolic environment essential for long-term persistence. Cell Host Microbe. 14(2):171–182. doi: 10.1016/j.chom.2013.07.010.

268. Brodsky, I. E. (2020). JAK-ing into M1/M2 polarization SteErs *Salmonella*-containing macrophages away from immune attack to promote bacterial persistence. Cell Host Microbe. 27(1):3–5. doi: 10.1016/j.chom.2019.12.007.

269. Ho, T. D., Figueroa-Bossi, N., Wang, M., Uzzau, S., Bossi, L., and Slauch, J. M. (2002). Identification of GtgE, a novel virulence factor encoded on the Gifsy-2 bacteriophage of *Salmonella enterica* serovar Typhimurium. J Bacteriol. 184(19):5234–5239. doi: 10.1128/JB.184.19.5234-5239.2002.

270. Neves, P., Lampropoulou, V., Calderon-Gomez, E., Roch, T., Stervbo, U., Shen, P., Kühl, A. A., Loddenkemper, C., Haury, M., Nedospasov, S. A., Kaufmann, S. H., Steinhoff, U., Calado, D. P., and Fillatreau, S. (2010). Signaling via the MyD88 adaptor protein in B cells suppresses protective immunity during *Salmonella* Typhimurium infection. Immunity. 33(5):777–790. doi: 10.1016/j.immuni.2010.10.016.

271. Fu, A., Mo, Q., Wu, Y., Wang, B., Liu, R., Tang, L., Zeng, Z., Zhang, X., and Li, W. (2019). Protective effect of *Bacillus* amyloliquefaciens against *Salmonella* via polarizing macrophages to M1 phenotype directly and to M2 depended on microbiota. Food Funct. 10(12):7653-7666. doi: 10.1039/c9fo01651a.

272. Wu, H., Zheng, J., Xu, S., Fang, Y., Wu, Y., Zeng, J., Shao, A., Shi, L., Lu, J., Mei, S., Wang, X., Guo, X., Wang, Y., Zhao, Z., and Zhang, J. (2021). Mer regulates microglial/macrophage M1/M2 polarization and alleviates neuroinflammation following traumatic brain injury. J Neuroinflammation. 18(1):2. doi: 10.1186/s12974-020-02041-7.

273. He, H., Genovese, K. J., and Kogut, M. H. (2011). Modulation of chicken macrophage effector function by T(H)1/T(H)2 cytokines. Cytokine. 53(3):363-369. doi: 10.1016/j.cyto.2010.12.009.

274. Li, K., Li, J., Wei, X., Wang, J., Geng, M., Ai, K., Liang, W., Zhang, J., Li, K., Gao, H., and Yang, J. (2023). IL-10 negatively controls the primary T cell response of tilapia by triggering the JAK1/STAT3/SOCS3 axis that suppresses NF-κB and MAPK/ERK signaling. J Immunol. 210(3):229-244. doi: 10.4049/jimmunol.2200335.

275. Stevens, M. P., and Kingsley, R. A. (2021). *Salmonella* pathogenesis and host-adaptation in farmed animals. Curr Opin Microbiol. 63:52-58. doi: 10.1016/j.mib.2021.05.013.

276. Luo, Y., Fang, Y., Kang, R., Lenahan, C., Gamdzyk, M., Zhang, Z., Okada, T., Tang, J., Chen, S., and Zhang, J.H. (2020). Inhibition of EZH2 (enhancer of zeste homolog 2) attenuates neuroinflammation via H3k27me3/SOCS3/TRAF6/NF-κB (trimethylation of histone 3 lysine 27/suppressor of cytokine signaling 3/tumor necrosis factor receptor family 6/nuclear factor-κB) in a rat model of subarachnoid hemorrhage. Stroke. 51(11):3320-3331. doi: 10.1161/STROKEAHA.120.029951.

277. Zhang, L., Lu, X., Gong, L., Cui, L., Zhang, H., Zhao, W., Jiang, P., Hou, G., and Hou, Y. (2021). Tetramethylpyrazine protects blood-spinal cord barrier integrity by modulating microglia polarization through activation of STAT3/SOCS3 and inhibition of NF-κB signaling pathways in experimental autoimmune encephalomyelitis mice. Cell Mol Neurobiol. 41(4):717-731. doi: 10.1007/s10571-020-00878-3.

278. Qin, H., Holdbrooks, A. T., Liu, Y., Reynolds, S. L., Yanagisawa, L.L., and Benveniste, E. N. (2012). SOCS3 deficiency promotes M1 macrophage polarization and inflammation. J Immunol. 189(7):3439-48. doi: 10.4049/jimmunol.1201168.

279. Karki, P., Ke, Y., Zhang, C. O., Li, Y., Tian, Y., Son, S., Yoshimura, A., Kaibuchi, K., Birukov, K. G., and Birukova, A. A. (2021). SOCS3-microtubule

interaction via CLIP-170 and CLASP2 is critical for modulation of endothelial inflammation and lung injury. J Biol Chem. 296:100239. doi: 10.1074/jbc.RA120.014232.

280. Liu, Y., Liao, S., Bennett, S., Tang, H., Song, D., Wood, D., Zhan, X., and Xu, J. (2021). STAT3 and its targeting inhibitors in osteosarcoma. Cell Prolif. 54(2):e12974. doi: 10.1111/cpr.12974.

281. Hansen, I. S., Schoonejans, J. M., Sritharan, L., van Burgsteden, J. A., Ambarus, C. A., Baeten, D. L. P., and den Dunnen, J. (2019). ER stress abrogates the immunosuppressive effect of IL-10 on human macrophages through inhibition of STAT3 activation. Inflamm Res. 68(9):775-785. doi: 10.1007/s00011-019-01261-9.

282. Cevey, Á. C., Penas, F. N., Soto, C. D. A., Mirkin, G. A., and Goren, N. B. (2019). IL-10/STAT3/SOCS3 axis is involved in the anti-inflammatory effect of Benznidazole. Front Immunol. 10:1267. doi: 10.3389/fimmu.2019.01267.

283. Gao, Y., Zhao, H., Wang, P., Wang, J., and Zou, L. (2018). The roles of SOCS3 and STAT3 in bacterial infection and inflammatory diseases. Scand J Immunol. 88(6):e12727. doi: 10.1111/sji.12727.

284. Sims, N. A. (2020). The JAK1/STAT3/SOCS3 axis in bone development, physiology, and pathology. Exp Mol Med. 52(8):1185-1197. doi: 10.1038/s12276-020-0445-6.

285. Zhao, F., Qu, J., Wang, W., Li, S., and Xu, S. (2020). The imbalance of Th1/Th2 triggers an inflammatory response in chicken spleens after ammonia exposure. Poult Sci. 99(8):3817-3822. doi: 10.1016/j.psj.2020.04.029.

286. Shen, X., Zhang, A., Gu, J., Zhao, R., Pan, X., Dai, Y., Yin, L., Zhang, Q., Hu, X., Wang, H., and Zhang, D. (2022). Evaluating *Salmonella* pullorum dissemination and shedding patterns and antibody production in infected chickens. BMC Vet Res. 18(1):240. doi: 10.1186/s12917-022-03335-z.

287. Niu, Y., Dong, Q., and Li, R. (2017). Matrine regulates Th1/Th2 cytokine responses in rheumatoid arthritis by attenuating the NF-κB signaling. Cell Biol Int. 41(6):611-621. doi: 10.1002/cbin.10763.

288. Ma, Q., Huang, W., Zhao, J., and Yang, Z. (2020). Liu Shen Wan inhibits influenza a virus and excessive virus-induced inflammatory response via suppression of TLR4/NF-κB signaling pathway *in vitro* and *in vivo*. J Ethnopharmacol. 252:112584. doi: 10.1016/j.jep.2020.112584.

289. Sun, H. J., Xiong, S. P., Cao, X., Cao, L., Zhu, M. Y., Wu, Z. Y., and Bian, J. S. (2021). Polysulfide-mediated sulfhydration of SIRT1 prevents diabetic nephropathy by suppressing phosphorylation and acetylation of p65 NF-κB and STAT3. Redox Biol. 38:101813. doi: 10.1016/j.redox.2020.101813.

290. Yin, C., Liu, Z., Xian, H., Jiao, Y., Yuan, Y., Li, Y., Li, Q., and Jiao, X. (2020). AvrA exerts inhibition of NF-κB pathway in its naïve *Salmonella* serotype through suppression of p-JNK and Beclin-1 molecules. Int J Mol Sci. 21(17):6063. doi: 10.3390/ijms21176063.

291. Liu, S., Yan, R., Chen, B., Pan, Q., Chen, Y., Hong, J., Zhang, L., Liu, W., Wang, S., and Chen, J. L. (2019). Influenza virus-induced robust expression of SOCS3 contributes to excessive production of IL-6. Front Immunol. 10:1843. doi: 10.3389/fimmu.2019.01843.

292. Yong, Y. H., Wang, P., Jia, R. M., Gooneratne, R., Wang, H. C. R., Liao, M., and Ju, X. H. (2019). SOCS3 control the activity of NF-κB induced by HSP70 via degradation of MyD88-adapter-like protein (Mal) in IPEC-J2 cells. Int J Hyperthermia. 36(1):151-159. doi: 10.1080/02656736.2018.1541484.

293. Zhang, H., Wang, Y., Li, S., Tang, X., Liang, R., and Yang, X. (2020). SOCS3 protects against neonatal necrotizing enterocolitis via suppressing NLRP3 and AIM2 inflammasome activation and p65 nuclear translocation. Mol Immunol. 122:21-27. doi: 10.1016/j.molimm.2020.03.019.

294. Zhang, X., Wang, Y., Yuan, J., Li, N., Pei, S., Xu, J., Luo, X., Mao, C., Liu, J., Yu, T., Gan, S., Zheng, Q., Liang, Y., Guo, W., Qiu, J., Constantin, G., Jin, J., Qin, J., and Xiao, Y. (2018). Macrophage/microglial Ezh2 facilitates autoimmune inflammation through inhibition of Socs3. J Exp Med. 215(5):1365-1382. doi: 10.1084/jem.20171417.

APPENDICES

Appendix A

List of works published on the topic of the dissertation

LIST OF WORKS PUBLISHED ON THE THEME OF THE DISSERTATION

Scientific works in which the main scientific results of the dissertation are published:

Articles in scientific professional publications of Ukraine

1. **Zhike, L.,** Fotina, T., Petrov, R., Klishchova, Z., & Fotin, A. (2021). Isolation, identification and analysis of drug resistance of *Salmonella* Pullorum. Ukrainian Journal of Veterinary and Agricultural Sciences, 4(1), 33-38. https://doi.org/10.32718/ujvas4-1.07. https://ujvas.com.ua/index.php/journal/article/view/79 (The applicant participated in research, analysis of the results and writing the article).

2. **Liu, Z.,** Fotina, T. I., Petrov, R. V., Fotin, A. I., & Ma, J. (2022). Construction and characterization of *steE* deletion mutant of *Salmonella* Pullorum. Bulletin of Sumy National Agrarian University. The Series: Veterinary Medicine, 2(57), 9-15. https://doi.org/10.32845/bsnau.vet. 2022.2.2. https://www.snaubulletin.com.ua/index.php/vm/article /view/665. (The applicant participated in research, analysis of the results and writing the article).

3. **Liu, Z.,** Fotin, A., Petrov, R., Ma, J., & Fotina, T. (2023). SteE enhances the colonization of *Salmonella* Pullorum in chickens. Ukrainian Journal of Veterinary and Agricultural Sciences, 6(1), 45-50. https://doi.org/10.32718/ujvas6-1.07. https://ujvas.com.ua/index.php/journal/article/view/145 (The applicant participated in research, analysis of the results and writing the article).

Articles in scopus journals

4. **Liu, Z.,** Yu, Y., Fotina, T., Petrov, R., Klishchova, Z., Fotin, A., Ma, J. (2022). Multiplex PCR assay based on the *citE2* gene and intergenic sequence for the rapid detection of *Salmonella* Pullorum in chickens. Poult Sci, 101(8), 101981. doi: 10.1016/j.psj.2022.101981.

https://www.ncbi.nlm.nih.gov/pmc/articles/PMC9264022/pdf/main.pdf. (The applicant participated in research, analysis of the results and writing the article).

5. **Liu, Z.,** Wang, L., Yu, Y., Fotin, A., Wang, Q., Gao, P., Zhang, Y., Fotina, T.,

& Ma, J. (2022). SteE enhances the virulence of *Salmonella* Pullorum in chickens by regulating the inflammation response. Front Vet Sci, 9, 926505. doi: 10.3389/fvets.2022.926505. https://www.ncbi.nlm.nih.gov/pmc/articles/PMC9330158/pdf/fvets-09-926505.pdf. (The applicant participated in research, analysis of the results and writing the article).

Theses of scientific reports

6. **Liu, Z.,** Fotina T., Petrov R., Kleshova J. (2021). Isolation, identification and drug resistance analysis of *Salmonella* Pullorum. BTRP Ukraine 2021 International BioThreat Reduction Symposium, (29 June - 2 July, 2021, Kyiv, Ukraine). (PhD participant in carrying out of experimental researches, processing of results, preparation of article for printing).

7. **Liu, Z.,** Yu, Y., Fotina, T., Petrov, R, Fotin, A., Ma, J. (2022). Multiplex PCR assay based on the *citE2* gene and intergenic sequence for the rapid detection of *Salmonella* Pullorum in chickens. Chinese Association of Animal Science and Veterinary Medicine, 2022 Academic Forum (14-16 August, 2022. Foshan, China). (PhD participant in carrying out of experimental researches, processing of results, preparation of article for printing).

8. **Liu, Z.,** Fotina, T., Fotin, A., Ma, J. (2022). *SteE* enhances the virulence of *Salmonella* Pullorum in chickens by regulating the inflammation response. Chinese Association of Animal Science and Veterinary Medicine, 2022 Academic Forum (14-16 August, 2022. Foshan, China). (PhD participant in carrying out of experimental researches, processing of results, preparation of article for printing).

9. **Liu, Z.,** Fotin, A., Fotina, T. (2023). The distribution of *Salmonella* Pullorum in different organs of chicken using in situ. The III Scientific and Practical International Distance Conference «Microbiological and Immunological Research in Modern Medicine», (24 March, 2023, Kharkiv, Ukraine). (PhD participant in carrying out of experimental researches, processing of results, preparation of article for printing).

10. **Liu, Z.,** Fotin, A., Petrov, R., Fotina, T. (2023). SteE regulates Th1/Th2

cytokine expression in chickens during *Salmonella* Pullorum infection. The III Scientific and Practical International Distance Conference «Microbiological and Immunological Research in Modern Medicine», (24 March, 2023, Kharkiv, Ukraine). (PhD participant in carrying out of experimental researches, processing of results, preparation of article for printing).

11. **Liu, Z.,** Fotin, A., Ma, J., Tetiana Fotina. (2023). *Salmonella* Pullorum effector SteE regulates Th1/Th2 balance by triggering the STAT33/SOCS3 axis that suppresses NF-κB activation. The III Scientific and Practical International Distance Conference «Microbiological and Immunological Research in Modern Medicine», (24 March, 2023, Kharkiv, Ukraine). (PhD participant in carrying out of experimental researches, processing of results, preparation of article for printing).

12. **Liu, Z.,** Fotina, T. (2023). Construction and characterization of *steE* deletion mutant of *Salmonella* Pullorum. The XI International Scientific and Practical Conference «Problems of the development of science and the view of society», (21-24 March, 2023, Graz, Austria). (PhD participant in carrying out of experimental researches, processing of results, preparation of article for printing).

13. **Liu, Z.,** Tetiana Fotina, T. (2023). SteE induces the colonization of *Salmonella* Pullorum in chickens.The XI International Scientific and Practical Conference «Problems of the development of science and the view of society», (21-24 March, 2023, Graz, Austria). (PhD participant in carrying out of experimental researches, processing of results, preparation of article for printing).

14. **Liu, Z.,** Fotin, A., Tetiana Fotina. (2023). *Salmonella* Pullorum effector SteE inhibits NF-κB activity by STAT3-mediated upregulation of SOCS3. Chinese Association of Animal Science and Veterinary Medicine, 2023 Academic Forum (12-15 May, 2023. Yangzhou, China). (PhD participant in carrying out of experimental researches, processing of results, preparation of article for printing).

Appendix B

BLAST search results using S. Pullorum *citE2* gene

BLAST® » blastn suite » results for RID-EF841XHX013

Job Title	emb|LK931482.1|
RID	EFKE7F3901R *Search expires on 07-10 12:17 pm* Download All
Program	BLASTN Citation
Database	nt See details
Query ID	LK931482.1
Description	Salmonella enterica subsp. enterica serovar Pullorum g ...
Molecule type	nucleic acid
Query Length	794

Description	Scientific Name	Max Score	Total Score	Query Cover	E value	Per. Ident	Acc. Len	Accession
Salmonella enterica subsp. enterica serovar Pullorum strain QJ-2D...	Salmonell...	1467	1467	100%	0.0	100.00%	4728875	CP022963.1
Salmonella enterica subsp. enterica serovar Pullorum str. ATCC 91...	Salmonell...	1467	1467	100%	0.0	100.00%	4694842	CP012347.1
Salmonella enterica subsp. enterica serovar Pullorum genome ass...	Salmonell...	1467	1467	100%	0.0	100.00%	4620579	LK931482.1
Salmonella enterica subsp. enterica serovar Gallinarum/pullorum s...	Salmonell...	1467	1467	100%	0.0	100.00%	4623089	CP003786.1
Salmonella enterica subsp. enterica serovar Pullorum str. S06004,...	Salmonell...	1467	1467	100%	0.0	100.00%	4682599	CP006575.1
Salmonella enterica subsp. enterica serovar Pullorum strain CFSA...	Salmonell...	1467	1467	100%	0.0	100.00%	4672899	CP075028.1
Salmonella enterica subsp. enterica serovar Pullorum strain CFSA...	Salmonell...	1467	1467	100%	0.0	100.00%	4689720	CP075018.1
Salmonella enterica subsp. enterica serovar Pullorum str. CFSAN0...	Salmonell...	1467	1467	100%	0.0	100.00%	4692377	CP074215.1
Salmonella enterica subsp. enterica serovar Gallinarum/pullorum s...	Salmonell...	1467	1467	100%	0.0	100.00%	4637962	CP003047.1
Salmonella enterica subsp. enterica serovar Enteritidis strain SAP1...	Salmonell...	839	1477	100%	0.0	99.35%	4679507	CP040646.1
Salmonella enterica subsp. enterica serovar Enteritidis strain SAP1...	Salmonell...	839	1477	100%	0.0	99.35%	4680325	CP040644.1
Salmonella enterica subsp. enterica serovar Enteritidis strain CFSA...	Salmonell...	839	1477	100%	0.0	99.35%	4668874	CP033340.1
Salmonella enterica subsp. enterica serovar Enteritidis strain SEO...	Salmonell...	839	1477	100%	0.0	99.35%	4676321	CP033090.1
Salmonella enterica subsp. enterica serovar Enteritidis str. RM2968...	Salmonell...	839	1477	100%	0.0	99.35%	4668875	CP028151.1
Salmonella enterica subsp. enterica serovar Enteritidis strain RM42...	Salmonell...	839	1477	100%	0.0	99.35%	4668881	CP028157.1
Salmonella enterica subsp. enterica serovar Enteritidis str. EC2012...	Salmonell...	839	1477	100%	0.0	99.35%	4685848	CP007332.2
Salmonella enterica subsp. enterica serovar Enteritidis strain ATCC...	Salmonell...	839	1477	100%	0.0	99.35%	4678516	CP025554.1
Salmonella enterica strain FDAARGOS_70 chromosome, complete ...	Salmonell...	839	1477	100%	0.0	99.35%	4679420	CP026052.1
Salmonella enterica subsp. enterica serovar Enteritidis strain 95-06...	Salmonell...	839	1477	100%	0.0	99.35%	4679622	CP018661.1
Salmonella enterica subsp. enterica serovar Enteritidis strain 93-06...	Salmonell...	839	1477	100%	0.0	99.35%	4679309	CP018659.1
Salmonella enterica subsp. enterica serovar Enteritidis strain 81-17...	Salmonell...	839	1477	100%	0.0	99.35%	4699800	CP018655.1
Salmonella enterica subsp. enterica serovar Enteritidis strain 81-17...	Salmonell...	839	1477	100%	0.0	99.35%	4698445	CP018651.1
Salmonella enterica subsp. enterica serovar Enteritidis strain 81-16...	Salmonell...	839	1477	100%	0.0	99.35%	4688972	CP018648.1
Salmonella enterica subsp. enterica serovar Enteritidis strain 81-14...	Salmonell...	839	1477	100%	0.0	99.35%	4699764	CP018647.1
Salmonella enterica subsp. enterica serovar Enteritidis strain 79-23...	Salmonell...	839	1477	100%	0.0	99.35%	4684909	CP018645.1
Salmonella enterica subsp. enterica serovar Enteritidis strain 77-29...	Salmonell...	839	1477	100%	0.0	99.35%	4686089	CP018644.1
Salmonella enterica subsp. enterica serovar Enteritidis strain 74-13...	Salmonell...	839	1477	100%	0.0	99.35%	4698044	CP018642.1
Salmonella enterica subsp. enterica serovar Enteritidis strain 70-16...	Salmonell...	839	1477	100%	0.0	99.35%	4679538	CP018640.1
Salmonella enterica subsp. enterica serovar Enteritidis strain 69-38...	Salmonell...	839	1477	100%	0.0	99.35%	4690881	CP018637.1
Salmonella enterica subsp. enterica serovar Enteritidis strain 56-39...	Salmonell...	839	1477	100%	0.0	99.35%	4678113	CP018635.1
Salmonella enterica subsp. enterica serovar Enteritidis strain 49-24...	Salmonell...	839	1477	100%	0.0	99.35%	4661885	CP018633.1
Salmonella enterica subsp. enterica serovar Enteritidis strain CFSA...	Salmonell...	839	1477	100%	0.0	99.35%	4679123	CP022003.1

Salmonella enterica subsp. enterica serovar Enteritidis strain CFS...	Salmonell...	839	1477	100%	0.0	99.35%	4679401	CP020825.1
Salmonella enterica subsp. enterica serovar Enteritidis strain CFS...	Salmonell...	839	1477	100%	0.0	99.35%	4679064	CP020823.1
Salmonella enterica subsp. enterica serovar Moscow str. S-1843, c...	Salmonell...	839	1477	100%	0.0	99.35%	4690402	CP019415.1
Salmonella enterica subsp. enterica serovar Blegdam str. S-1824,...	Salmonell...	839	1477	100%	0.0	99.35%	4693979	CP019406.1
Salmonella enterica subsp. enterica serovar Gallinarum str. 9184,...	Salmonell...	839	1477	100%	0.0	99.35%	4609911	CP019035.1
Salmonella enterica subsp. enterica serovar Enteritidis strain OLF-...	Salmonell...	839	1477	100%	0.0	99.35%	4679487	CP011942.1
Salmonella enterica subsp. enterica serovar Enteritidis str. SA200...	Salmonell...	839	1477	100%	0.0	99.35%	4685839	CP007468.2
Salmonella enterica subsp. enterica serovar Enteritidis str. EC201...	Salmonell...	839	1477	100%	0.0	99.35%	4686198	CP007323.2
Salmonella enterica subsp. enterica serovar Enteritidis str. EC201...	Salmonell...	839	1477	100%	0.0	99.35%	4685833	CP007339.2
Salmonella enterica subsp. enterica serovar Enteritidis str. EC201...	Salmonell...	839	1477	100%	0.0	99.35%	4685846	CP007344.2
Salmonella enterica subsp. enterica serovar Enteritidis str. EC201...	Salmonell...	839	1477	100%	0.0	99.35%	4686258	CP007378.2
Salmonella enterica subsp. enterica serovar Enteritidis str. EC201...	Salmonell...	839	1477	100%	0.0	99.35%	4685847	CP007412.2
Salmonella enterica subsp. enterica serovar Enteritidis str. EC201...	Salmonell...	839	1477	100%	0.0	99.35%	4685847	CP007325.2
Salmonella enterica subsp. enterica serovar Enteritidis str. EC201...	Salmonell...	839	1477	100%	0.0	99.35%	4685842	CP007498.2
Salmonella enterica subsp. enterica serovar Enteritidis str. SA200...	Salmonell...	839	1477	100%	0.0	99.35%	4685835	CP007469.2
Salmonella enterica subsp. enterica serovar Enteritidis str. SA200...	Salmonell...	839	1477	100%	0.0	99.35%	4685836	CP007467.2
Salmonella enterica subsp. enterica serovar Enteritidis str. SA200...	Salmonell...	839	1477	100%	0.0	99.35%	4685836	CP007466.2
Salmonella enterica subsp. enterica serovar Enteritidis str. EC201...	Salmonell...	839	1477	100%	0.0	99.35%	4685731	CP007464.2
Salmonella enterica subsp. enterica serovar Enteritidis str. EC201...	Salmonell...	839	1477	100%	0.0	99.35%	4685736	CP007463.2
Salmonella enterica subsp. enterica serovar Enteritidis str. EC201...	Salmonell...	839	1477	100%	0.0	99.35%	4685849	CP007438.2
Salmonella enterica subsp. enterica serovar Enteritidis str. EC201...	Salmonell...	839	1477	100%	0.0	99.35%	4685846	CP007433.2
Salmonella enterica subsp. enterica serovar Enteritidis str. EC201...	Salmonell...	839	1477	100%	0.0	99.35%	4685848	CP007429.2
Salmonella enterica subsp. enterica serovar Enteritidis str. EC201...	Salmonell...	839	1477	100%	0.0	99.35%	4685846	CP007428.2
Salmonella enterica subsp. enterica serovar Enteritidis str. SA201...	Salmonell...	839	1477	100%	0.0	99.35%	4685849	CP007427.2
Salmonella enterica subsp. enterica serovar Enteritidis str. EC201...	Salmonell...	839	1477	100%	0.0	99.35%	4685847	CP007432.2
Salmonella enterica subsp. enterica serovar Enteritidis str. SA200...	Salmonell...	839	1477	100%	0.0	99.35%	4685841	CP007431.2
Salmonella enterica subsp. enterica serovar Enteritidis str. EC200...	Salmonell...	839	1477	100%	0.0	99.35%	4685846	CP007430.2
Salmonella enterica subsp. enterica serovar Enteritidis str. EC201...	Salmonell...	839	1477	100%	0.0	99.35%	4685845	CP007404.2
Salmonella enterica subsp. enterica serovar Enteritidis str. EC201...	Salmonell...	839	1477	100%	0.0	99.35%	4685847	CP007401.2
Salmonella enterica subsp. enterica serovar Enteritidis str. EC201...	Salmonell...	839	1477	100%	0.0	99.35%	4685840	CP007368.2
Salmonella enterica subsp. enterica serovar Enteritidis str. EC201...	Salmonell...	839	1477	100%	0.0	99.35%	4685975	CP007367.2
Salmonella enterica subsp. enterica serovar Enteritidis str. EC201...	Salmonell...	839	1477	100%	0.0	99.35%	4685832	CP007366.2
Salmonella enterica subsp. enterica serovar Enteritidis str. EC201...	Salmonell...	839	1477	100%	0.0	99.35%	4685838	CP007373.2
Salmonella enterica subsp. enterica serovar Enteritidis str. SA201...	Salmonell...	839	1477	100%	0.0	99.35%	4685840	CP007372.2

Salmonella enterica subsp. enterica serovar Enteritidis str. EC201...	Salmonell...	839	1477	100%	0.0	99.35%	4685786	CP007371.2
Salmonella enterica subsp. enterica serovar Enteritidis str. EC201...	Salmonell...	839	1477	100%	0.0	99.35%	4685833	CP007370.2
Salmonella enterica subsp. enterica serovar Enteritidis str. EC201...	Salmonell...	839	1477	100%	0.0	99.35%	4685835	CP007369.2
Salmonella enterica subsp. enterica serovar Enteritidis str. EC200...	Salmonell...	839	1477	100%	0.0	99.35%	4685834	CP007422.2
Salmonella enterica subsp. enterica serovar Enteritidis str. EC200...	Salmonell...	839	1477	100%	0.0	99.35%	4685838	CP007421.2
Salmonella enterica subsp. enterica serovar Enteritidis str. EC201...	Salmonell...	839	1477	100%	0.0	99.35%	4685835	CP007420.2
Salmonella enterica subsp. enterica serovar Enteritidis str. EC201...	Salmonell...	839	1477	100%	0.0	99.35%	4685849	CP007424.2
Salmonella enterica subsp. enterica serovar Enteritidis str. EC201...	Salmonell...	839	1477	100%	0.0	99.35%	4685847	CP007423.2
Salmonella enterica subsp. enterica serovar Enteritidis str. EC201...	Salmonell...	839	1477	100%	0.0	99.35%	4685836	CP007419.2
Salmonella enterica subsp. enterica serovar Enteritidis str. EC201...	Salmonell...	839	1477	100%	0.0	99.35%	4685849	CP007418.2
Salmonella enterica subsp. enterica serovar Enteritidis str. SA201...	Salmonell...	839	1477	100%	0.0	99.35%	4685793	CP007417.2
Salmonella enterica subsp. enterica serovar Enteritidis str. EC201...	Salmonell...	839	1477	100%	0.0	99.35%	4685841	CP007416.2
Salmonella enterica subsp. enterica serovar Enteritidis str. EC201...	Salmonell...	839	1477	100%	0.0	99.35%	4685839	CP007415.2
Salmonella enterica subsp. enterica serovar Enteritidis str. EC201...	Salmonell...	839	1477	100%	0.0	99.35%	4685835	CP007354.2
Salmonella enterica subsp. enterica serovar Enteritidis str. SA201...	Salmonell...	839	1477	100%	0.0	99.35%	4685835	CP007361.2
Salmonella enterica subsp. enterica serovar Enteritidis str. EC201...	Salmonell...	839	1477	100%	0.0	99.35%	4685849	CP007359.2
Salmonella enterica subsp. enterica serovar Enteritidis str. EC201...	Salmonell...	839	1477	100%	0.0	99.35%	4685849	CP007358.2
Salmonella enterica subsp. enterica serovar Enteritidis str. EC201...	Salmonell...	839	1477	100%	0.0	99.35%	4685841	CP007357.2
Salmonella enterica subsp. enterica serovar Enteritidis str. EC201...	Salmonell...	839	1477	100%	0.0	99.35%	4685838	CP007382.2
Salmonella enterica subsp. enterica serovar Enteritidis str. EC201...	Salmonell...	839	1477	100%	0.0	99.35%	4685847	CP007381.2
Salmonella enterica subsp. enterica serovar Enteritidis str. EC201...	Salmonell...	839	1477	100%	0.0	99.35%	4685838	CP007380.2
Salmonella enterica subsp. enterica serovar Enteritidis str. EC201...	Salmonell...	839	1477	100%	0.0	99.35%	4685833	CP007379.2
Salmonella enterica subsp. enterica serovar Enteritidis strain CFS...	Salmonell...	839	1477	100%	0.0	99.35%	4679257	CP075120.1
Salmonella enterica subsp. enterica serovar Enteritidis strain CFS...	Salmonell...	839	1477	100%	0.0	99.35%	4685965	CP075019.1
Salmonella enterica subsp. enterica serovar Enteritidis strain CFS...	Salmonell...	839	1477	100%	0.0	99.35%	4668867	CP074661.1
Salmonella enterica subsp. enterica serovar Enteritidis strain CFS...	Salmonell...	839	1477	100%	0.0	99.35%	4679535	CP075118.1
Salmonella enterica subsp. enterica serovar Javiana str. CFSAN00...	Salmonell...	839	1477	100%	0.0	99.35%	4679849	CP074314.1
Salmonella enterica subsp. enterica serovar Montevideo str. CFSA...	Salmonell...	839	1477	100%	0.0	99.35%	4594713	CP074299.1
Salmonella enterica subsp. enterica serovar Enteritidis strain CFS...	Salmonell...	839	1477	100%	0.0	99.35%	4679790	CP074254.1
Salmonella enterica subsp. enterica serovar Enteritidis strain CFS...	Salmonell...	839	1477	100%	0.0	99.35%	4718780	CP074252.1
Salmonella enterica subsp. enterica serovar Enteritidis str. 607307...	Salmonell...	839	1477	100%	0.0	99.35%	4679730	CP074238.1
Salmonella enterica strain FDAARGOS_1066 chromosome, compl...	Salmonell...	839	1477	100%	0.0	99.35%	4677108	CP066047.1
Salmonella enterica subsp. enterica serovar Enteritidis strain CP2...	Salmonell...	839	1477	100%	0.0	99.35%	4736564	CP063705.1
Salmonella enterica subsp. enterica serovar Enteritidis strain D77...	Salmonell...	839	1477	100%	0.0	99.35%	4749264	CP063702.1

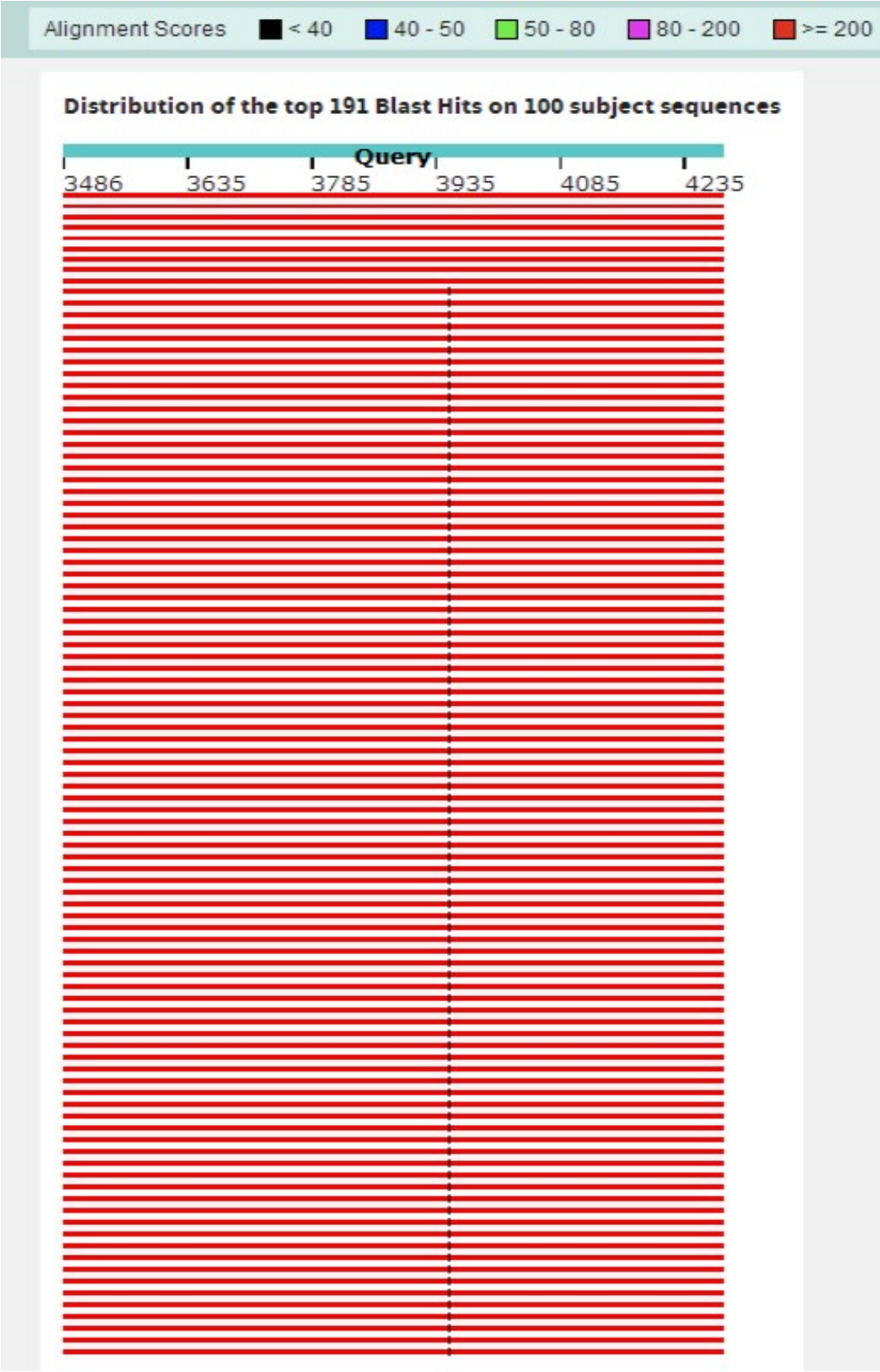

Supplementary Fig. 3.1 BLAST search results using S. Pullorum *citE2* gene (GenBank accession No: LK931482.1, region 3,486-4,279) against the nucleotide collection (nr/nt) database.

The results indicated that *citE2* exists in Salmonella enterica subsp. enterica serotypes, and *S*. Pullorum has a 76 bp deletion in *citE2* gene , which could be designed to identify *S*. Pullorum from other *Salmonella enterica* subsp. *enterica* serovars and non-*Salmonella enterica* subsp. *enterica* pathogens.

BLAST® » blastn suite » results for RID-UW4B3VSS013

Job Title	**emb|LK931482.1|**
RID	UW4B3VSS013 *Search expires on 12-07 20:34 pm* Download All
Program	BLASTN Citation
Database	nt See details
Query ID	LK931482.1
Description	Salmonella enterica subsp. enterica serovar Pullorum gen ...
Molecule type	nucleic acid
Query Length	167
Other reports	Distance tree of results MSA viewer

Description	Scientific Name	Max Score	Total Score	Query Cover	E value	Per. Ident	Acc. Len	Accession
Salmonella enterica subsp. enterica serovar Infantis strain CVM N17S1509 chromosome, complete genome	Salmonella ente...	309	1982	100%	5e-80	100.00%	4727152	CP052817.1
Salmonella enterica subsp. enterica serovar Paratyphi C strain 07-0715 chromosome, complete genome	Salmonella ente...	309	1341	100%	5e-80	100.00%	4794211	CP053400.1
Salmonella enterica strain 2016K-0213 chromosome, complete genome	Salmonella ente...	309	1523	100%	5e-80	100.00%	4761338	CP053402.1
Salmonella enterica subsp. enterica serovar Infantis strain CVM N16S024 chromosome, complete genome	Salmonella ente...	309	1982	100%	5e-80	100.00%	4727142	CP052839.1
Salmonella enterica subsp. enterica serovar Infantis strain CVM N16S097 chromosome, complete genome	Salmonella ente...	309	1982	100%	5e-80	100.00%	4727141	CP052837.1
Salmonella enterica subsp. enterica serovar Infantis strain CVM N16S103 chromosome, complete genome	Salmonella ente...	309	1982	100%	5e-80	100.00%	4727146	CP052835.1
Salmonella enterica subsp. enterica serovar Infantis strain CVM N17S041 chromosome, complete genome	Salmonella ente...	309	1982	100%	5e-80	100.00%	4727150	CP052833.1
Salmonella enterica subsp. enterica serovar Infantis strain CVM N17S1040 chromosome, complete genome	Salmonella ente...	309	1982	100%	5e-80	100.00%	4727118	CP052831.1
Salmonella enterica subsp. enterica serovar Infantis strain CVM N17S1105 chromosome, complete genome	Salmonella ente...	309	1982	100%	5e-80	100.00%	4728347	CP052829.1
Salmonella enterica subsp. enterica serovar Infantis strain CVM N17S1126 chromosome, complete genome	Salmonella ente...	309	1982	100%	5e-80	100.00%	4728349	CP052827.1
Salmonella enterica subsp. enterica serovar Infantis strain CVM N17S1245 chromosome, complete genome	Salmonella ente...	309	1982	100%	5e-80	100.00%	4727130	CP052825.1
Salmonella enterica subsp. enterica serovar Infantis strain CVM N17S1265 chromosome, complete genome	Salmonella ente...	309	1982	100%	5e-80	100.00%	4727126	CP052823.1
Salmonella enterica subsp. enterica serovar Infantis strain CVM N17S1349 chromosome, complete genome	Salmonella ente...	309	1982	100%	5e-80	100.00%	4727144	CP052821.1
Salmonella enterica subsp. enterica serovar Infantis strain CVM N17S1442 chromosome, complete genome	Salmonella ente...	309	1982	100%	5e-80	100.00%	4727121	CP052819.1
Salmonella enterica subsp. enterica serovar Infantis strain CVM N17S1598 chromosome, complete genome	Salmonella ente...	309	1982	100%	5e-80	100.00%	4727100	CP052815.1
Salmonella enterica subsp. enterica serovar Enteritidis strain SE211 chromosome, complete genome	Salmonella ente...	309	1441	100%	5e-80	100.00%	4679414	CP084532.1
Salmonella enterica subsp. enterica serovar Newlands strain ZC-S1 3rd chromosome, complete genome	Salmonella ente...	309	1441	100%	5e-80	100.00%	4679998	CP082916.1
Salmonella enterica subsp. enterica serovar Infantis strain CVM N18S2198 chromosome, complete genome	Salmonella ente...	309	1982	100%	5e-80	100.00%	4738019	CP082521.1
Salmonella enterica subsp. enterica serovar Reading strain CVM N18S2042 chromosome, complete genome	Salmonella ente...	309	1982	100%	5e-80	100.00%	4833661	CP082536.1
Salmonella enterica subsp. enterica serovar 4 [5],12,i:- strain CVM N18S0736 chromosome, complete genome	Salmonella ente...	309	1660	100%	5e-80	100.00%	4866552	CP082588.1
Salmonella enterica subsp. enterica serovar Infantis strain CVM N17S1592 chromosome, complete genome	Salmonella ente...	309	1982	100%	5e-80	100.00%	4726954	CP082617.1
Salmonella enterica subsp. enterica serovar Heidelberg strain CVM N17S1352 chromosome, complete geno...	Salmonella ente...	309	1660	100%	5e-80	100.00%	4854520	CP082629.1
Salmonella enterica subsp. enterica serovar Enteritidis strain CVM N17S192 chromosome, complete genome	Salmonella ente...	309	1447	100%	5e-80	100.00%	4679415	CP082726.1
Salmonella enterica subsp. enterica serovar 4 [5],12,i:- strain CVM N17S166 chromosome, complete genome	Salmonella ente...	309	1660	100%	5e-80	100.00%	4997193	CP082668.1
Salmonella enterica subsp. enterica serovar Enteritidis strain CVM N17S111 chromosome, complete genome	Salmonella ente...	309	1447	100%	5e-80	100.00%	4679495	CP082729.1
Salmonella enterica subsp. enterica serovar Heidelberg strain CVM N16S098 chromosome, complete genome	Salmonella ente...	309	1559	100%	5e-80	100.00%	4837915	CP082658.1
Salmonella enterica subsp. enterica serovar Infantis strain FSIS1703084 chromosome, complete genome	Salmonella ente...	309	1982	100%	5e-80	100.00%	4727480	CP082372.1
Salmonella enterica subsp. enterica serovar Heidelberg strain CVM N16S074 chromosome, complete genome	Salmonella ente...	309	1660	100%	5e-80	100.00%	4751723	CP082736.1
Salmonella enterica subsp. enterica serovar Heidelberg strain FSIS11706780 chromosome, complete genome	Salmonella ente...	309	1660	100%	5e-80	100.00%	4881640	CP082394.1
Salmonella enterica subsp. enterica serovar Heidelberg strain FSIS11704575 chromosome, complete genome	Salmonella ente...	309	1660	100%	5e-80	100.00%	4841713	CP082415.1
Salmonella enterica subsp. enterica serovar Infantis strain FSIS1700566 chromosome, complete genome	Salmonella ente...	309	1982	100%	5e-80	100.00%	4660612	CP082389.1

Salmonella enterica subsp. enterica serovar Heidelberg strain FSIS1606640 chromosome, complete genome	Salmonella ente...	309	1660	100%	5e-80	100.00%	4985524	CP082503.1
Salmonella enterica subsp. enterica serovar Infantis strain CVM N18S1988 isolate 18TX11CB22-S1 chromos...	Salmonella ente...	309	1982	100%	5e-80	100.00%	4730425	CP082538.1
Salmonella enterica subsp. enterica serovar Weltevreden strain Colony70 chromosome	Salmonella ente...	309	1421	100%	5e-80	100.00%	5047093	CP078529.1
Salmonella enterica subsp. enterica serovar Weltevreden strain Colony65 chromosome	Salmonella ente...	309	1421	100%	5e-80	100.00%	5047093	CP078530.1
Salmonella enterica subsp. enterica serovar Java strain P7704 chromosome	Salmonella ente...	309	1523	100%	5e-80	100.00%	4755347	CP065185.1
Salmonella enterica subsp. enterica serovar Enteritidis strain CFSAN051827 chromosome, complete genome	Salmonella ente...	309	1447	100%	5e-80	100.00%	4679656	CP075122.1
Salmonella enterica subsp. enterica serovar Enteritidis strain CFSAN051882 chromosome, complete genome	Salmonella ente...	309	1447	100%	5e-80	100.00%	4679257	CP075120.1
Salmonella enterica subsp. enterica serovar Stanleyville strain CFSAN059881 chromosome, complete genome	Salmonella ente...	309	1568	100%	5e-80	100.00%	4688242	CP075116.1
Salmonella enterica strain CFSAN012373 chromosome, complete genome	Salmonella ente...	309	1660	100%	5e-80	100.00%	4701728	CP075043.1
Salmonella enterica subsp. enterica serovar Infantis strain CFSAN012496 chromosome, complete genome	Salmonella ente...	309	1982	100%	5e-80	100.00%	4679931	CP075042.1
Salmonella enterica subsp. enterica serovar Pullorum strain CFSAN022627 chromosome, complete genome	Salmonella ente...	309	1259	100%	5e-80	100.00%	4672899	CP075028.1
Salmonella enterica subsp. enterica serovar Enteritidis strain CFSAN022640 chromosome, complete genome	Salmonella ente...	309	1447	100%	5e-80	100.00%	4685965	CP075019.1
Salmonella enterica subsp. enterica serovar Pullorum strain CFSAN022642 chromosome, complete genome	Salmonella ente...	309	1259	100%	5e-80	100.00%	4689720	CP075018.1
Salmonella enterica strain CFSAN024184 chromosome, complete genome	Salmonella ente...	309	2348	100%	5e-80	100.00%	4611122	CP075015.1
Salmonella enterica subsp. enterica serovar Enteritidis strain CFSAN008104 chromosome, complete genome	Salmonella ente...	309	1447	100%	5e-80	100.00%	4668867	CP074661.1
Salmonella enterica subsp. enterica serovar Enteritidis strain CFSAN051890 chromosome, complete genome	Salmonella ente...	309	1447	100%	5e-80	100.00%	4679535	CP075118.1
Salmonella enterica subsp. enterica serovar Kunzendorf strain CFSAN022623 chromosome, complete genome	Salmonella ente...	309	1335	100%	5e-80	100.00%	4726369	CP075031.1
Salmonella enterica subsp. enterica serovar Choleraesuis strain CFSAN022628 chromosome, complete gen...	Salmonella ente...	309	1335	100%	5e-80	100.00%	4784901	CP075026.1
Salmonella enterica subsp. enterica serovar Kunzendorf strain CFSAN022631 chromosome, complete genome	Salmonella ente...	309	1335	100%	5e-80	100.00%	4784246	CP075024.1
Salmonella enterica subsp. enterica serovar Hartford strain CFSAN008725 chromosome, complete genome	Salmonella ente...	309	1489	100%	5e-80	100.00%	4717025	CP074660.1
Salmonella enterica subsp. enterica serovar Weltevreden strain CFSAN028546 chromosome, complete geno...	Salmonella ente...	309	1421	100%	5e-80	100.00%	4920208	CP074657.1
Salmonella enterica subsp. enterica serovar Paratyphi B str. CFSAN000535 strain SGSC 2233 isolate SARA...	Salmonella ente...	309	1335	100%	5e-80	100.00%	4694564	CP074611.1
Salmonella sp. SJTUF14523 chromosome, complete genome	Salmonella sp. ...	309	1441	100%	5e-80	100.00%	4679991	CP074428.1
Salmonella sp. SJTUF15034 chromosome, complete genome	Salmonella sp. ...	309	1441	100%	5e-80	100.00%	4679426	CP074425.1
Salmonella enterica subsp. enterica serovar Infantis strain CFSAN059939 chromosome, complete genome	Salmonella ente...	309	1982	100%	5e-80	100.00%	4726984	CP074343.1
Salmonella enterica subsp. enterica serovar Infantis strain CFSAN059940 chromosome, complete genome	Salmonella ente...	309	1982	100%	5e-80	100.00%	4727146	CP074341.1
Salmonella enterica subsp. enterica serovar Weltevreden strain CFSAN024549 chromosome, complete geno...	Salmonella ente...	309	1421	100%	5e-80	100.00%	4939325	CP074328.1
Salmonella enterica subsp. enterica serovar Soerenga str. 695 chromosome, complete genome	Salmonella ente...	309	1958	100%	5e-80	100.00%	4766925	CP074317.1
Salmonella enterica subsp. enterica serovar Javiana str. CFSAN001992 chromosome, complete genome	Salmonella ente...	309	1441	100%	5e-80	100.00%	4679849	CP074314.1
Salmonella enterica subsp. enterica serovar Montevideo str. CFSAN004346 chromosome, complete genome	Salmonella ente...	309	1499	100%	5e-80	100.00%	4594713	CP074299.1
Salmonella enterica subsp. enterica serovar Hartford strain CFSAN008740 chromosome, complete genome	Salmonella ente...	309	1489	100%	5e-80	100.00%	4815272	CP074274.1
Salmonella enterica subsp. enterica serovar Infantis strain CFSAN024778 chromosome, complete genome	Salmonella ente...	309	1982	100%	5e-80	100.00%	4713725	CP074257.1
Salmonella enterica subsp. enterica serovar Enteritidis strain CFSAN026631 chromosome, complete genome	Salmonella ente...	309	1447	100%	5e-80	100.00%	4679790	CP074254.1
Salmonella enterica subsp. enterica serovar Infantis strain CFSAN024781 chromosome, complete genome	Salmonella ente...	309	1977	100%	5e-80	100.00%	4705145	CP074256.1
Salmonella enterica subsp. enterica serovar Livingstone strain CFSAN024717 chromosome, complete genome	Salmonella ente...	309	1726	100%	5e-80	100.00%	4762862	CP074262.1
Salmonella enterica subsp. enterica serovar Enteritidis strain CFSAN026633 chromosome, complete genome	Salmonella ente...	309	1447	100%	5e-80	100.00%	4718780	CP074252.1
Salmonella enterica subsp. enterica serovar Enteritidis str. 607307-2 chromosome, complete genome	Salmonella ente...	309	1447	100%	5e-80	100.00%	4679730	CP074238.1
Salmonella enterica subsp. enterica serovar Paratyphi B str. CFSAN000545 strain SGSC 2500 isolate SARB...	Salmonella ente...	309	1523	100%	5e-80	100.00%	4726964	CP074225.1
Salmonella enterica subsp. enterica serovar Paratyphi B str. CFSAN000546 strain SGSC 2501 isolate SARB...	Salmonella ente...	309	1335	100%	5e-80	100.00%	4453147	CP074223.1
Salmonella enterica subsp. enterica serovar Pullorum str. CFSAN000606 strain SGSC 2508 isolate SARB51...	Salmonella ente...	309	1265	100%	5e-80	100.00%	4692377	CP074215.1
Salmonella enterica subsp. enterica serovar Dublin str. CFSAN000517 strain SGSC 2470 isolate SARB13 ch...	Salmonella ente...	309	1542	100%	5e-80	100.00%	4935048	CP074226.1
Salmonella enterica subsp. enterica serovar Heidelberg str. SARA37 strain SGSC 2217 chromosome, compl...	Salmonella ente...	309	1660	100%	5e-80	100.00%	4969969	CP074234.1
Salmonella sp. SAL-045 chromosome, complete genome	Salmonella sp. ...	309	1441	100%	5e-80	100.00%	4679327	CP071693.1
Salmonella sp. SAL-007 chromosome, complete genome	Salmonella sp. ...	309	1441	100%	5e-80	100.00%	4679742	CP071686.1
Salmonella sp. SAL-020 chromosome, complete genome	Salmonella sp. ...	309	1441	100%	5e-80	100.00%	4679997	CP071690.1
Salmonella enterica subsp. enterica serovar Infantis strain 114061 chromosome, complete genome	Salmonella ente...	309	1982	100%	5e-80	100.00%	4720865	CP070302.1
Salmonella enterica subsp. enterica serovar Infantis strain 91264 chromosome, complete genome	Salmonella ente...	309	1982	100%	5e-80	100.00%	4757543	CP070301.1
Salmonella enterica subsp. enterica serovar Weltevreden strain colony_64 chromosome	Salmonella ente...	309	1421	100%	5e-80	100.00%	5047093	CP067990.1
Salmonella enterica subsp. enterica serovar Weltevreden strain colony_68 chromosome	Salmonella ente...	309	1421	100%	5e-80	100.00%	5047093	CP067988.1
Salmonella enterica subsp. enterica serovar Weltevreden strain colony_80 chromosome	Salmonella ente...	309	1421	100%	5e-80	100.00%	5047093	CP067980.1
Salmonella enterica strain UWI_PP31 isolate CFSAN103816 chromosome	Salmonella ente...	309	1982	100%	5e-80	100.00%	4703182	CP066324.1
Salmonella enterica subsp. enterica serovar Infantis strain CFSAN103796 chromosome, complete genome	Salmonella ente...	309	1982	100%	5e-80	100.00%	4727424	CP066335.1
Salmonella enterica subsp. enterica serovar Heidelberg strain CVM 20760 chromosome, complete genome	Salmonella ente...	309	1660	100%	5e-80	100.00%	4744872	CP051410.1
Salmonella enterica subsp. enterica serovar Heidelberg strain CVM 24359 chromosome, complete genome	Salmonella ente...	309	1660	100%	5e-80	100.00%	4792518	CP051381.1
Salmonella enterica subsp. enterica serovar Choleraesuis strain CVM 28296 chromosome, complete genome	Salmonella ente...	309	1335	100%	5e-80	100.00%	4744179	CP051366.1
Salmonella enterica subsp. enterica serovar Heidelberg strain CVM 28322 chromosome, complete genome	Salmonella ente...	309	1660	100%	5e-80	100.00%	4856212	CP051358.1
Salmonella enterica subsp. enterica serovar Heidelberg strain CVM 35161 chromosome, complete genome	Salmonella ente...	309	1660	100%	5e-80	100.00%	4856293	CP051310.1
Salmonella enterica strain FDAARGOS_1066 chromosome, complete genome	Salmonella ente...	309	1447	100%	5e-80	100.00%	4677108	CP066047.1
Salmonella enterica strain FDAARGOS_879 chromosome	Salmonella ente...	309	1330	100%	5e-80	100.00%	4742560	CP065890.1
Salmonella enterica subsp. enterica serovar Enteritidis strain P125109 chromosome, complete genome	Salmonella ente...	309	1441	100%	5e-80	100.00%	4685852	CP063700.1
Salmonella enterica subsp. enterica serovar Enteritidis strain CP255 chromosome, complete genome	Salmonella ente...	309	1447	100%	5e-80	100.00%	4736564	CP063705.1
Salmonella enterica subsp. enterica serovar Enteritidis strain A1636 chromosome, complete genome	Salmonella ente...	309	1441	100%	5e-80	100.00%	4685812	CP063708.1
Salmonella enterica subsp. enterica serovar Enteritidis strain D7795 chromosome, complete genome	Salmonella ente...	309	1447	100%	5e-80	100.00%	4749264	CP063702.1
Salmonella enterica subsp. enterica serovar Enteritidis strain R17.4111 chromosome, complete genome	Salmonella ente...	309	1441	100%	5e-80	100.00%	4713149	CP063289.1
Salmonella enterica strain SLR1_8250 chromosome, complete genome	Salmonella ente...	309	1441	100%	5e-80	100.00%	4679617	CP060522.1
Salmonella enterica strain SLR1_7966 chromosome, complete genome	Salmonella ente...	309	1982	100%	5e-80	100.00%	4686427	CP060512.1
Salmonella enterica subsp. enterica serovar Infantis strain VNSEC001 chromosome, complete genome	Salmonella ente...	309	1982	100%	5e-80	100.00%	4727130	CP039445.1
Salmonella enterica subsp. enterica serovar Infantis strain VNSEC002 chromosome, complete genome	Salmonella ente...	309	1982	100%	5e-80	100.00%	4727131	CP039443.1
Salmonella enterica subsp. enterica serovar Infantis strain VNSEC003 chromosome, complete genome	Salmonella ente...	309	1982	100%	5e-80	100.00%	4727127	CP039441.1

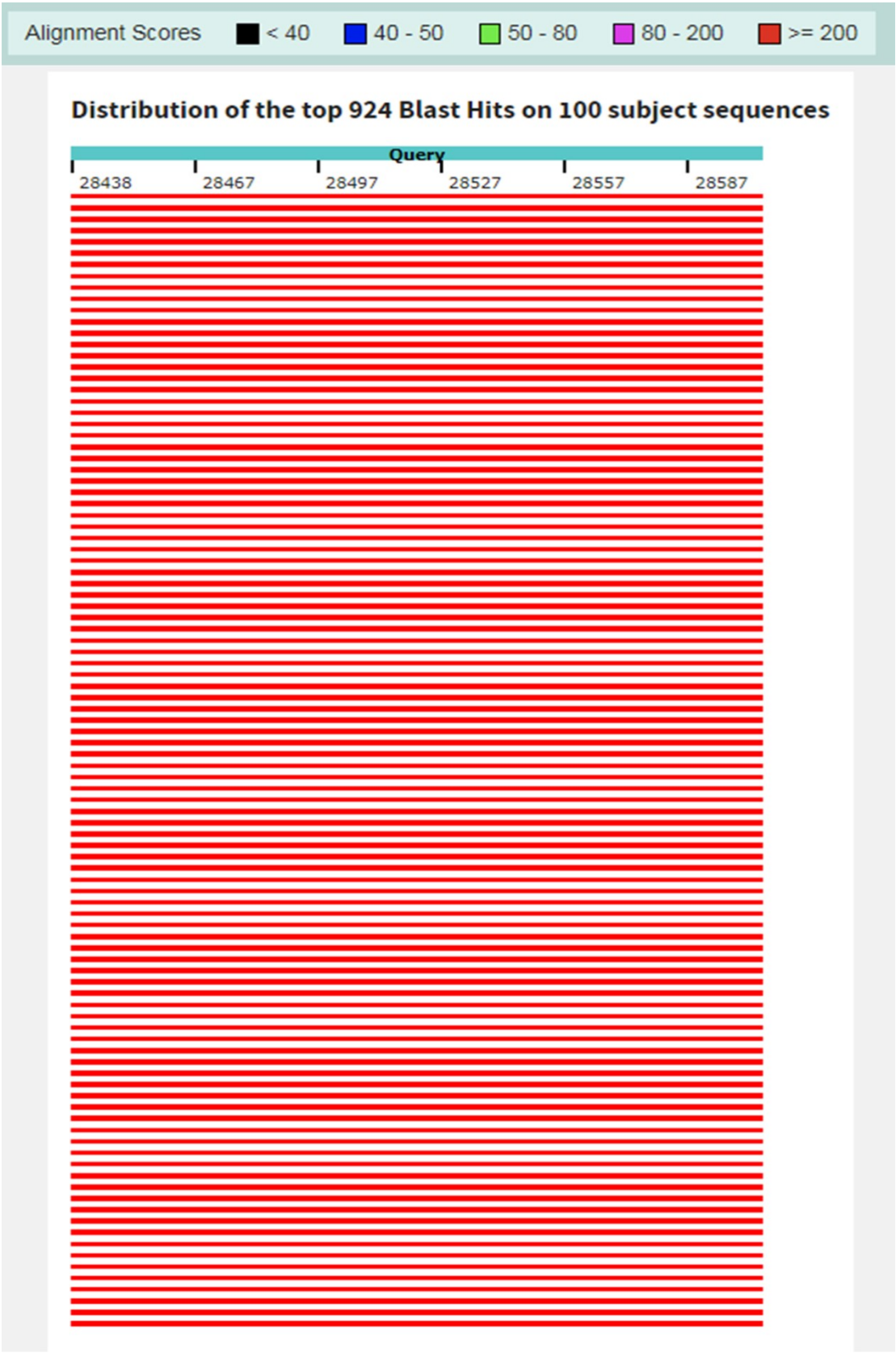

Supplementary Fig. 3.2 BLAST search results using the interval sequence of *S.* Pullorum SPS4_00301–SPS4_00311 (GenBank accession No: LK931482.1, region 28,438-28,604) against the nucleotide collection (nr/nt)

database.

The results indicated that SPS4_00301-SPS4_00311 exists in Salmonella enterica subsp. enterica serotypes, which could be designed to identify Salmonella from other *Salmonella enterica* subsp. *enterica* serovars and non-*Salmonella enterica* subsp. *enterica* pathogens.